THE UNIVERSITY OF CHICAGO

DEVELOPMENT OF MOTOR CIRCUITS: FROM NEURONAL STEM CELLS AND NEURONAL DIVERSITY TO MOTOR CIRCUIT ASSEMBLY

A DISSERTATION SUBMITTED TO
THE FACULTY OF THE DIVISION OF THE BIOLOGICAL SCIENCES
AND THE PRITZKER SCHOOL OF MEDICINE
IN CANDIDACY FOR THE DEGREE OF
DOCTOR OF PHILOSOPHY

GRADUATE PROGRAM IN CELL AND MOLECULAR BIOLOGY

BY
JULIA L. MENG

CHICAGO, ILLINOIS
MARCH 2022

Copyright © 2022 by Julia L. Meng

All Rights Reserved

In memory of Wilhelm Sailer-Schättin who through his life and death taught me that life is too short and painful to put off doing the things that offer joy and happiness

We have to remember that what we observe is not nature itself, but nature exposed to our method of questioning. — Werner Heisenberg

TABLE OF CONTENTS

LIST OF FIGURES ix

LIST OF TABLES xii

ACKNOWLEDGMENTS xiii

ABSTRACT xiv

1 INTRODUCTION 1
1.1 Introduction 1
1.2 Motor Circuits 2
1.2.1 Drosophila larva motor neuron circuit membership defined by muscle groups 4
1.3 Neuronal stem cells in the motor system 5
1.4 From neuronal diversity to motor circuit assembly 7
1.5 Why is neuron birth timing an important factor in motor circuit assembly? . 10

2 TEMPORAL COHORTS 11
2.1 Introduction 11
2.2 NB3-3 generates early-born EL and late-born EL temporal cohorts 12
2.3 Motor neuron temporal cohorts in Drosophila larvae 16
2.4 Atlas linking motor neuron lineage/hemilineage identity to muscle groups to reveal putative novel motor neuron temporal cohorts and more avenues for future projects 17
2.5 Temporal cohorts are born contiguously or in a tight developmental time window 23
2.6 Motor neuron temporal cohorts in adult Drosophila 24
2.7 In many systems, motor circuits are specified sequentially 24
2.8 Remaining questions about the lineage-based organization of motor circuits . 26
2.9 Conclusion 27

3 TEMPORAL TRANSCRIPTION FACTORS 28
3.1 Introduction 28
3.1.1 To what extent do temporal transcription factors control mature neuronal Identity? 28
3.1.2 Temporal transcription factor expression in neuroblasts regulates motor neuron temporal cohort size and composition 30
3.1.3 In some cases, the CNS can compensate for temporal transcription factor-induced changes 31
3.1.4 Remaining questions about how temporal transcription factors impact motor circuit assembly 32
3.2 Meng et al., 2019 eLife 34
3.2.1 Abstract 34

3.2.2 Introduction . . . 35
3.2.3 Results . . . 37
3.2.4 Discussion . . . 66
3.2.5 Materials and methods . . . 76
3.3 Meng et al., 2020 eLife . . . 82
3.3.1 abstract . . . 82
3.3.2 Introduction . . . 82
3.3.3 Results . . . 85
3.3.4 Discussion . . . 109
3.3.5 Conclusion . . . 114
3.3.6 Materials and methods . . . 116
3.4 misexpression of the temporal transcription factor Kruppel . . . 120
3.4.1 Introduction . . . 120
3.4.2 Past studies where Kr expression is manipulated . . . 120
3.4.3 Misexpression of Kruppel in NB7-1 . . . 122
3.4.4 Misexpression of Kruppel in NB3-1 . . . 124
3.4.5 Discussion of why there may be a discrepancy between previous findings and our data . . . 125

4 NB7-1 INTERNEURON STORY . . . 129
4.1 Introduction . . . 129
4.2 Results: Characterization of the entire NB7-1 lineage . . . 132
4.2.1 Embryonic Molecular Identity . . . 132
4.2.2 Morphology of NB7-1 interneurons . . . 135
4.3 In NB7-1>Hb embryos, ectopic Hunchback is expressed throughout the NB7-1 lineage . . . 140
4.4 Impact of Hunchback misexpression on NB7-1 interneuron morphology . . . 142
4.5 Mismatch between inherited information of interneurons and birth time? . . . 148
4.6 Castor is not required nor sufficient to specify interneuron outgrowth, projection, and arborization within the dorsal region of the neuropil . . . 151
4.7 Discussion . . . 156
4.7.1 What controls the timing of neuroblast's transition from generating motor neurons to making interneurons? . . . 161
4.7.2 Relationships between birth time and interneuron morphological fate 162

5 NOTCH TRANSCRIPTION FACTOR . . . 165
5.1 Introduction . . . 165
5.2 Results: Expressing Notch∧intra in the NB7-1 lineage transforms NotchOFF to the NotchON hemilineage . . . 171
5.2.1 Misexpressing Notch∧intra in the NB7-1 lineage permanently transforms the NotchOFF U sib fate to NotchON U and VO motor neuron to muscle synaptic partnership fate . . . 174
5.3 Results: Misexpressing Notch∧intra in the NB3-1 lineage permanently transforms the NotchOFF RP1,4,3,5 motor neuron fates to NotchON sib. . . . 177

5.4 Results: Misexpressing Numb using the NB7-1 driver does not transform the NotchON to the NotchOFF hemilineage . . . 178
5.5 Discussion: Does numb exclusively inhibit Notch signaling in the context of sibling fate specification? . . . 179
5.6 Notch/Numb pathway is involved in NB3-3 lineage development . . . 180
5.7 Results: Misexpressing Notch∧intra in NB7-1 causes Eve+ U motor neuron cell bodies to be abnormally clustered and positioned abnormally medially . 182
5.8 Future Directions: Could NB7-1's U motor neurons be a model system to study mechanisms underlying cell migration? . . . 186
5.8.1 Introduction . . . 186
5.8.2 First, I think there may be some general migration patterns of early born neurons, most of which are motor neurons . . . 187
5.8.3 Third, I think it is worthwhile to explore the extent to which circuit wiring decisions rely on proper cell body migration in the developing nerve cord . . . 194

6 CARDINAL TRANSCRIPTION FACTORS . . . 206
6.1 Introduction: What role do post-mitotic transcriptional programs play in motor circuit assembly? . . . 206
6.2 Results . . . 208
6.2.1 Introduction to the Drosophila motor system . . . 208
6.2.2 Loss of Nkx6 and Hb9 has no impact on third instar larval motor neuron-to-muscle synaptic connectivity . . . 209
6.2.3 Loss of hb9 and nkx6 delays ISNb outgrowth? . . . 212
6.3 Discussion: An update view on the cross-repressive relationships between cardinal factors . . . 215
6.4 Further characterization of the double loss of hb9 and nkx6 mutant larvae . . 216
6.5 Eve misexpression manipulation . . . 219
6.5.1 Background . . . 219
6.5.2 Results . . . 220
6.6 Discussion for the whole section on cardinal TFs . . . 230

7 ELECTRON MICROSCOPY . . . 237
7.1 Comparative EM connectomics project of nerve cord volumes containing APEX labeled neurons . . . 237
7.2 EM protocol background . . . 239
7.3 EM protocol . . . 241

8 APPENDIX . . . 250
8.1 Misexpressing Hunchback in NB7-1 reduces larval crawling speed . . . 250
8.2 Characterization of the NB3-1 driver and lineage . . . 255
8.3 Characterization of the NB7-1 driver and lineage . . . 256
8.4 Unpublished VP16::Hb related experiments . . . 257

8.4.1 Impact misexpressing VP16::HB2x and Hb1x using the NB7-1 GAL4 driver . . . 258
8.4.2 Impact misexpressing VP16::HB using the CQ GAL4 driver . . . 263

9 CONCLUSION . . . 266
9.1 Historical overview of the field of neurobiology's major goals . . . 266
9.2 Historical overview of developmental neurobiology's approaches and goals . . . 267
9.3 My PhD thesis's contribution to the field of developmental neurobiology . . . 268
9.4 My PhD thesis's major takeaway points . . . 269

10 METHODS . . . 273
10.1 Julia Meng's Gateway Cloning Protocol . . . 273
10.2 HL3 recipe for calcium imaging of the MHC tethered GCaMP6f . . . 278
10.3 live imaging protocol . . . 280
10.4 Illustrations of the adult Drosophila thoracic muscles . . . 280
10.5 Matching L3 bodywall segments to nerve cord hemisegments . . . 284

REFERENCES . . . 286

LIST OF FIGURES

1.1 Anatomical and functional definition of motor circuits. 3
1.2 Developmental organization of neuronal stem cell lineage 6
1.3 Molecular programs contributing to diverse neuronal identities 9

2.1 Temporal cohorts are an organizational unit linking neuronal stem cell lineages to motor circuit membership 13
2.2 Early-Born and Late-Born ELs Differentially Respond to Sound 14
2.3 Motor neuron to muscle target atlas including motor neuron's lineage/hemilineage identity 19

3.1 U motor neurons have unique embryonic molecular identities and unique terminal features. 39
3.2 U Motor Neuron axon projection in third instar (L3) Drosophila larva. 41
3.3 In embryos with prolonged Hb expression, U motor neurons are produced at abnormally late times in development. 44
3.4 Characterization of NB7-1-GAL4. 46
3.5 Prolonged expression of Hb in NB7-1 produces more U motor neurons. 49
3.6 Prolonged expression of Hb in NB7-1 alters U motor neuron dendritic arbors. . . 50
3.7 Prolonged expression of Hb in NB7-1 alters U motor neuromuscular synapses. . 54
3.8 U Motor neuron ablation. 56
3.9 Altered synaptic arbors on dorsal muscles contain functional synapses. 58
3.10 U motor neuron axonal trajectories are not accurately predicted by embryonic molecular identity or birth timing. 60
3.11 In NB7-1>Hb, U1 motor neuron identity is only transiently specified. 62
3.12 Altering the number of Hb(+) U motor neurons at L3 is correlated with synaptic partnerships. 65
3.13 Summary of Hunchback control on circuit wiring. 70
3.14 Calcium imaging protocol, analysis, and examples. 80
3.15 Prolonged expression of Hunchback alters RP motor neuron synapses. 87
3.16 NB3-1 generates RP motor neurons, with known features. 89
3.17 In embryos, prolonged expression of Hunchback generates more RP motor neurons with early born molecular identity. 90
3.18 Increased synaptic branches contain pre and postsynaptic markers necessary for function. 92
3.19 Altered synapses onto Ventral muscles are functional. 94
3.20 Precocious expression of Castor alters U motor neuron synapses. 98
3.21 In embryos, precocious expression of Castor generates fewer U motor neurons at the expense of later born neurons. 100
3.22 In embryos, precocious expression of Pdm generates either more or fewer U motor neurons depending on A/P positioning. 103
3.23 Precocious expression of Pdm alters U motor neuron synapses. 105
3.24 Altered synapses onto Dorsal muscles are functional 107

3.25 Calcium imaging protocol, analysis, and examples. 108
3.26 Summary of results in this study. 115
3.27 Impact misexpression of Kruppel in NB7-1 has on motor neuron molecular identity and permanent motor neuron to muscle synaptic partnerships. 123
3.28 Impact misexpression of Kruppel in NB3-1 has permanent motor neuron to muscle synaptic partnerships 125

4.1 Characterization embryonic molecular identity for the entire NB7-1 lineage . . . 133
4.2 Characterization of NB7-1 interneuron morphology 137
4.3 Light Microscopy of single clones of NB7-1 interneuron morphology. 139
4.4 Ectopic Huncback is expressed throughout the NB7-1 lineage at late embryonic stages 141
4.5 NB7-1 interneuron morphologies in 1st instar NB7-1>Hb animals 144
4.6 Arborless cells in the wildtype NB7-1 lineage in 1st instar larva nerve cord. . . . 145
4.7 Clones of interneurons with 'arrested' outgrowth fate in 1st instar NB7-1>Hb nerve cords 146
4.8 Clones of interneurons with 'wildtype-like' outgrowth fate in 1st instar NB7-1 >Hb nerve cords. 150
4.9 Clones of interneurons with 'wildtype-like' outgrowth fate in 1st instar NB7-1>Hb nerve cords expressing Hunchback. 152
4.10 In NB7-1> Castor, ectopic Castor is expressed throughout the NB7-1 lineage at late embryonic stages. 153
4.11 In 1st instar NB7-1>Cas, clones of interneurons with 'lateral-late' morphologies first identified in the EM volume in 1st instar. 154
4.12 In 1st instar NB7-1>Cas, clones of interneurons with 'lateral-late' morphologies first identified in the EM volume in 1st instar. 155
4.13 Summary (**A**) Illustration representing NB7-1 derived neuronal progeny's molecular marker expression and arborization pattern within the neuropil at around late-stage embryos and 1st instar larvae.*Cont'd* 158

5.1 Type I division of neuroblasts within the Drosophila larval nerve cord. 166
5.2 Notch∧intra misexpression in NB7-1 increases the number of neurons with NotchON molecular markers at the expense of NotchOFF molecular markers. 169
5.3 Notch∧intra misexpression in NB7-1 permanently increases the number of synaptic branches onto the NotchON U motor neuron muscle targets. 175
5.4 Notch∧intra misexpression in NB7-1 permanently increases the number of synaptic branches onto the NotchON VO motor neuron muscle targets. 176
5.5 Numb-GFP misexpression in NB7-1 has no impact on molecular marker expression in late-stage embryos. 179
5.6 Notch∧intra misexpression in NB7-1 impacts Eve+ U motor neuron cell body position along the medial-lateral axis. 183
5.7 Possible Eve+ U motor neuron migration pattern during embryogenesis. 188
5.8 Previously published data suggesting that NotchOFF siblings may influence the migration of the NotchON sibling. 192

5.9 Evidence that the Dbx+ sibling neurons of the Eve+ U motor neurons are not Repo+ glial cells. 197
5.10 Characterization of the position of small undifferentiated neurons in the A1 segment of the 1st instar larval CNS EM volume. 198

6.1 Loss of Hb9 and Nkx6 does not impact permanent motor neuron to muscle synaptic partnership decisions 210
6.2 ISNb nerve outgrowth in late-stage embryos. 213
6.3 In hb9 nkx6 mutants, there is no change in the permanent synaptic partnership decisions of thoracic motor neurons onto mouthook-related muscles. 218
6.4 Misexpression of Eve in Hb9+ motor neurons permanently reduces the number of type 1b and 1s motor neuron-to-muscle synaptic branches onto ventral muscles. 222
6.5 Characterization of the Hb9 driver. The image is of the full length of a nerve cord in a late-stage embryo (E16/17). 224
6.6 Misexpression of Eve in Hb9+ motor neurons permanently increases the number of type 1b and 1s motor neuron-to-muscle synaptic branches onto dorsal muscle 4. 225
6.7 Misexpressing Eve in neurons that are normally Hb9+ variably represses endogenous Hb9+ expression. 226

7.1 APEX-GFP expression in 1st instar larval nerve cords when driven by the NB7-1 driver 240
7.2 Possible APEX-mediated reaction product accumulation in neuronal cell bodies 242
7.3 Possible APEX-mediated reaction product accumulation in neuronal cell bodies of serial section taken by Gregg Wildenberg 243
7.4 Schematics for EM protocol 248
7.5 EM images obtained when Julia prepared samples using the provided protocol . 249

8.1 larval crawling speed behavior 251
8.2 NB3-1 driver 255
8.3 NB7-1 driver 256
8.4 Misexpressing constitutively activated form of Hunchback, VP16::Hb can only lead to an average of 5 Hb+, Eve+ neurons at L3 regardless of the number of Eve+ neurons generated. 259
8.5 Misexpressing constitutively activated form of Hunchback, VP16::Hb transiently in U motor neuron GMC precursor and U motor neurons during early development can lead to endogenous expression of Hb in ‘U3’ but not impact permanent synaptic partnership with dorsal muscle targets. 264

10.1 Diagram of adult flight muscles part I 281
10.2 Diagram of adult flight muscles part II 282
10.3 Protocol for dissecting, fixing, and staining the adult thorax 283
10.4 Matching L3 bodywall segments to nerve cord hemisegments 285

LIST OF TABLES

3.1 Source Data for Figure 3.27 127
3.2 Source Data for Figure 3.28 128

4.1 Source Data for Figure 4.1 163
4.2 Source Data for Figure 4.4 164

5.1 Source Data for Figure 5.2 202
5.2 Source Data for Figure 5.3 203
5.3 Source Data for Figure 5.4 204
5.4 Source Data for Figure 5.6 205

6.1 Correlation between molecular marker expression and synaptic connectivity decisions. Note, both tables are sub-tables within this table 232
6.2 Source Data for Figure 6.1 233
6.3 Source Data for Figure 6.2 234
6.4 Source Data for Figure 6.4 235
6.5 Source Data for Figure 6.6 236

8.1 Source Data for Behavior data in 8.1 254
8.2 Source Data for Figure 8.4 258
8.3 Source Data for Figure 8.5 265

ACKNOWLEDGMENTS

Thank you Ellie for your abounding optimism, support, and mentorship. Your excitement and wonder of the Drosophila motor system is what drew me to the field of developmental neurobiology. Thank you to all of the Heckscher lab members (former and current), the devneuro super group, and the 9th floor fly community for being wonderful colleagues. I want to thank my entire thesis committee: Ed Munro, Ilaria Rebay, Chip Ferguson, and Xiaoxi Zhuang for their feedback and support throughout my thesis journey. Thank you to my funding sources: National Institute of General Medical Sciences (T32 GM007183) and the National Science Foundation (DGE-1746045)

Words cannot express the gratitude and thankfulness I have for my best friend and husband, Kyle Lathem. You are the secret sauce for keeping me balanced and productive, particularly during graduate school. Even though I often did not heed your advice, thank you for gently encouraging me to rest more and have a more positive view of myself. You have been my biggest cheerleader throughout my PhD journey. Thank you for eagerness and excitement when it comes to talking about science, philosophy, and life. I am so lucky to have you by my side. Franzl, my furbabe, thank you for the countless hours you have spent nestled next to me while I worked late into the evening hours.

Last but not least, I want to thank the rest of my family. Thank you to my parents Jonathan and Ruth Meng who imparted upon me their hard work ethic and independence. Thank you to my twin Daniel and sisters Joy and Catherine, along with my siblings-in-law Jerissa, Jonas, and Alex. You are all so wonderful and have so many amazing talents. I thank my parent-in-laws, Laura and John for their kindness. Thank you to my cousin Yana, Aunt Reni, and Aunt Debbie for being so good to me.

ABSTRACT

How circuits assemble starting from stem cells is a fundamental question in developmental neurobiology. Dynamic gene expression in stem cells contribute to molecular diversity of neuronal progeny. Morphology and synaptic connections of neurons are important for circuit organization and function. However, less clear is the relationship between molecular diversity and the specification of neuronal morphology and synaptic partnerships. Here, I tested the hypothesis that dynamic gene expression in neural stem cells is a general strategy underlying neuronal integration into circuits. To do so, I used the Drosophila larval motor system. This system offers unparalleled resolution of neural stem cells as well as neurons at single-cell and -synapse resolution. The Heckscher lab discovered that neuronal birth time and circuit membership are correlated (Wreden et al., 2017)[1]. This finding implies that time-linked information plays an instructive role for circuit membership. At the time of birth, neurons receive information from two sources: intrinsic –inherited from their stem cell parent and extrinsic –cues from their environment. As development progresses, intrinsic and extrinsic cues change simultaneously. To uncouple intrinsic cues from developmental time in stem cells, I specifically manipulated dynamically-expressed transcription factors called temporal factors. Temporal factors act in Drosophila stem cells (neuroblasts), to specify embryonic molecular marker expression in neuronal progeny. Using genetic approaches, I altered the temporal dynamics of transcription factor expression in a neuroblast lineage-specific manner. Then, I performed neuromuscular dissections, single-cell tracing, labeling with marker genes, confocal imaging, electrophysiology (in collaboration), and calcium imaging to examine motor neuron morphology and synaptic connectivity (Meng et al., 2019; 2020)[2, 3]. I found that temporal transcription factors acting in neuroblast are potent regulators of functional motor neuron-to-muscle synaptic partnerships, but that the local local synaptic environment can also influence synaptic partnerships. Further, my data revealed that molecular markers used to assess embryonic neuronal fate do not faithfully correlate with motor neuron to

muscle synaptic partnerships. Altogether, my data demonstrates that intrinsic information strongly influences circuit assembly decisions. Next, since the environment greatly differs in the bodywall muscle periphery vs the CNS I characterized the dendrite morphology of single motor neurons and interneurons within the larval CNS. Here, I found evidence that intrinsic information strongly influences motor neuron dendrite morphology (Meng et al., 2019)[2], but may have less of an impact on interneuron dendrite morphologies (unpublished, work in progress). This suggests, there are likely differences in strategies underlying synaptic partnership decisions in the periphery versus the CNS. To understand these differences, future research will need to obtain single-synapse resolution of synaptic partnerships formed within the CNS. To further elucidate intrinsic molecular programs specifying motor neuron to muscle synaptic partnership decisions, I manipulated other intrinsic, early acting factors (e.g. Notch, Hb9, and Eve). These unpublished experiments further support the hypothesis that inherited information from neural stem cell parents is likely a general strategy underlying neuronal integration into circuits. More broadly, strategies underlying motor circuit assembly identified in the Drosophila larval system are likely repeated throughout the Animal Kingdom where motor circuits are essential for locomotion.

CHAPTER 1

INTRODUCTION

In this chapter, I borrow text and figures I previously wrote and created for a published review [4].

1.1 Introduction

Every time you move, feel a touch, or sense your body move, you rely on the activity of neurons in your spinal cord. These neurons are organized into motor circuits. When motor circuits are dysfunctional or develop abnormally this can lead to debilitating perceptual abnormalities such as allodynia, or movement disorders like paraplegia (Zeilig et al., 2012)[5]. Understanding how motor circuits develop is a fundamental question in developmental neurobiology, which has implications for various fields including robotics, evolution, and medicine.

Motor circuit development starts with neurogenesis and culminates with the assembly of functional motor circuits. Motor circuit assembly is a multi-step process. First, neuronal stem cells divide to generate neurons. These neurons inherit gene expression from their stem cell parent. Then dendrites and axons must navigate through a dynamic, three-dimensional space; dendritic and axonal arbors must be elaborated; neurotransmitter phenotypes must be established; electrical properties must be acquired, and synaptic partnerships must be formed. Each of these events represents a key developmental decision that every neuron must make. The field of developmental neurobiology seeks to understand the cellular and molecular processes that control these motor circuit assembly decisions.

In the past, neuronal stem cells were studied for their role in generating the large diversity of neurons found in the motor system. Specifically, in my thesis, I address the question: to what extent are the decisions that occur during motor circuit assembly controlled by the

same information that generates a large diversity of neurons from a relatively small pool of neuronal stem cells?

1.2 Motor Circuits

Motor circuits are unique from circuits found elsewhere in the CNS. They are the only circuits able to generate movement. Motor circuits are also unique in that they are required to detect and process multiple different types of somatosensory stimuli in parallel. For example, they can simultaneously detect touch, heat, and even light (exteroception) as well as self-movement (interoception) (Koch et al., 2018; Kohsaka et al., 2017; Im and Galko, 2012)[6, 7, 8].Anatomically, motor circuits are composed of three fundamental neuron types. 1) Motor neurons send axons from the CNS and control the activity of muscles (Stifani, 2014)[9]. Patterned muscle activity moves animals. 2) Sensory neurons have dendrites in the periphery. Sensory neurons directly detect somatosensory stimuli (Abraira and Ginty, 2014)[10]. 3) Interneurons have both dendrites and axons within the CNS. In the motor system of many organisms, interneurons are by far the most abundant neuron type, and often interneurons are the most morphologically and functionally diverse (Bikoff, 2019; Osseward and Pfaff, 2019)[11, 12]. However, due to their relative experimental inaccessibility interneurons are the least well-understood neuron type in motor circuits.

Conceptually, motor circuits are fundamental functional modules. That is, each circuit performs a specific computation. One motor circuit can be disrupted without perturbing the function of other motor circuits (Clark et al., 2016)[13], and individual motor circuits can be combined in different ways to generate complex outputs (Masson et al., 2020; Ohyama et al., 2015; Blitz and Nusbaum et al., 2012)[14, 15, 16]. Historically, motor circuits were studied using sharp electrodes in aquatic animals with large neuronal bodies, such as leech, lamprey, and lobster (Marder and Bucher, 2001; Friesen et al., 1976)[17, 18]. These animals are long-lived and therefore are not good genetic models. Consequently, our understanding

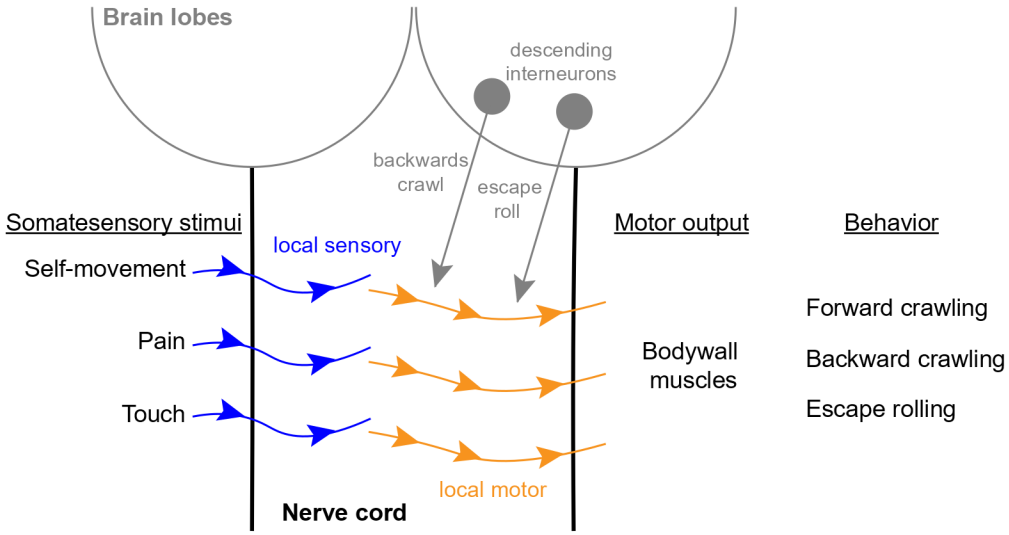


Figure 1.1: Anatomical and functional definition of motor circuits. Illustration of the Drosophila larval nerve cord (black) and motor circuits (depicted as lines with nodes representing direction of circuit information flow). Sensory processing circuits, in blue to the left, relay somatosensory stimuli such as self-movement, pain, and touch. Motor circuits, in yellow to the right, can receive input from sensory neurons or descending neurons from the brain. Motor circuits control the patterned activity of bodywall muscles, which in turn generate patterned behaviors such as forward crawling, backward crawling, and escape rolling.

of motor circuit assembly was extremely limited. In recent years the developmental genetic model, Drosophila, has become a prominent model to identify and study the function of motor circuits (Clark et al., 2018; Tastekin and Louis, 2017)[19, 20]. This has been enabled by technological innovation—highly specific driver lines (Manning et al., 2012; Li et al., 2014; Jenett et al., 2012; Pfeiffer et al., 2008)[21, 22, 23, 24], genetically-encoded calcium indicators (Dana et al., 2019; Vaadia et al., 2019)[25, 26], optogenetics (Simpson and Looger, 2018)[27], and connectomics (Schneider-Mizell et al., 2016)[28]. Now, many motor circuits have been identified at cellular and synaptic resolution. Some motor circuits generate patterned forward and reverse crawling (Kohsaka et al., 2019; Zarin et al., 2019; Takagi et al., 2017; Kohsaka et al., 2017; Fushiki et al., 2016; Kohsaka et al., 2012)[29, 30, 31, 7, 32, 33]. These circuits can generate crawling or crawling-like motor neuron firing patterns without input from the central brain (Berni et al., 2012)[34] or input from sensory neurons (Pulver et al. 2015;

Lemon et al., 2015)[35, 36] (Figure 1.1). Motor circuits in the nerve cord can be controlled by neurons descending from the central brain such as Goro neurons for escape movement or MDN neurons for backward crawling (Figure 1.1) (Carreira-Rosario et al., 2018; Namiki et al., 2018)[37, 38]. Other circuits in the Drosophila nerve cord include those that process different types of somatosensory stimuli (e.g. noxious stimuli, proprioceptive stimuli, light touch, etc.) (Figure 1.1) (Heckscher et al., 2015; Ohyama et al., 2015; Jovanic et al., 2019; Miroschnikow et al., 2018; Tastekin et al., 2018; Burgos et al., 2018; Babski et al., 2019)[39, 15, 20, 40, 41, 42, 43]. These sensory processing circuits relay somatosensory information to other nerve cord circuits or to the central brain. One of the first circuits to be identified in the Drosophila nerve cord contains a set of Even-skipped Lateral neurons (ELs) (Heckscher et al., 2015)[39]. This EL circuit maintains left-right symmetrical muscle contraction during Drosophila larval crawling. Notably, when ELs are ablated many aspects of movement are normal, such as the timing of muscle contraction. Thus, even without ELs other circuits still function normally, demonstrating the modular nature of motor circuits. Ultimately, the identification of motor circuits in Drosophila larvae has opened the door for study of their assembly using a powerful developmental genetic toolkit.

1.2.1 Drosophila larva motor neuron circuit membership defined by muscle groups

The Drosophila motor system is organized into anterior-posterior repeated, left-right symmetrical hemisegements (Figure 1.2A). Each hemisegment contains about 300 neurons, 32 of which are motor neurons (Ohyama et al., 2015)[15]. Nearly each motor neuron innervates a unique bodywall muscle in a 1:1 fashion (Landgraf et al., 1997; Schmid et al., 1999; Menon et al., 2013; Zarin et al., 2019)[44, 45, 46, 30]. Each bodywall segment contains 30 muscle cells, which are organized into three main groups—dorsal, transverse, and ventral. Each muscle group is controlled by a unique circuit (Heckscher et al., 2012)[47], and populating

each circuit are non-overlapping sets of motor neurons. Importantly, by late larval stages Drosophila motor neuron-to-muscle synapses are large, experimentally accessible, and extremely well-characterized. For these reasons, I used the Drosophila neuromuscular junction (NMJ) as a system to understand how motor neuron to muscle synaptic partnership decisions are specified in development. While the bulk of my work focuses on circuit-relevant fate features made in the peripheral nervous system, using sparse neuron labeling approaches, I was able to interrogate circuit-relevant fate features at the level of neurite and arborization morphology of motor neuron dendrites and interneurons within the 1st instar larval nerve cord. (Meng et al., 2019)[2] (See NB7-1 interneuron chapter).

1.3 Neuronal stem cells in the motor system

Neuronal stem cells, like other stem cells, divide asymmetrically to self-renew and to generate a daughter that will go on to make a post-mitotic neuronal cell (Knoblich, 2010)[48]. Neuronal stem cells change their potency over time, such that at different points in development the same stem cell produces different neurons. The set of neurons generated from a single neuronal stem cell is referred to as a lineage (Figure 1.2C). Lineages are stereotyped from animal to animal and are composed of sets of non-identical neurons (Hartenstein and Stollewerk, 2018)[49]. Neuronal stem cell lineages can be considered fundamental developmental units of the nervous system.

In Drosophila, neuronal stem cells are called "neuroblasts". Nerve cord neuroblasts are among the most-intensely studied and best-characterized neuronal stem cells in the field (Birkholz et al., 2015; Birkholz et al., 2013; Broadus et al., 1995; Goodman and Doe, 1993)[50, 51, 52, 53]. The Drosophila nerve cord is composed of repeating segments along the anterior-posterior (A-P) axis (Figure 1.2A) (Technau et al., 2014)[54]. Segmentally repeating units are morphologically and functionally similar. Each segment can be further broken down into left-right symmetrical hemisegments that are separated by the midline (Figure 1.2A).

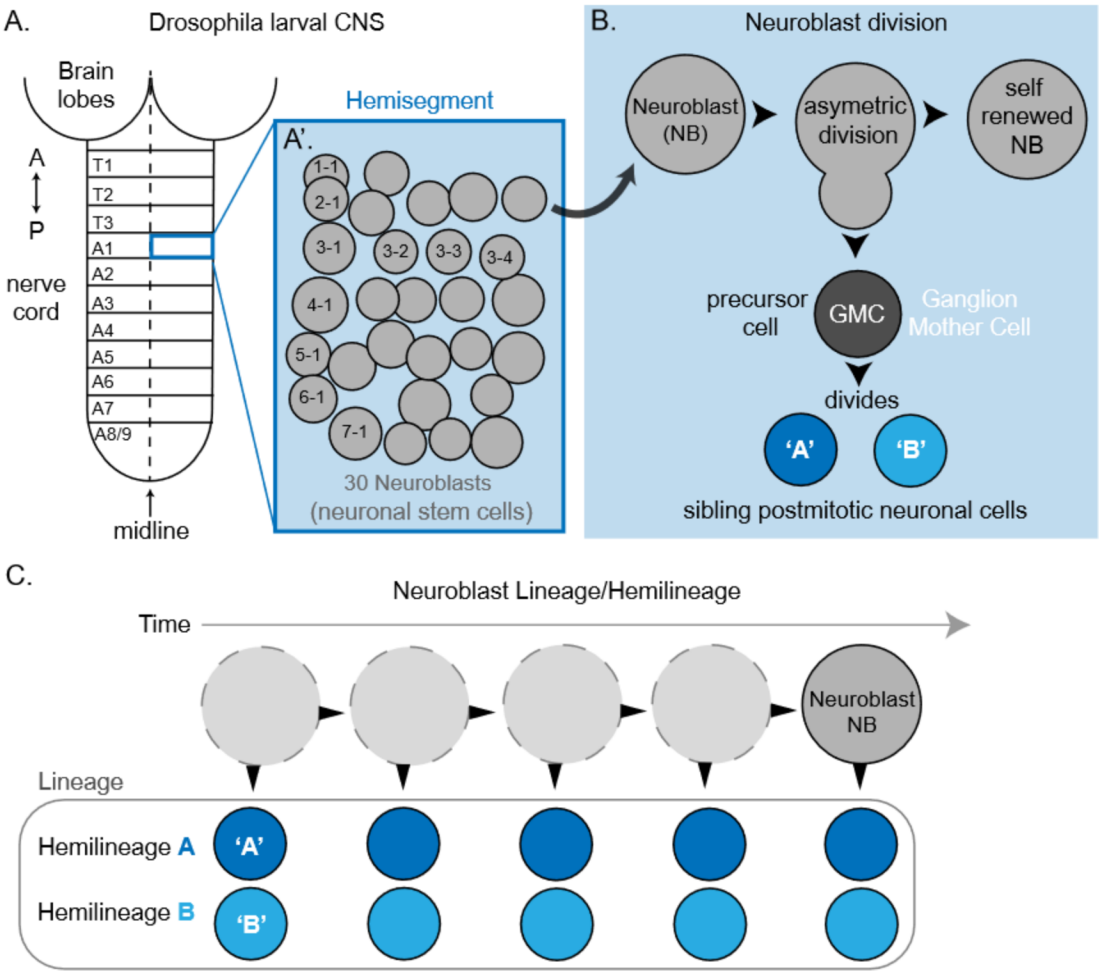


Figure 1.2: Developmental organization of neuronal stem cell lineages (**A**) Illustration of the Drosophila larvae Central Nervous System. The nerve cord is composed of repeating segments along the anterior–posterior (A–P) axis. There are three thoracic segments (T1–T3), seven abdominal segments (A1–A7), and two terminal segments (A8/9). Each segment can be further broken down into left-right symmetrical hemisegments that are separated by the midline (dotted line). (A') Illustration of a hemisegment, which contains the same 30 neuronal stem cells called neuroblasts (NB), in gray. Each neuroblast is numerically named based on stereotyped row and column position (e.g., NB in row "1" and column "1" is named "1-1"). (**B**) Illustration depicting that neuroblasts divide asymmetrically to selfrenew. Asymmetric divisions can generate precursor cells, dark gray, called a Ganglion Mother Cell (GMC) that generates two sibling postmitotic neuronal cells, "A" and "B."(**C**) Illustration of a single dividing Neuroblast over time, lighter gray circles with a dashed perimeter represent the Neuroblast at previous time points. The "A" and "B" neurons born from GMCs populate separate hemilineages A and B, respectively.

Each hemisegment contains the same 30 neuroblasts (Figure 1.2A') (Broadus et al., 1995; Doe, 1992)[52, 55]. During embryogenesis, one set of 30 neuroblasts generates approximately 300 neurons (Schmidt et al., 1997; Heckscher et al., 2015; Ohyama et al., 2015; Bossing et al., 1996)[56, 39, 15, 57], each of which is thought to have a unique morphology (Rickert et al., 2011; Bossing and Technau, 1994; Bossing et al., 1996; Schmid et al., 1999; Schmidt et al., 1997)[58, 59, 57, 45, 56]. Neurons produced during embryogenesis from nerve cord neuroblasts populate larval motor circuits.

In the Drosophila nerve cord, neuroblast lineages are often subdivided into two hemilineages. Hemilineages have been suggested to be an organizational unit of motor circuits. In the nerve cord, neuroblasts often divide asymmetrically to self-renew and bud off a ganglion mother cell (GMC) (Figure 1.2B) (Goodman and Doe, 1993)[53]. The GMC divides once to produce two post-mitotic daughter cells (Figure 1.2B). One of the two GMC daughters will become an 'A' cell and will become part of the A hemilineage. The other GMC daughter will become a 'B' cell and will populate the B hemilineage (Figure 1.2C) (Truman et al., 2010)[60]. In the adult Drosophila nerve cord, a comprehensive study showed that activation of distinct hemilineages of neurons generate distinct motor behaviors, with a majority of behaviors being unique (Harris et al., 2015)[61]. Behavior was used as a proxy for underlying circuit configuration. Notably, caution must be taken to avoid over-interpreting circuit structure from behavior. Nonetheless, this study supports the idea that hemilineages produce groups of neurons that occupy specific motor circuits. Thus, a currently held view in the field is that neuroblast lineages can be considered fundamental developmental units of the motor system and also fundamental functional units of motor circuits.

1.4 From neuronal diversity to motor circuit assembly

Historically, the stem cell field has focused on understanding how early events in neurogenesis generate a diversity of different types of neurons (Pearson and Doe, 2004; Jessell,

2000)[62, 63]. In the past, the terms neuronal diversity, neuronal fate, and neuronal identity have been used nearly interchangeably. Here, we will use the term identity to refer to all three. Past studies have provided a wealth of information regarding molecular programs that contribute to diverse neuronal identities (Doe, 2017)[64]. In this review, we divide these molecular programs into four classes: 1) Anterior-posterior diversity is regulated by Hox transcription factors (Figure 1.3A) Estacio-Gómez and Díaz-Benjumea, 2014)[65]. 2) Within a single hemisegment, neuroblasts become different from each other based on Spatial patterning transcription factors (Figure 1.3B) (Skeath and Thor, 2003; Skeath, 1999)[66, 67]. 3) Over time, a single neuroblast can generate a diversity of neuronal identities (Figure 1.3C) (a.k.a., temporal identities), which is regulated by the activity of Temporal transcription factors (Figure 1.3C') (Isshiki et al., 2001; Pearson and Doe, 2003; Grosskortenahus et al., 2006; Tran and Doe, 2008)[68, 62, 69, 70]. 4) An additional layer of diversity is achieved at the level of GMC daughter cells by Notch signaling (Figure 1.3C") (Skeath and Doe, 1998; Truman et al., 2010)[71, 60]. Thus we have a basic framework for understanding how neuronal diversity is generated.

In the past, neuronal identity has been measured by many criteria—embryonic neuronal gene expression, gross anatomical features, neurotransmitter expression, and physiological properties (Rickert et al., 2018; Lacin and Truman, 2016; Allan and Thor, 2015)[72, 73, 74]. A major gap in our knowledge, however, is that these definitions of identity are largely unlinked to mature neuronal features like presynaptic and postsynaptic partnerships, dendrite morphologies, neuronal firing patterns, or roles in behavior. The field needs to include mature neuronal features in the definition of neuronal identity if it hopes to link knowledge about the generation of neuronal diversity to motor circuit assembly. A major current focus of the field is to precisely define how regulators of neuronal identity impact circuit relevant fate features of neurons and ultimately their integration into motor circuits. Understanding how neurons integrate into circuits will shed light onto the underlying logic of motor circuit

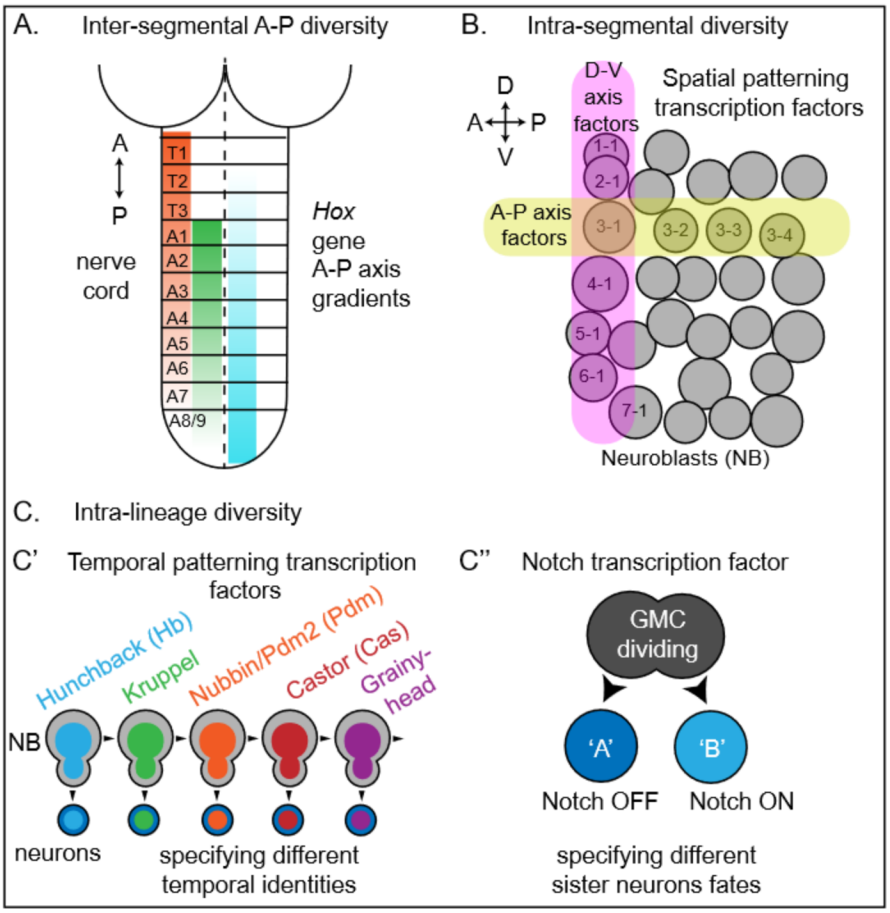


Figure 1.3: Molecular programs contributing to diverse neuronal identities (**A**) Illustration of representative Hox gene gradients, different colored bars, along the A-P axis of the Drosophila larval nerve cord. (**B**) Illustration of representative neuroectoderm spatial transcription factors expressed along the A-P axis, green bar, and D-V axis, pink bar. The intersection, pink and green overlayed, of these spatial transcription factors specify neuroblast identity. (**C**) Illustration of intra-lineage diversity factors. (**C'**) Illustration of a single neuroblast (NB) dividing and expressing a series of temporal patterning transcription factors called temporal transcription factors, labeled and color coded, found in most, if not all, neuroblasts. Neuronal progeny inherit temporal transcription factor expressed during division. (**C"**) Illustration of a GMC dividing to produce two sibling neuronal cells, where one is Notch ON whereas the other is Notch OFF. Notch ON/OFF promotes different molecular fates in the sibling cells.

assembly.

1.5 Why is neuron birth timing an important factor in motor circuit assembly?

Once stem cell to circuit relationships are identified, the next step in understanding circuit assembly is to identify the underlying cellular and molecular mechanisms that give rise to these relationships. The identification of temporal cohorts as an organizational unit of Drosophila motor circuits revealed a correlation between neuronal birth timing, within a single neuroblast lineage, and neuronal circuit membership. This finding raised the question of how those relationships are established. During stem cell division, there are several simultaneously changing factors that could influence the circuit membership of the resulting neuron. One factor is the dynamic, instructive environment—earlier-born neurons and later-born neurons might encounter different physical substrates or receive different signaling cues. A second factor is that earlier-born neurons have more time for cell biological processes to occur, such as axon outgrowth. Third, the chromatin landscape within the nucleus of a neuronal stem cell can change over time. Finally, earlier-born and later-born neurons have different molecular profiles, which are controlled by temporal transcription factors. Determining the precise role of each factor associated with neuronal birth time is crucial for understanding how motor circuits assemble.

CHAPTER 2

TEMPORAL COHORTS

In this chapter, I borrow text I previously wrote for a published review (Meng and Heckscher, 2021)[4]. For clarity, thoroughness, and to present my most up-to-date view, I expand on what I previously wrote in my published review. The following section is entirely new and a launch point for future experiments: Atlas linking motor neuron lineage/hemilineage identity to muscle groups to reveal putative novel motor neuron temporal cohorts and more avenues for future projects

2.1 Introduction

A required first step in understanding how motor circuits arise from neural stem cells is to describe the circuit membership of neurons from a given stem cell lineage. A major concept that emerged from the Heckscher lab at around the time I joined the group are temporal cohorts, which are defined by three criteria. Temporal cohorts are sets of neurons that come from one neuronal stem cell, are contiguously born, and have similar function at the circuit level (Figure 2.1). This concept emerged from investigating the relationship between birth time and circuit membership of the NB3-3's Even-skipped (Eve)+ EL interneurons (Wreden et al., 2017)[1]. I am dedicating a whole chapter to the concept of temporal cohorts because it not only motivated my thesis project but from my project, I am confident we have identified more examples of temporal cohorts, further solidifying this concept as a useful framework when thinking about the relationship between neuroblast lineages and motor circuit assembly in the developing Drosophila larva motor system. There is also evidence to strongly suggest that the concept of temporal cohorts extends beyond Drosophila.

2.2 NB3-3 generates early-born EL and late-born EL temporal cohorts

In the Drosophila larval nerve cord, a pioneering study used the neuroblast NB3-3 lineage as a model to investigate the relationship between neuronal stem cell lineages and motor circuits (Wreden et al., 2017)[1]. NB3-3 generates a single motor neuron followed by a series of interneurons characterized by the expression of the transcription factor Even-skipped (Eve) and a lateral cell body position in the nerve cord (Figure 2.1B) (Schmid et al., 1999)[45].

These interneurons are called "ELs" (Fujoka et al., 1999; Wreden et al., 2017)[75, 1], showed that ELs could be split into early-born and late-born sets of neurons based on the expression of an enhancer called 11F02 (Wreden et al., 2017)[1]. For each set of ELs, circuit membership was assessed anatomically and functionally. Optogenetic activation of early-born ELs triggered escape rolling behavior, and optogenetic activation of late-born ELs resulted in abnormal left-right crawling. Connectomic data showed at least a subset of early-born ELs receive synapses directly and indirectly from chordotonal (sound/vibration sensitive) sensory neurons, and late-born ELs received synapses directly and indirectly from proprioceptive sensory neurons (Wreden et al., 2017; Heckscher et al., 2015; He et al., 2019)[1, 39, 76]. For my rotation project, I used calcium imaging as a readout for EL activity in response to a sound stimuli mimicking wasp buzz. Using Calcium imaging we confirmed that only early-born ELs were activated by sound stimuli, which activate chordotonal sensory neurons (Figure 2.2).

Taken together, this study demonstrated that NB3-3 generates ELs that contribute to two circuits. Early-born ELs populate a fast escape circuit that processes chordotonal input, and late-born ELs populate a circuit that refines movement and processes proprioceptive stimuli (Figure 2.1B). In both circuits, ELs are somatosensory processing interneurons. Thus, it appears that the NB3-3 lineage endows ELs with the capacity to process sensory information regardless of circuit Identity and information associated with neuronal birth-timing segre-

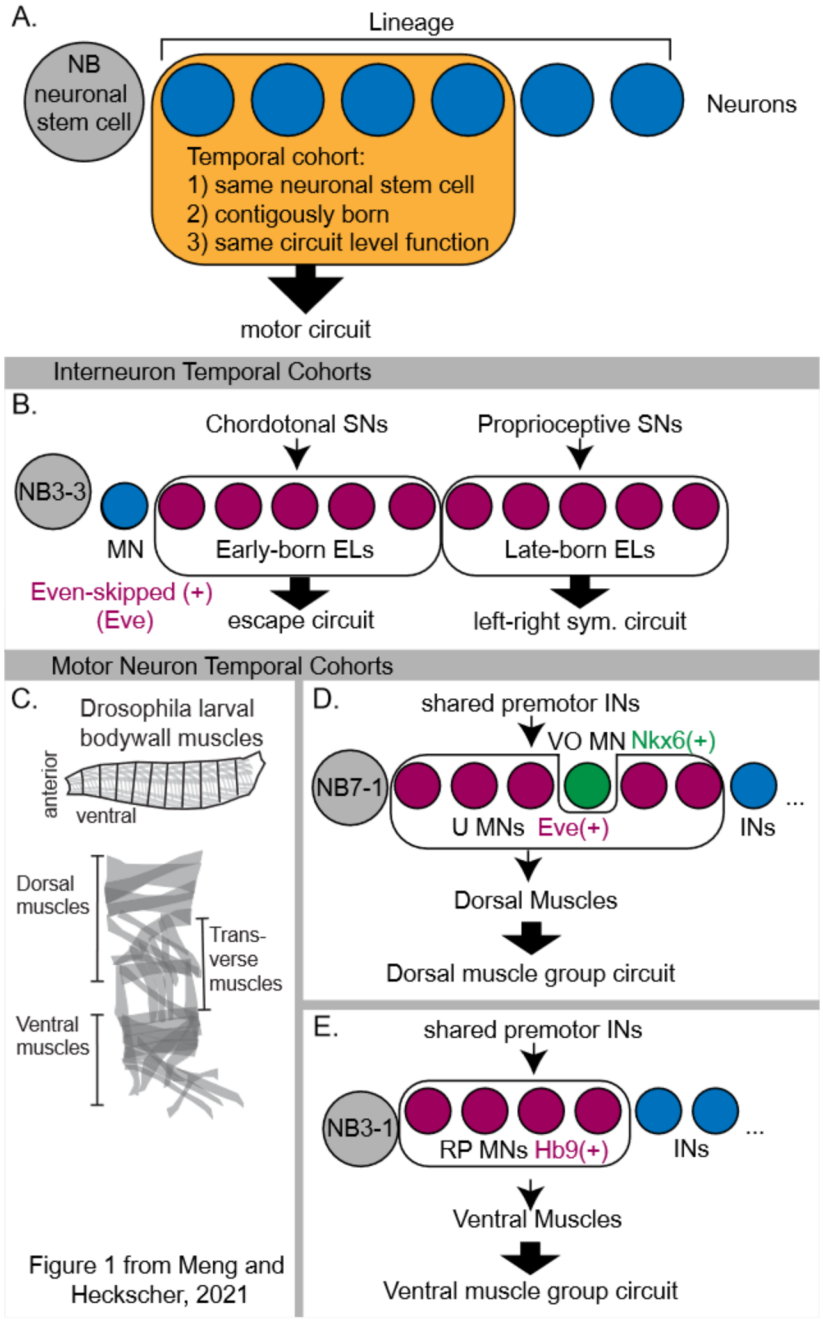


Figure 2.1: Temporal cohorts are an organizational unit linking neuronal stem cell lineages to motor circuit membership (**A**) Illustration depicting the criteria that must be met for a group of neurons to be considered a temporal cohort. (**B**) Illustration of the NB3-3 lineage, which after producing a single motor neuron, generates an Eve(+) early-born EL and late-born EL temporal cohorts. *Continued*

Figure 2.1: *Cont'd.* Temporal cohorts are an organizational unit linking neuronal stem cell lineages to motor circuit membership.(**C**) Illustration of the Drosophila larvae body wall musculature. Each body wall hemisegment contains 30 muscles. Each muscle is organized into three anatomical and functional groups: dorsal, transverse, and ventral.(**D**) Illustration of the NB7–1 lineage, which generates the Eve(+) U motor neurons, Nkx6(+) VO motor neuron, and a number, denoted by "...," of interneurons. The U motor neuron temporal cohort is not contiguously born because it is disrupted by the recently discovered VO motor neuron, which projects to the ventral oblique muscles, yet also shares premotor INs with several U MNs. (**E**) Illustration of the NB3-1 lineage, which generates the Hb9(+) RP motor neurons followed by a number, denoted by "...," of interneurons.

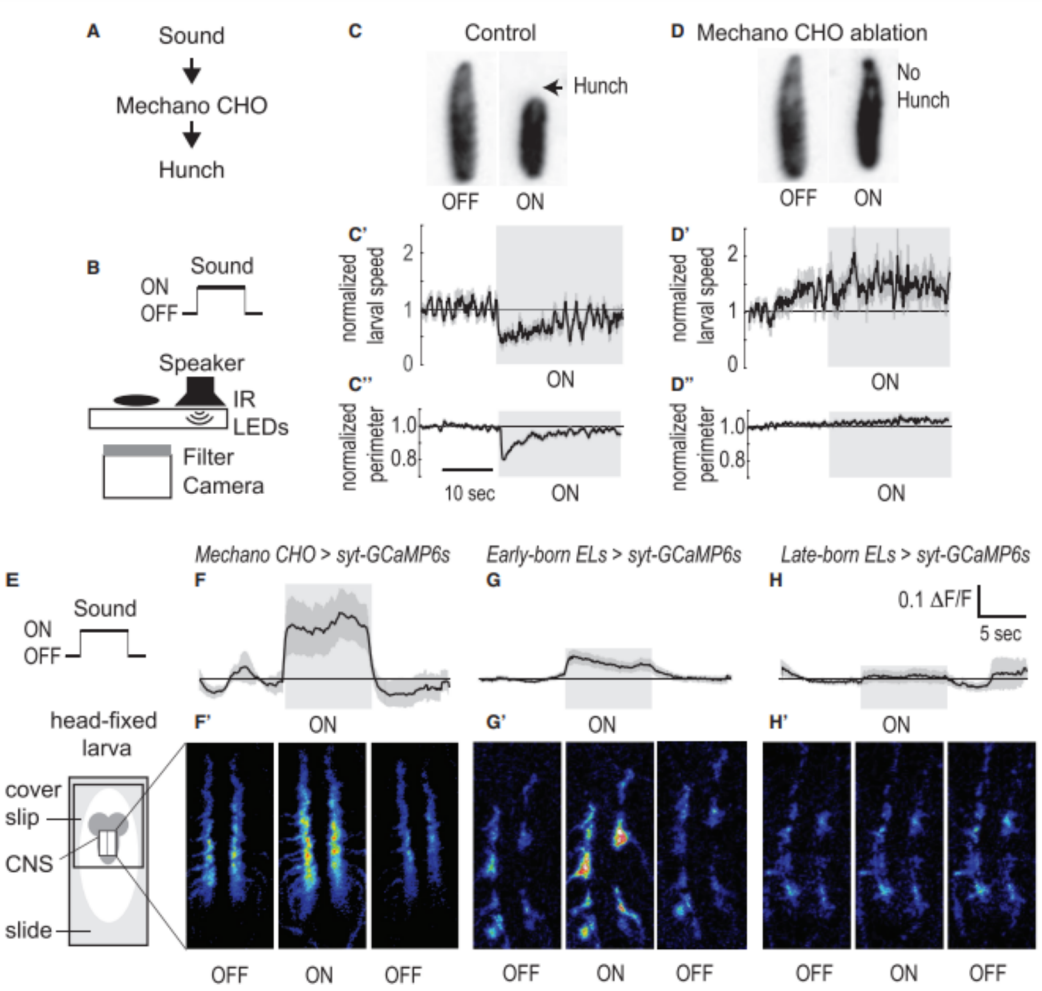


Figure 2.2: Early-Born and Late-Born ELs Differentially Respond to Sound (**A**) Sound/vibration activates mechanosensitive chordotonal sensory neurons (Mechano CHOs) and causes larval hunching. *Continued*

Figure 2.2: *Cont'd.* (**B**) Behavioral arena used to record responses to stimulus (Sound ON, gray in C and D, and F and H). (**C and D**) Larvae hunch upon sound/vibration only when CHOs are present. Larvae before (left) or during (right) sound/vibration. Anterior up, head-to-tail larval length 3.5 mm (C and D). Average (± SEM) larval speeds normalized to pre-stimulus speed (C' and D') or larval perimeter normalized to pre-stimulus perimeter (C" and D"). Genotypes were as follows: control (C; n = 14), UAS-RPR, UAS-HID/+ ; R11F02-DBD/+ ; and CHO ablation (D; n = 11), UAS-RPR, UAS-HID/+ ; IAVGAL4/+. See Movie S2 and Audio S1.(**E**) The stimulus was played to a larva with the anterior portion, containing the CNS, immobilized and the posterior free.(F–H) Neuronal activity was monitored with GCaMP6s. Average (± SEM) change in fluorescence (DF/F) over time is shown, scale in H (F–H). Example responses to sound stimulation (F0 and H0). Fluorescence in pseudo color, red = maximum, blue = minimum. Anterior up; box width 72 mm. Genotypes were as follows: CHOs (F; n = 11), IAV-GAL4/UAS-syt-GCaMP6s; early-born ELs (G; n = 25), UAS-FLP, actin-FRT-stop-FRT-GAL4/+; R11F02-GAL80/UAS-syt-GCaMP6s; EL-GAL4/+;and late-born ELs (H; n = 17), UAS-FLP, actin-FRT-stop-FRT-GAL4/+; EL-AD/UAS-syt-GCaMP6s; R11F02-DBD/+.

gates ELs into different circuits. Assembling motor circuits according to these rules provides a developmental mechanism for generating motor circuits able to process different types of sensory stimuli in parallel.

Wreden et al. was the first study to suggest that lineage-related neurons could be subdivided into temporal cohorts. To put this finding into context, it has been known for many years that there can be abrupt changes during lineage progression with respect to some neuronal features, such as morphology, gene expression, and neurotransmitter phenotype. For example, during lineage progression a neuroblast can abruptly change from producing projection interneurons to producing local interneurons (Schmid et al., 1999) [45], or from producing Eve(+) to Eve(-) neurons (Pearson and Doe, 2004)[62]. The observation that lineages can be organized into temporal cohorts demonstrated that there can also be abrupt changes in the types of synaptic partnerships formed by neurons in a lineage. Of note, temporal cohort borders cannot necessarily be predicted based on differences in other features such as gene expression. This is illustrated by the example of ELs, which all share Eve marker expression yet contribute to two distinct circuits.

2.3 Motor neuron temporal cohorts in Drosophila larvae

There are also known examples of motor neuron temporal cohorts. In Drosophila larvae, in each hemisegment there are 30 glutamatergic motor neurons that can be divided into two types. There are 28 type Ib motor neurons with big boutons innervate the 30 bodywall muscles in a near 1:1 fashion (Landgraf et al., 1997; Schmid et al., 1999; Menon et al., 2013; Zarin et al., 2019)[44, 45, 46, 30]. In each hemisegment there are 2 type 1s motor neurons with small boutons that innervate the dorsal and ventral muscle fields, respectively (see Non-type Ib motor neuron group (Figure 2.3)). The remaining 4 motor neurons (type II and III) are modulatory and do not use glutamatergic. Here, I will only discuss glutamatergic motor neurons, because they are required for normal locomotion and the type Ibs greatly contribute to excitatory postsynaptic potentials (EPSPs), which if strong enough initiate action potential causing muscle contraction.

Body wall muscles are organized into three anatomical and functional groups—dorsal, transverse, and ventral (Figure 2.1C) (Snodgrass, 1935; Bate, 1993)[77, 78]. Each muscle group is driven by a unique motor circuit (Heckscher et al., 2012)[47]. Therefore, sets of motor neurons that synapse onto muscles in each group share circuit membership. I want to acknowledge that our understanding of defining muscle groups based on firing unison is evolving and is something being pursued in the Heckscher lab and others (Zarin et al., 2019)[30]. Therefore, future work will likely uncover unique combinations of muscles involved in specific motor circuits. This information will undoubtedly update our understanding of current putative motor neuron temporal cohorts.

To date, we have identified unique temporal cohorts that innervate dorsal and ventral muscle groups, respectively. Dorsal and ventral muscle groups are innervated by motor neuron temporal cohorts. For the ventral muscle group, NB3-1 generates four consecutively born, RP motor neurons (RP1, RP4, RP3, RP5) (Figure 2.1E) (Tran and Doe, 2008)[70]. Single neuron labeling shows each RP motor neuron forms unique and stereotyped synapses

onto a ventral muscle (Landgraf et al., 1997; Choi et al., 2004; Zarin et al., 2019; Meng et al., 2020)[44, 79, 30, 3]. Furthermore, connectomic analysis shows that RP motor neurons share common premotor interneuron synaptic inputs (Zarin et al., 2019)[30]. For the dorsal muscle group, NB7-1 generates five U motor neurons (U1-U5) (Figure 2.1D) (Isshiki et al., 2001)[68]. Single cell labeling approaches showed that each U motor neuron forms a unique and stereotyped synapse onto a muscle in the dorsal muscle group (Landgraf et al., 1997; Meng et al., 2019; Seroka and Doe, 2019)[44, 2, 80]. U motor neurons share many premotor interneuron inputs (Zarin et al., 2019)[30]. Both NB7-1 and NB3-1 generate interneurons after the window of motor neuron production. In summary, the Drosophila motor system contains at least two temporal cohorts of motor neurons that are defined both by muscle synaptic outputs and by presynaptic inputs.

An attractive model is that each circuit controlling a muscle group (dorsal, ventral, and transverse) is populated by a different motor neuron temporal cohort. In support of this idea, DiI clonal data of Drosophila neuroblasts lineages shows at least one lineage generates multiple motor neurons that project to the transverse muscle group (Schmid et al., 1999)[45]. Notably, also based on these DiI data, it is likely that not all motor neurons are organized into temporal cohorts because some lineages generate only one motor neuron. Currently, it is unclear why some lineages make multiple motor neurons and others just a single motor neuron.

2.4 Atlas linking motor neuron lineage/hemilineage identity to muscle groups to reveal putative novel motor neuron temporal cohorts and more avenues for future projects

To gain a comprehensive view of our current knowledge of the relationship between lineages and putative motor circuits I combined previously published literature on Drosophila

larva motor neuron innervation and muscle patterns with my first hand experience to compile an atlas distinguishing muscle groups based on muscle anatomy and nerve membership (Figure 2.3) (Landgraf et al., 1997; Schmid et al., 1999; Menon et al., 2013; Zarin et al., 2019)[44, 45, 46, 30].

For each muscle group I list all motor neurons and include their known lineage and hemilineage membership (Note '?' denote unknown or not confident assignments). Remarkably, for nearly all motor neurons we can identify their neuroblast lineage membership (Figure 2.3). For roughly 60% (18 out of 28) of all motor neurons we can also identify their hemilineage membership. This resolution offers enough insight to let us reasonably speculate about lineage/circuit membership relationships involving motor neuron to muscle synaptic partnerships. Below I expand on the speculative insights offered by the atlas.

First, when focusing on each muscle group based on nerve identity we find that the dorsal muscle group can be further broken down into the dorsal longitudinal (DL) muscles that receive innervation from motor neurons routed in the ISN dorsal-most nerve branch and the dorsal oblique (DO) muscles that are innervated by motor neurons in the ISN lateral nerve branch (Figure 3). Similarly the ventral muscle groups can be further broken down into the ventral longitudinal (VL), ventral acute (VA), and ventral oblique (VO) muscles. Here, I don't include the ventral transverse (VT) muscle group because it consists of one muscle and this muscle is only present in A2-A7 and not A1.

Second, strikingly DL, DO, LT, VL, and VA muscle groups are each innervated by a group of lineage related type Ib motor neurons (represented by similarly colored NB lineage). NB7-1's U motor neurons innervate all DL muscles except for muscle 1, which is innervated by NB1-1's aCC. A group of NB3-2's motor neurons innervate all DO muscles. Another group of NB3-2's motor neurons innervate half of the LT muscles while the remaining LT muscles are innervated by motor neurons from different lineages (lineages that only generate one motor neuron are denoted by underlining). NB3-1's RP motor neurons innervate more than

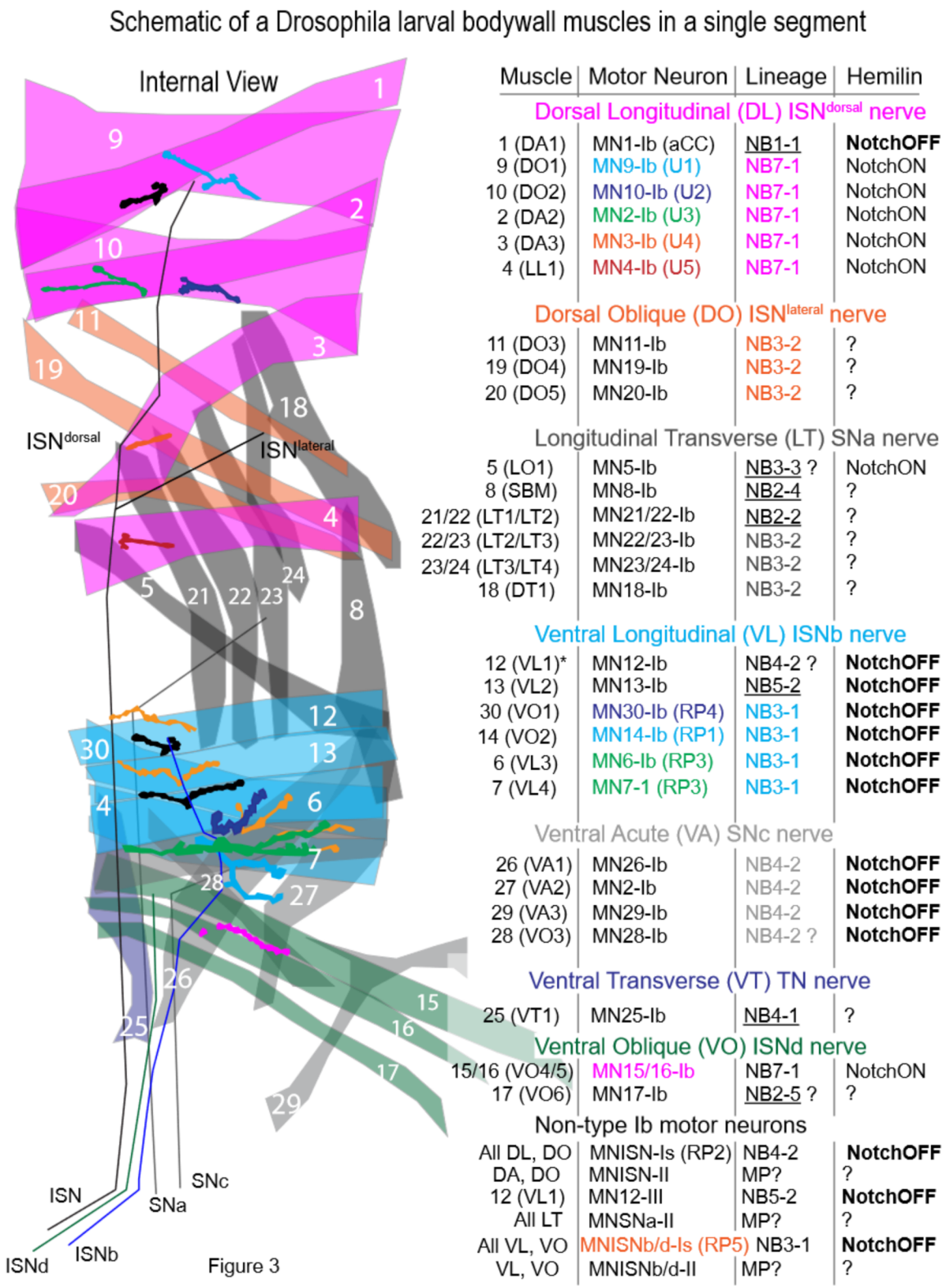


Figure 2.3: Motor neuron to muscle target atlas including motor neuron's lineage/hemilineage identity *Continued*

Figure 2.3: *Cont'd.* Motor neuron to muscle target atlas including motor neuron's lineage/hemilineage identity. Illustration of a single bodywall segment with all 30 muscles labeled, dorsal up, ventral down, anterior to the left. Each muscle group accessed by a nerve is color-coded. Synapses of motor neurons I have studied are included in the schematic. NB lineages that generate a single motor neuron are underlined. Conflicting or unknown information have a '?'. The color-coded lineages represent confirmed or putative temporal cohorts. For example, for the U motor neurons, their 'NB7-1' is magenta to represent that the U motor neurons are a likely cohort that populate the ISN dorsal nerve accessing the Dorsal Longitudinal (DL) muscles. '*' next to muscle 12(VL1) denotes that this muscle uniquely receives type III innervation.

half of the VL muscles while the remaining VL muscles are innervated by motor neurons from different lineages. NB4-2's CoR motor neurons innervate all VA muscles. Combined with what we know about NB7-1 and NB3-1 motor neurons, these data suggest that there are unique temporal cohorts dedicated to each of these five muscle groups. Strikingly, the DO and VA muscle groups are exclusively innervated by motor neurons with shared lineage identity. The DL muscle group is nearly exclusively innervated by the NB7-1 motor neurons. The LT and VL muscle groups receive innervation from the most lineage-diverse group of motor neurons. However, we still find a single heavily represented lineage-related group of motor neurons innervating these groups (NB3-1 for VL group and NB3-2 for LT group). Since we never observe two groups of lineage related neurons innervating a single muscle group, a general takeaway rule is that only 1 motor neuron temporal cohort is dedicated to each muscle group. That being said, if we collapse all dorsal muscles into one group and all ventral muscles into one group this rule no longer applies.

The NB3-2 lineage is unique in that it likely gives rise to two distinct motor neuron temporal cohorts dedicated to DO and LT muscle groups, respectively. This also means that the NB3-2 generates motor neurons innervating one bodywall segment (Segmental nerve SNa routes to the LT muscle group) and the next bodywall segment (Intersegmental nerve ISN lateral routes to the DO muscle group). Elegant work characterizing motor neuron dendrite position in the nerve cord found dendrites are parasegmentally organized, meaning

that motor neurons populating intersegmental nerves form dendrites in a similar region of the nerve cord distinct from overlapping dendrites of motor neurons populating segmental nerves (Landgraf et al., 2003)[81]. In this study, single clones were obtained. Strikingly motor neurons populating intersegmental vs segmental nerves have very different cell body position in the nerve cord. Coupled with the general feature in the nerve cord that cell body migration is minimal, meaning position can be a general proxy for birth time, it is likely that there is a correlation between birth time and motor neuron group assignment. If so, the two groups of motor neurons in NB3-1 represent bona fide temporal cohorts. To further investigate these questions, there is a split GAL4 that consistently marks NB3-2 lineage and occasionally NB4-2 (R21EO9∧AD-R16H11∧DBD) (Lacin and Truman, 2016)[73]. Investigating the birth order relationship within this lineage will reveal if indeed these two groups of motor neurons are indeed temporal cohorts. Based on our current understanding, this suggests that a single neuroblast lineage can generate two distinct motor neuron temporal cohorts. This is reminiscent of the two interneuron temporal cohorts generated in NB3-3.

Third, only a small fraction of neuroblast lineages generate only one type I motor neuron. A general idea in the field is that a number of neuroblast lineages generate a motor neuron during the first division window. While this is certainly true for some lineages including NB3-3, only a small fraction of neuroblast lineages generate 1 motor neuron, denoted by underlining. There are 7 of these lineages, meaning they represent only around 1/5th (7 out of 30) of all neuroblast lineages. Remarkably the majority of type I motor neurons (count 30) are generated by 4 lineages: NB7-1 (count 6), NB3-2 (count 6), NB3-1 (count 4), and NB4-2 (count 6). Combined, only around 1/3rd (11 out of 30) of all neuroblasts generate motor neurons.

Fourth, currently the majority of type I motor neurons with known hemilineage identity are generated in the ‘B’ NotchOFF hemilineage. Most of these motor neurons innervate muscles in the VL, VA, and DL groups. Both VL and VA groups receive innervation

from NotchOFF motor neurons while the DL group receives innervation predominantly from NotchON motor neurons (aka NB7-1's U motor neurons). Currently aside from NB3-3's NotchON motor neuron innervating a muscle in the LT group we do not know the hemilineage identity of motor neurons innervating the DO and LT muscle groups. To learn these motor neurons' hemilineage identity, future experiments misexpressing Notch∧intra using the split GAL4 (Lacin and Truman, 2016)[73], which drives in the NB3-2 lineage need to be done. An alternative broad-based approach is to label all motor neurons with GFP (nuclear localized or membrane bound) using the OK6-GAL4 driver and stain for Hey, a reporter for Notch signaling (Bertet et al., 2014; Monastirioti et al., 2010)[82, 83] and pMad, a decent reporter of motor neurons (note, all motor neurons are pMad+ but some pMad+ neurons are interneurons). Once we know the hemilineage identity of the NB3-2 motor neurons we can distinguish between several currently valid hypotheses. 1) The DL muscle group is uniquely innervated by predominantly NotchON motor neurons. 2) DL, DO, and LT muscle groups are innervated predominantly by NotchON motor neurons whereas VL and VA muscle groups are innervated predominantly by NotchOFF motor neurons.

The data we have so far here is counter to a recently published framework where NotchON hemilineages project their neurites to the dorsal/motor region of the neuropil whereas NotchOFF hemilineages project their neurites to the ventral/sensory region of the neuropil (Mark et al., 2021)[84]. Based on this framework we would predict that motor neurons are overwhelmingly in the NotchON hemilineage but surprisingly, our current understanding supports a model where motor neurons are overwhelmingly from the NotchOFF hemilineage. It is also tempting to speculate about possible NotchON vs NotchOFF motor neuron differences between dorsal/lateral vs ventral muscle groups, respectively. Could these differences be relevant for assembly of unique motor circuits involved in locomotion? Looking at anatomy, the dorsal and ventral muscles are strikingly different. We have evidence to suggest that the DL muscle group may be dispensable for normal locomotion behavior. We know that loss of innerva-

tion of the U motor neurons by cell death ablation (CQGAL4>UAS-RPRHID) does not impact 1st instar larval crawling speed (unpublished data Zarion Marshall). While the same experiment has yet to be done for the ventrally projecting motor neurons, we know the ventral muscles are required for forward and backward locomotion (Heckscher et al., 2012)[47]. A robust manipulation to effectively remove NB3-1's RP motor neuron innervation is to misexpress Notch∧intra using the NB3-1 lineage. I imagine using the Hb9GAL4 driver to misexpress Notch∧intra could effectively remove nearly all ventrally projecting innervation. Assessing the behavior of these larvae, will reveal the extent to which motor neuron innervation onto ventral muscles is critical for various motor circuit output behaviors including backward/forward locomotion, rolling, hunching, etc.

2.5 Temporal cohorts are born contiguously or in a tight developmental time window

It is possible that temporal cohorts are not always comprised of contiguously-born neurons, but instead comprised of neurons born in a limited developmental time window. This idea is supported by a recent study that refuted the long-held perception that NB7-1 generates the five U motor neurons consecutively (Seroka et al., 2020)[85]. Seroka et al, showed that after the third-born U motor neuron, but before the fourth-born U motor neuron, an additional motor neuron is produced by NB7-1 (Figure 2.1D). The newly identified NB7-1 motor neuron, VO, projects to ventral oblique muscles, meaning it is not a member of the dorsal muscle circuit (Seroka et al., 2020)[85]. This finding reveals a break in the previously identified U motor neuron temporal cohort. Notably, the VO motor neuron shares many presynaptic, premotor neuron inputs with U motor neurons (Zarin et al., 2019)[30]. This observation raises questions about how motor circuits evolve over time. Overall, these findings suggest that temporal cohorts are not always made up of neurons that are contiguously born, but can instead be comprised of neurons that are born in a tight developmental time

window.

2.6 Motor neuron temporal cohorts in adult Drosophila

Beyond larval motor circuits, there is evidence of temporal cohorts of leg motor neurons in the Drosophila adult motor system. Clonal analysis revealed that out of eleven neuroblast lineages producing leg motor neurons, the majority are produced by two neuroblasts (Baek and Mann, 2009)[86]. In one lineage, LinA, birth dating of motor neurons showed a striking correlation between birth time and muscle targeting. All early-born LinA motor neurons synapse onto muscles (mostly long tendons) in the proximal tibia or proximal femur portion of the leg, whereas nearly all later-born LinA motor neurons synapse onto muscles (mostly reductors) in the distal tibia or distal femur portion of the leg. A second lineage, LinB, produces a group of late-born LinB motor neurons that synapse onto the coxa levator muscle. Each group of motor neurons in LinA (early-born and late-born) and LinB (late-born) had its own field of overlapping dendrites. Overlapping dendritic fields suggest that these neurons may receive common premotor input, and therefore they are predicted to be functionally recruited together. These findings provide evidence of leg motor neuron temporal cohorts. Therefore, temporal cohorts may be a widespread developmental strategy in motor systems throughout Drosophila life stages.

2.7 In many systems, motor circuits are specified sequentially

In the mouse spinal cord, there are examples of temporal cohort-like sets of neurons. These neurons are generated from stem cells within a small progenitor domain of the developing spinal cord, and these neurons perform analogous functions in different circuits. For example, Renshaw cells and Ia interneurons are sequentially produced by stem cells in the p1 progenitor domain (Benito-Gonzalez et al., 2012; Stam et al., 2012)[87, 88]. Renshaw cells

contribute to a motor neuron feedback circuit, whereas Ia interneurons contribute to a stretch reflex circuit. Despite participation in distinct circuits, Renshaw cells and Ia interneurons perform analogous functions—directly synapsing onto motor neurons and terminating firing (Hultborn, 2006)[89]. In addition, for extensor and flexor premotor interneurons, many of which originate from the same progenitor domain, time of neurogenesis is correlated with spatial and inferred functional segregation (Tripodi et al., 2011)[90]. Thus, Renshaw cells and Ia interneurons are examples of temporal-cohort like units in the spinal cord.

In the vertebrate spinal cord, lineage tracing studies are limited. In general, neuronal origins are traced to only progenitor domains that contain a large number of individual self-renewing stem cells (Woodworth et al., 2017; Sanes and Lichtman, 1999)[91, 92]. This means in spinal cords it is not possible to distinguish the origin of temporal cohort-like sets of neurons. They may originate from neuronal stem cells by one of two ways, based on the following models: stem cell heterogeneity model and a common stem cell model (Ravanelli and Appel, 2015)[93]. The heterogeneity model predicts that different stem cells are activated at different developmental times, and each stem cell gives rise to a distinctive temporal cohort-like set of neurons. The common model, analogous to the Drosophila neuroblast system, predicts that one stem cell divides to generate different neurons over time to make one or more temporal cohort. Therefore, it is unknown if there are convergent or homologous cell biological mechanisms generating temporal cohort-like sets of neurons in the vertebrate spinal cord with respect to the Drosophila nerve cord. Nonetheless, the observation that there are temporal cohort-like groups of neurons in evolutionarily distant species points to the fundamental importance of temporally defined cohorts as a developmental strategy in the assembly of motor circuits.

The need for temporal specification of subsets of neurons in motor system development is likely driven by the fact that motor circuits develop sequentially. Indirect evidence for sequential motor circuit assembly comes from behavioral observations in species as diverse

as humans and flies. For example, using ultrasound, reflex movements are first detected in human fetuses at 7 weeks post fertilization and then more complex behaviors such as hand-mouth coordination appear around 27 weeks (Geertsen et al., 2017; De Vries and Fong, 2006)[94, 95]. Similarly, in Drosophila embryos, the earliest motor behaviors involve forward peristalsis waves followed by more refined behaviors such as self-righting (Crisp et al., 2008)[96]. Work in zebrafish has pushed beyond behavioral observations to show that early-born neurons contribute to circuits for fast escape, whereas later-born neurons contribute to circuits for refined movements (McLean and Fetcho, 2009; Fetcho and McLean, 2010; Jay and McLean 2019)[97, 98, 99]. These observations directly show that there is sequential assembly of motor circuits rather than just sequential expression of behavior from a set of pre-assembled circuits. Analogously, Wreden et al, found that in Drosophila larvae, early-born EL interneurons contribute to circuits for fast escape, whereas later-born EL interneurons contribute to circuits for proprioceptive refinement of movements (Wreden et al., 2017)[1]. This observation may point to a conserved developmental principle. Temporal cohorts or cohort-like groups of neurons may underlie motor circuit assembly across species, despite their separation by hundreds of millions of years of evolution.

2.8 Remaining questions about the lineage-based organization of motor circuits

There remain many questions about the relationships between stem cells and motor circuit configuration. Despite NB3-3 being currently the most completely characterized lineage, several key questions still remain. Can one EL be part of multiple temporal cohorts? NB3-3 makes additional neurons during larval stages. To what adult circuits do they contribute? How do the circuits to which NB3-3 contribute vary along the anterior-posterior axis of the larvae? In other insects, what circuits do NB3-3 neurons contribute to? Beyond NB3-3, to what extent are there additional examples of other interneuron temporal cohorts? For

example, Saaghi neurons and Basin neurons, which synapse onto ELs, have been proposed to be temporal cohorts (Wreden et al., 2017)[1]. What is the relationship between neurons from different lineages that synapse with each other? For example, do temporal cohorts of early-born neurons preferentially wire together? Do early-born neurons from multiple lineages promote fast escape movements? Do all lineages synapse with each other, or is there some selectivity?

2.9 Conclusion

Work reviewed in this chapter provides evidence that temporal cohorts are fundamental, lineage-based organizational units of the Drosophila motor system. Temporal cohorts link neuron birth time within a neuronal stem cell lineage to motor circuit membership. Sequential development of motor circuits appears to be an ancient feature of motor system development. Thus, the observed link between neuronal birth time and functional circuit assembly may be representative of an ancient, widely-occurring strategy driving motor circuit assembly.

CHAPTER 3

TEMPORAL TRANSCRIPTION FACTORS

3.1 Introduction

In this chapter's introduction, I borrow text and figures I previously wrote and created for a published review [4].

3.1.1 To what extent do temporal transcription factors control mature neuronal Identity?

As neuronal stem cells divide, they sequentially express temporal transcription factors (Pearson and Doe, 2004)[62]. In Drosophila nerve cord neuroblasts, the following temporal transcription factors are expressed in neuroblasts in this sequence: Hunchback (Hb), Kruppel, Nubbin/Pdm2 (Pdm), Castor (Cas), and Grainyhead (Isshiki et al., 2001; Kambadur et al., 1998; Brody and Odenwald, 2000)[68, 100, 101]. Loss-of-function and misexpression experiments showed that temporal transcriptions collectively specify embryonic temporal identity of neuronal progeny (Pearson and Doe, 2004; Isshiki et al., 2001; Grosskortenhaus et al., 2006; Tran and Doe, 2008)[62, 68, 69, 70]For example, when Hunchback is lost, expression of molecular markers for first-born neuronal progeny are lost (Isshiki et al., 2001; Tran and Doe, 2008)[68, 70]. When Hunchback expression is prolonged in neuroblasts, more neurons express first-born molecular markers, and fewer neurons express later-born molecular markers. Limited anatomical evidence collected in embryos suggested that neurons with early-born molecular marker expression have initial axonal trajectories similar to those of early-born neurons (Pearson and Doe, 2003; Isshiki et al., 2001)[102, 68]. Therefore collectively, there was strong evidence in the field to show that embryonic neuronal identity could be regulated by temporal transcription factors.

The relationship between temporal transcription factor-induced changes in embryonic molecular identity and mature neuronal Identity, and therefore circuit assembly, was far less clear. Notably, no data had been collected on mature features such as synaptic partnerships or dendrite morphology. Despite limited evidence, however, a widely-held model was that temporal transcription factors controlled all aspects of neuronal Identity, including mature neuronal features (Allan and Thor, 2015)[74]. This is an important model to test because, if true, it means that the information that controls all of a neuron's developmental decisions is present prior to the neuron's time of birth. It would mean that circuit assembly could be predicted and controlled by programs of gene expression in the neuroblast and would suggest that the environment in which motor circuits assemble is relatively stable and permissive. Finally, because temporal transcription factors are at the top of a molecular cascade, it would provide a molecular entry point for identifying important downstream factors that control motor circuit assembly.

Three recent studies, discussed below, directly probed the role of temporal transcription factors in controlling mature features of motor neurons (Meng et al., 2019; Meng et al., 2020; Seroka and Doe, 2019)[2, 80, 3]. These studies used NB7-1 and NB3-1 lineage-specific gene expression of temporal transcription factors. This allowed the authors to rule out any non-lineage specific effects and to grow animals to mature larval stages. The manipulations in the recent studies generated the same embryonic phenotypes as seen in previous studies that focused only on embryonic stages (Isshiki et al., 2001; Tran and Doe, 2008; Grosskortenhaus et al., 2006)[68, 70, 69]. What sets the recent studies apart from previous studies is that they track motor neurons into mature larval stages. Collectively, these recent studies use neuromuscular junction fillet preparations, single-cell tracing techniques, labeling with marker genes, confocal imaging, electrophysiology, and calcium imaging. They assess how temporal transcription factors regulate neuronal mature features such as anatomical and functional synaptic connectivity. Together they provide insight into how temporal transcription factors

impact motor circuit assembly. They show: 1) temporal transcription factor expression in neuroblasts regulates motor neuron temporal cohort size and composition and 2) temporal transcription factor-induced changes in embryonic marker gene expression do not always accurately predict motor neuron-to-muscle synaptic partnerships.

3.1.2 Temporal transcription factor expression in neuroblasts regulates motor neuron temporal cohort size and composition

Recent studies support a model in which temporal transcription factors act as molecular switches in the neuroblast to regulate circuit membership of neuronal progeny. Bi-directional manipulation of the duration of temporal transcription factor expression in NB7-1 bi-directionally modulates the number of motor neurons produced by NB7-1. It does so without altering the total number of neurons in the lineage (Meng et al., 2019; Seroka and Doe, 2019)[2, 80]. Prolonged expression of Hb in NB7-1 generates extra motor neurons that form functional synapses on muscles in the dorsal muscle group (Meng et al., 2019)[2]. Hb expression in post-mitotic neurons does not have these effects. Forcing NB7-1 to precociously transition out of the Hb expression window by expressing the Hb switching factor Seven-up decreases the number of motor neurons synapsing on dorsal muscles. Additionally, when Hb expression is prolonged in NB3-1, there is an increase in the number of motor neurons synapsing on the muscles in the ventral muscle group (Meng et al., 2020)[3]. Together these data demonstrate that Hb expression is a potent regulator of motor neuron temporal cohort size in neuroblasts.

Other temporal transcription factors also regulate the size of motor neuron temporal cohorts. After the Hb expression window, Pdm and Castor are expressed (Pearson and Doe, 2004)[62]. Precocious expression of Castor in NB7-1 decreases the number of motor neurons that populate the dorsal muscle circuit. Precocious expression of Pdm in NB7-1 can either increase or decrease the number of U motor neurons that populate the dorsal muscle

circuit, depending on which anterior-posterior segment is examined (Meng et al., 2020)[3]. The observation that the effect of Pdm varies with anterior-posterior position suggests there may be a synergistic interaction with A-P patterning Hox genes. In summary, there is now strong evidence that multiple temporal transcription factors can modulate the proportion of neurons from a lineage that populate a given motor circuit.

When temporal transcription factor expression alters the size of a motor neuron temporal cohort, it does not linearly scale the proportion of neuronal Identities within the temporal cohort. That is, a temporal cohort, which is twice as large as wild-type would not contain twice as many early-born and late-born motor neurons as wild-type. Instead, neurons with certain Identities are overrepresented and other Identities underrepresented, depending on the specific temporal transcription factor manipulated (Meng et al., 2020; Meng et al., 2019; Seroka and Doe, 2019)[3, 2, 80]. For example, when Hb expression is prolonged in NB7-1, there is a dramatic increase in the number of synaptic branches onto the early U muscle targets and a significant decrease in the number of synaptic branches onto late U muscle targets (Meng et al., 2019; Seroka and Doe, 2019)[2, 80]. These studies show that when temporal transcription factor manipulations change motor neuron temporal cohort size, certain motor neuron Identities are over-represented and other Identities are lost.

3.1.3 In some cases, the CNS can compensate for temporal transcription factor-induced changes

As described above, temporal transcription factor manipulation results in two phenotypes—over innervated muscles and under innervated muscles. How does the motor system respond to these changes?

For over-innervated muscles, there is evidence for functional compensation. When Hb expression is prolonged in NB3-1, several ventral muscles get extra synaptic branches. Electrophysiological recordings show a significant increase in the number of vesicles released

during stimulated synaptic activity. This is consistent with the idea that the total number of functional synapses is increased (Meng et al., 2020)[3]. However, the overall muscle response to nerve stimulation (EPSP) remained at wild-type levels. These data show functional compensation occurs. Although the specific cell biological mechanism for compensation is unclear, it is likely to be a form of synaptic homeostasis (Frank et al., 2020)[103].

There is evidence that under-innervated muscles receive anatomical compensation. When Hb expression is prolonged in NB7-1 or NB3-1, late-born U motor neurons and late-born RP motor neurons appear to be missing. Late-born U motor neuron and late-born RP motor neuron muscle targets are under-innervated. However, these muscles do not entirely lack synapses. Instead, what little synaptic branches are seen appear to be abnormally placed branches from motor neurons innervating other muscles. This phenotype is also seen on the RP3 motor neuron target when RP3 is laser ablated during development (Chang and Keshishian, 1996)[104]. This phenotype is seen on U motor neuron muscle targets when U motor neurons are genetically ablated during development by expression of pro-apoptotic genes (Meng et al., 2019)[2]. Taken together these data support the idea that when muscles lack innervation due to loss of their normal motor neuron partner, other motor neurons excessively branch to compensate for the loss of innervation.

In summary, manipulation of temporal transcription factors in neuroblasts has long-lasting effects on physiology of the motor system and is capable of triggering different types of plasticity.

3.1.4 Remaining questions about how temporal transcription factors impact motor circuit assembly

The observation that temporal transcription factors are potent regulators of motor neuron mature features raises the question of how manipulation of temporal transcription factors impacts interneuron mature features. There are two major gaps in our knowledge. 1) When

motor neuron dendrite morphology is transformed by temporal transcription factor manipulation, how are premotor interneuron-to-motor neuron input synapses impacted? 2) How do temporal transcription factor manipulations impact axons and synaptic partner choice of interneurons whose axons do not leave the CNS? These questions must be addressed because motor neurons develop in a different context in comparison to interneurons. Interneurons form synaptic connections within the CNS, which is a dynamic environment constantly changing due to ongoing neurogenesis. Larval motor neurons acquire many of their mature features while projecting into a periphery that contains large, pre-existing muscles. Answering these questions will further elucidate the logic of motor circuit assembly.

The observation that temporal transcription factors can profoundly influence motor circuit assembly in Drosophila larvae raises questions about the impact of temporal transcription factors in other contexts. 1) In the spinal cord, temporal programs drive neuronal identity (Philippidou and Dasen, 2013; Sagner and Briscoe, 2019)[105, 106]. However, the specific underlying molecular mechanisms are currently poorly-understood. Consequently, the degree to which stem cell intrinsic temporal transcriptional programs influence motor circuit assembly remains un-tested in the spinal cord. 2) Temporal transcription factors have been identified in other Drosophila circuits (Sullivan et al., 2019; Rossi et al., 2017; Doe, 2017; Stratmann and Thor, 2017; Allan and Thor, 2015)[107, 108, 64, 109, 74], but their impact on mature neuronal features and circuit assembly in these contexts is uncharacterized. 3) It would be valuable to see the degree to which there are alterations in temporal transcription factor expression in neuroblasts in other insects. This is because all insect motor systems are generated from the same basic set of 30 neuroblasts (Doe, 1992; Truman and Ball, 1998; Shepherd and Bate, 1990; Tamarelle et al., 1985; Doe and Goodman, 1985)[55, 110, 111, 112, 113]. Yet, insect body plans have dramatically changed during the course of 300 million years of evolution (Niven et al., 2008)[114]. To accommodate changes in body plan, the duration of neuroblast division is altered (Biffar and Stollewerk, 2014;

Truman and Ball, 1998)[115, 110]. How temporal transcription factor expression changes over evolutionary time scales and how expression changes might impact diversification of motor system wiring are open questions.

The finding that temporal transcription factors strongly influence motor circuit assembly demonstrates that this class of transcription factors are at the top of a transcriptional hierarchy. A major unsolved question is what are the relevant programs of gene expression downstream of temporal transcription factors that regulate motor circuit assembly.

3.2 Meng et al., 2019 eLife

In this first paper entitled 'How prolonged expression of Hunchback, a temporal transcription factor, re-wires locomotor circuits', Zarion Marshall contributed by preparing, fixing, and staining CQGAL4>UAS-MCFO late stage embryos in Figure 1. During a rotation, Meike Lobb-Rabe contributed by dissecting, fixing, and staining for synaptic markers in NB7-1>UAS-Hb2X 3rd instar animals in Figure 6.

3.2.1 Abstract

How circuits assemble starting from stem cells is a fundamental question in developmental neurobiology. We test the hypothesis that, in neuronal stem cells, temporal transcription factors predictably control neuronal terminal features and circuit assembly. Using the Drosophila motor system, we manipulate expression of the classic temporal transcription factor Hunchback (Hb) specifically in the NB7-1 stem cell, which produces U motor neurons (MNs), and then we monitor dendrite morphology and neuromuscular synaptic partnerships. We find that prolonged expression of Hb leads to transient specification of U MN identity, and that embryonic molecular markers do not accurately predict U MN terminal features. Nonetheless, our data show Hb acts as a potent regulator of neuromuscular wiring decisions. These data introduce important refinements to current models, show that molecular infor-

mation acts early in neurogenesis as a switch to control motor circuit wiring, and provide novel insight into the relationship between stem cell and circuit.

3.2.2 Introduction

In complex brains, a relatively small pool of neuronal stem cells generates a large diversity of neurons. Ultimately, this diversity of neurons wire together to generate functional neuronal circuits that underlie sensation, cognition, and action. How circuits are assembled starting from neuronal stem cells is a fundamental question in developmental neurobiology that has implications for the fields of biomedicine and evolution.

As a neuronal stem cell divides it generates a diverse set of neurons in a predictable, orderly fashion through stem cell-intrinsic molecular programs. This process is often referred to as temporal patterning. In past decades, intense molecular genetic work has shown that early step of temporal patterning—the establishment of unique profiles of gene expression in newly-born post mitotic neurons—can be controlled by a class of transcription factors called temporal transcription factors (Doe, 2017)[64]. Despite decades of work on temporal transcription factors, however, the biological relevance of most published manipulations is unknown. This is because the role of temporal transcription factors at later steps of neuronal development—establishing terminal neuronal features such as dendrite morphology, axonal trajectory, and functional synaptic partnerships—are almost completely unexplored.

Temporal patterning has been proposed to play a role in circuit assembly (Deguchi et al., 2011)[116]. An attractive and often cited model is that temporal transcription factors are master regulators of entire developmental programs (Allan and Thor, 2015)[74]. From a circuit wiring perspective, this would mean that manipulating temporal transcription factor expression in a given stem cell would be sufficient to predictably alter the wiring of neuronal progeny. If this is true, it has important implications for the evolution of neuronal circuits and for stem-cell based biomedical interventions. In support of such a model, there is an

association between neuronal birth time and neuronal circuit membership in many organisms and many brain regions (Bhansali et al., 2014; Deguchi et al., 2011; Eerdunfu et al., 2017; Greaney et al., 2017; Jefferis et al., 2001; Kulkarni et al., 2016; McLean et al., 2007; McLean and Fetcho, 2009; Morrow et al., 2008; Osterhout et al., 2014; Petrovic and Hummel, 2008; Pujol-Martí et al., 2012; Tripodi et al., 2011) [117, 116, 118, 119, 120, 121, 122, 97, 123, 124, 125, 126, 90]. However, such a simple model over emphasizes the idea that temporal transcription factors are master regulators of temporal cell fate and de-emphasizes the role of dynamic factors in the environment or in the stem cell that change as temporal patterning occurs. These other dynamic factors could also play a major role in circuit wiring. Thus, it is far from clear how manipulating temporal transcription factors impacts circuit assembly.

The objective of this study is to test the hypothesis that temporal transcription factor activity in neuronal stem cells is sufficient to control neuronal terminal features and therefore circuit assembly. The Drosophila embryonic/larval nerve cord is a model system ideally suited to study how temporal transcription factors regulate circuit wiring. Here, we focus on one stem cell, neuroblast NB7-1, and five of its progeny, the U motor neurons, U1-U5 (Figure 3.1A). Molecular markers are available to uniquely identify each U motor neuron (Figure 3.1A), and the temporal transcription factors involved in establishing U motor neuron diversity have been studied for decades (Grosskortenhaus et al., 2006; Isshiki et al., 2001; Pearson and Doe, 2003)[127, 68, 102]. For example, one of the first-identified and best-characterized temporal transcription factors, Hb (Hb), is involved in establishing early-born U1/U2 motor neuron identities (Isshiki et al., 2001)[68]. Notably, the mammalian homolog of Hb, Ikaros, acts as a temporal transcription factor in both retina and cortex (Alsiö et al., 2013; Elliott et al., 2008)[128, 129]. In this study, to use the Drosophila motor system, and specifically NB7-1 and U motor neurons, to study the role of temporal transcription factors in circuit wiring, first we characterize each U motor neuron's terminal features—dendrite morphology, axonal trajectory, and neuromuscular synaptic partner—and link these features to U motor

neuron marker gene expression at single neuron resolution. Next, we manipulate temporal patterning in NB7-1 using three different Hb manipulations: we prolong the expression of wild type Hb, we prolong expression of an activating Hb protein (tethered to the VP16 transcriptional activation domain), and we shorten the expression of wild type Hb by precocious expression of the switching factor, Seven-up (Kanai et al., 2005; Tran et al., 2010) [130, 131]. In these backgrounds, we monitor establishment of U motor neuron molecular identity (i.e., embryonic marker gene expression), as well as maintenance (i.e., larval marker gene expression), and assess U motor neuron terminal features.

Our data uncover the biological relevance of manipulating temporal transcription factors. We find that Hb is a potent regulator of neuromuscular wiring decisions. But, surprisingly, we find prolonged expression of Hb leads to a transient rather than permanent specification of U motor neuron molecular identity, and that the embryonic molecular markers which have been used for decades to monitor U motor neuron embryonic molecular identity cannot accurately predict U motor neuronal terminal features. Nonetheless, our data support a general model in which neuromuscular synaptic partner choice and circuit wiring can be established before neuronal birth by early programs of gene expression acting in neuronal stem cells.

3.2.3 Results

Characterizing terminal features of U motor neurons at single neuron resolution

We take advantage of a well-characterized neuronal stem cell (neuroblast) lineage in the Drosophila embryonic larval nerve cord to test the hypothesis that temporal transcription factor activity controls neuronal terminal features and circuit assembly. Specifically, we focus on NB7-1, which generates five U motor neurons in this order: U1, U2, U3, U4, U5,

followed by a series of poorly-characterized neurons (Figure 3.1AA). U motor neurons are easily identified because they express the homeobox transcription factor, Even-skipped (Eve, Evx1/2 in vertebrates), and in embryos each U motor neuron can be uniquely identified by a distinctive combination of transcription factors (Figure 3.1A) (Isshiki et al., 2001)[68]. Furthermore, each U motor neuron occupies a distinctive position within the CNS characteristic of its birth time, with earliest-born U motor neurons found closest to the midline (Figure 3.1C). Cell body position in the Drosophila CNS is roughly correlated with birth time because there is little neuronal migration, and so as laterally positioned neuroblasts divide, later-born neurons displace earlier-born neurons to a deeper and more medial CNS position. The establishment of distinct U motor neuron identities has been intensely studied, but the biological relevance of altering embryonic identity markers is poorly understood (Doe, 2017)[64]. Here, we characterize terminal features of each U motor neuron in wild type.

First, we label individual U motor neurons in whole mount, late-stage embryos when neuroblasts have stopped dividing and circuit wiring is being established (Figure 3.1B). We find dendrites of the earliest-born U motor neurons, U1 and U2, are contralateral (i.e., cross the midline) and dendrites of U3-U5 are ipsilateral (i.e., do not cross the midline) (Figure 3.1C'–G'). Notably, U1 and U2 are generated from NB7-1 while Hb is expressed in NB7-1 (Figure 3.1A). Therefore these data establish a correlation between Hb expression and U motor neuron dendrite morphology and raise the possibility of a causal link.

We visualize single U motor neuron axons and their muscle targets and find every U motor neuron axon projects to a unique dorsal muscle (Figure 3.1C"–G"). The earliest-born U motor neuron, U1 has the longest axon and reaches the distal most muscle, muscle 9 (M9). Progressively later-born U motor neurons have progressively shorter axons, reaching progressively less distal muscles, with U2 reaching muscle 10, U3 reaching muscle 2, U4 reaching muscle 3, and U5 reaching muscle 4. These data agree with previous reports

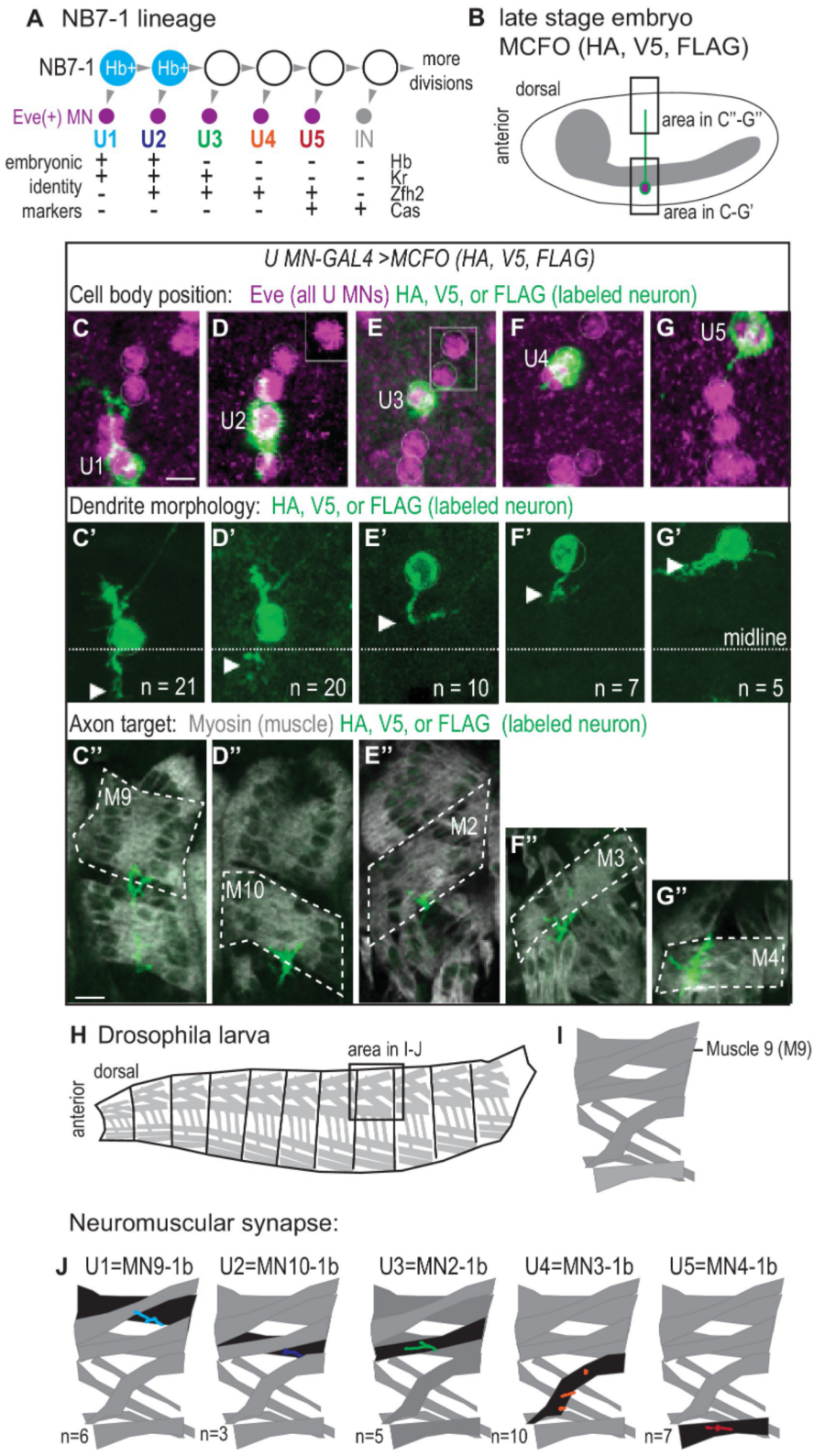


Figure 3.1: U motor neurons have unique embryonic molecular identities and unique terminal features. *Continued*

Figure 3.1: *Cont'd.* U motor neurons have unique embryonic molecular identities and unique terminal features. (**A**) Illustration of the divisions of NB7-1. Each gray arrowhead represents cell division. Abbreviations: MN is motor neuron, IN is interneuron, Eve is Even-skipped, Hb is Hunchback, Kr is Kruppel, Zfh2 is Zinc finger homeodomain 2, and Cas is Castor. (**B**) Illustration of a Drosophila late stage embryo, CNS in gray, motor neuron in green, with cell body in magenta. (**C–G"**) Images of individually labeled U motor neuron cell bodies in the CNS of late stage embryos. The same cell is shown in ventral view (**C–G'**) or lateral view (**C"–G"**). Multi-Color Flip Out (MCFO) transgenes were used to stochastically label neurons within a GAL4 pattern with membrane tethered epitope tags (HA, V5, FLAG). (**C–G**) Boxes are insets from a different focal plane. (**C'–G'**) U1/U2 motor neurons dendrite tips (arrowhead) cross the midline (dotted white line), whereas U3-U5 neurons do not. n = number of single-labeled Eve(+) cells. (**C"–G"**) Axons project to unique dorsal muscles (dotted outline, M stands for muscle, for example M9 is muscle 9). (**H–I**) Illustrations of Drosophila larval muscles. (H) The larval body is organized into repeated left-right, mirror image hemisegments. (I) In a hemisegment, individual muscles are identified and named by characteristic morphology. (**J**) Illustration of individual U motor neuron neuromuscular synapses onto dorsal muscles in larvae. Embryonic motor neuron (e.g., U1) and larval motor neuron synapse (e.g. MN9-1b) names are shown. n = number of single-labeled Eve(+) cells. Color code as in A. For sample of larval image data see Figure 1—figure supplement 1. Images in (C–G') are shown anterior to the left. Scale bars represent five microns (C'–G') and 10 microns (C"–G"). MCFO transgenes were driven with a U MN-GAL4 line, CQ2-GAL4 (hsFLP; CQ2-GAL4/+; UAS(FRT.stop)myr::smGdP-HA, UAS(FRT.stop)myr::smGdP-V5-THSUAS(FRT.stop)myr::smGdP-FLAG/+).

showing that, in general, U motor neurons project to dorsal (and possibly ventral) muscles (Bossing et al., 1996; Landgraf et al., 1997; Schmid et al., 1999) [57, 44, 45].

Next, we label individual U motor neurons in late stage larvae (L3), at a time when there are large, well-established, well-characterized neuromuscular synapses (Hoang and Chiba, 2001). Consistent with embryo data, U1 generates a synapse on muscle 9 that has been called MN9-1b (i.e., motor neuron that targets muscle 9 and has a type 1 big synapse), U2 generates the MN10-1b synapse, U3 generates the MN2-1b synapse, U4 generates the MN3-1b synapse, and U5 generates the MN4-1b synapse (Figure 3.1H–J and 3.2). We conclude that in wild type there is a perfect correspondence between axonal target and neuromuscular synapse and that a majority of dorsal muscles are innervated by neurons from NB7-1.

Together these data link markers of U motor neuron embryonic temporal identity to U

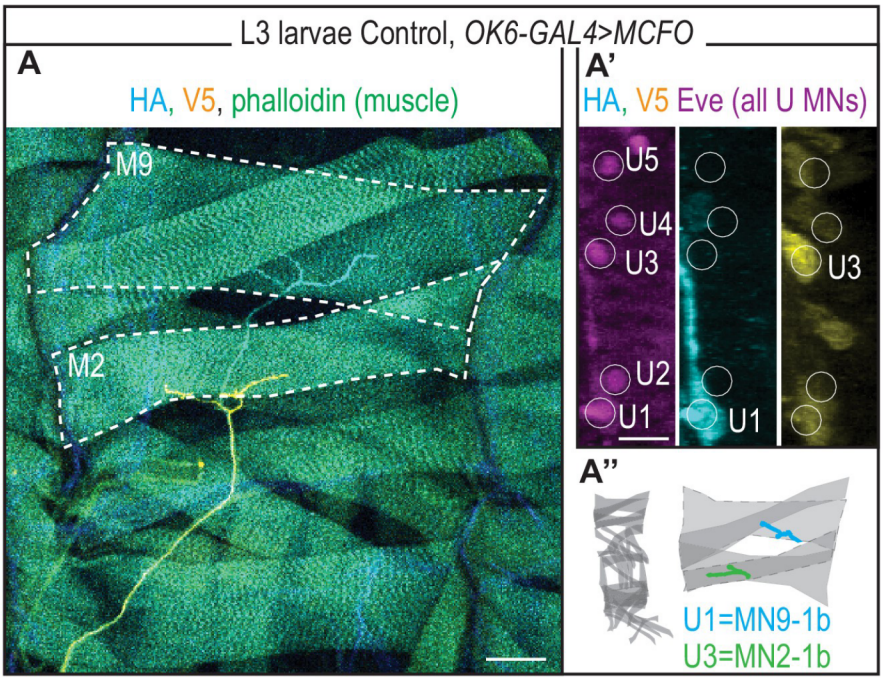


Figure 3.2: U Motor Neuron axon projection in third instar (L3) Drosophila larva.(**A**) Image of individually labeled U motor neuron axons. The dorsal-most region in a body wall segment of a L3 fillet dissected larva is shown. MCFO transgenes were driven with a pan motor neuron-GAL4 line, OK6-GAL4 (hsFLP; OK6-GAL4/+; UAS(FRT.stop)myr::smGdP-HA, UAS(FRT.stop)myr::smGdP-V5-THSUAS(FRT.stop)myr::smGdP-FLAG/+). Axons project to unique dorsal muscles (dotted). Midline is down. (**A'**) Image of individually labeled U motor neuron cell bodies (in white circles) from A in the CNS of L3 larvae. (**A"**) Illustration of a Drosophila L3 bodywall segment imaged in A. Embryonic (e.g., U1) and larval (e.g. MN9-1b) motor neuron names are color coded with neuromuscular synapse location. Color code as in Figure 1. Image in (A) shown with dorsal up, anterior to the left. Image in (A') shown with lateral up, anterior to the left. Scale bars represent 50 microns (A) and five microns (A').

motor neuron terminal features—dendrite morphology, axonal target, and neuromuscular synapses- at single neuron resolution, which allows us to predict which terminal features should be associated with a particular U motor neuron marker gene expression profile, regardless of neuronal birth time.

Prolonged expression of Hunchback in NB7-1 generates ectopic Eve-expressing neurons with U1 embryonic molecular identities at abnormally late times in development

To test the hypothesis that temporal transcription factor activity in neuronal stem cells is sufficient to control neuronal terminal features and circuit assembly, we manipulate temporal transcription factor expression. In wild type, a given temporal transcription factor is expressed in nearly all neuronal stem cells during a limited time window. For example, in NB7-1, the temporal transcription factor Hunchback (Hb) is expressed during the first two neuroblast divisions (Figure 3.3A). In this study, we prolong Hb expression specifically in NB7-1, and then we assay NB7-1 progeny for embryonic marker gene expression (Figure 3.3), the extent to which progeny are motor neurons (Figure 3.5), dendrite morphology (Figure 3.6), functional neuromuscular synapse formation (Figures 3.7,3.9), axonal trajectory (Figure 3.10), and larval marker gene expression (Figure 3.11). Hb expression has been prolonged in NB7-1 in many ways (e.g., hs-GAL4, En-GAL4, Pros-GAL4, removal of Hb switching factor SVP; Cleary and Doe, 2006; Grosskortenhaus et al., 2005; Isshiki et al., 2001; Kanai et al., 2005; Pearson and Doe, 2003)[69, 68, 102], and in general, these manipulations produce a large number of ectopic Eve(+) cells that express U1 molecular markers. Here, we use a previously uncharacterized, NB7-1-specific method to prolong Hb expression. NB7-1-specific manipulation is essential when examining circuit wiring because it rules out possible effects of Hb acting in another lineages. Specifically, we use NB7-1-GAL4 (Figure 3.4) to drive Hb expression from either one or two copies of UAS-Hb (Kohwi et al., 2013)[132]. In both manipulations, we find an average of ten Eve(+) cells (Figure 3.3A–D',H). Notably, however, there is hemisegment to hemisegment variability in how long NB7-1-GAL4 drives gene expression, which results in variability in the number of Eve(+) cells (Figure 3.3H,Q). We also note driving two copies of Hb generates slightly stronger phenotypes (Figure 3.4E–G), and so unless otherwise noted, we drive two copies of Hb, which we refer to as 'NB7-1>Hb'. In

comparison to NB7-1>Hb, a similar number of Eve(+) cells are found when Hb expression in NB7-1 is prolonged by eliminating Seven-up, a factor that promotes Hb switching (Kanai et al., 2005)[130]. This suggests that the level of Hb expression we achieve in the NB7-1>Hb manipulation is in a physiological range.

Because we use a previously uncharacterized manipulation of Hb, we perform a series of control experiments to show that we elicit changes in temporal patterning similar to those described previously. We track all NB7-1 progeny in control and NB7-1>Hb embryos using a GFP reporter (Figure 3.3C–I). First, we find a slight, but not significant increase in the total number of GFP(+) NB7-1 progeny in NB7-1>Hb in comparison to Control, which is not enough to account for the number of extra U motor neurons (Figure 3.3G). Second, in Control, later-born NB7-1 interneurons express the transcription factor, Castor (Cas), but not Eve, and are located dorsolaterally to U motor neurons (Figure 3.3E–E',I). In NB7-1>Hb embryos, there is a near complete loss of the later-born NB7-1 Cas(+) neurons (Figure 3.3E–F',I). Taken together, we conclude that in NB7-1>Hb, extra Eve(+) neurons are generated at the time when neurons with later-born molecular identities are normally born.

Next, we characterize embryonic molecular identities of the Eve(+) cells in NB7-1>Hb using the combination of molecular markers Hb (Hb), Krupple (Kr), and Zfh2, which together label U1 (Hb[+] Kr[+] Zfh2[-]), U2 (Hb[+] Kr[+] Zfh2[+]), U3 (Hb[-] Kr[+] Zfh2[+]), and U4/U5 (Hb[-] Kr[-] Zfh2[+]) (Figure 3.3J–Q). Note, we use Hb in two capacities in this experiment. We manipulate Hb in the neuroblast, and we use Hb as marker for U1/U2 molecular identity because in wild type U1 and U2 motor neurons actively transcribe Hb (Kohwi et al., 2013)[132]. To distinguish actively-transcribed Hb (an identity marker) from Hb inherited from neuroblast cytoplasm, we stain at late embryonic stages to allow for Hb protein turnover as in Pearson and Kohwi (Kohwi et al., 2013; Pearson and Doe, 2003)[132, 102]. In NB7-1>Hb embryos, 86% of Eve(+) cells are U1-like (Figure 3.3P-Q and Figure

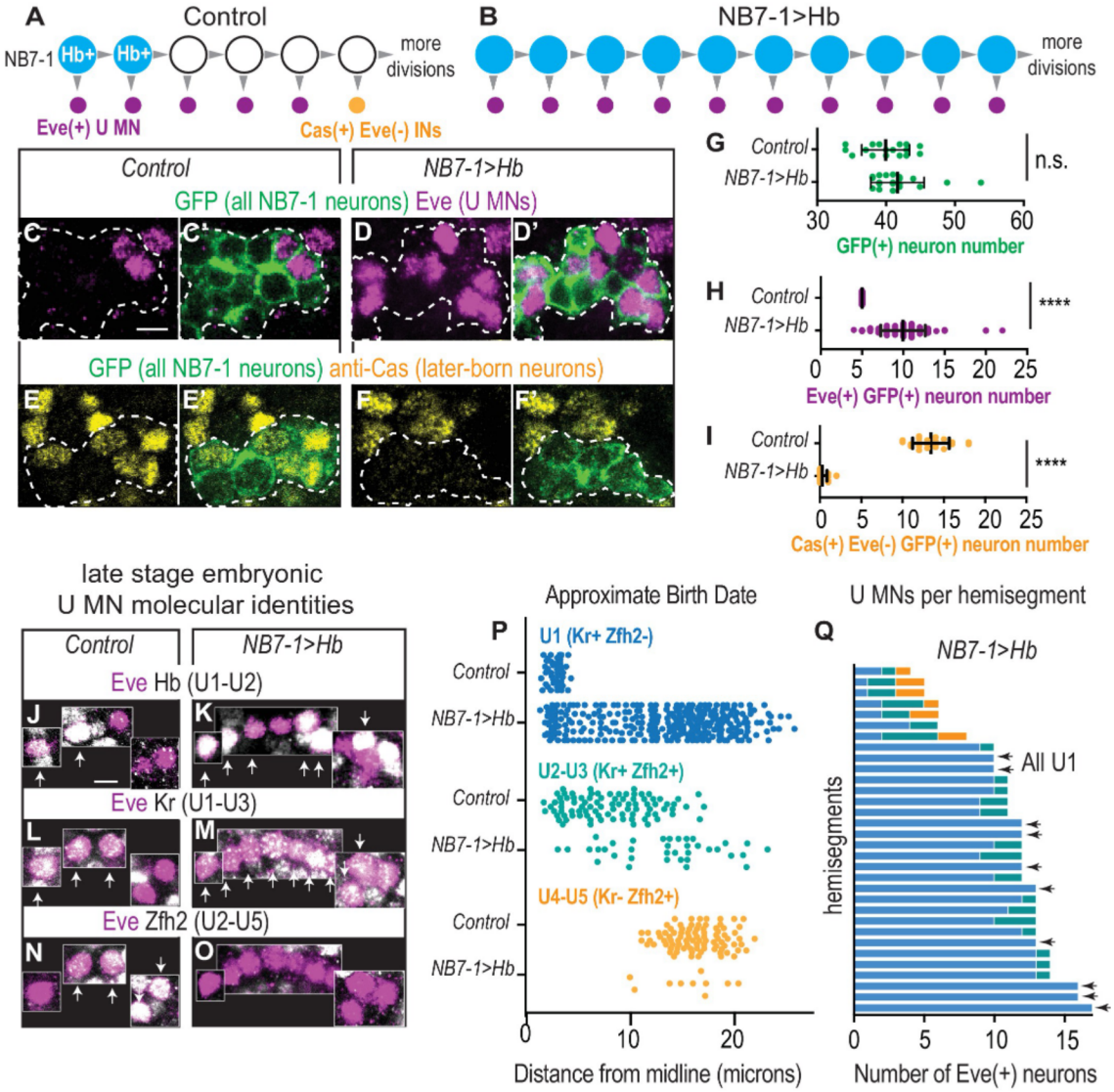


Figure 3.3: In embryos with prolonged Hb expression, U motor neurons are produced at abnormally late times in development. (**A-B**) Illustrations of NB7-1 lineage progression. Each gray arrowhead represents cell division. Large circles are neuroblasts, and smaller circles are neurons. In NB7-1>Hb, ectopic Eve(+) neurons (magenta) are produced when later-born Cas(+) NB7-1 interneurons (yellow) are normally produced. (**C–F'**) Images of late stage embryonic CNSs show distribution of Eve(+) and Cas(+) neurons. Data quantified in (G–I). GFP (+) neurons from NB7-1 are outlined in white dotted lines. *Continued*

Figure 3.3: *Cont'd.* In embryos with prolonged Hb expression, U motor neurons are produced at abnormally late times in development. (**G–I**) Quantification of NB7-1 neurons in Control and NB7-1>Hb. (G) Total neurons (H) Eve(+) neurons (I) Cas(+) neurons. For Controls n = 17, 23, 19 and for NB7-1>Hb n=20, 30, 14 for (G–I), respectively. (**J–O**) Images of embryonic molecular identity marker expression in Eve(+) cells in late stage embryonic CNSs. In NB7-1>Hb, extra Eve(+) cells are produced, most of which have U1 molecular identities. Boxes are neurons from different z-planes. Arrows indicate co-expression. (**P**) Quantification of distance from midline is a proxy for neuronal birth time. In NB7-1>Hb, Eve(+) cells co-labeled with U1 molecular markers are born at abnormally late times in lineage progression. Control n = 44, 88, 88, NB7-1>Hb n=301, 40, 10. (**Q**) Quantification of Eve(+) neuron molecular identity in single hemisegments. In NB7-1>Hb, there is hemisegment by hemisegment variability. Arrows point to hemisegments in which all Eve(+) neurons have U1 molecular identity. Color code follows (P). All images are shown in ventral view, anterior up and midline to the left. Scale bars represent five microns. For quantifications each dot represents single neuron cell bodies in abdominal hemisegments. Average and standard deviation are overlaid. Un-paired t-Test.' n.s.' not significant, '****'$p<0.0001$. In C-I, Control is NB7-1-GAL4/+; UAS-myr-GFP/+ and NB7-1>Hb is NB7-1-GAL4/UAS-Hb; UAS-myr-GFP/UAS-Hb. In J-Q, Control is w1118 and NB7-1>Hb is NB7-1-GAL4/UAS-Hb; UAS-Hb/+.

3.4F-G). Furthermore, in nearly one-third of all hemisegments all Eve(+) cells have U1 molecular identities (Figure 3.3Q arrows). To demonstrate that in NB7-1>Hb Eve(+) cells with U1 identities are born at abnormally late times in development we measure the distance of each cell body from the CNS midline as a proxy for neuronal birth time, and then plot the position of Eve(+) cells along the medio-lateral axis (Figure 3.3P and Figure 3.4E). Together these data demonstrate that prolonging Hb expression with NB7-1-GAL4 is sufficient to generate extra Eve(+) neurons, a majority of which have U1 molecular identities regardless of birth time. Thus, in NB7-1>Hb, a neuron's birth time and its temporal identity are decoupled, which allows us to parse the contribution of Hb versus other birth time related factors in controlling terminal features of U motor neurons.

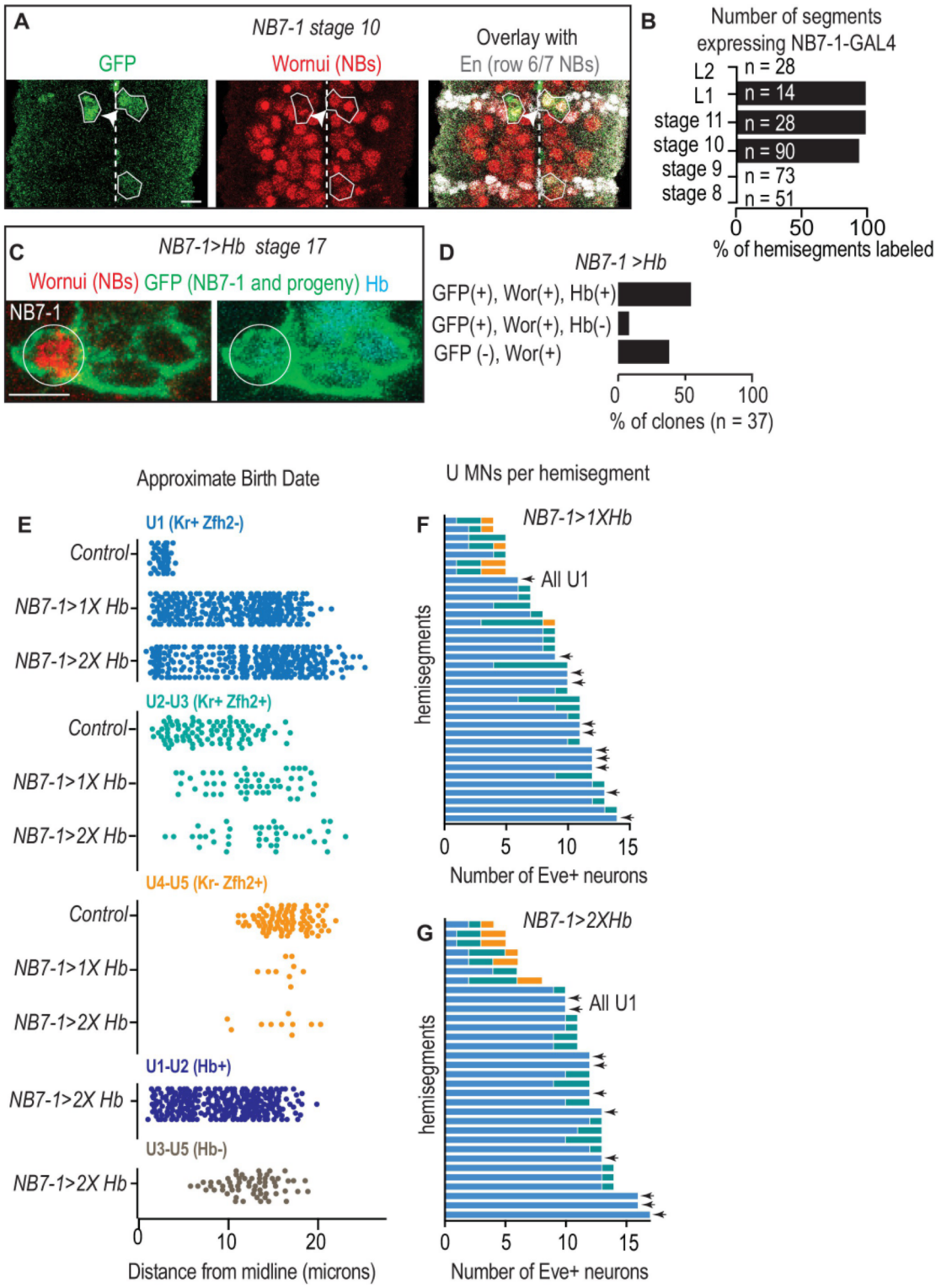


Figure 3.4: Characterization of NB7-1-GAL4. (**A**) Image of GFP in NB7-1 as a reporter of NB7-1-GAL4 activity. NB7-1 is gooseberry-DBD, achaete-VP16/+; UAS-nls-GFP/+. NB is neuroblast. Arrowhead points to NB6-1, which is occasionally labeled. One complete abdominal segment is shown with anterior up, and midline dotted. *Continued*

Figure 3.4: *Cont'd.* Characterization of NB7-1-GAL4. (**B**) Quantification of percent of hemisegments expressing GFP under the control of NB7-1-GAL4 at different stages. n = number of hemisegments scored per stage. (**C**) Image of a late stage embryo showing NB7-1 and its latest born progeny in NB7-1¿Hb. Genotype is gooseberry-DBD, achaete-VP16/UAS-Hb; UAS-nls-GFP/UAS-Hb. NB7-1 is circled. (**D**) Quantification of Hb expression in NB7-1 in late stage embryos. In a majority of segments, there are GFP(+) Wor(+) Hb(+) cells, showing Hb is expressed throughout neurogenesis in NB7-1. In fewer segments, there are GFP(+) Wor(+) Hb(-) cells, in which GFP expression persists but Hb expression does not, suggesting NB7-1-GAL4 is no longer active, or there are GFP(-) Wor (+) cells in which no GFP expression exists, again suggesting that NB7-1-GAL4 is not active in NB7-1. Genotype is the same as C. (**E**–**G**) Quantification of Eve(+) neuron molecular identities in NB7-1¿Hb with different levels of Hb. (**E**) Quantification of distance from midline, which is a proxy for neuronal birth time, for Eve(+) cells with different molecular markers. For Control n = 44, 88, 283, NB7-1>1X Hb n = 284, 51, 9, NB7-1>2X Hb n = 301, 40,10, 283, 61. (**F**–**G**) Quantification of Eve(+) neurons in single hemisegments. Color code as in E. Control is w1118, NB7-1>1X Hb is NB7-1 GAL4/+; UAS-Hb/+, and NB7-1>Hb is NB7-1-GAL4/UAS-Hb; UAS-Hb/+. All images are shown in ventral view, anterior up, and lateral to the left. Scale bars represents five microns.

When Hb expression is prolonged in NB7-1, all ectopic Eve(+) cells are motor neurons

After establishing prolonged Hb expression in NB7-1 is sufficient to generate ectopic Eve(+) neurons with embryonic U1 molecular identities, we next examine the terminal features of the ectopic neurons, and in this section we focus on motor neuron identity. In Drosophila, the gold-standard for determining if a neuron is a bona fide motor neuron is to show the neuron has a cell body in the CNS and extends a neurite out of the CNS (Figure 3.5C). This distinguishes motor neurons from interneurons whose axons do not leave the CNS, and from sensory neurons whose cell bodies are in the periphery and send axons into the CNS. We make single neuron clones in both Control and NB7-1>Hb genetic backgrounds and score for CNS exit. Regardless of genotype and birth time, every labeled Eve(+) neuron sends a neurite out of the CNS (Figure 3.5A–D). As a second, independent confirmation that ectopic Eve(+) neurons in NB7-1>Hb are motor neurons, we show a vast majority of Eve(+) neurons from NB7-1 co-stain with the pan- motor neuron marker (phosopho-Mad)

(Figure 3.5E–F). We conclude that in NB7-1>Hb, Eve(+) cells are motor neurons.

There are complete and incomplete transformations of dendrite morphology when Hb expression is prolonged in NB7-1

Next, we focus on characterizing dendrite morphology of U motor neurons in NB7-1>Hb. In Control, Hb(+) U motor neurons have contralateral dendrites that cross the midline, whereas Hb(-) U motor neurons have ipsilateral dendrites that do not cross the midline (Figure 3.6A). This raises the possibility that expression of Hb in NB7-1 is sufficient to generate contralateral U motor neuron dendrite morphology. We test this by labeling single neurons in a NB7-1>Hb genetic background and examining dendrite morphology of U motor neurons. We label 79 U motor neurons and find a majority (77%) have contralateral dendrites (Figure 3.6A–D). This demonstrates that Hb expression has a major influence on dendrite morphology, but raises the question of why in NB7-1>Hb there are a mix of ipsilateral and contralateral dendrite morphologies.

In NB7-1>Hb, a small number of U motor neurons do not express Hb (Figure 3.4E), and so an attractive idea is that these Hb(-) U motor neurons may be the U motor neurons with ipsilateral dendrites. We generate a second set of individually labeled neurons (n = 39), this time staining with Hb, and find most (79%), but not all Hb(+) U motor neurons have contralateral dendrites (Figure 3.6E–F). Because Hb(+) U motor neurons are generated from NB7-1 that expressed Hb, these data show that in NB7-1>Hb, Hb expression generates both full and partial transformations of dendrite morphology.

A recent report from Kohwi et al., showed that when Hb expression is prolonged in NB7-1, there are both full and partial transformations in U motor neuron identity, as assessed by marker gene expression (Kohwi et al., 2013)[132]. Specifically, they found only five Eve(+) cells are bona fide U1/U2 motor neurons (maintain endogenous Hb expression) and that the remaining Eve(+) cells have mixed molecular identity, which is due to a nuclear architecture

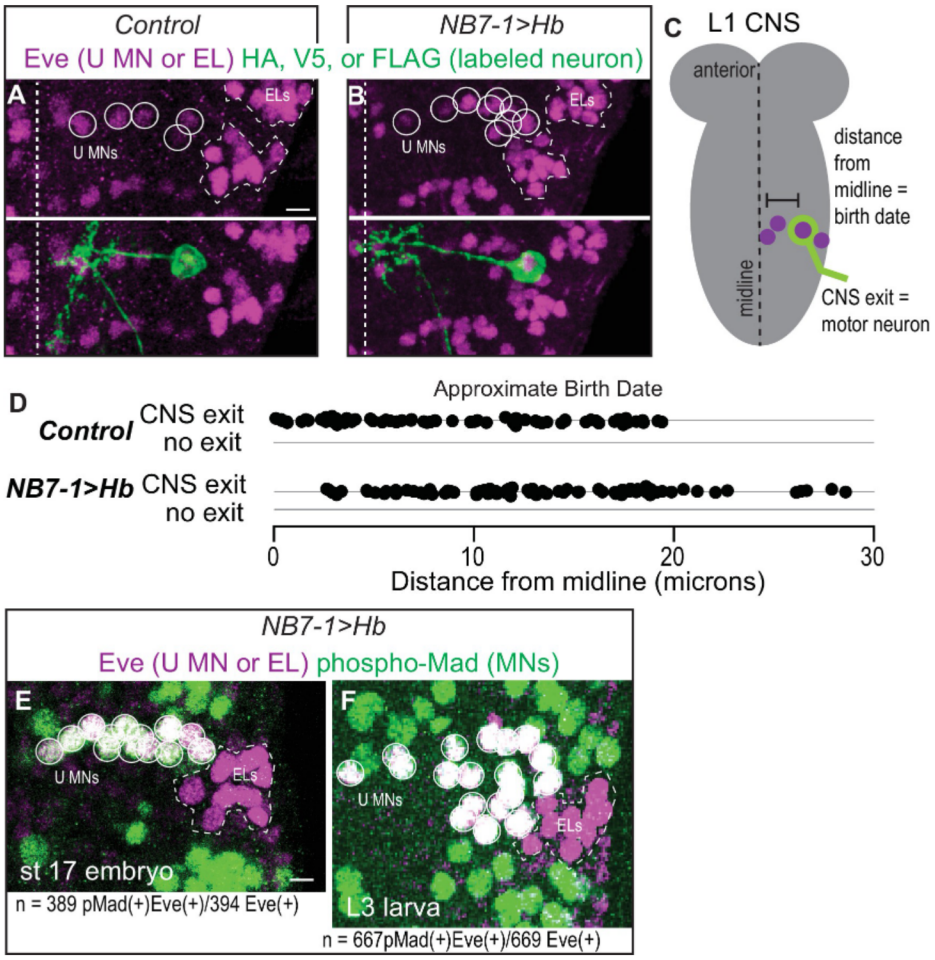


Figure 3.5: Prolonged expression of Hb in NB7-1 produces more U motor neurons. (**A**–**B**) Images of individually-labeled Eve(+) neurons in isolated first instar larvae (L1) CNSs. U motor neurons from NB7-1 are circled in white. Dotted line outlines EL interneurons (from NB3-3). Midline is dashed. (**C**) Illustration of isolated L1 CNS shows how data plotted in D were generated. Distance from the midline of stochastically labeled (green) motor neurons was measured. (**D**) Quantification of distance from midline, which is a proxy for neuronal birth time, for stochastically labeled Eve(+) cells in Control and NB7-1>Hb. Each dot represents a single neuron. Every Eve(+) neuron sends a process out of the CNS regardless of birth time. For Control n = 75, for NB7-1>Hb n=78. (**E**–**F**) Images of co-expression of Eve and the pan-motor neuron marker, pMad in NB7-1>Hb CNS of various stages. Eve(+) neurons in NB7-1 are motor neurons that survive until late larval stages. White circles outline individual U motor neurons and dotted white lines outline EL interneurons. All images are shown in ventral view, anterior up and midline to the left. Scale bars represent five microns. (A–D) Control is hsFLP; NB7-1-GAL4/+; UAS(FRT.stop)myr::smGdP-HA, UAS(FRT.stop)myr::smGdP-V5-THSUAS(FRT.stop)myr::smGdP-FLAG/+ and NB7-1>Hb is hsFLP; NB7-1-GAL4/UAS-Hb;UAS(FRT.stop)myr::smGdP-HA,UAS(FRT.stop)myr::smGdP-V5-THSUAS(FRT.stop)myr::smGdP-FLAG/UAS Hb. (E–F) NB7-1>Hb is NB7-1-GAL4/UAS-Hb; UAS-Hb/+.

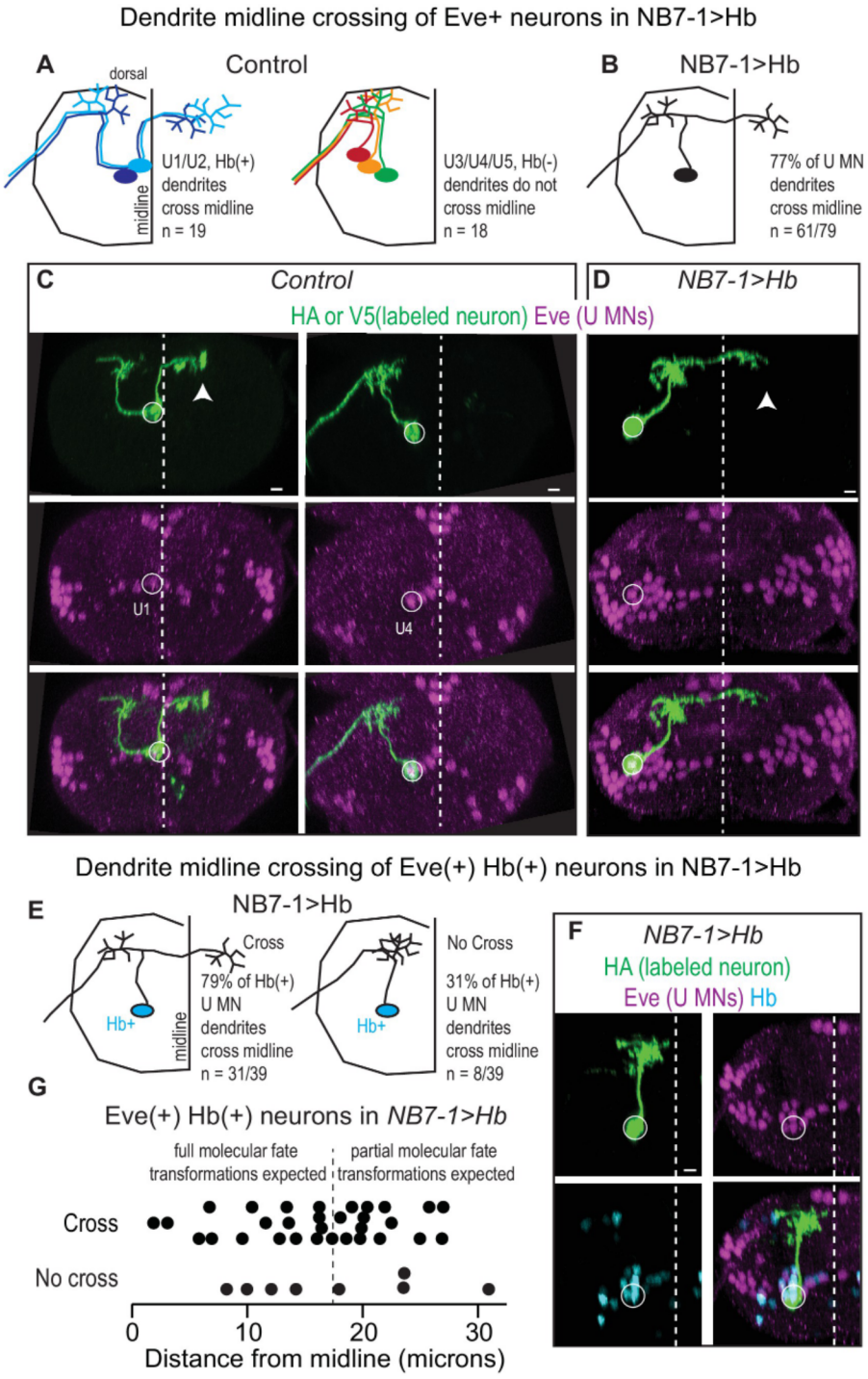


Figure 3.6: Prolonged expression of Hb in NB7-1 alters U motor neuron dendritic arbors. (**A**–**B**) Illustrations of U motor neuron dendrite morphology in Control and NB7-1>Hb shown in transverse view. In Control, light blue is U1, dark blue is U2, green is U3, orange is U4, and red is U5. In NB7-1>Hb, black is a Eve(+) U motor neuron. *Continued*

Figure 3.6: *Cont'd.* Prolonged expression of Hb in NB7-1 alters U motor neuron dendritic arbors. (**C**–**D**) Images of individually-labeled U motor neurons in the L1 CNS of Control and NB7-1>Hb. In Control, U1 has contralateral dendrites (white arrow) crossing the midline (white dotted line), whereas U4 has ipsilateral dendrites. In this NB7-1>Hb example, a contralaterally projecting U motor neuron is shown (white arrow). (**E**) Illustrations of different dendrite morphologies in NB7-1>Hb, for Hb(+) U motor neurons (blue). Most, but not all are contralateral. (**G**) Quantification of distance from midline for Eve(+) Hb(+) U MN neurons in L1 CNS of NB7-1>Hb. Black dotted line marks the distance from the midline for the lateral-most Eve(+) U motor neuron in Control (W1118), which is produced by the fifth division of NB7-1. After the fifth division of NB7-1 a nuclear remodeling event occurs. When Hb expression is prolonged in NB7-1 this remodeling event restricts the molecular fate transformations of U motor neurons born after the fifth division (Kohwi et al., 2013)[132]. (**F**) Image of Hb(+) U MN neuron dendrite morphology in L1 CNS of NB7-1>Hb. Here, in NB7-1>Hb, a Hb(+) U MN has an ipsilateral dendrite that does not cross the midline (white dotted line). All images are shown in transverse view, dorsal up, arrowheads pointing to dendrites crossing midline (white dotted line). The cell body location for labeled neurons are circled. Scale bar represents five microns. Control is hsFLP; NB7-1-GAL4/+; UAS(FRT.stop)myr::smGdPHA, UAS(FRT.stop)myr::smGdP-V5-THS-UAS(FRT.stop)myr::smGdP-FLAG/+ and NB7-1>Hb MCFO is hsFLP; NB7-1-GAL4/UAS-Hb; UAS(FRT.stop)myr::smGdP-HA, UAS(FRT.stop)myr::smGdP-V5-THS-UAS(FRT.stop)myr::smGdP-FLAG/UAS-Hb.

remodeling event in the neuroblast that occurs after the fifth division. We reason that remodeling of nuclear architecture might also explain partial transformation of U motor neuron dendrite morphology. If true, we expect that in NB7-1>Hb, Hb(+) U motor neurons born before the fifth division would have contralateral dendrites, and those born after the fifth division would have ipsilateral dendrites. We measure distance from midline of the cell body for each Hb(+) U motor neuron as a proxy for neuron birth time, plot dendrite morphology versus distance from midline, but find no association (Figure 43.6G). These data show that although prolonged expression of Hb generates partial transformations in dendrite morphology, changes in NB7-1 nuclear architecture are unlikely to account for this phenomenon. Furthermore, these data demonstrate that embryonic U motor neuron marker gene expression does not accurately predict U motor neuron dendrite morphology.

Prolonged expression of Hb shifts the distribution of neuromuscular synapses on dorsal muscles

Next, we ask to what extent does U motor neuron marker gene expression predict U motor neuron-to-muscle synaptic partnerships. Based on characterization of U motor neuron neuromuscular synapses in wild type larvae (Figure 3.7A) and on the average number of U motor neurons expressing markers of U1 through U5 embryonic identities in NB7-1>Hb embryos (Figure 3.3), we make the following predictions about neuromuscular synapses in NB7-1>Hb larvae (Figure 3.7B): MN3-1b and MN4-1b synapses should be absent because there are almost no U motor neurons with U4 and U5 molecular identities in NB7-1>Hb embryos. There should be MN9-1b, MN10-1b and MN2-1b branches, and of these there should be many more MN9-1b synaptic branches than MN10-1b and MN2-1b branches because there are more neurons with U1 identities than U2 and U3 identities in NB7-1>Hb embryos. To test these predictions, we assay mature circuit wiring in NB7-1>Hb larvae by labeling all neuronal membranes, including nerves and neuromuscular synaptic terminals (Figure 3.7C–H). We count the number of type 1b branches on dorsal muscles because in wild type larvae, U motor neurons make type 1b synapses on dorsal muscles. Notably, this method allows us to look at the population of motor neurons, not just individually-labeled neurons, as described above.

Our hypothesis predicts that in NB7-1>Hb larvae, MN3-1b and MN4-1b synapses should be absent. In wild type larvae, U motor neurons and other neurons exit the CNS and travel to the dorsal muscles through the Intersegmental Nerve (ISN), and U5 and U4 each have unique and reproducible nerve exit sites off of ISN before making MN4-1b and MN3-1b synapses, respectively (Figure 3.7A). In NB7-1>Hb animals there is a lack of normal nerve exits from ISN onto muscles 3 and 4 (Figure 3.7B,G–H). Thus, our data are in general agreement with our prediction, but we note two differences. First, there are no normally placed MN4-1b branches, and instead branches are reduced rather than eliminated (Figure 3.7K).

In Drosophila, when a ventral motor neuron is eliminated by laser ablation, other motor neurons excessively branch to innervate the target muscle of the ablated neuron (Chang and Keshishian, 1996)[104]. Thus, in NB7-1>Hb, we suspect that non U-motor neurons are the source of the MN4-1b branches. To test this idea, we ablate U-motor neurons using a U motor neuron specific GAL4 line to express pro-apoptotic genes. In this manipulation, the number and placement of MN4-1b branches is indistinguishable from that seen in NB7-1>Hb (Figure 3.8). We consider this phenotype to be an example of compensation, which occurs when a muscle is under innervated. The second difference between our prediction that in NB7-1>Hb, MN4-1b and MN3-1b should be absent, is that there are often synaptic branches found dorsally on muscle 3 rather than at the normal ventral location (arrow, Figure 3.7B,E–H). These abnormally located synapses are found adjacent to muscles (muscles 10 and 2 see below) that are hyper-innervated. It is likely that this phenotype occurs when a muscle has too many synapses on it, and some synapses spill over onto nearby muscles. We conclude that prolonged expression of Hb in NB7-1 can force U motor neurons to bypass the normal nerve exit point that leads to muscles 3 and 4, but that in NB7-1>Hb, there are still 1b synapses on muscles 3 and 4 likely due to compensation and spillover.

A second prediction is that in NB7-1>Hb, there should be many MN9-1b synaptic branches and fewer MN10-1b and MN2-1b synapses. We find significant increases in MN9-1b, MN10-1b and MN2-1b branch number (Figure 3.7K). Counter to our prediction, there are significantly more MN10-1b branches than MN9-1b branches (Figure 3.7B–F,K). To confirm that this unexpected phenotype is not due to an unknown role of Hb in promoting excessive branching of U motor neurons, we do two follow up experiments. First, we express Hb in post-mitotic U motor neurons and find no increase in synapse branching (Figure 3.7J). Second, we confirm that in NB7-1>Hb animals, each U motor neuron generates one or two synaptic branches, as in wild type (Figure 3.7L–N). In summary, our data reveal an unexpectedly large number of MN10-1b branches on muscle 10 (U2 target) and an unexpect-

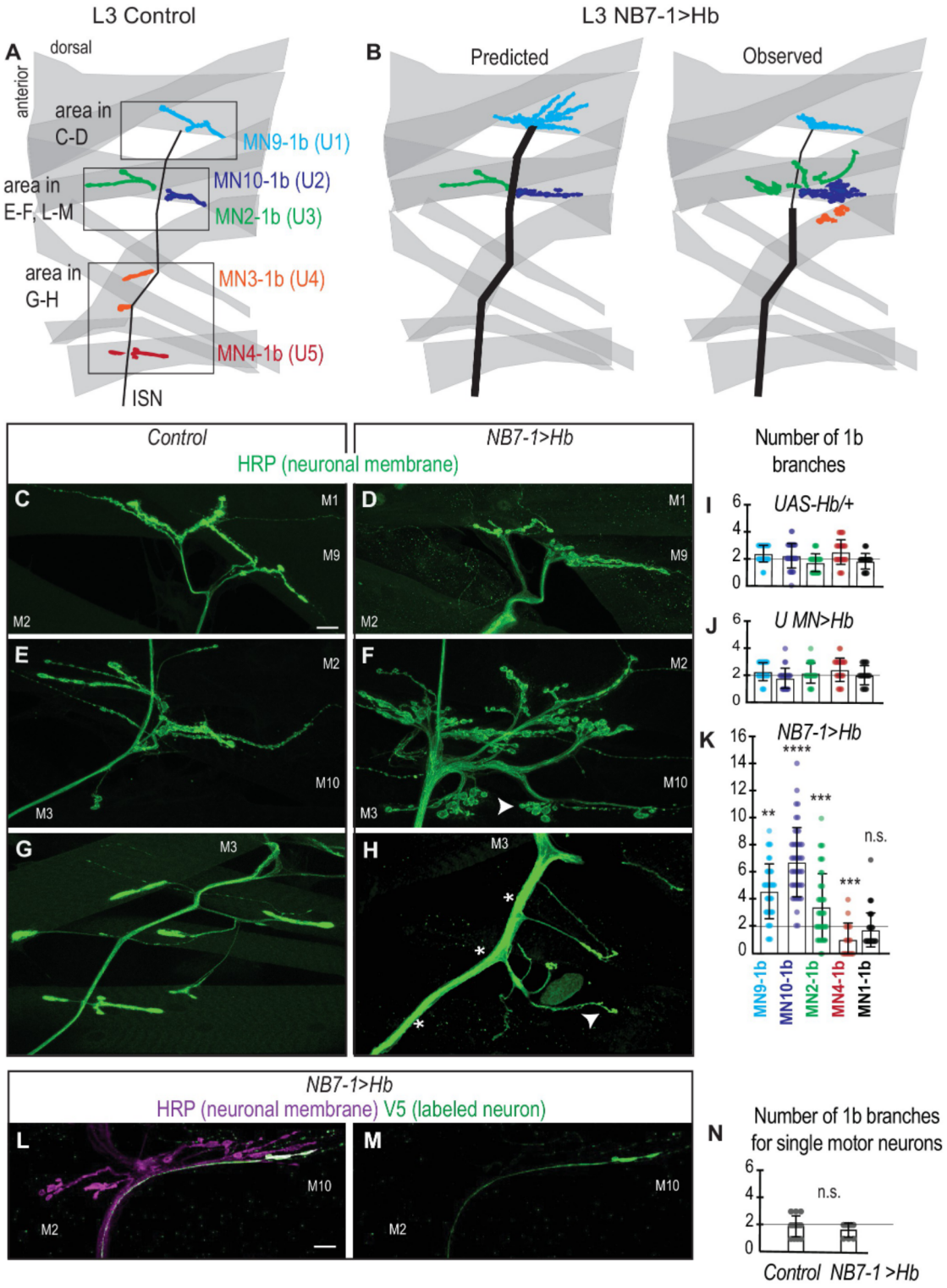


Figure 3.7: Prolonged expression of Hb in NB7-1 alters U motor neuromuscular synapses. (**A**–**B**) Illustrations of neuromuscular synapses on dorsal muscles in a L3 body wall segment. Control synapses are based on third instar larval MCFO data (see Figure 1—figure supplement 13.2). *Continued*

Figure 3.7: *Cont'd.* Prolonged expression of Hb in NB7-1 alters U motor neuromuscular synapses. In NB7-1>Hb, predicted neuromuscular synapses are inferred from Control neuromuscular wiring patterns and from NB7-1>Hb embryonic molecular identity data (see Figure 23.3). Observed neuromuscular synapses are described in C-H. ISN is intersegmental nerve. (**C**–**H**) Images of neuronal membrane—both axons and neuromuscular synapses—on dorsal muscles in L3 bodywall segments. Arrow indicates branching onto M3. An asterisk * indicates missing synapses. Data quantified in (I–K). (**I**–**K**) Quantification of the number of 1b branches on L3 muscles. Color code as in (A). Line intersects the y-axis at 2. Each dot represents the number of branches onto a single muscle. (I) For UAS-Hb/+ n = 32, 35, 33, 36, 36, (J) For U MN>Hb n=11, 11, 11, 12, 11, (K) For NB7-1>Hb n=39, 46, 44, 18, 46, numbers listed from MN9-1b to MN1-1b. (**L**–**M**) Images of all neuronal membrane (magenta) on dorsal muscles in L3 bodywall segments of NB7-1>Hb with a single U motor neuron labeled (green). (**N**) Quantification of the number of 1b branches from individual U motor neurons on dorsal L3 muscles in Control and NB7-1>Hb. Line intersects the y-axis at two branch number. For WT n = 13, NB7-1>Hb n=8. All images are shown dorsal up, anterior left. Scale bars represent 10 microns. Control is w1118 (C, E, G), or hsFLP; OK6-GAL4/+; UAS-MCFO/+ (N). UAS-Hb/+ is UAS-Hb/+, UAS-Hb/+. U MN>Hb is CQ2-GAL4/UAS-Hb; CQ2-GAL4/UAS-Hb. NB7-1>Hb is NB7-1-GAL4/UAS-Hb; UAS-Hb/+ (D–H, K) and hsFLP; Vglut-lexA/NB7-1-GAL4; lexAop-FRT-stop-FRT-EGFP/UAS-Hb (L–N). For quantifications average and standard deviation are overlaid. ANOVA, corrected for multiple samples 'ns' not significant, '**' $p<0.05$, '***' $p<0.001$, '****' $p<0.0001$.

edly low number of MN9-1b branches on muscle 9 (U1 target). These data show that Hb has profound effects on neuromuscular synapse formation and suggest that U motor neuron embryonic molecular identity does not accurately predict neuromuscular partner.

Our reason for examining the ability of Hb to control terminal features is to connect early developmental programs with circuit assembly. Therefore, it is important to determine the extent to which the synaptic branches in NB7-1>Hb contained functional synapses. To characterize the NB7-1>Hb neuromuscular synapses, first in fixed tissue L3 fillets, we stain for a panel of synaptic marker proteins. There is normal abundance and localization of pre-synaptic markers—for active zones (Brp), stable microtubule loops (Fustch), and synaptic vesicles (Syn)—as well as post-synaptic markers—for post-synaptic density (DLG) and neurotransmitter receptors (GluRIIA) (Figure 3.9A–G). Thus, on the cell biological level, neuromuscular synapses in NB7-1>Hb are not different from Control. In addition, we

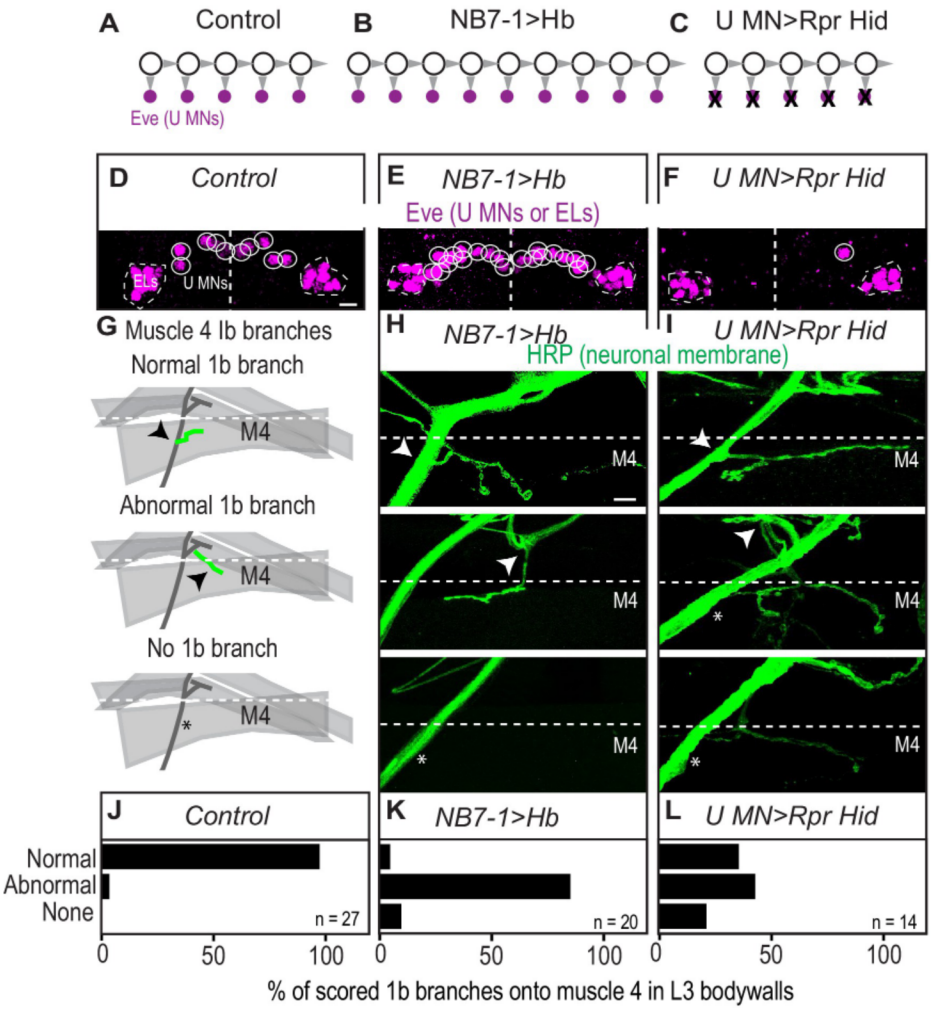


Figure 3.8: U Motor neuron ablation.(**A**–**C**) Illustration of the number of Eve(+) U motor neurons in (A) Control, (B) NB7-1>Hb and (C) U motor neuron ablated genotype, U MN>Rpr Hid. NB7-1 is represented by large circles. Each gray arrowhead represents cell division. Small magenta circles represent Eve(+) U motor neurons. Black Xs represent cell death. (**D**–**F**) Images of Eve(+) U motor neurons in late stage embryo CNS segments with midline running through the middle (white dotted line). U motor neurons from NB7-1 are circled in white. Dotted line, outlines EL interneurons (from NB3-3). (**G**) Illustration of scored branch point of 1b branches on L3 muscle 4 (M4). Arrow indicates branch point from intersegmental nerve on m 4.* indicates missing branches. Dotted line represents dorsal edge of muscle 4 (see H-I). (**H**–**I**) Images of neuronal membrane on L3 muscle 4 (M4). Markings same as in G. (**J**–**L**) Quantification of the percentage of total 1b branches that were scored as either normal, abnormal, or absent on L3 muscle 4 (see G-I). n = number of total branches that were scored. Images in (D–F) are shown in ventral view, anterior up, lateral left. Scale bar represents five microns. Images in (H–I) are shown dorsal up, anterior left. Scale bar represents 10 microns. Control is w1118. NB7-1>Hb is NB7-1/+; NB7-1/UAS-Hb. U MN>RPR HID is UAS-Rpr Hid; CQ2-GAL4/+; CQ2-GAL4/+.

visualize neuromuscular synapse activity with a post-synaptically localized calcium sensor (Newman et al., 2017)[133]. In L3 larval fillets, we image spontaneous release of individual synaptic vesicles from 1b branches on muscles 1, 2, 9, and 10. In both Control and NB7-1>Hb animals, within a five-minute imaging period, we find at least one post-synaptic response in every 1b synaptic branch on every muscle imaged (Control [n = 6] and NB7-1>Hb [n = 5] Figure 6H–I and Figure 6—figure supplement 1). We conclude in NB7-1>Hb, extra branches on dorsal muscles contain functional synapses. Taken together this demonstrates that prolonged expression of the temporal transcription factor, Hb, in single neuroblast lineage has profound effects on functional circuit wiring.

U motor neuron embryonic molecular identity and neuronal birth time do not accurately predict axonal targeting

Our neuromuscular synapse data strongly suggests that U motor neuron embryonic molecular identity does not accurately predict neuromuscular partnerships in NB7-1>Hb. We test this idea by labeling single neurons in late stage embryos, tracking axonal trajectories, and staining for embryonic U motor neuron molecular markers. Specifically we stain for Hb and Zfh2, which together distinguish U1 (Hb[+] Zfh2[-]), U2-U3 (Hb[+] Zfh2[+]), and U4-U5 (Hb[-] Zfh2[+]). We label 18 single neurons in NB7-1>Hb and find five examples where embryonic identity and axonal trajectory match as in wild type, and 13 examples where neurons with U1 identities innervate either muscle 10 or 2 (Figure 3.10A–B'). This provides direct evidence that driving Hb with NB7-1-GAL4 results in both full and partial transformations in axonal trajectory.

Next, we ask why molecular identity does not accurately predict axonal target in NB7-1>Hb. An attractive model is that in NB7-1>Hb, first-born U1 neurons reach muscle 9, make synapses on the muscle and the muscles become 'occupied', and so that later-born U1 neurons instead of synapsing on muscle 9 make synapses on muscle 10. This model predicts

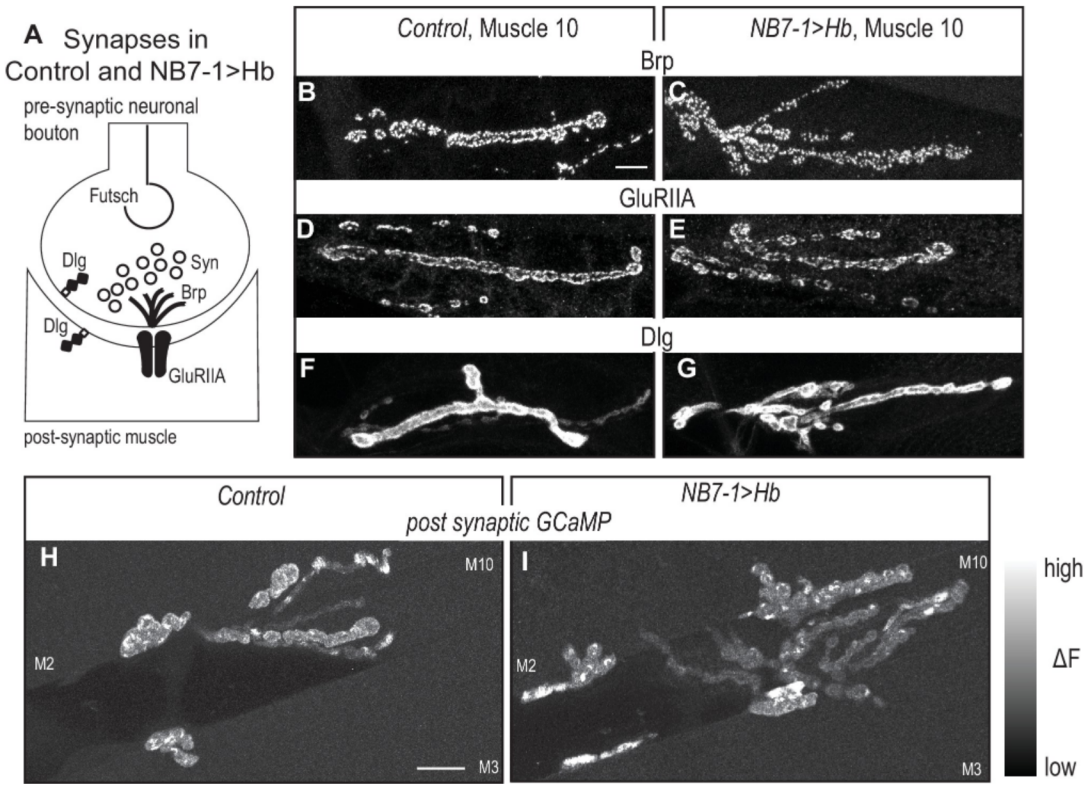


Figure 3.9: Altered synaptic arbors on dorsal muscles contain functional synapses. (**A**) Illustration of subcellular localization of neuromuscular synapse markers. Futsch labels microtubules; Synapsin (Syn) labels neurotransmitter filled synaptic vesicles; Brunchpilot (Brp) labels active zones; Glutamate Receptor IIA (GluRIIA) labels neurotransmitter receptors; Discs large (Dlg) is a scaffolding protein. (**B**–**G**) Images of neuromuscular synapses on L3 muscle 10. There is no difference in distribution or abundance of synaptic markers between Control (w1118) and NB7-1>Hb (NB7-1-GAL4/UASHb, UAS-Hb/+). (**H**–**I**) Images of fluorescence intensity changes in a calcium indicator of synaptic activity. GCaMP was targeted to the post-synaptic density for example (DLG in F-G). When pre-synaptic vesicles are released from active zones (Brp in B-C) post-synaptic neurotransmitter receptors respond (GluRIIA in D-E), increasing GCaMP fluorescence intensity (see Figure 6—figure supplement 1 for details). Images show post-synaptic responses (delta F) in L3 muscles 2, 3, and 10 (M2, M3, M10) in Control (NB7-1-GAL4/+; MHC-CD8-GCaMP6f-Sh/+) and NB7-1>Hb (NB7-1 GAL4/UAS Hb; MHC-CD8-GCaMP6f-Sh/UAS Hb) over a 5 min imaging period. All images are shown dorsal up, anterior to the left. Scale bar represents 10 microns.

a correlation between the birth time of a neuron and its synaptic partner. We generate a second set of singly labeled U motor neurons (n = 52) in a NB7-1>Hb genetic background, and score both the cell body distance from midline and axonal targets. These data reveal no strong correlation between the birth time of a neuron and its axonal target (Figure 3.10C–D). They suggest that muscle occupancy as well as other time-linked factors such as changes in nuclear architecture do not strongly influence U motor neuron axon targeting in NB7-1>Hb.

Molecular cues inherited from the neuroblast can convey wiring specificity

We were puzzled as to why prolonged expression of Hb in NB7-1 is sufficient to generate a large number of U motor neurons with U1 embryonic molecular identities, but yet these neurons do not always project axons to, and make synapses with, 9. One possibility is that in NB7-1>Hb, Hb expression may not fully transform Eve(+) neurons into bona fide U1 motor neurons. To test this, we screen all available embryonic U motor neuron molecular markers for expression in U motor neurons at late (L3) larval stages. In wild type, U1 and U2 maintain Hb expression, indicating that expression of Hb at L3 is a marker for U1/U2 temporal identity (Figure 3.11A,C,D). In NB7-1>Hb, we stain for Hb at L3, and often found two, and rarely three, bona fide Hb(+) U1/U2 motor neurons (Figure 3.11E,F), even though in late stage embryos, U motor neurons in NB7-1>Hb expressed Hb as well as other markers of U1/U2 embryonic molecular identity (Figure 3.11C). We conclude that in NB7-1>Hb, prolonged Hb in NB7-1 is only sufficient to transiently transform U motor neurons into U1 neurons.

Next, we wonder if increasing the expression level of Hb in NB7-1 increases the number of bona fide U1/U2 motor neurons at late larval stages. We increase Hb expression by raising NB7-1>Hb embryos at higher temperature or increasing transgene copy number, and confirm the efficacy of these manipulations by showing slightly higher average number of Eve(+) neurons at L3 (Figure 3.11G). However, there is absolutely no change in the number of

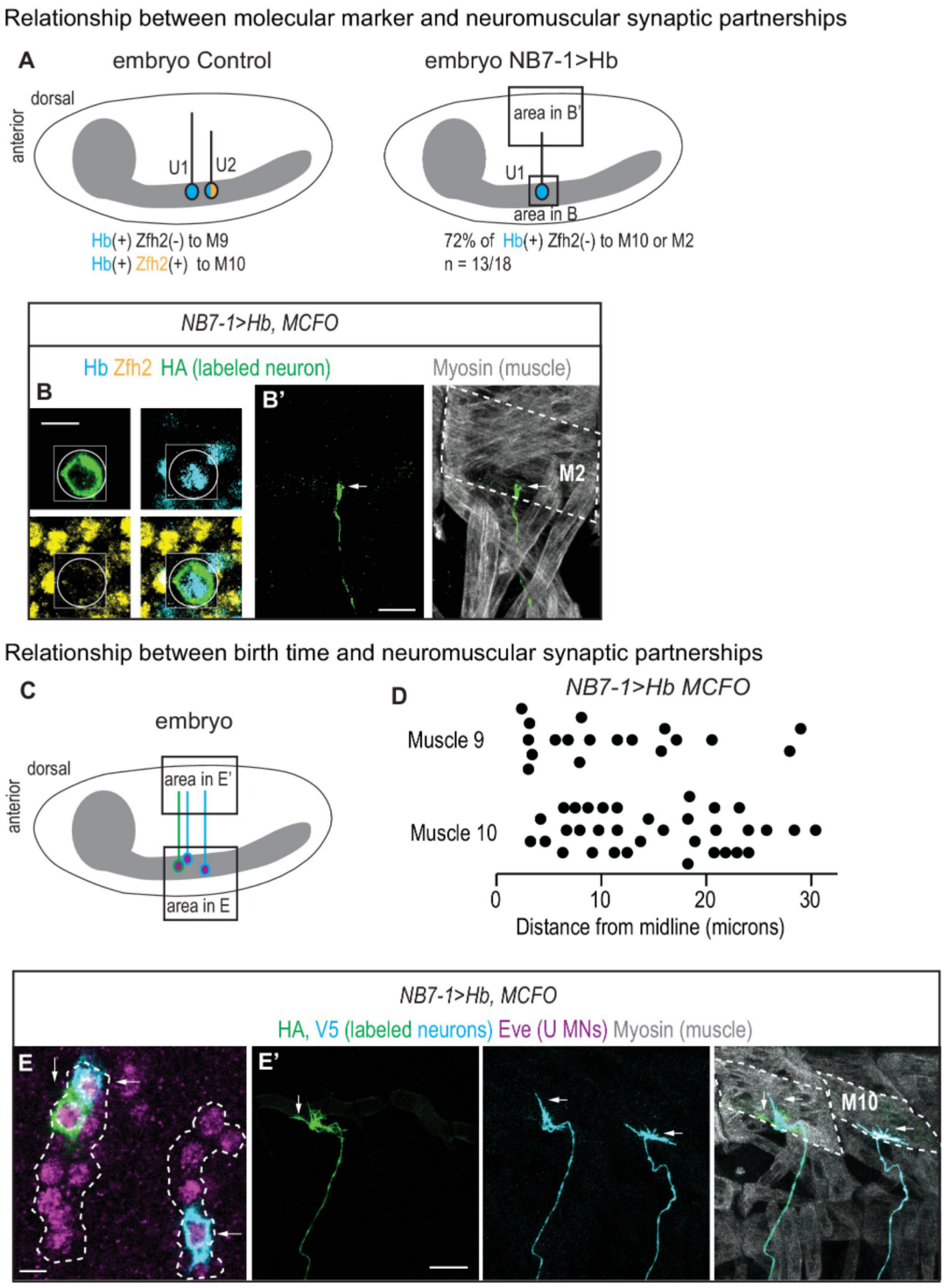


Figure 3.10: U motor neuron axonal trajectories are not accurately predicted by embryonic molecular identity or birth timing. (**A**) Illustrations of Drosophila late stage embryos, CNS is gray. In Control, Hb(+) and Zfh2(-) neurons (U1) send axons to muscle 9, and Hb(+) Zfh2(+) neurons (U2) send axons to muscle 10. Whereas in NB7-1>Hb, Hb(+) Zfh2(-) (U1) neurons often send axons to muscle 10 or muscle 2. *Continued*

Figure 3.10: *Cont'd.* U motor neuron axonal trajectories are not accurately predicted by embryonic molecular identity or birth timing. (**B**–**B'**) Images of an individually-labeled U motor neuron in a late stage, whole-mount, NB7-1>Hb embryo in ventral (B) and lateral views (B'). An individual Hb(+) (cyan) Zfh2(-) (yellow) cell is labeled with MCFO (circled). Boxes are neurons from different z-planes. (B') The labeled U motor neuron axon projects (arrow) to muscle 2 (M2, dotted). (**C**) Illustration of a Drosophila late stage embryo. In NB7-1>Hb, U motor neurons at different positions along the medio-lateral axis all send axons to dorsal-most muscles, muscles 9 and 10. (**D**) Quantification of distance from midline, which is a proxy for neuronal birth time, for individual Eve(+) U motor neurons labeled with MCFO. Dots represent single neurons. For muscle 9 and muscle 10, n = 18, 34, respectively. (**E**–**E'**) Images of a late stage, whole-mount, NB7-1>Hb embryo shown in ventral (E) and lateral (E') views. (E) There are >5 U motor neurons from NB7-1 in each hemisegment (dotted line), three of which are labeled by MCFO. (E') Axons from Eve(+) cells project to muscle 10 (M10, dotted). Vertical and horizontal arrows point to the same HA(+) and V5(+) cells, respectively (E–E'). Images in (B,E) are shown lateral up, anterior to the left. Images in (B',E") are shown with dorsal up, anterior to the left. Scale bar represents five microns for B and E. Scale bar represents 10 microns for B' and E'. NB7-1>Hb, MCFO is hsFLP; NB7-1-GAL4/UASHb; UAS(FRT.stop)myr::smGdP-HA, UAS(FRT.stop)myr::smGdP-V5 THSUAS(FRT.stop)myr::smGdP-FLAG/UAS-Hb.

Hb(+) Eve(+) neurons at L3 (Figure 3.11G). These data suggest the existence of a lineage intrinsic mechanism present after the second division of NB7-1 that restricts the ability of Hb to permanently transform U motor neurons into bona fide U1/U2 neurons. Furthermore, these data demonstrate that in NB7-1>Hb, neurons with embryonic U1 molecular marker gene expression are a heterogeneous population.

Next, we test the idea that heterogeneity in embryonic U motor neurons in NB7-1>Hb, can explain why some neurons with U1 molecular markers make synapses onto 9, while others make synapses elsewhere. First, to test this idea at L3, we individually-label U motor neurons, stain with Hb, and characterize neuromuscular synaptic partnerships (Figure 3.11I–K). A majority (n = 7) of the individually-labeled U motor neurons in this dataset are Hb(-) and are therefore not bona fide U1/U2 motor neurons. All of these neurons project to 10 (U2 target). There is one Hb(+) bona fide U1/U2 motor neuron, which targets the 9 (U1 target). Next, for each hemisegment, we score the number of Hb(+) U motor neurons at L3 and the number of synaptic branches on s 9 and 10. We pool data for all segments with three

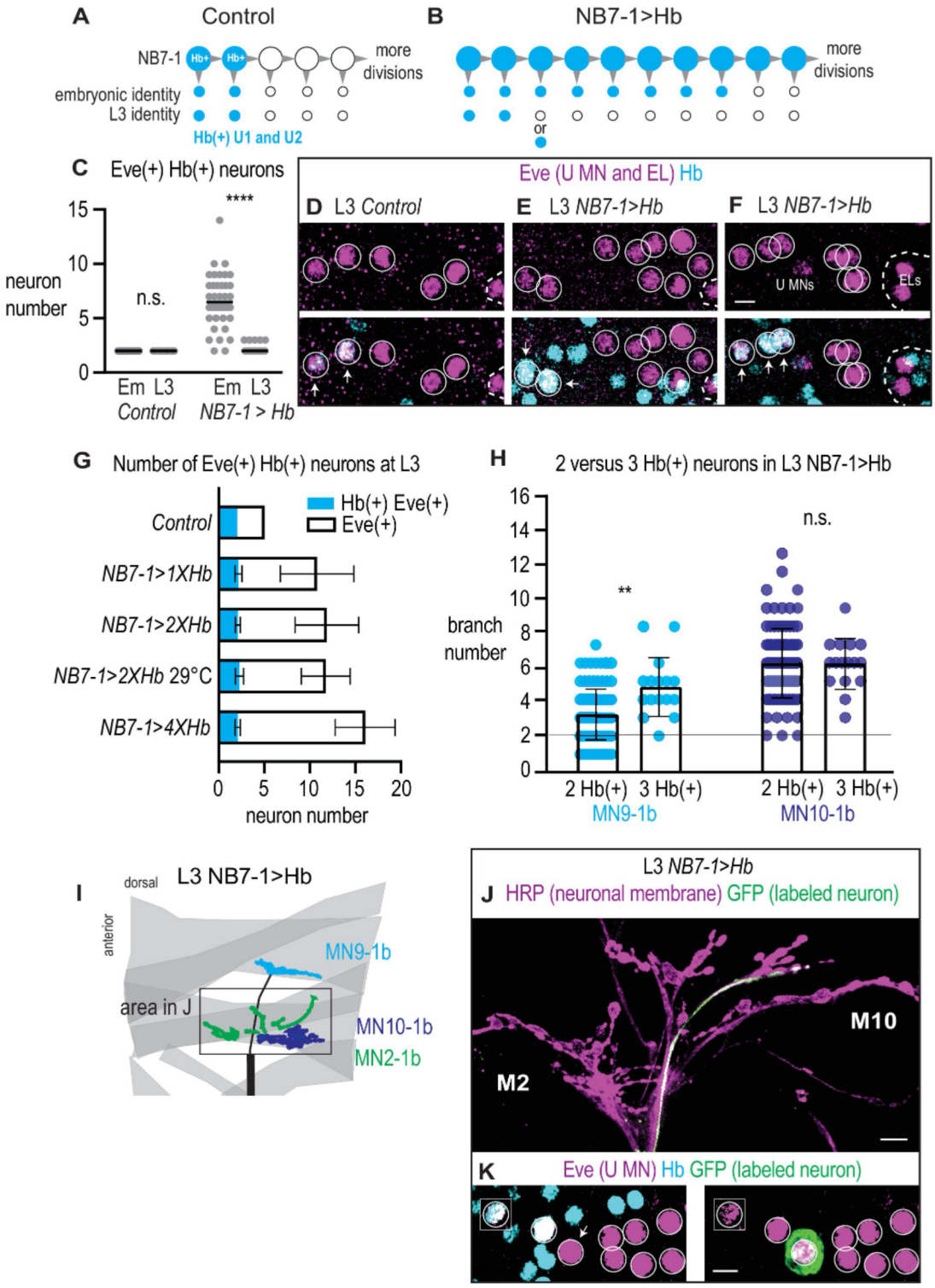


Figure 3.11: In NB7-1>Hb, U1 motor neuron identity is only transiently specified. (**A**–**B**) Illustrations of the divisions of NB7-1 in Control and in NB7-1>Hb. Each gray arrowhead represents cell division, large circles represent NB7-1. The top row of small circles represent U motor neurons in late stage embryos and the bottom row represent U motor neurons in L3. *Continued*

Figure 3.11: *Cont'd.* In NB7-1>Hb, U1 motor neuron identity is only transiently specified. In Control, two neurons are Hb(+) (blue) at both stages, whereas in NB7-1>Hb many neurons are Hb(+) in embryos, but by late L3 there only two or three Hb(+) neurons. (**C**) Quantification of Eve(+) Hb(+) U motor neurons at two different stages: late stage embryos (Em) and late stage larvae (L3), n = 36, 28, 38, 84 from left to right. (**D**–**F**) Images of molecular identity, Hb(+), expression in isolated third instar larvae (L3) CNS. Eve(+) U motor neurons from NB7-1 are circled in white and co-localization with Hb(+) is shown (arrows). Dotted line outlines EL interneurons (from NB3-3). Data quantified in (G). (**G**) Quantification of Eve(+) Hb(+) U motor neuron (blue) number and total Eve(+) U motor neurons (white) neuron number at L3. Altering Hb expression level in NB7-1 by changing transgene copy number and temperature has little effect on the total number of Eve(+) neurons and has no effect on the number of Hb(+) Eve(+) neurons. For Control n = 28, NB7-1>1X Hb n = 68, NB7-1>2X Hb n = 84, NB7-1>2X Hb 29 °C n = 27, NB7-1>4X Hb n = 12. (**H**) Quantification of the number of 1b branches onto L3 muscle 9 and muscle 10 in NB7-1>Hb manipulations with either 2 or 3 Hb(+) Eve(+) U motor neurons. Line intersects the y-axis at two branch number. For MN9-1b 2 Hb(+) neurons n = 98, MN9-1b 3 Hb(+) neurons n = 16, MN10-1b 2 Hb(+) neurons n = 98, MN10-1b 3 Hb(+) neurons n = 16. (**I**) Illustration of neuromuscular synapses on dorsal L3 muscles in NB7-1>Hb. Black box marks area in J. A single labeled Hb(+) Eve(+) neuron projects to muscle 9, whereas seven single-labeled Hb(-) Eve(+) neurons project to muscle 10. (**J**–**K**) Images of a single-labeled U motor neuron in NB7-1>Hb. Eve(+) Hb(-) U motor neuron (K) projects to muscle 10 (J). Boxes are insets from a different focal plane (K). U motor neurons are circled. Images in (D–F,K) are shown in ventral view, anterior up, and midline to the left. Image in (J) are shown dorsal up anterior to the left. Scale bar represents five microns (D–F, K), and 10 microns for (J). Genotypes: Control is w1118. NB7-1>1X Hb is NB7-1-GAL4/+; UAS-Hb/+. NB7-1>2X Hb is NB7-1-GAL4/UAS-Hb; UAS-Hb/+, and NB7-1>4X Hb is NB7-1-GAL4/UAS-Hb; NB7-1-GAL4/UAS-Hb (for C-H). For I-K NB7-1>Hb is hsFLP; Vglut-lexA/NB7-1-GAL4; lexAop-FRT-stop-FRT-EGFP/UAS-Hb. For quantifications dot is number of 1b branches onto a specified muscle within a bodywall hemisegment. Average and standard deviation are overlaid. ANOVA, corrected for multiple samples. Un-paired t-tests. '**' $p<0.05$.

Hb(+) U motor neurons and pool data for all segments with two Hb(+) U motor neurons, and find a significant increase in 9 branches in hemisegments with three versus two Hb(+) neurons (Figure 3.11H). These data show that molecular differences in U motor neurons at L3 correlate with neuromuscular targeting.

Because we find a positive correlation between the number of Hb(+) U motor neurons at L3 and the number of branches on muscle 9, we next alter the number of Hb(+) U motor

neurons using different molecular manipulations, and then assay neuromuscular synaptic partnerships. We screen through a number of manipulations and find two that alter the number of Hb(+) U motor neurons in L3 larvae. First, when we express a wild-type Hb protein tethered to the transcriptional activation domain VP16 (NB7-1>VP16::Hb), in NB7-1 we see an increase in the number of Hb(+) neurons, reaching on average nearly 5 Hb(+) U motor neurons (Figure 3.12B,D,F). Note, that unlike NB7-1>Hb, in NB7-1>VP16::Hb the total number of Eve(+) neurons does not increase, consistent with previous publications (Tran et al., 2010)[131]. Second, we precociously express the Hb switching factor, Seven-up in NB7-1 and other neuroblasts, using the strong EN-GAL4 driver (EN>SVP), and we find a reduction in both the total number of U motor neurons and the number of Hb(+) U motor neurons at L3, finding on average just one Hb(+) U motor neuron per hemisegment (Figure 3.12C,E,F). Together these data show that genetic manipulations in NB7-1 can permanently alter the expression of Hb in U motor neurons.

Next, in both EN>SVP and in NB7-1>VP16::Hb, we characterize the number of Hb(+) U motor neurons versus the number of muscle 9 and muscle 10 neuromuscular synapses in L3 larvae. Within each genetic background, we pool data based on the number of L3 Hb(+) U motor neurons and then plot the number of synaptic branches on muscles 9 and 10. We find a strong correlation between the number of L3 Hb(+) U motor neurons and the number of synaptic branches on muscle 9 (Figure 3.12G–M). In contrast, there is no significant change in the number of synaptic branches onto muscle 10. Taken together these data demonstrate early manipulation of gene expression in NB7-1 is sufficient to permanently alter the molecular identity of U motor neurons and to predictably re-wire the neuronal circuits to which they contribute.

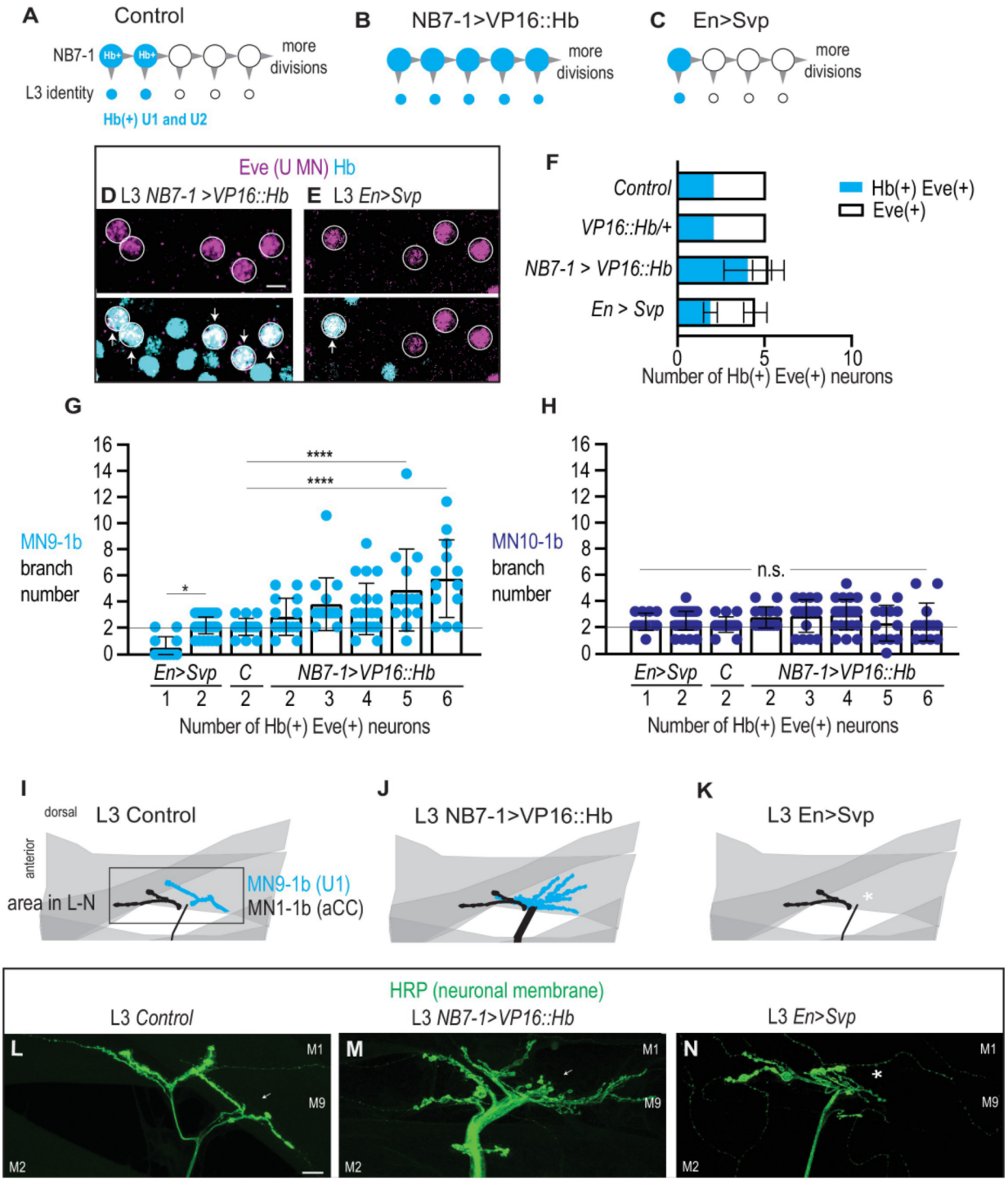


Figure 3.12: Altering the number of Hb(+) U motor neurons at L3 is correlated with synaptic partnerships. (**A**–**C**) Illustrations of the divisions in NB7-1 in Control, NB7-1>VP16::Hb, and En>Svp. Each gray arrowhead represents cell division, large circles represent NB7-1. Row of small circles represent U motor neuron identity at L3. In Control, two neurons are Hb(+) (blue), in NB7-1>VP16::Hb most neurons are Hb(+), and in En>Svp, only one Hb(+) remains. *Continued*

Figure 3.12: *Cont'd.* Altering the number of Hb(+) U motor neurons at L3 is correlated with synaptic partnerships. (**D**–**E**) Images of molecular identity, Hb(+), expression in isolated third instar larvae (L3) CNS, shown in ventral view, anterior up, and midline to the left. Eve(+) U motor neurons from NB7-1 are circled in white and co-localization with Hb(+) is shown (arrows). In NB7-1>VP16::Hb there are five Hb(+) Eve(+), whereas in En>Svp there are two (arrows). Data quantified in (F). (**F**) Quantification of Eve(+) Hb(+) U motor neuron (blue) number and total Eve(+) U motor neurons (white) neuron number at L3. Expressing an activated form of Hb in NB7-1 (NB7-1>VP16::Hb) has little effect on the total number of Eve(+) neurons but increases the number of Hb(+) Eve(+) neurons. Expressing a switching factor, Svp in NB7-1 (En>Svp) can decrease the total number of Eve (+) neurons by one and decrease the total number of Hb(+) Eve(+) neurons by one. For Control n = 28, VP16::Hb n = 29, NB7-1>VP16::Hb n = 65, En>Svp n=70. (**G**–**H**) Quantification of the number of 1b branches onto muscle 9 and muscle 10. C. stands for Control. Line intersects the y-axis at two branch number. Number of Eve-expressing neurons are shown below each genotype. For columns left to right n = 12,44,16,14,16,21,14,13, (G) n = 12,43,17,14,15,21,13,13 (H). (**I**–**K**) Illustrations of neuromuscular synapses on L3 dorsal muscles 1 and 9. Black box marks area imaged in L-N. MN1-1b (black) comes from a non-U Motor neuron called aCC. (**L**–**N**) Images of neuronal membrane—both axons and neuromuscular synapses—on L3 dorsal muscles shown dorsal up, anterior left of Control (W1118) (L), NB7-1>vp16::Hb (NB7-1-GAL4/UAS-vp16::Hb; UAS-vp16::Hb/+) (M), and En>Svp1 (Engrailed-GAL4/UAS-svp1) (N). Arrow indicates branching onto muscle 9 (M9). An asterisk * indicates missing synapse. Scale bar represents five microns for E-F. Scale bar represents 10 microns for L-N. Control (W1118), vp16::Hb (UAS-vp16::Hb/+; UAS-vp16::Hb/+), NB7-1>vp16::Hb (NB7-1-GAL4/UAS-vp16::Hb; UAS-vp16::Hb/+), En>Svp1 (Engrailed-GAL4/UAS-svp1). For quantifications, each dot represents the number of 1b branches onto a specified muscle within a bodywall hemisegment that corresponds to a hemisegment with specified number of Hb(+) neurons. Black bars are averages. Error bars represent standard deviation. ANOVA, corrected for multiple samples. Un-paired t-tests. '*' p=0.02, '****' p<0.0001, n.s. (not significant).

3.2.4 Discussion

The existing model in the field is that temporal transcription factors are master regulators of entire developmental programs that are linked to a neuron's birth time (Allan and Thor, 2015)[74]. For example, it is often said that high expression of Hb in NB7-1 is both necessary and sufficient to specify U1 motor neurons fates, where fates have been taken to mean both embryonic molecular identity as well as terminal neuronal features, such as axonal trajectory (Isshiki et al., 2001; Pearson and Doe, 2003) [68, 102](Figure 3.13A). From the

perspective of circuit assembly, this suggests that manipulating temporal transcription factor expression in a given stem cell should predictably alter the wiring of neuronal progeny. However, recent work has introduced important refinements to the existing model, showing that prolonged expression of Hb is only sufficient to generate five bona fide U1/U2 motor neurons by embryonic molecular marker expression (Kohwi et al., 2013)[132]. After five divisions, NB7-1 continues to produce U motor neurons, but the molecular identity of these later-born U motor neurons is mixed. The limited production of bona fide U motor neurons has been linked to the closing of a competence window in NB7-1 mediated by a nuclear remodeling event (Kohwi et al., 2013)[132]. The biological relevance of this nuclear remodeling event has never been explored. Furthermore, the existence of this nuclear remodeling event highlights the idea that during neurogenesis there is a complex set of time-linked factors, including the dynamic expression of temporal transcription factors, all of which have the potential to impact neuronal wiring decisions. The objective of this study was to unravel this complexity by explicitly testing the hypothesis that the activity of the temporal transcription factor, Hb, in NB7-1 is sufficient to control terminal features of its U motor neuron progeny regardless of birth time.

Manipulation of temporal transcription factors provides insight into neuromuscular plasticity and identifies developmental decision points for wiring specificity

Neuromuscular targeting is thought to be controlled in a step-wise fashion with motor neurons making a series of decisions that culminate in specific wiring decisions. First, a neuron must decide to exit the nerve cord, then it must decide to branch off the main nerve, and finally it must pick a specific muscle with which to synapse. For decades the Drosophila neuromuscular system has been a model to identify molecular mechanisms underlying these steps. Notably, the phenotypes we report here are among the most dramatic morphological

rearrangements of neuromuscular synapses ever reported in this system (Figures 3.7, 3.12). In general, in Drosophila larva, in mutants—for cell adhesion, axon guidance cues, and post-mitotic neuronal transcription factor genes—there is delayed rather than impaired synapse formation, which indicates there is enormous plasticity, redundancy and complexity in neuromuscular wiring decisions (Desai et al., 1996; Krueger et al., 1996; Landgraf et al., 1999; Nose et al., 1994)[134, 135, 136, 137]. Here, we show that by manipulating gene expression early in neuronal development, in the neuronal stem cell, we dramatically alter neuromuscular synapse partner selection of motor neurons (Figures 3.7, 3.12). This argues against a model in which post-mitotic motor neurons are gradually restricted to adopt specific synaptic partnerships, and instead argues that in general, when a motor neuron is born, it already 'knows' its synaptic partner. Furthermore, our data show that transcription factors acting early in neuronal development, in neuroblasts, control the ensemble of molecular effectors necessary to specify neuromuscular wiring. Thus, we identify a powerful entry point for future studies to uncover the suite of effectors controlling neuromuscular synapse selection.

The Drosophila neuromuscular system is a prominent model for studying synaptic homeostasis and plasticity. The neuromuscular wiring phenotypes documented in this study provide evidence for two types of plasticity in neuromuscular wiring, which we refer to as compensation and spillover. Compensation occurs when a muscle does not have enough innervation. In this case, neurons that do not normally innervate a muscle form extra branches to innervate a muscle that is devoid of its normal innervation (either because the motor neuron has been ablated or genetically mis-specified). We find evidence for compensation on dorsal muscles, muscle 3 and 4, similar to that which has been found for ventral muscles (Chang and Keshishian, 1996)[104], showing that compensation is not a muscle- or neuron-specific phenomenon. Spillover occurs when a muscle has too much innervation. To our knowledge this type of plasticity has not yet been described because no manipulations have been identified that increase innervation on a single muscle to the degree we describe. In

spillover, motor neurons that exit from the ISN at a specific branch point do not innervate the muscle target which is normally innervated by neurons exiting at that point, but instead these neurons synapse onto other nearby muscles, such that synapses form on muscle surfaces normally devoid of synapses (e.g., the top of muscle 3, Figure 3.7). Spillover phenotypes suggests that molecular cues are sufficient to send neurons out of the nerve cord, and instruct them where to branch off the main nerve, but that once neurons reach a muscle field they can innervate one of several nearby muscles. In addition, we note that the neuromuscular synaptic branches that form in NB7-1>Hb, contain functional synapses, but we know little about the function of these neurons otherwise. It will be important to undertake a detailed functional analysis of multi-innervated muscles to gain insight into homeostatic and other synaptic plasticity mechanisms.

Hb is a limited master regulator of temporal-specific developmental programs

A widely held model in the field is that temporal transcription factors are master regulators of temporal-specific developmental programs (Allan and Thor, 2015; Jacob et al., 2008)[74, 138] (Figure 3.13A). This is an attractive model, but there is limited data to support it because experiments in general have assayed establishment of molecular marker gene expression in embryos, which provides limited information about an entire developmental program. We argue that understanding the role of temporal transcription factors in regulating terminal neuronal features is critically important because it provides insight into functional neural diversity and circuit wiring and because it is the end product of an entire developmental program.

One of our most surprising findings is that embryonic molecular identity markers do not accurately predict neuronal terminal features. For example, in NB7-1>Hb early stage larvae, we find some Hb(+) neurons with ipsilateral dendrites, although in wild type all Hb(+) neurons have contralateral dendrites (Figure 3.6). In late stage embryos, we find

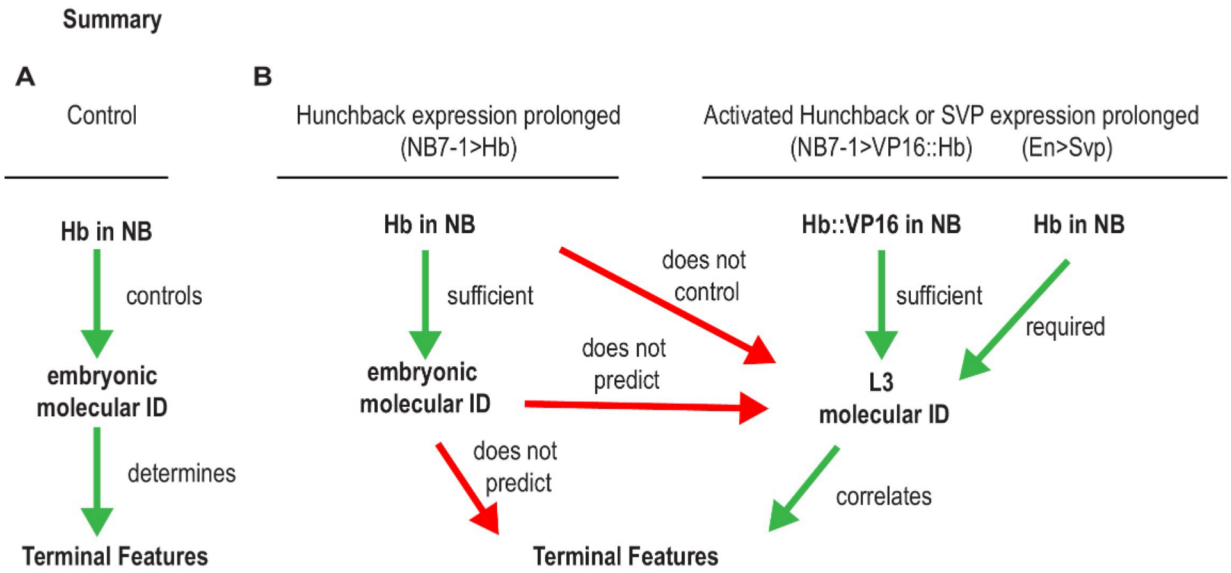


Figure 3.13: Summary of Hunchback control on circuit wiring. (**A**–**B**) Illustration summary of findings reported in this study. In Wildtype (WT) conditions, NB7-1 expresses Hunchback (Hb), Hb is involved in establishing U1/U2 motor neuron embryonic identities which was proposed to determine terminal features (dendrite morphology, axonal trajectory, and functional synaptic partnerships) (A). When Hb is overexpressed in NB7-1>Hb, Hb expression in NB7-1 is prolonged (Figure 3.3). The overwhelming majority of embryonic identities seen in motor neurons resemble U1 (Figure 3.3) however the terminal features do not entirely resemble U1 (Figures 3.7, 3.9, 3.10). We find that prolonging Hb expression in NB7-1 produces, in a majority of cases, the same number or, infrequently, one additional neuron possessing molecular identity that resembles U1 at late larval stage (L3), therefore we conclude that prolonging Hb expression in NB7-1 does not control L3 identities (Figure 3.11). Similarly, in this background, we learn that U1 embryonic identities do not predict U1 L3 identities. We find that if we overexpress an activated form of Hb (VP16::Hb) or the switching factor, Seven-up (Svp1), U1 L3 identities can be controlled. We find that L3 identities in these manipulations are correlated to terminal features of U motor neurons (Figure 3.12).

a majority of Hb(+) Zfh2(-) U1 neurons project axons to muscles 10 and 2 rather than the wild type U1 target muscle 9 (Figure 3.10). In late stage larvae, we find that Hb(-) U motor neurons often project to muscle 10, despite the fact that in wild type muscle 10 in innervated by Hb(+) U motor neurons (Figure 3.11). These data show that Hb can generate complete and partial transformations of neuronal terminal features, and demonstrate that only in certain contexts does Hb act as a master regulator of temporal-specific developmental programs.

Temporal transcription factors are known to act in the context of a dynamically changing stem cell. For example, providing pulses of Hb to NB7-1 generates extra U motor neurons, if the pluses of Hb are provided before the fifth division. If, however, Hb is provided after the fifth division, the 'competence window' closes and NB7-1 no longer generates U motor neurons (Cleary and Doe, 2006; Pearson and Doe, 2003)[139, 102]. Furthermore, Kohwi et al., recently showed that even if Hb is provided continuously to NB7-1, and NB7-1 generates a large number of U motor neurons, only the first five express an endogenously HA-tagged Hb transgene, suggesting that only the first five U motor neurons are bona fide U1/U2 motor neurons. Our data suggest the existence of an additional competence window that closes after two divisions of NB7-1. This is because we find that although prolonged expression of Hb produces a large number of U motor neurons, most of which express markers for U1 in late stage embryos (Figure 3.3, 3.4), this same manipulation assayed at late larval stages produces only two bona fide Hb(+) U1/U2 motor neurons (Figure 3.11). One possibility is that if we were able to drive Hb at higher levels in NB7-1, we would generate five bona fide U1/U2 motor neurons at L3. Although our data do not completely rule out this possibility, we note that varying the expression level of Hb had no effect on the number of Hb(+) U motor neurons at L3 (Figure 3.11). We also note that expressing an artificial construct, VP16::Hb using the same NB7-1-GAL4 driver produces five Hb(+) neurons at L3 (Figure 3.12). Although, the mechanism is still unclear, this VP16::Hb manipulation demonstrates that NB7-1 is capable of generating a large number of ectopic, bona fide U1/U2 motor neurons at L3, and it controls for the NB7-1-GAL4 expression pattern. Together these data show that in response to prolonged expression of wild type Hunchback protein, NB7-1 is only able to produce two bona fide U1/U2 motor neurons.

In sum, our study adds an entirely new and unexplored level to the existing model by focusing on the role of Hb in circuit wiring rather than establishment of molecular identity, which has been intensely studied for decades (Figure 3.13B). It examines the biological

relevance for a number of previously described molecular manipulations (Kanai et al., 2005; Kohwi et al., 2013; Tran et al., 2010)[130, 132, 131]. In so doing, we showed that on a cell biological level the original fate specification model was too simple. Rather than completely transform the terminal features of later-born neurons into terminal features characteristic of early-born neurons, we find that Hb can only completely control whether or not a neuron in the NB7-1 lineage is a dorsally-projecting U motor neuron or an interneuron. For all other terminal features examined, we find partial transformations. Furthermore, our data suggest that this is linked to a previously un-identified NB7-1 competence window.

One conclusion of our paper is that individual temporal transcription factors influence, but do not entirely determine, neuronal fate, terminal differentiation, dendritic arborization, and neuronal partners. That is to say, overexpression of one single temporal factor can only transiently change the fate of neurons, which later fail to differentiate into the correct type of neuron. A second conclusion of our paper is that neuromuscular synaptic partner choice and circuit wiring can be established before neuronal birth by early programs of gene expression acting in neuronal stem cells. While these two conclusions may seem to contradict one another, this contradiction can be resolved by pointing out that our data, do not provide the identities of all of the genes acting in the neuronal stem cells, but point to their existence and suggest that Hb is among these genes.

Insights into the lineage-based organization of motor circuits

In many CNS regions there are notable relationships between neuronal stem cell lineage and circuit wiring, but these relationships differ depending on the circuit configuration with a given CNS region (Xu et al., 2014; Yu et al., 2009)[140, 141]. These observations have led to the hypothesis that lineage is an important element in circuit assembly, but that lineage-circuit relationships differ for different circuits. Little is known about lineage-circuit relationships in the motor system. In the Drosophila motor system, we recently showed

that neurons from a single neuroblast, NB3-3 are organized into blocks of non-identical, yet functionally-related sets (Wreden et al., 2017)[1]. These early-born and late-born blocks of lineage-related interneurons are called 'temporal cohorts', defined as groups of contiguously-born neurons from a single stem cell that have similar circuit level function. To be a bona fide temporal cohort requires a large amount of information about individual neurons, including their exact stem cell parent, birth order, as well as a functional demonstration of circuit membership. It is important to have all of these pieces of information for a single neuron because ultimately this is critically required to identify molecular mechanisms underlying cell fate specification of neurons in a circuit.

Temporal cohorts are likely to be found in many lineages, brain regions, and organisms, and therefore could be fundamental, developmentally-based units of neuronal circuit organization. Furthermore, there are many examples of sets of neurons that partially fulfill the criteria to be considered a temporal cohort. It is likely that temporal cohorts are found in several regions of the Drosophila CNS. For example, in the Drosophila central complex, early-born neurons from Type II neuroblasts have shared dendrite and axonal projection patterns and later-born neurons have distinctive targets (Sullivan et al., 2019)[107]. Similarly, in mushroom bodies there is a relationship between neuronal birth time from mushroom body neuroblasts and neuronal morphology (Zhu et al., 2003)[142]. However, in both of these examples, the developmental origin of neurons has been mapped only to a small pool of molecularly heterogeneous neuroblasts, and so the precise stem cell origin of neurons in these CNS regions remains undefined (Kunz et al., 2012; Walsh and Doe, 2017)[143, 144]. There are also likely to be temporal cohorts in the vertebrate spinal cord. For example, inhibitory Renshaw cells, which contribute to a motor neuron feedback circuit and Ia interneurons, which contribute to a reflex circuit are sequentially produced by progenitors in a small domain (Benito-Gonzalez and Alvarez, 2012; Stam et al., 2012)[87, 88]. However, the precise birth time and exact stem cell parent of these spinal cord neurons is unknown.

Together these studies provide evidence that developmental origin is often tightly linked to neuronal morphology and connectivity, and they illustrate the technical difficulties associated with identifying additional examples of temporal cohorts.

Here, we identify a temporal cohort in the NB7-1 lineage comprised of U motor neurons (Figure 3.1). U motor neurons are from a single neuronal stem cell, contingously-born, and because they innervate a group of synergistic muscles they share circuit membership. This finding demonstrates that temporal cohorts can be found in lineages other than NB3-3 and that temporal cohorts can be composed not just of interneurons, but also of motor neurons. Notably, the U motor neuron temporal cohort innervates the dorsal muscles, which is just one of three distinct groups of synergistic muscles in the Drosophila larval motor system (Heckscher et al., 2012)[47]. This raises the question of whether other groups of muscles are innervated by other temporal cohorts. Nonetheless, the identification of the U motor neuron temporal cohort supports the idea that temporal cohorts are developmental units fundamental to motor circuit organization.

One question raised by the concept of temporal cohorts is what regulates the borders of temporal cohorts, that is, how do neuronal stem cells make abrupt, rather than gradual, changes in lineage progression. For example, in NB7-1, for several divisions, motor neurons are produced, and then NB7-1 stops making motor neurons and starts making interneurons. Our data show that Hb regulates the U motor neuron temporal cohort border because when Hb expression is prolonged in NB7-1, NB7-1 produces many more functional, dorsally-projecting motor neurons at the time when NB7-1 would normally be making interneurons. Interestingly, prolonged expression of VP16::Hb does not alter the U motor neuron temporal cohort border. Nonetheless, our data argue that rather than specify specific cell fates, a general function of temporal transcription factors is to regulate temporal cohort boundaries. They also raise the possibility that alterations in temporal transcription factor expression could be a major driver of evolution of neuronal circuits.

Parsing the source(s) of information that control circuit wiring

In many CNS regions in many organisms there is an association between birth time and circuit membership (Bhansali et al., 2014; Deguchi et al., 2011; Eerdunfu et al., 2017; Greaney et al., 2017; Jefferis et al., 2001; Kulkarni et al., 2016; McLean et al., 2007; McLean and Fetcho, 2009; Morrow et al., 2008; Osterhout et al., 2014; Petrovic and Hummel, 2008; Pujol-Martí et al., 2012; Tripodi et al., 2011). [117, 116, 118, 119, 120, 121, 122, 97, 123, 124, 125, 126, 90]. The mechanisms underlying this association are likely to be varied and are still poorly understood. Identifying sources of information that control circuit wiring is critically required for understanding molecular underpinnings of circuit assembly. In complex brains, neurons are born from pools of neuronal stem cells. As stem cells divide, several factors are simultaneously changing each of which could influence the circuit membership of the resulting neuron. One factor is a dynamic environment—earlier-born neurons and later-born neurons can encounter different physical substrates or receive different signaling cues. A second type of factor is that earlier-born neurons have more time for processes like migration and axon extension. Third, over time, within the nucleus of a neuronal stem cell, the chromatin landscape can change. Finally, earlier-born and later-born neurons have different molecular profiles, which is controlled by temporal transcription factors. Determining the precise role of each of the factor associated with birth time is crucial for understanding how circuits assemble. Our data show that in NB7-1>Hb animals, even the latest-born U motor neuron can adopt terminal features characteristic of the earliest-born U motor neuron—including CNS exit, dendrite morphology, axonal targeting and functional neuromuscular synaptic partner selection. Thus, we find no limit on the ability of late-born neurons to adopt early-born features. These findings rule out many time-linked processes in circuit wiring decisions. Furthermore, we show that manipulation of temporal patterning via manipulation of gene expression in the neuroblast is sufficient to re-wire locomotor circuits, indicating that circuit wiring can be established before neuronal birth by early programs of gene expression acting

in neuronal stem cells.

While this manuscript was in review, a manuscript describing similar experiments was published (Seroka and Doe, 2019)[80].

3.2.5 Materials and methods

Fly genetics

Standard methods were used for propagating fly stocks. For all experiments, embryos and larvae were raised at 25 °C, unless otherwise noted. The following lines were used: CQ2-GAL4 (Bloomington stock center [BL] 7468), OK6-GAL4 (BL 64199), hsFLP; UAS(FRT.stop)myr::smGdP-HA, UAS(FRT.stop)myr::smGdP-V5-THS UAS(FRT.stop)myr::smGdP-FLAG (BL 64085), UAS-myr-GFP (BL 32198), UAS-nls-GFP (BL 6452), UAS-Hb; UAS-HB/TM2 (BL 8504), w1118 (BL 36005), MHC-CD8-GCaMP6f-Sh (BL 67739) ac:VP16, gsb:v8v (aka NB7-1-GAL4, gift of M. Kohwi), VGlut-lexA/cyo (BL 60314), lexA(stop.FRT)mCD8.GFP (BL 57588), UAS-VP16::Hb/-;UAS-VP16::Hb (gift of C. Doe), UAS-svp1 1.12 (gift of M. Kowhi), Engrailed-GAL4 (BL 1973) (gift of M. Kowhi), UAS-hid,rpr (Zhou et al., 1997).

Tissue preparation

Three tissue preparations were used: Late stage whole mount embryos, in which antibody can still penetrate cuticle; isolated first instar (L1) CNSs, in which the CNS is removed from other larval tissue so that antibody reach the CNS; and third instar (L3) fillet preparations, in which the neuromuscular tissue and cuticle are dissected away from other tissue and pinned open like a book, allowing for superb immuno-labeling and visualization of larval neuromuscular synapses. For all preparations, standard methods were used for fixation in fresh 3.7% formaldehyde (Sigma-Aldrich, St. Louis, MO) [49-51]. For calcium imaging, L3

larvae expressing MHC-CD8-GCamp6f-Sh construct were dissected in HL3 solution containing 1.5 mM Ca2+ and 25 mM Mg2+, brains removed, body walls rinsed fresh saline, and samples imaged.

Immunostaining

Tissue was blocked for an hour at room temperature or overnight at 4 °C in phosphate buffered saline with 2% Normal Donkey Serum (Jackson ImmunoResearch), followed by 2 hr at room temperature in primary antibodies, and 1 hr at room temperature in secondary antibodies. Primary antibodies include: rabbit anti-Eve (1:1000, Heckscher lab, see below), chicken anti-GFP (1:1000, Aves GFP-1020), chicken anti-V5 (1:300, Bethyl A190-118A), mouse anti-HA (1:100, BioLegend 901501), rat anti-FLAG (1:300 Novus NBP1-06712), rat anti-Worniu (1:250 Abcam ab196362), goat anti-HRP-Cy3 (1:300, Jackson ImmunoResearch 123-165-021) rat anti-Runt (1:300, John Rientz, UChicago), guinea pig anti-Hb (1:1000, John Rientz, UChicago), guinea pig anti-Kruppel (1:1000, John Rientz, UChicago), rat anti-Zfh2 (1:800 Chris Doe, UOregon), rabbit anti-Castor (1:1000 Chris Doe, UOregon), guinea pig anti-Dbx (1:500 Heather Broiher, Case Western) guinea pig anti-HB9 (1:1000 Heather Broiher, Case Western), rabbit anti-Smad3 (pMad) (1:300 Abcam 52903). The following monoclonal antibodies were obtained from the Developmental Studies Hybridoma Bank, created by the NICHD of the NIH and maintained at The University of Iowa, Department of Biology, Iowa City, IA: mouse anti-myosin (1:100, 3E8-3D3), mouse anti-Futsch (1:50 22C10) mouse anti-Brp (1:50, NC82), mouse anti-DLG (1:500, 4F3), mouse anti-GluRIIA (1:25, 8B4D2), mouse anti-En (1:5, 4D9). Secondary antibodies were from Jackson ImmunoResearch and were reconstituted according to manufacturer's instructions and used at 1:400. 647-Phalliodin (1:600, Thermofisher A22287), Cy3-HRP (Jackson ImmunoResearch 123-025-021). Embryos were staged for imaging based on morphological criteria. Whole mount embryos and larval fillets were mounted in 90% Glycerol with 4% n-propyl gallate.

Larvae brain preparations were mounted in DPX (Sigma-Aldrich, St. Louis, MO).

Antibody generation

An anti-Even-skipped antibody was generated by GenScript (Piscataway, NJ). Rabbits were inoculated three times with a bacterial fusion protein containing an N-terminal 6xHis tag fused with the first 129 amino acids of Eve (Met..Arg Gln Arg). The resulting antiserum was immunopurified using the bacterial fusion protein.

Single neuron labeling

Single U motor neurons were labeled by crossing a Multi-Color Flip Out fly line (Nern et al., 2015)[145], harboring a heat-shock inducible FLP recombinase construct, to other lines of interest. For late stage embryo and L1 larval labeling, heat shock (37 °C for 10 min) was delivered to embryos aged 6–24 hr on apple juice caps. For L3 labeling, late stage embryos and 1st instar larvae were heat shocked and incubated at 25 °C. All CNS tissue was co-stained with Eve antibody to confirm the identity of single cell clones. In Control, U MNs were identified by their characteristic position in the CNS with U1 positioned most medial and U5 lateral.

Image acquisition

For fixed tissue images, data were acquired on a Zeiss 800 confocal microscope with 40X oil (NA 1.3) or 63 X oil (NA 1.4) objectives, or a Nikon C2+ confocal microscope with 40X (NA 1.25) or 60X (NA 1.49) objectives. For calcium imaging, data were acquired using a Zeiss 800 confocal microscope with a 40X dipping objective (NA 1.0) using 488 nm laser power with the pinhole entirely open. Images were acquired on a Zeiss 800 confocal microscope. Images were cropped in ImageJ (NIH) and assembled in Illustrator (Adobe).

Image analysis

Cell body counting: We used NB7-1-GAL4 driving UAS-myristoylated-GFP to count the number of cells within the NB7-1 lineage during late stage (16-17) embryos. Embryos were co-stained with Worniu and Eve antibodies to confirm that only the NB7-1 lineage clone was labeled. To ensure the entire lineage was labeled by GFP, we scored only segments in which both an Eve(+) U1 neuron (earliest born neuron in the lineage) and NB7-1 was labeled. Since the NB7-1 lineage clone is a dense cluster of cells in x-y-z, we used a custom Fiji plug-in, that employs the Multi point tool to count cells.

Type 1b branch counting: We stained against HRP to detect the neuronal membrane and Discs large (Dlg) in L3 fillet preparations. Dlg allowed us to distinguish between type 1b and type 1s boutons. We counted contiguous stretches of Dlg staining that overlapped with HRP as a single branch. In (Figures 3.11G–H,3.12) innervation onto muscle 9 included innervation that branched off over muscle 9 but synapsed onto the most dorsal edge of muscle 10 or muscle 2.

Calcium imaging: X-y-z-t stacks (Figure 3.14B–C) were converted into x-y time series images using the Maximum Intensity projection function (Fiji). X-y time series images were then registered using the Register Virtual Stack Slices plug-in (Fiji) to reduce movement artifacts. Time series images were projected into two different x-y single images using either the Maximum Intensity projection function (Fiji) or Average Intensity projection function (Fiji), and then the average intensity was subtracted from the maximum to get a change in fluorescence image (Figure 3.14D).

Statistics

Descriptive statistics: average and standard deviation are reported, except for behavior, where the average of average speed and standard error of the mean are reported. Every data point is plotted in figures. Test statistics: All data was assumed to follow a Gaussian

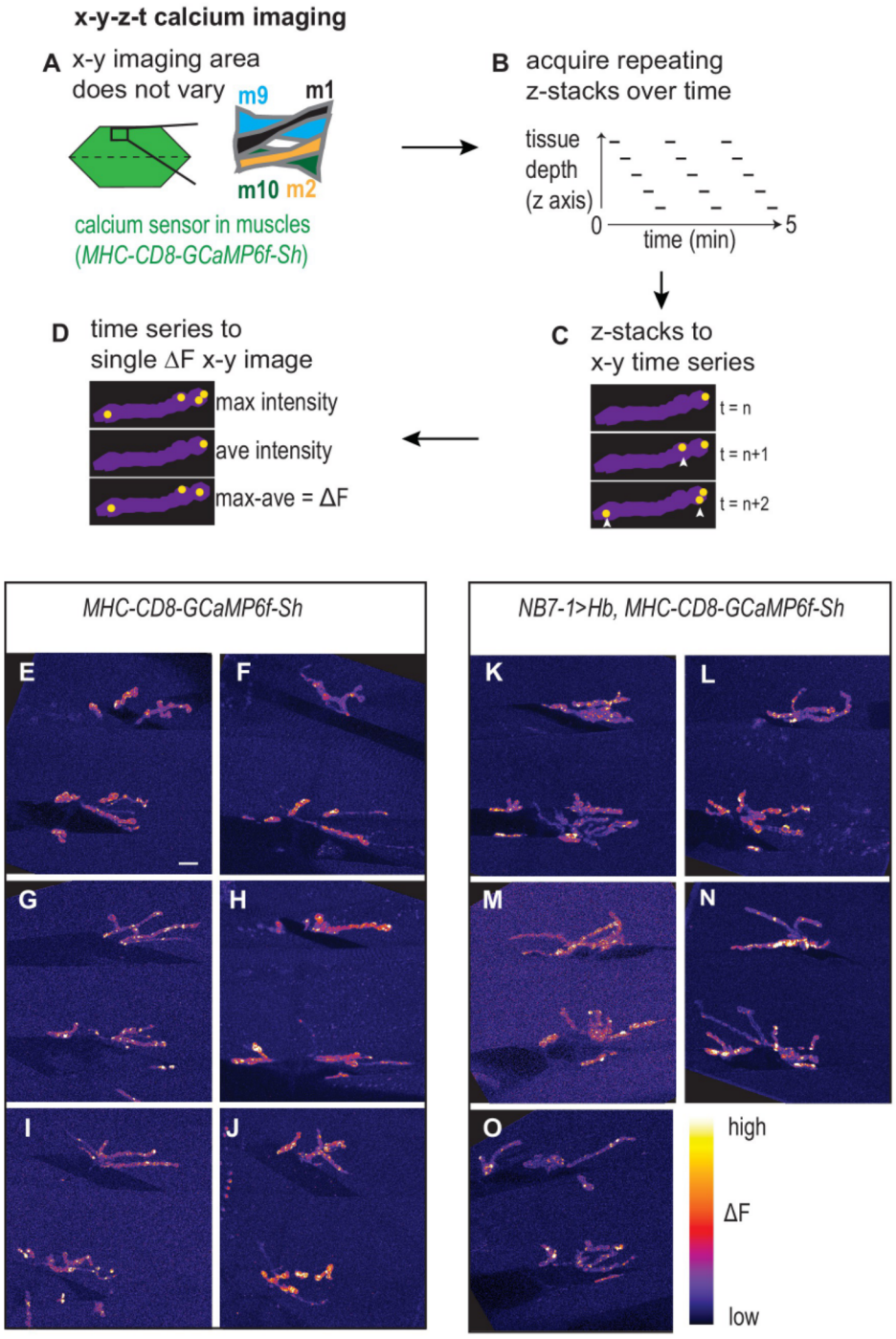


Figure 3.14: Calcium imaging protocol, analysis, and examples. (**A**–**D**) Illustration of calcium imaging protocol and analysis are shown. See Materials and methods for details. (**E**–**O**) Images of calcium signals on L3 muscles 1, 2, 9, 10 for Control (NB7-1-GAL4/+; MHC-CD8-GCaMP6f-Sh/+) and NB7-1>Hb (NB7-1 GAL4/UAS Hb; MHC-CD8-GCaMP6f-Sh/UAS Hb). Images are dorsal up, anterior to the left. Scale bar represents five microns.

distribution. If standard deviations were unmatched Welch's correction was applied. For numerical data in two populations, we used un-paried, two-tailed t tests. For numerical data in more than two populations, we used ordinary one-way ANOVAs with Dunnett or Games-Howell correction for multiple comparison. Analysis done using GraphPad Prism.

3.3 Meng et al., 2020 eLife

In this second paper entitled, 'Temporal transcription factors determine circuit membership by permanently altering motor neuron-to-muscle synaptic partnerships', Yupu Wang, graduate student in Robert Carrillo's lab, contributed by performing all electrophysiology experiments in Figure 3.5.

3.3.1 abstract

How circuit wiring is specified is a key question in developmental neurobiology. Previously, using the Drosophila motor system as a model, we found the classic temporal transcription factor Hunchback acts in NB7-1 neuronal stem cells to control the number of NB7-1 neuronal progeny form functional synapses on dorsal muscles (Meng et al., 2019)[2]. However, it is unknown to what extent control of motor neuron-to-muscle synaptic partnerships is a general feature of temporal transcription factors. Here, we perform additional temporal transcription factor manipulations—prolonging expression of Hunchback in NB3-1, as well as precociously expressing Pdm and Castor in NB7-1. We use confocal microscopy, calcium imaging, and electrophysiology to show that in every manipulation there are permanent alterations in neuromuscular synaptic partnerships. Our data show temporal transcription factors, as a group of molecules, are potent determinants of synaptic partner choice and therefore ultimately control circuit membership.

3.3.2 Introduction

During neural development, neurons are born from neuronal stem cells. Post-mitotic neurons then make a series of cell biological decisions that culminate in each neuron becoming a member of a specific neuronal circuit. For example, motor neurons first decide to send axons out of the CNS; then axons decide to travel to a particular muscle field; once within a

muscle field, axonal growth cones decide which muscle fiber to contact; and finally, growth cones decide to form functional synapses. Thus, circuit membership of neurons is determined by a series of decisions that impact many cell biological events. Where, when, and what the information is that regulates these decisions are key questions in developmental neurobiology.

The class of molecules termed temporal transcription factors are poised to be potent regulators circuit membership. This is because temporal transcription factors have been postulated to control entire time-linked developmental programs, and because in many systems there is a strong association between the birth time of a neuron and its ultimate circuit membership (Bhansali et al., 2014; Deguchi et al., 2011; Eerdunfu et al., 2017; Greaney et al., 2017; Jefferis et al., 2001; Kulkarni et al., 2016; McLean et al., 2007; McLean and Fetcho, 2009; Morrow et al., 2008; Osterhout et al., 2014; Petrovic and Hummel, 2008; Pujol-Martí et al., 2012; Tripodi et al., 2011; Li et al., 2013; Elliott et al., 2008; Alsiö et al., 2013; Doe, 2017; Allan and Thor, 2015; Wreden et al., 2017; Suzuki et al., 2013)[117, 116, 118, 119, 120, 121, 122, 97, 123, 124, 125, 126, 90, 22, 129, 128, 64, 74, 1, 146]. Consistent with the idea that temporal transcription factors control time-linked developmental programs, in many brain regions and model systems, temporal transcription factors control marker gene expression in newly-formed, post-mitotic neurons (Isshiki et al., 2001; Moris-Sanz et al., 2014; Novotny et al., 2002; Pearson and Doe, 2003; Tran and Doe, 2008; Cleary, 2006; Grosskortenhaus et al., 2006; Baumgardt et al., 2009; Stratmann et al., 2016)[68, 147, 148, 102, 70, 139, 69, 149, 109]. In some cases, temporal transcription factors have been shown to control later events in the development of a neuron. This includes regulation of neurotransmitter phenotype (Stratmann and Thor, 2017; Isshiki et al., 2001; Allan and Thor, 2015)[109, 68, 74], as well as regulation of axon pathfinding, dendrite targeting, and neuron morphology (Pearson and Doe, 2003; Seroka and Doe, 2019; Meng et al., 2019; Sullivan et al., 2019; Rossi et al., 2017; Doe, 2017)[102, 80, 2, 107, 108, 64]. Thus, temporal transcription factors regulate many of the decisions a neuron makes towards circuit

membership.

It is still poorly understood how manipulation of temporal transcription factors impacts final neuronal decisions–synaptic partner choice and synapse formation–which are the critical final steps of determining circuit membership. Notably, synapse formation is distinct from other aspects of neuronal maturation in that it is obligately non-cell autonomous because it requires two permissive partner cells to form a functional synapse. Furthermore, synapse formation may be particularly sensitive to dynamic environmental factors in developing animals (e.g., availability of synaptic partners or transient signaling cues). A recent study in Drosophila central complex showed that loss of the temporal transcription factor Eyeless/Pax6 impacted the adult navigation behavior, demonstrating a long-lasting change in navigational circuits (Sullivan et al., 2019)[107]. However, it is unknown how Eyeless alters neuronal function, or whether it impacts synaptic partner selection. Another recent study in Drosophila nerve cord showed prolonged expression of the temporal transcription factor Hunchback in neuroblast (NB) 7–1 neuronal stem cells impacts motor neuron-to muscle synaptic connections made by NB7-1 progeny (Meng et al., 2019)[2]. These data demonstrate that Hunchback activity in NB7-1 controls synaptic partner choice. However, it is still unknown to what extent regulation of synaptic partner choice is a general feature of temporal transcription factors. For example, it is unknown to what extent the temporal transcription factor Hunchback can control synaptic partner selection of neuronal progeny from neuroblasts other than NB7-1, and it is unknown how temporal transcription factors other than Hunchback impact motor neuron-to-muscle synaptic partnerships in NB7-1.

In this study, we manipulate temporal transcription factors and characterize synaptic partner selection and functional synapse formation using the Drosophila larval motor system as a model. The Drosophila motor system is organized into anterior-posterior repeated, left-right symmetrical hemisegements (Figure 3.15A). Each hemisegment contains 30 muscle cells that are organized into three main groups—dorsal, transverse, and ventral (Figure 3.15B).

Each muscle group is targeted by non-overlapping sets of motor neurons. Importantly, by late larval stages Drosophila motor neuron-to-muscle synapses are large, experimentally-accessible, and extremely well-characterized (Nose, 2012)[150]. First, we find that Hunchback acting in NB3-1 is sufficient to specify synaptic partnerships. Thus, the ability of the temporal transcription factor Hunchback to regulate synaptic partner selection is not limited to one stem cell lineage. Second, we find that the temporal transcription factors Castor and Pdm are sufficient to specify motor neuron-to-muscle targeting of NB7-1 neuronal progeny. Thus, multiple temporal transcription factors can control synaptic partner selection. Together, these findings provide evidence that temporal transcription factors, as a class of molecule, are potent regulators of synaptic partner selection and therefore circuit membership.

3.3.3 Results

Prolonged expression of Hunchback in NB3-1 anatomically alters RP motor neuromuscular synapses

In the Drosophila motor system, temporal transcription factors are expressed in nearly all neuroblasts, where they are thought to control the temporal identity (e.g., first-born, second-born) of neurons. To show that temporal transcription factors, as a class of molecules, control motor neuron-to-muscle synaptic partnerships, we need to show that Hunchback can determine neuromuscular targeting of neuronal progeny from more than one neuroblast lineage. In this section, we use NB3-1 as a model lineage, and we assay synaptic partnership by anatomical criteria.

We focus on NB3-1 because temporal transcription factors have been characterized in this lineage, and because NB3-1 produces a group of well-characterized motor neurons (Tran and Doe, 2008)[70]. Specifically, NB3-1 generates four RP motor neurons in the following

birth order: RP1, RP4, RP3, and RP5 (Figure 3.15C). All RP motor neurons express the transcription factor Hb9 and project to ventral muscles (Figure 3.15C). At larval stages, RP1, RP4, and RP3 make stable type one big (1b) neuromuscular synapses onto ventral Muscles 14, 30, and 6/7, respectively (Landgraf et al., 1997; Choi, 2004; Zarin et al., 2019)[44, 79, 30] (Figure 3.15C, Figure 3.16B). Previous studies, which relied on retrograde Dil labeling, do not agree on the specific ventral muscle target(s) of RP5 (Hoang and Chiba, 2001; Landgraf et al., 1997; Sink and Whitington, 1991; Mauss et al., 2009; Schmid et al., 1999)[151, 44, 152, 153, 45]. Here, we show RP5 is a type one small (1s) motor neuron (Figure 3.16D). To do so, we used a Dip-alpha-GAL4, which drives GFP expression in 1s motor neurons (herein Dip-alpha>GFP, Ashley et al., 2019; Pérez-Moreno and O'Kane, 2019)[154, 155], and we immunolabel RP1/4/3 (Hb9+, Kr+, Cut-) and RP5 (Hb9+, Kr-, Cut+) (Figure 3.16A,C). We find Dip-alpha>GFP expression specifically in RP5. We conclude RP5 is the ventrally-projecting 1s motor neuron. Further, NB3-1 is a model lineage in which we can test the extent to which Hunchback regulates neuron-to-muscle synaptic partnerships.

We prolonged the expression of Hunchback specifically in the NB3-1 lineage (Figure 3.17A–B). To prolong expression of Hb, we drive UAS-Hunchback using a NB3-1 specific GAL4 line NB3-1-GAL4 (herein, NB3-1>Hb) (Figure 3.17C; Lacin and Truman, 2016)[73]. Using a NB3-1 specific driver is critical to rule out lineage non-specific effects, and allows embryos to be healthy enough to grow to larval stages. We confirmed that NB3-1>Hb transforms RP motor neuron identities in a manner consistent with previous work, where Hunchback expression was prolonged in all neuroblasts (Tran and Doe, 2008)[70]. In NB3-1>Hb embryos, there is an average of six ventral motor neurons (Hb9+, pMad+), that express markers characteristic of early-born RP motor neuron identity (RP1/RP4 Hb+, Kr+, Zfh2-, Cut-), but not later-born RP motor neuron identity (RP3 Hb- Kr+ Zfh2+ Cut- and RP5 Hb- Kr- Zfh2+ Cut+) (Figure 3.17B,D–F). These data confirm that our reagents are working as expected. They show that prolonged expression of Hunchback in NB3-1

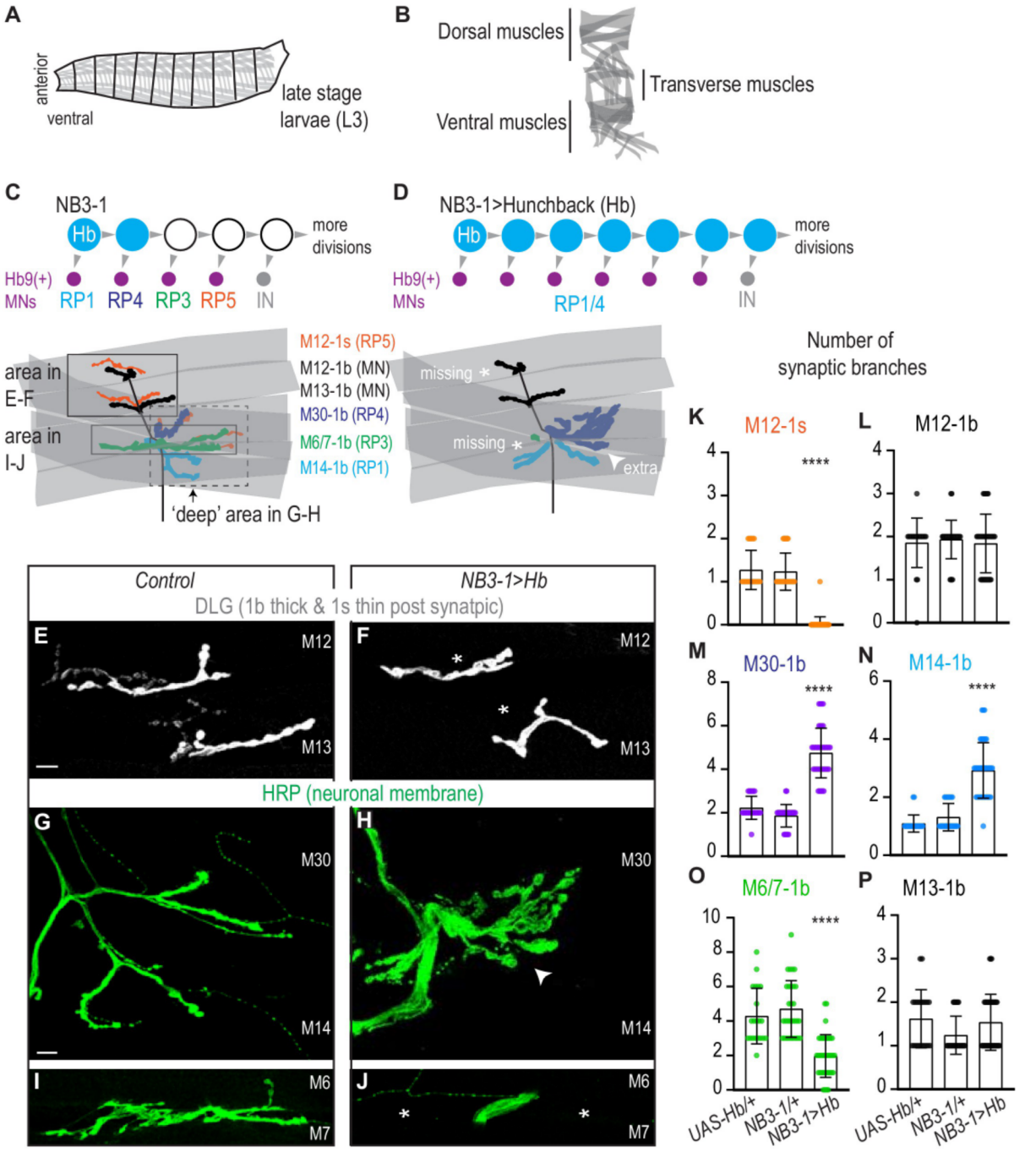


Figure 3.15: Prolonged expression of Hunchback alters RP motor neuron synapses. (**A**) Illustration of the late stage larvae (L3), body is organized into repeated left-right, mirror image hemisegments. Muscles (in gray) have a stereotyped pattern. (**B**) Illustration of muscles in a single hemisegment of a late stage larvae (L3). *Continued*

Figure 3.15: *Cont'd.* Prolonged expression of Hunchback alters RP motor neuron synapses. (**C**–**D**) Illustrations of NB3-1 lineage progression. Each gray arrowhead represents cell division. Each gray arrowhead represents cell division. Large circles are neuroblasts, and smaller circles are neurons. Abbreviations: IN is interneuron. Illustrations of neuromuscular synapses on dorsal muscles in a L3 body wall segment and embryonic molecular identity depicted as circles (blue = RP1/4, green = RP3, orange = RP5). In NB3-1>Hb the number of synaptic branches (in blue) are increased (white arrowhead) onto Muscle 14 and 30 (RP1 and RP4 muscle targets, respectively), 1b synaptic branch number is decreased (asterisk) on Muscle 6 and 7 (RP3 muscle target) and 1s synaptic branch number is lost (asterisk) assessed on Muscle 12 (RP5 muscle target). (**E**–**J**) Images of neuronal membrane, both axons and neuromuscular synapses, on ventral muscles in L3 abdominal segments. Arrowhead indicates increased branching onto Muscle 30. An asterisk * indicates missing synapses. Data quantified in (K-P). (**K**–**P**) Quantification of the number of 1b or 1s branches on L3 muscles. Color code as in (A). Each dot represents the number of branches onto a single muscle. (K-P) For UAS-Hb/+ n = 22,21,22,22,21,21. For NB3-1/+ n = 30,30,29,29,30,29. For NB3-1>Hb n = 39,38,39,39,38,39. Control is NB3-1/+. NB3-1>Hb is NB3-1 GAL4/UAS Hb; UAS Hb/+. All images are shown dorsal up, anterior left. Scale bars represent 10 microns. For quantifications average and standard deviation are overlaid. ANOVA, corrected for multiple samples '****' $p<0.0001$.

increases the total number of ventral motor neurons at embryonic stages.

We asked if prolonged expression of Hb in NB3-1 results in permanent anatomical changes to motor neuron-to-ventral muscle synapses in late stage larvae. First, we counted the number of 1b and 1s synaptic branches on ventral muscles. In wild-type, one 1b motor neuron makes one or two synaptic branches per muscle (Figure 3.15C,E,L–P). In NB3-1>Hb, which has increased numbers of RP1/4 motor neurons compared to control, we find a significant increase in the number of 1b synaptic branch onto Muscle 14 and 30 (RP1 and RP4 muscle targets, respectively)(Figure 3.15D,H,M–N). Additionally, in NB3-1>Hb, which has a decrease in numbers of RP3 and RP5 motor neurons, we see a significant decrease in 1b branch number onto Muscles 6/7 (RP3 muscle target) and a significant decrease in 1s branch number onto Muscle 12 (a RP5 muscle target) (Figures 3.15D,F,J,K,O–P). These data show that the alterations in embryonic RP motor neuron in NB3-1>Hb correlate with changes in the number of synaptic branches on ventral muscles at larval stages.

Next, we examine the extent to which extra synaptic branches in NB3-1 > Hb are likely to

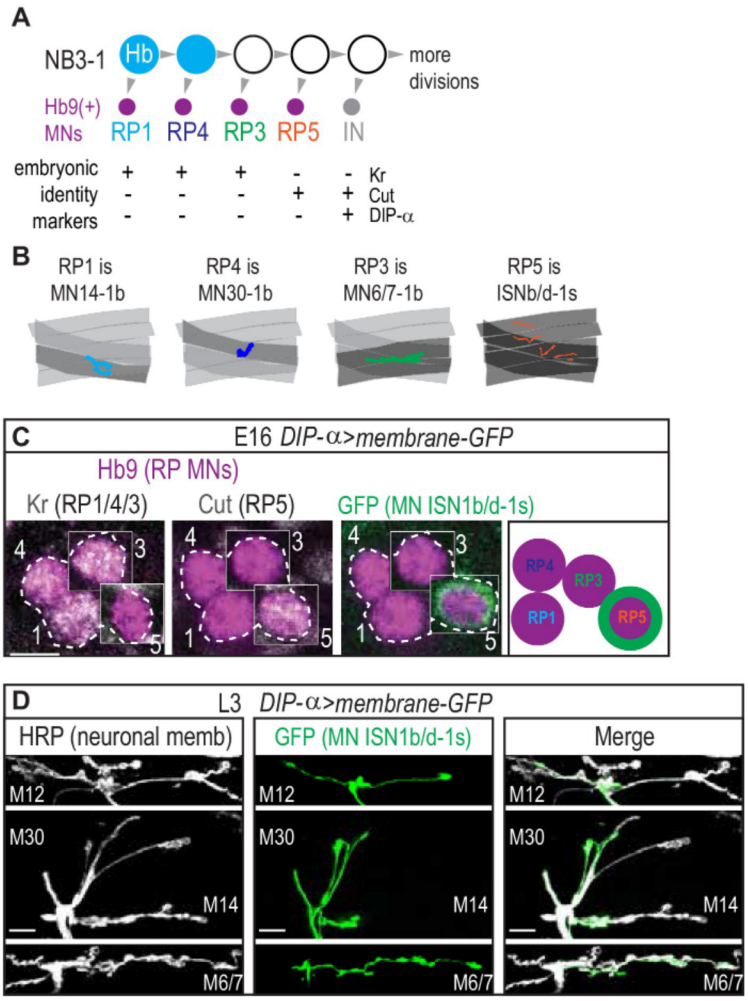


Figure 3.16: NB3-1 generates RP motor neurons, with known features. (**A**) Illustration of NB3-1 lineage progression. Each gray arrowhead represents cell division. Large circles are neuroblasts and smaller circles are neurons. Abbreviations: MN is motor neuron, IN is interneuron, Hb is Hunchback, and Kr is Kruppel. (**B**) Illustration of individual RP motor neuron neuromuscular synapses onto ventral muscles in third instar larvae. RPs populate the ventral muscle group motor circuit, which is independently recruited during locomotion. (**C**) Image of embryonic molecular identity marker and GFP expression driven by DIP alpha driver in Hb9(+) cell bodies in late stage embryonic CNSs. RP5 expresses GFP in late stage embryos. Boxes are insets from different z-planes (dotted outline around the RP motor neurons labeled by number). Scale bars represent five microns. Images are shown anterior up, midline to the left. (**D**) Images of individually labeled DIP alpha(+) motor neuron axon in third instar larvae (L3) fillet dissected larval prep. Scale bars represent 10 microns. Images shown in ventral view, anterior to the right, midline down. DIP-alpha>membrane GFP is DIP-alpha-GAL4/+; UAS-myr-GFP/+.

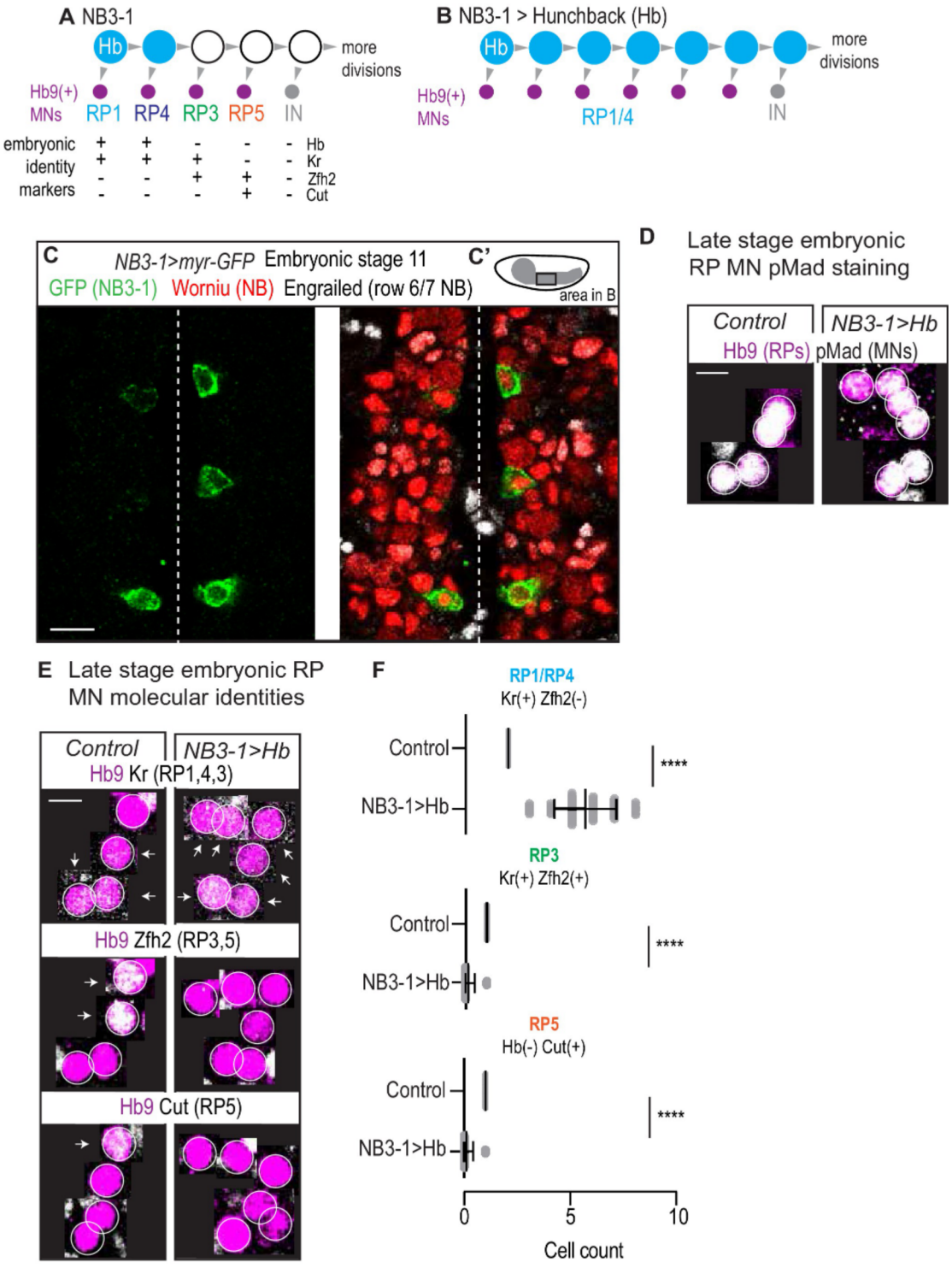


Figure 3.17: In embryos, prolonged expression of Hunchback generates more RP motor neurons with early born molecular identity. (**A**–**B**) Illustrations of NB3-1 lineage progression. Each gray arrowhead represents cell division. Each gray arrowhead represents cell division. Large circles are neuroblasts, and smaller circles are neurons. *Continued*

Figure 3.17: *Cont'd.* Abbreviations: IN is interneuron, Hb is Hunchback, Kr is Kruppel, Zfh2 is Zinc finger homeodomain 2. In NB3-1>Hb, there is an increase in the number of Hb9(+) with RP1/4 embryonic molecular identity. In embryos, prolonged expression of Hunchback generates more RP motor neurons with early born molecular identity. (**C**) Image of GFP in NB3-1 as a reporter of NB3-1-GAL4 activity. Three complete abdominal segments are shown with anterior up, and midline dotted. (**C'**) Illustration of a Drosophila late stage embryo, CNS in gray. For NB3-1>myr GFP, n = 28 hemisegments. Scale bar represents 10 microns. (**D**) Images of co-expression of Hb9 and the pan-motor neuron marker pMad in Control and NB3-1>Hb CNS of late stage embryos. For Control, n = 160 hemisegments from four embryos. For NB3-1>Hb, n = 360 from six embryos. Scale bar represents five microns. (**E**) Images of embryonic molecular identity marker expression in Hb9(+) cells in late stage embryonic CNSs. In NB3-1>Hb, extra Hb9(+) cells with RP1/4 molecular identity are produced. Boxes are neurons from different z-planes. Arrows indicate co-expression. Scale bar represents 5 microns. (**F**) Quantification of NB3-1 neurons in Control and NB3-1>Hb. Cells with RP1/RP4, RP3, and RP5 molecular markers. Each dot represents a single hemisegment. For Control, n = 31,31,31 hemisegments from top to bottom graph. For NB3-1>Hb, n = 60,90,60 hemisegments from top to bottom graph. NB3-1>myr GFP is NB3-1 GAL4/UAS-myr GFP. Control is W1118. NB3-1>Hb is NB3-1 GAL4/UAS Hb; UAS Hb/+. Images are shown anterior up, midline to the left. For quantifications average and standard deviation are overlaid. ANOVA, corrected for multiple samples '****' $p<0.0001$.

contain functional synapses. To do so, we stained for pre-synaptic active zone marker (Bruchpilot), a post-synaptic marker (Discs large), and a post-synaptic neurotransmitter receptor (GluRIIA) (Figure 3.18A). In NB3-1>Hb, in comparison to controls, we find normal abundance and localization for all markers (Figure 3.18C–H). These data strongly suggest that the extra synaptic branches on ventral muscles in NB3-1>Hb contain functional synapses.

In summary, in wild type, NB3-1 produces four RP motor neurons that synapse on ventral muscles. When Hb expression is prolonged in NB3-1, this generates additional RP motor neurons at embryonic stages, all of which have markers for the earliest-born RP motor neuron identities. In NB3-1>Hb, at larval stages, there is an increase in functional neuronal branches on early-born RP motor neuron targets and a decrease in neuron branch number on late-born RP motor neuron targets. We conclude prolonged expression of Hb in NB3-1 leads to long-lasting changes in motor neuron-to-muscles synapses.

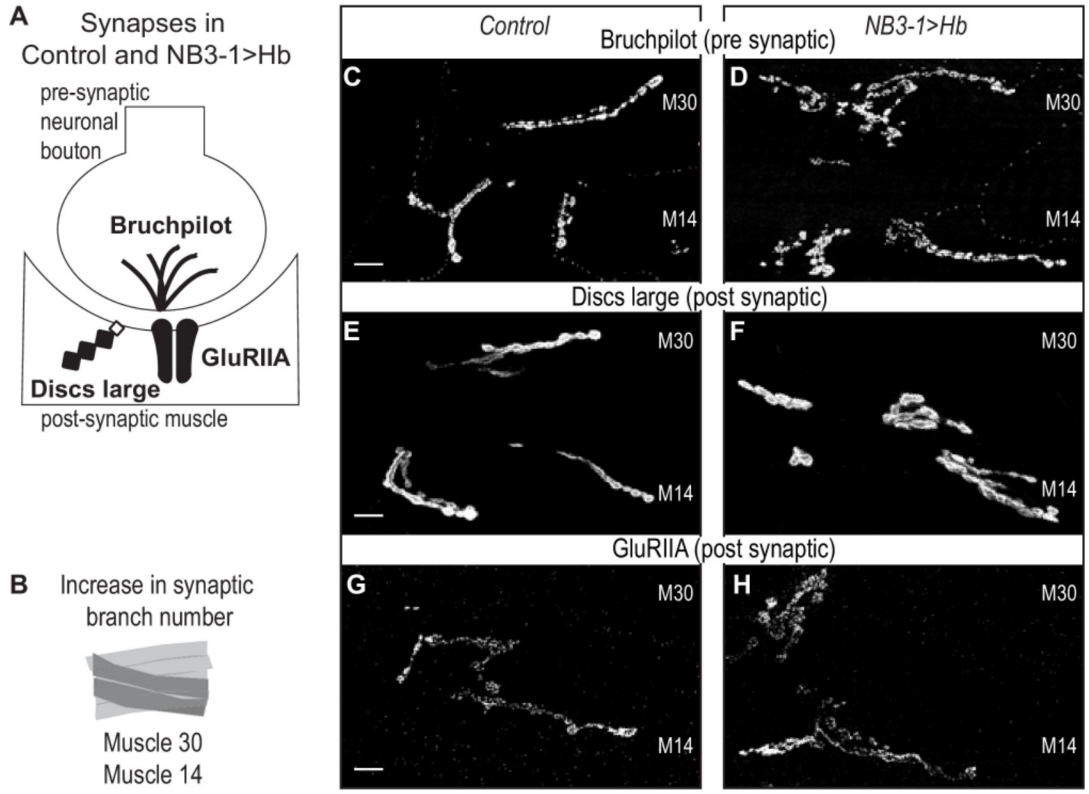


Figure 3.18: Increased synaptic branches contain pre and postsynaptic markers necessary for function. (**A**) Illustration of subcellular localization of neuromuscular synapse markers. Brunchpilot labels active zones, Discs large is a scaffolding protein strongly localized at post-synapse, and GluRIIA is the post-synaptic glutamate receptor IIA. (**B**) Illustration highlighting (darkened) muscles 14 and 30, which have increased synaptic branching in NB3-1¿Hb (see Figure 1). (**C**–**H**) Images of neuromuscular synapses on L3 Muscle 14 and 30 (see B). There is no difference in distribution or abundance of synaptic markers between Control and NB3-1>Hb. Control is Hb/+ and NB3-1>Hb is NB3-1-GAL4/UAS-Hb; UAS-Hb/+. All images are shown dorsal up, anterior to the left, scale bars represent 10 microns.

Prolonged expression of Hunchback in NB3-1 functionally alters RP motor neuromuscular synapses

In this section, we determine the extent to which prolonged expression of Hunchback in NB3-1 impacts larval physiology. This is an open question because changing the number of synaptic contacts onto a muscle does not necessarily mean that there will be a corresponding functional change in the muscle. In the Drosophila motor system, there exist well-characterized, homeostatic mechanisms that keep the muscle's response to nerve stim-

ulation within a set range of values (Frank et al., 2020)[103]. This means that anatomical changes do not necessarily lead to functional alterations.

Here, we use electrophysiology to determine the extent to which prolonged expression of Hb in NB3-1 affects motor system physiology. Specifically, we place a stimulating electrode on the nerve root to stimulate release of synaptic vesicles from pre-synaptic motor neurons, and we use a sharp electrode in the muscle to record the post-synaptic response. This provides three measurements: (1) excitatory post-synaptic potential (EPSP), which quantifies the muscles response to nerve stimulation; (2) miniature-EPSP (mEPSP), which quantifies the muscle response to spontaneous release of single synaptic vesicles and is a proxy for postsynaptic receptor sensitivity; and (3) quantal content (EPSP/mEPSP), which estimates the numbers of vesicles released during nerve stimulation (Figure 3.19A). First, we examined the physiology of Muscle 30 (Figure 3.19B). In NB3-1>Hb, there is an increase in nerve branches and synaptic markers on Muscle 30. Increases in synapse number on a muscle is expected to increase the response of the muscle to nerve stimulation. However, we observe no increase in EPSP amplitude in NB3-1>Hb, compared to wild type (Figure 3.19C–D). This suggests homeostasis alters the system to maintain the muscle response to nerve stimulation. Conceptually, there are two ways homeostasis could be working in this system. First, neurotransmitter receptors on the postsynaptic muscle could be less sensitive to neurotransmitters (Frank et al., 2006)[156]; alternatively, synapses might release fewer vesicles upon nerve stimulation. To examine these possibilities, we measured mEPSP and quantal content. In NB3-1>Hb, there is a significant increase in quantal content when compared to control animals (Figure 3.19F). This suggests that upon nerve root stimulation, the number of presynaptic vesicles released is increased, consistent with the idea that the total number of synapses is increased in NB3-1>Hb. However, in NB3-1>Hb, there is a significant decrease in mEPSP amplitude compared to control animals (Figure 3.19C,E). These data suggest that the postsynaptic receptor sensitivity to neurotransmitter is reduced.

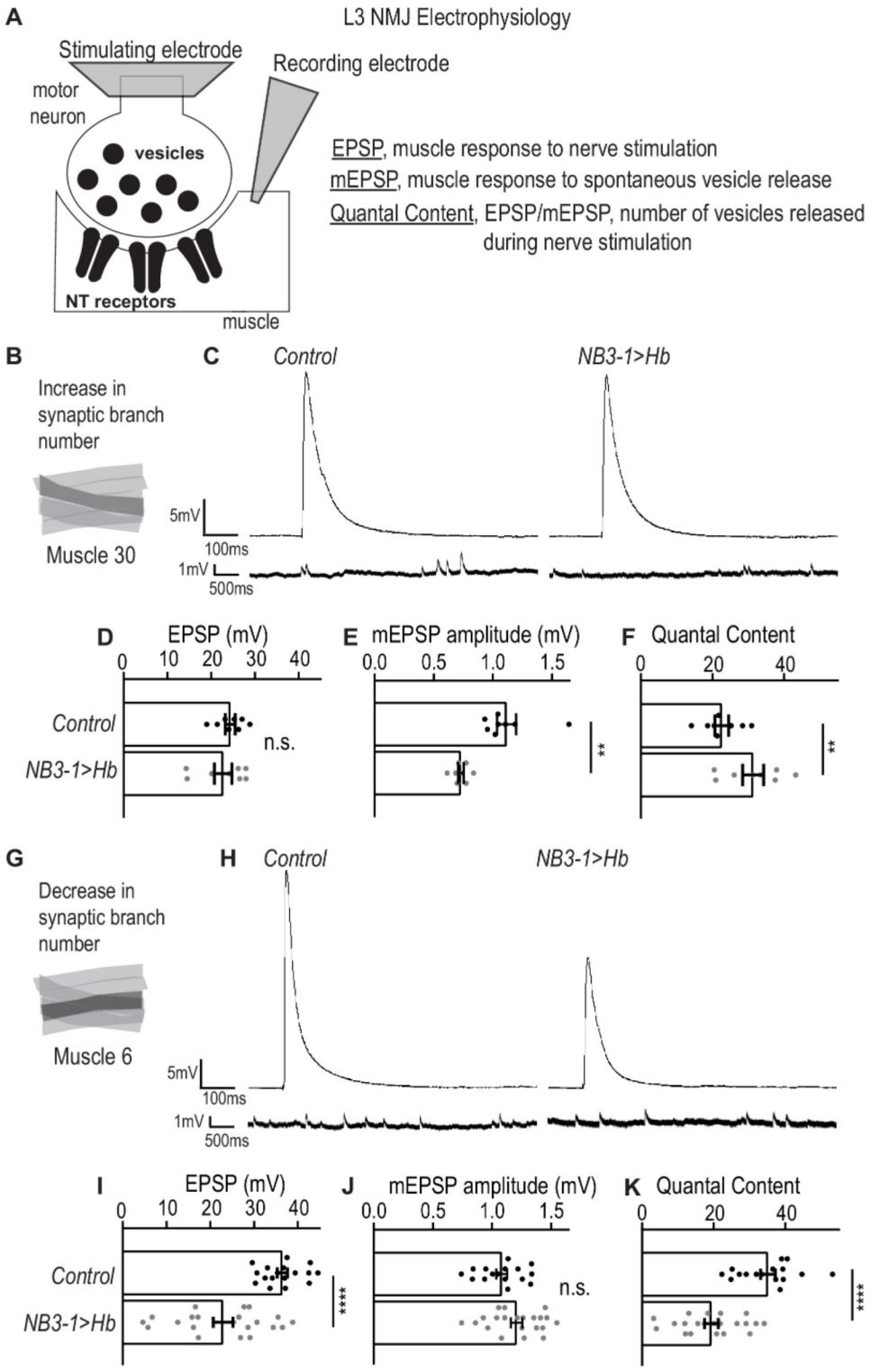


Figure 3.19: Altered synapses onto Ventral muscles are functional. (**A**) Illustration of neuromuscular junction (NMJ) electrophysiology approach on third instar larvae (L3). Abbreviation NT is neurotransmitter. (**B**) Illustration highlighting (darkened) Muscle 30 whose electrophysiological recordings are presented in C-F. *Continued*

Figure 3.19: *Cont'd.* Altered synapses onto Ventral muscles are functional. (**C**) Traces of EPSP and mEPSPs for Muscle 30. (**D–F**) Quantification of electrophysiological recordings for Muscle 30. (D) Evoked response (EPSP) is not changed in Muscle 30 in NB3-1>Hb vs Control. (**E**) Spontaneous response (mEPSP) is significantly decreased in Muscle 30 in NB3-1 vs Control. (**F**) Transmitter release (Quantal Content (EPSP/mEPSP)) is slightly significantly increased in Muscle 30 NB3-1 vs Control. (D–F) For Control, n = 8. For NB3-1¿Hb, n = 8. For C-E and H-J, each dot (black represents Control and gray represents NB3-1>Hb) on the graph represents a single recording from a unique bodywall segment from A2-A4. (**G**) Illustration highlighting (darkened) Muscle 6 whose electrophysiological recordings are presented in H-K. (**H**) Traces of EPSP and mEPSPs for Muscle 6. (I–K) Quantification of electrophysiological recordings for Muscle 6. (**I**) Evoked response (EPSP) is significantly decreased in Muscle 6 in NB3-1>Hb vs Control. (**J**) Spontaneous response (mEPSP) is not changed in Muscle 6 in NB3-1 vs Control. (**K**) Transmitter release (Quantal Content (EPSP/mEPSP)) is significantly decreased in Muscle 6, NB3-1 vs Control. (**I–K**) For Control, n = 17,16,16. For NB3-1>Hb, n = 21. Control is NB3-1/+ and NB3-1>Hb is NB3-1-GAL4/UAS-Hb; UAS-Hb/+. All images are shown dorsal up, anterior to the left. For quantifications, average and standard deviation are overlaid. Unpaired t-test 'ns' not significant, '**' $p<0.05$, '****' $p<0.0001$.

Next, we examined the physiology of Muscle 6, which has a decrease in synaptic branches in NB3-1>Hb (Figure 3.19G). If there is no homeostatic compensation, then decreased number of synapses is expected to decrease the amount of presynaptic neurotransmitter released (quantal content), not affect postsynaptic receptor sensitivity (mEPSP amplitude), and lead to an overall decrease in the muscle response to nerve stimulation (EPSP amplitude). Our data are consistent with these expectations (Figure 3.19H–K). Thus, in NB3-1>Hb, there is impaired synaptic function and lack of homeostatic compensation on Muscle 6. Similar phenotypes have been observed in a previous study (Goel et al., 2019)[157].

We conclude that in NB3-1>Hb, on Muscle 30, there are wild type levels of synaptic function. Whereas, in NB3-1>Hb, Muscle 6 synaptic function is impaired. Taken together these data show that prolonged expression of Hunchback in NB3-1 results in functional changes in motor system physiology.

Precocious expression of castor in NB7-1 decreases the number of U motor neurons and causes loss of synaptic connectivity onto later-born U muscle targets

In the Drosophila motor system, Hunchback is one of several temporal transcription factors in a well-characterized cascade that also includes Kruppel, Pdm, and Cas (Doe, 2017)[64]. To show that temporal transcription factors, as a class of molecules, control motor neuron-to-muscle synaptic partnerships, we need to manipulate temporal transcription factors other than Hunchback. For the remainder of this paper, we focus on two temporal transcription factors, Castor and Pdm. We focus on Castor and Pdm because, although they are temporal transcription factors like Hunchback, they differ from Hunchback in important ways. First, Hunchback is the earliest transcription factor in the cascade, whereas Castor and Pdm are expressed later in the cascade. Second, Hunchback is thought to specify early-born temporal identities, whereas Castor and Pdm specify later-born temporal identities. Third, prolonged expression of Hunchback extends the time that neuroblasts produce early-born neurons, whereas precocious expression of Castor and Pdm can truncate the time that neuroblasts produce early-born neurons. Together the series of experiments described in the sections below probe the extent to which changes in temporal transcription factors Cas and Pdm produce long lasting changes in motor neuron-to-muscle synaptic connectivity.

Here, we use NB7-1 as a model lineage because temporal transcription factors are arguably the most well-characterized in the NB7-1 lineage. Early divisions of NB7-1 give rise to five U motor neurons in the following birth order: U1, U2, U3, U4, and U5 (Figure 3.20A). All U motor neurons express the transcription factor Eve and synapse on dorsal muscles (Figure 3.20A). In embryos, each U motor neuron can be identified by a unique combination of marker genes, and in larvae, each U motor neuron forms a synapse on a unique dorsal muscle (Figure 3.21A). Studying NB7-1 as a model lineage allows us to investigate the impact of manipulating temporal transcription factors on embryonic temporal identities and to

link this to mature synaptic partnerships. Before examining larval synapses, we confirmed that our Cas manipulation generates embryonic motor neuron phenotypes. In wild type, in NB7-1, Cas is first expressed during the division that generates the U5 motor neuron, and Cas continues to be expressed in NB7-1 during subsequent divisions that give rise to a set of Cas(+) interneurons (Figure 3.21A). Cas expression closes the window of U motor neuron production. This can be seen by driving UAS-Cas with En-GAL4, which is expressed from the first division in all nerve cord row six and seven neuroblasts, and observing the production of fewer than five U motor neurons (Grosskortenhaus et al., 2006)[69]. Here, we express Castor starting during the earliest divisions of NB7-1 using a NB7-1 specific driver, NB7-1-GAL4 to drive UAS-Cas (herein, NB7-1>Cas)(Figure 3.21B). NB7-1>Cas allows us to grow animals to late larval stages and to rule out any non-lineage specific effects. We stained NB7-1>Cas embryos with a U motor neuron marker (Eve), a pan-motor neuron marker (pMad), and markers for individual U motor neuron identities (Figure 3.21D,F). In a majority of hemisegments in NB7-1>Cas, we see decreases to sets of three or four U motor neurons (Figure 3.21D–F). These U motor neuron sets have molecular identities of U1, U2, U3 or U1, U2, U3, U4/U5, respectively (Figure 3.21D–E). These data show our reagents are working as expected. We conclude that at embryonic stages, precocious expression of Cas, specifically in NB7-1, decreases the number of U motor neurons.

Next, in NB7-1>Cas, we characterize mature neuromuscular synapses at larval stages. Because NB7-1>Cas has different numbers of U motor neurons in different hemisegments, we matched nerve cord hemisegments to corresponding body wall segments (Figure 3.20C–D). In hemisegments in NB7-1>Cas with fewer U motor neurons (three or four), we counted mature synaptic branches onto individual dorsal muscles. Compared to controls, we find no change in 1b branch number onto Muscles 9, 10, and 2 (U1, U2, and U3 muscle targets, respectively) (Figure 3.20E–H,K–L). However, compared to our control, we see a significant decrease in 1b branch number onto Muscles 3 and 4 (U4 and U5 muscle targets, respectively)

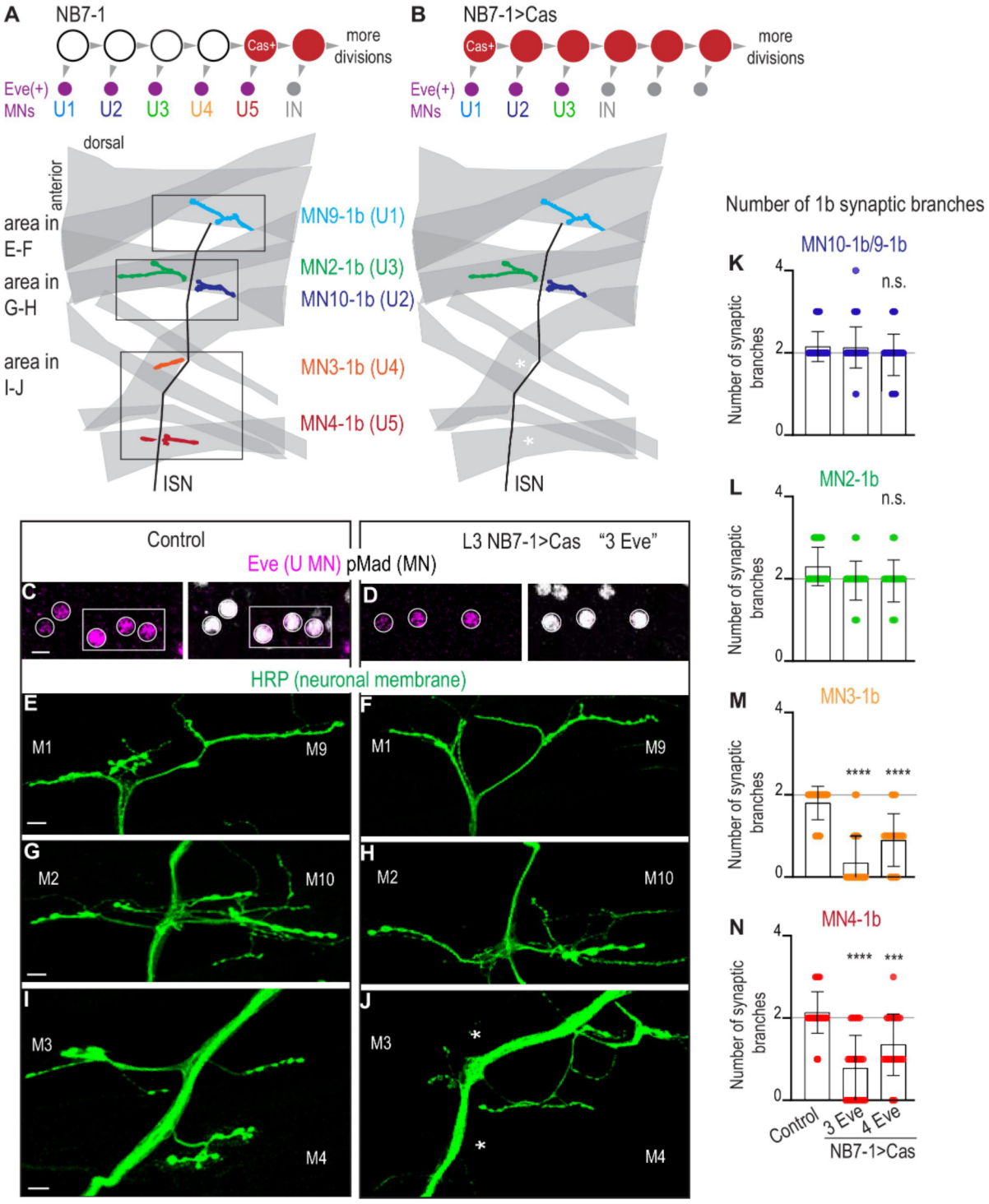


Figure 3.20: Precocious expression of Castor alters U motor neuron synapses. (**A**–**B**) Illustrations of NB7-1 lineage progression. Each gray arrowhead represents cell division. Each gray arrowhead represents cell division. Large circles are neuroblasts, and smaller circles are neurons. IN is interneuron. In NB7-1>Cas there is a decrease in the number of Eve(+) neurons with U4/U5 embryonic molecular identity. *Continued*

Figure 3.20: *Cont'd.* Precocious expression of Castor alters U motor neuron synapses. Illustrations of neuromuscular synapses on dorsal muscles in a L3 body wall segment and embryonic molecular identity depicted as circles (light blue = U1, dark blue = U2, green = U3, orange = U4, red = U5). In NB7-1>Cas the number of 1b synaptic branches (in orange and red) are lost (white asterisks) onto Muscle 3 and Muscle 4 (U4 and U5 muscle targets, respectively). (**C**–**D**) Images of L3 nerve cord abdominal hemisegment Eve(+) neurons co-expressing the motor neuron marker pMad. For Control, n = 12 hemisegments in three animals. For NB7-1>Cas, n = 23 hemisegments in seven animals. All images are shown anterior up, midline left, scale bar represents five microns. (**E**–**J**) Images of neuronal membrane, both axons and neuromuscular synapses, on ventral muscles in L3 abdominal segments corresponding to hemisegments containing the number of Eve(+) neurons as imaged in (D–E). An asterisk * indicates missing synapses on Muscle 3 and Muscle 4. All images are shown dorsal up, anterior left, scale bar represents 10 microns. Data quantified in (K–N). (**K**–**N**) Quantification of the number of 1b branches on L3 muscles. Color code as in (A). Line intersects the y-axis at 2. Each dot represents the number of branches onto a single muscle. Decrease in synaptic branching onto Muscle 4 and Muscle 3 in experimental conditions (3 Eve(+) neurons and 4 Eve(+) neurons) vs Control (K). No change (L). (K–N) For Control n = 59,30,30,30. For NB7-1>Cas hemisegments with 3 Eve(+) neurons, n = 46,23,23,23. For NB7-1>Cas hemisegments with 4 Eve(+) neurons, n = 40,20,20,20. Control is Cas/+ and NB7-1>Cas is NB7-1 GAL4/Cas. For quantifications, average and standard deviation are overlaid. ANOVA, corrected for multiple samples 'ns' not significant, '***' $p<0.001$, '****' $p<0.0001$.

(Figure 3.20I–J,M–N). These data suggest that precocious expression of Cas in NB7-1 leads to changes in embryonic U motor neuron number, and that these changes correspond to long-lasting changes in motor neuron-to-dorsal muscle synapses at larval stages. We conclude that at least one temporal transcription factor other than Hunchback can control motor neuron-to-muscle synaptic partnerships.

Precocious expression of pdm in NB7-1 anatomically and functionally alters U motor neuromuscular synapses

Here, we continue to address the question to what extent do temporal transcription factors other than Hb control motor neuron-to-muscle synaptic partnerships. Specifically, we manipulate the temporal transcription factor Pdm to generate 'heterochronic' mismatches

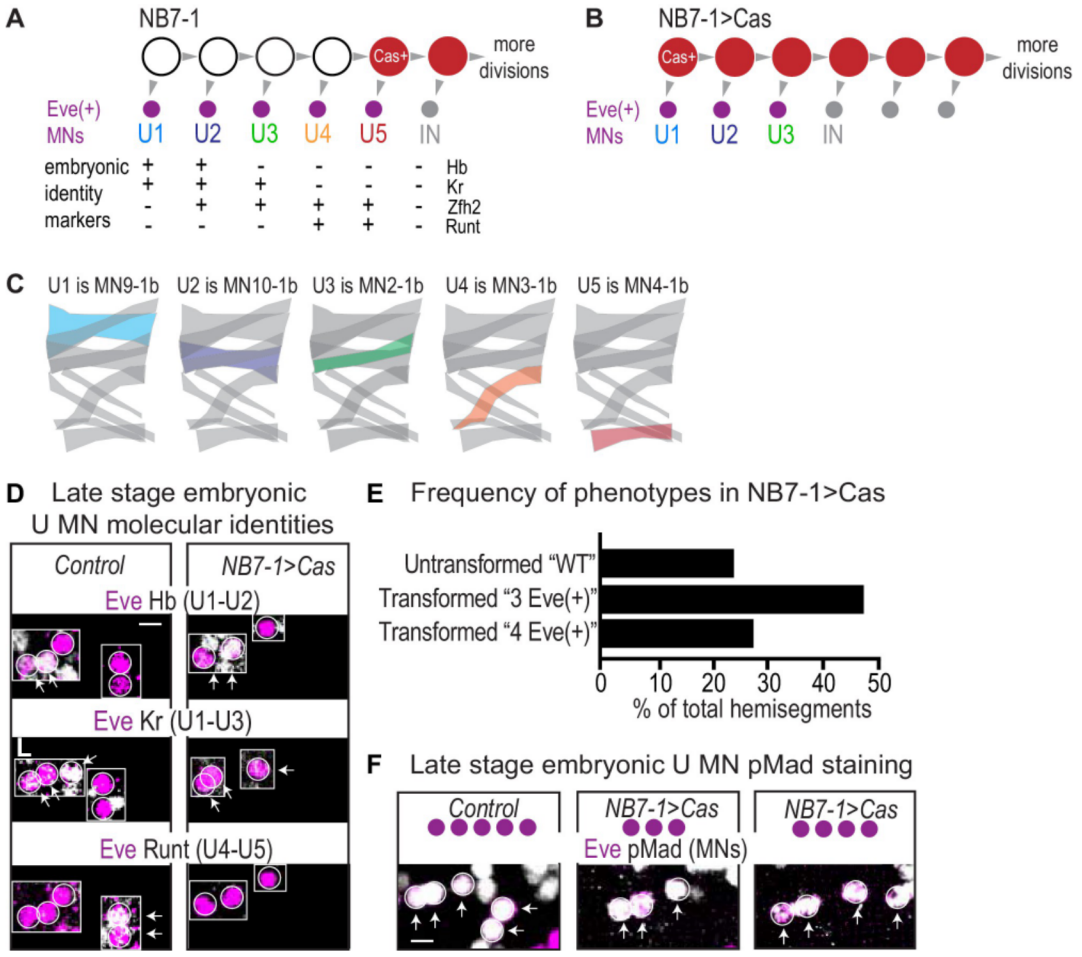


Figure 3.21: In embryos, precocious expression of Castor generates fewer U motor neurons at the expense of later born neurons. (**A**–**B**) Illustrations of NB7-1 lineage progression. Each gray arrowhead represents cell division. Each gray arrowhead represents cell division. Large circles are neuroblasts, and smaller circles are neurons. Abbreviations: IN is interneuron, MN is motor neuron, IN is interneuron, Eve is Even-skipped, Hb is Hunchback, Kr is Kruppel, and Zfh2 is Zinc finger homeodomain 2. In NB7-1>Cas, there is a decrease in the number of Eve(+) neurons with U4/U5 embryonic molecular identity. (**C**) Illustration of individual U motor neuron neuromuscular synapses onto dorsal muscles in larvae. Embryonic motor neuron (e.g., U1) and larval motor neuron synapse (e.g. MN9-1b) names are shown. Color code as in (A). (**D**) Images of embryonic molecular identity marker expression in Eve(+) cells in late stage embryonic CNSs. In NB7-1>Cas, Eve(+) cells with U4/U5 molecular identity are not produced. Boxes are neurons from different z-planes. Arrows indicate co-expression. *Continued*

Figure 3.21: *Cont'd.* (**E**) Quantification of the % of hemisegments in late stage embryonic NB7-1>Cas that give rise to f5 Eve(+) neurons (Untransformed 'WT'), 3 Eve(+) neurons (Transformed '3 Eve(+)"), and 4 Eve(+) neurons (Transformed '4 Eve(+)"). n = 44/180, n = 86/180, n = 50/180, respectively for the three phenotypes. (**F**) Images of co-expression of Eve and the pan-motor neuron marker, pMad in Control and NB7-1>Cas CNS of late stage embryos. All images are shown anterior up, midline to the left, scale bars represent 5 microns.

between a U motor neuron's embryonic temporal identity and its birth time. By studying heterochronic mismatches we can assess the relative contribution of intrinsic factors (e.g., neuronal gene expression) versus extrinsic factors (e.g., availability of synaptic partners or transient signaling cues) in control of synaptic partner selection.

Prolonged Hb expression in NB7-1 generates a heterochronic mismatch. It produces a large number of ectopic motor neurons with U1-like molecular identities (Isshiki et al., 2001)[68]. This means that in NB7-1>Hb, early-born U motor neurons are generated at abnormally late times in development. In NB7-1>Hb, at late larval stages there are increases in motor neurons innervating the dorsal muscles (Meng et al., 2019)[2]. This demonstrates that prolonged expression of Hb causes early-born U motor neurons to target dorsal muscles without regard to time-linked environmental cues. Notably, precocious expression of the temporal transcription factor Cas in NB7-1, described in the section above, reduces the total number of U motor neurons, but does not create a heterochronic mismatch. Here, using Pdm, we produce two heterochronic mismatches that allow us to determine the extent to which late-born U motor neurons born either at abnormally late or abnormally early times in development can target particular dorsal muscles. These experiments are critical for determining the extent to which factors other than Hb specify synaptic partner selection.

We manipulate Pdm, which is expressed during the fourth and fifth division window of NB7-1 (Figure 3.23A). Pdm specifies the U4 temporal identity and represses Kruppel, the temporal transcription factor that specifies the U3 temporal identity (Grosskortenhaus et al., 2006)[69]. We precociously express Pdm in the NB7-1 using NB7-1-GAL4 to drive UAS-Pdm

(herein, NB7-1>Pdm). We characterize this manipulation by immunostaining with markers in embryos for U motor neurons (Eve), all motor neurons (pMad), and individual U motor neuron temporal identity markers (Figure 3.22). We find that NB7-1>Pdm transforms U motor neuron identities in a manner consistent with other GAL4 drivers (Grosskortenhaus et al., 2006)[69]. Specifically, in NB7-1>Pdm, we see two phenotypes–either decreases or increases in the number of U motor neurons per abdominal hemisegment in comparison to controls (Figure 3.23B–C, Figure 3.22F). Each phenotype is discussed in a separate paragraph below.

In NB7-1>Pdm, hemisegments with additional U motor neurons are examples of heterochronic mismatches in which later-born U motor neurons are born at abnormally late times in development. Notably, we observe this phenotype selectively in segments A1-A3 (Figure 5B). In these segments, U motor neurons have the following embryonic molecular identities: U1, U2, U3, U4, followed by a variable number of U5-like neurons (Figure 3.23B, Figure 3.22C–G). Therefore, in NB7-1>Pdm, neurons with U5-like identities are born at abnormally late times, that is, when interneurons are usually made.

In NB7-1>Pdm, hemisegments with fewer U motor neurons are examples of heterochronic mismatches in which later-born U motor neurons are born at abnormally early times in development. Notably, we observe this phenotype selectively in segments A4-A7 (Figure 3.23C). In these segments, U motor neurons have the following embryonic molecular identities: U1, U2, U4, and U5, but not U3 (Figure 3.23C, Figure 3.22D–G). To confirm this heterochronic mismatch, we co-stained for the U4 and U5 marker Runt and the U motor neuron marker Eve in stage late 11 to early 12 embryos. At this stage in wild type, four Eve(+) neurons are generated, one of which is Runt(+) (Figure 3.22H). In NB7-1>Pdm, at the same stage, of the four Eve(+) neurons two can be Runt(+) (Figure 3.22H). Therefore, in NB7-1>Pdm, NB7-1 can skip production of U3 and produce neurons with U4 and U5 molecular identities at abnormally early times in development.

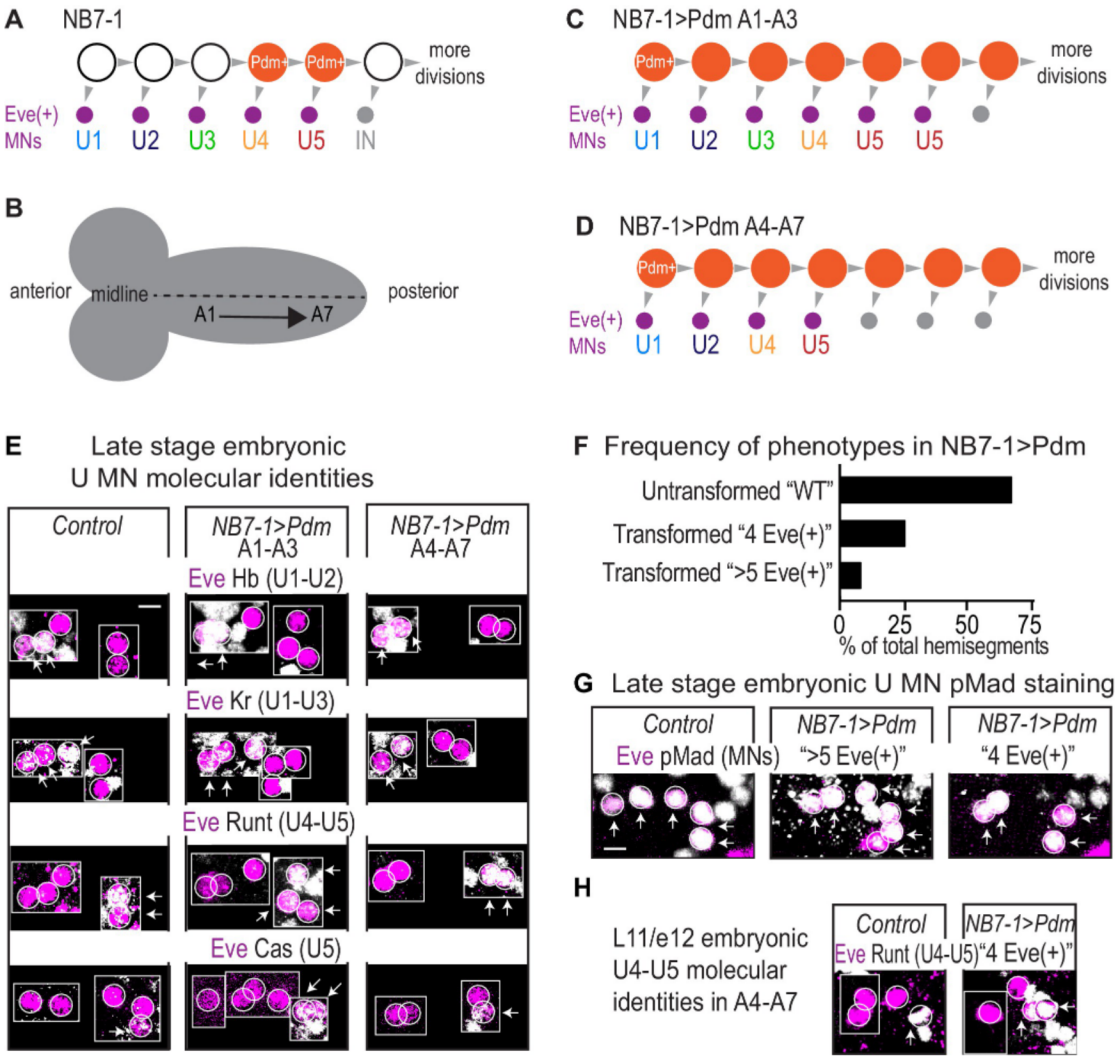


Figure 3.22: In embryos, precocious expression of Pdm generates either more or fewer U motor neurons depending on A/P positioning. (**A**) Illustration of NB7-1 lineage progression. Each gray arrowhead represents cell division. Each gray arrowhead represents cell division. Large circles are neuroblasts, and smaller circles are neurons. Abbreviations: IN is interneuron. (**B**) Illustration of a Drosophila embryo CNS. Nerve cord abdominal hemisegments are represented as (A). A1 is most anterior and A2-A7 are progressively more posterior. Dotted line represents the midline. (**C**–**D**) Illustration follows (A). In NB7-1>Pdm for A1-A3, there is an increase in the number of Eve(+) neurons with U5 embryonic molecular identity (C). In NB7-1>Pdm for A4-A7, there is a decrease in the number of Eve(+) neurons with U3 embryonic molecular identity. (**E**) Images of embryonic molecular identity marker expression in Eve(+) cells in late stage embryonic CNSs. In NB7-1>Pdm A1-A3, extra Eve(+) cells with U5 molecular identity are produced. In NB7-1>Pdm A4-A7, Eve(+) cells with U3 molecular identity are not produced. Boxes are neurons from different z-planes. Arrows indicate co-expression. *Continued*

Figure 3.22: *Cont'd.* In embryos, precocious expression of Pdm generates either more or fewer U motor neurons depending on A/P positioning. (**F**) Quantification of the % of hemisegments in late stage embryonic NB7-1>Pdm that give rise to 5 Eve(+) neurons (Untransformed 'WT'), 4 Eve(+) neurons (Transformed '4 Eve(+)"), and more than 5 Eve(+) neurons (Transformed '>5 Eve(+)"). n = 103/154, n = 39/154, n = 12/154, respectively for the three phenotypes. (**G**) Images of co-expression of Eve and the pan-motor neuron marker, pMad in Control and NB7-1>Pdm CNS of late stage embryos. (**H**) Images of embryonic stage late 11 to early 12 (l11/e12) embryonic stage of co-expression of Eve and the U4/U5 marker Runt. In NB7-1>Pdm, cell division rate is not altered because 4 Eve(+) neurons are born, similar to Control. During l11/e12 in NB7-1>Pdm, two neurons expressing Runt are born, while in Control only one neuron expressing Runt is born. Control is Pdm/+ and NB7-1>Pdm is NB7-1 GAL4/Pdm; Pdm/+. All images are shown anterior up, midline to the left. Scale bars represent 5 microns.

Next, in NB7-1>Pdm, we looked at motor neuron-to-dorsal muscle synapses in late stage larvae. First, we looked at neuroanatomy, matching nerve cord hemisegments to corresponding body wall segments, and staining for muscle (phalloidin) and neuronal membrane (anti-HRP) (Figure 3.23A–F). When hemisegments contain >5 Eve(+) pMad(+) neurons (e.g., those with U5-like neurons born at abnormally late times), we find a significant increase in 1b branch number selectively Muscle 4 (i.e., wild type U5 target, Figure 3.23B,K,P), while all other muscles had no change in branch number compared to our control (Figure 3.23). When hemisegments contain 4 Eve(+) pMad(+) neurons (e.g., those with U4 and U5 generated at abnormally early time and lacking a U3-like neuron), compared to our control, we find a significant decrease in 1b branch number on Muscle 2 (U3 muscle target, Figure 3.23C,I,N), and no changes in 1b branch number on other muscles (Figure 3.23). These data show that the alterations in embryonic motor neuron markers in NB7-1 > Pdm correlates with changes in the number of synaptic branches on dorsal muscles at larval stages.

Next, we confirmed that in NB7-1>Pdm in abdominal segments A1-A3, the increased nerve branches on Muscle 4 contained neuromuscular synapses. We stained for synaptic proteins for active zones (Bruchpilot), postsynaptic densities (Discs large), and neurotransmitter receptors (GluRIIA) (Figure 3.24A). We find a normal abundance and localization for

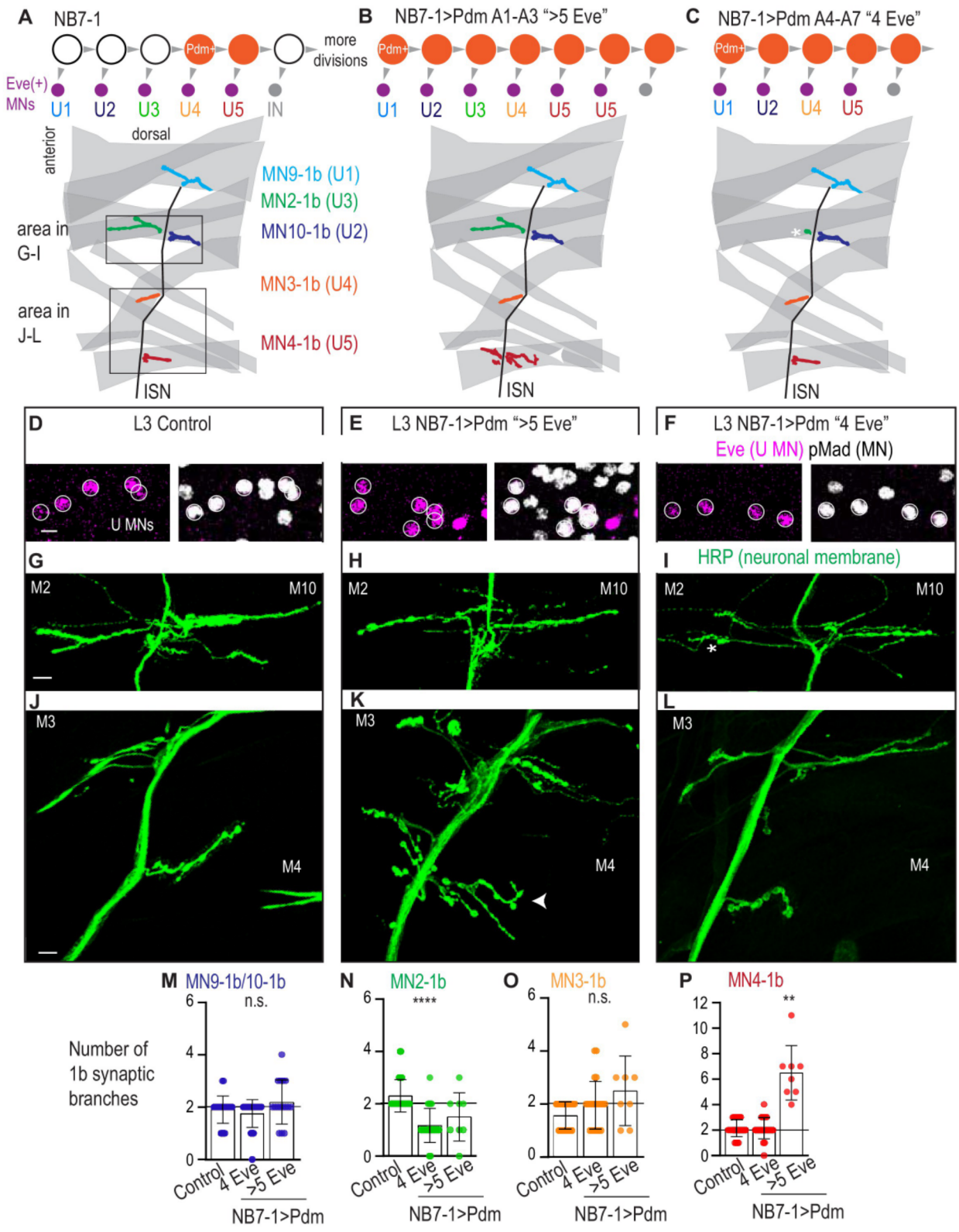


Figure 3.23: Precocious expression of Pdm alters U motor neuron synapses. *Continued*

Figure 3.23: *Cont'd.* Precocious expression of Pdm alters U motor neuron synapses.(**A**–**C**) Illustration of NB7-1 lineage progression. Each gray arrowhead represents cell division. Each gray arrowhead represents cell division. Large circles are neuroblasts, and smaller circles are neurons. Abbreviations: IN is interneuron. Illustrations of neuromuscular synapses on dorsal muscles in a L3 body wall segment and embryonic molecular identity depicted as circles (light blue = U1, dark blue = U2, green = U3, orange = U4, red = U5). In NB7-1>Pdm in A1-A3 segments where there are more than 5 Eve(+) U motor neurons, the number of 1b synaptic branches (in red) are increased (white arrowhead) onto Muscle 4 (U5 muscle target). In NB7-1>Pdm in A4-A7 segments where there are 4 Eve(+) U motor neurons, the number of 1b synaptic branches (in green) is nearly lost on Muscle 2 (U3 muscle target). (**D**–**F**) Images of L3 nerve cord abdominal hemisegment Eve(+) neurons co-expressing the motor neuron marker pMad. All images are shown anterior up, midline left. Scale bars represent 5 microns. (**G**–**L**) Images of neuronal membrane, both axons and neuromuscular synapses, on ventral muscles in L3 abdominal segments corresponding to hemisegments containing the number of Eve(+) neurons as imaged in (D–E). An asterisk * indicates missing synapses on Muscle two and an arrowhead indicates increase in synapses on Muscle 4. Data quantified in (M–P). All images are shown dorsal up, anterior left. Scale bars represent 10 microns. (**M**–**P**) Quantification of the number of 1b branches on L3 muscles. Color code as in (A). Line intersects the y-axis at 2. Each dot represents the number of branches onto a single muscle. Control is Pdm/+. NB7-1>Pdm is NB7-1 GAL4/Pdm; Pdm/+. In H, Control is NB7-1 GAL4/UAS myr GFP. (M–P) For Control, n = 33,26,28,28. For NB7-1>Pdm with 4 Eve(+), n = 45,23,22,23. For NB7-1>Pdm with 5 Eve(+), n = 16,8,8,8. For quantifications average and standard deviation are overlaid. ANOVA, corrected for multiple samples 'ns' not significant, '**' $p<0.05$, '****' $p<0.0001$.

all markers (Figure 3.24B–G). Thus, on the cell biological level, neuromuscular synapses in NB7-1>Pdm are not different from Control. Finally, for NB7-1>Pdm (A1-A3), we visualize neuromuscular synapse activity onto Muscle 4 with a post-synaptically localized calcium sensor (Newman et al., 2017)[133]. In late larval neuromuscular synapses, we imaged spontaneous release of individual synaptic vesicles from 1b branches on Muscle 4, that have increased numbers of synaptic branches. In both Control and NB7-1>Pdm, we see that within a five-minute imaging period, there is at least one postsynaptic response (Figure 3.24H–I, Figure 3.25). From these findings, we conclude that Pdm can impact functional synaptic connections onto muscles made by U motor neurons.

In summary, we find that precocious expression of Pdm in NB7-1 leads to two different types of heterochronic mismatches: one in which later-born U motor neurons are born at

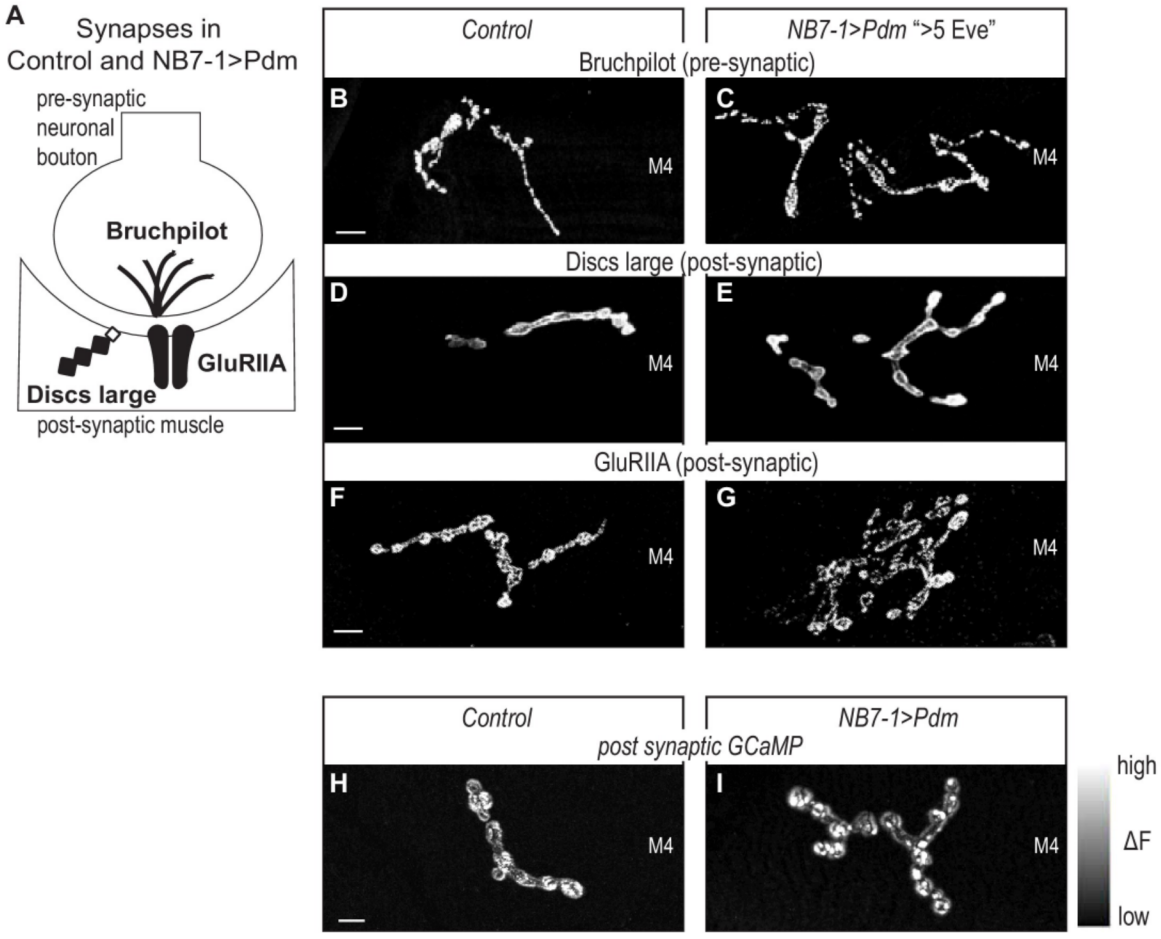


Figure 3.24: Altered synapses onto Dorsal muscles are functional. (**A**) Illustration of subcellular localization of neuromuscular synapse markers. Brunchpilot labels active zones, Discs large is a scaffolding protein strongly localized at post-synapse, GluRIIA is a glutamate receptor IIA. (**B**–**G**) Images of neuromuscular synapses on L3 Muscle 4. There is no difference in distribution or abundance of synaptic markers between Control and NB7-1>Pdm. Control is Pdm/+ and NB7-1>Pdm is NB7-1-GAL4/UAS-Pdm; UAS-Pdm/+ (**H**–**I**) Images of fluorescence intensity changes in a calcium indicator of synaptic activity. GCaMP was targeted to the post-synaptic density for example (DLG in E-G). When pre-synaptic vesicles are released from active zones (Brp in B-C), post-synaptic neurotransmitter receptors respond (GluRIIA in G-F), increasing GCaMP fluorescence intensity (see Figure 3.25 for details). Images show post-synaptic responses (delta F) in L3 Muscle 4 (M4) in Control and NB7-1>Pdm. Control is Pdm/+; MHC-CD8-GCaMP6f-Sh/Pdm and NB7-1>Pdm is NB7-1-GAL4/Pdm; MHC-CD8-GCaMP6f-Sh/Pdm. All images are shown dorsal up, anterior to the left. Scale bars represent 10 microns.

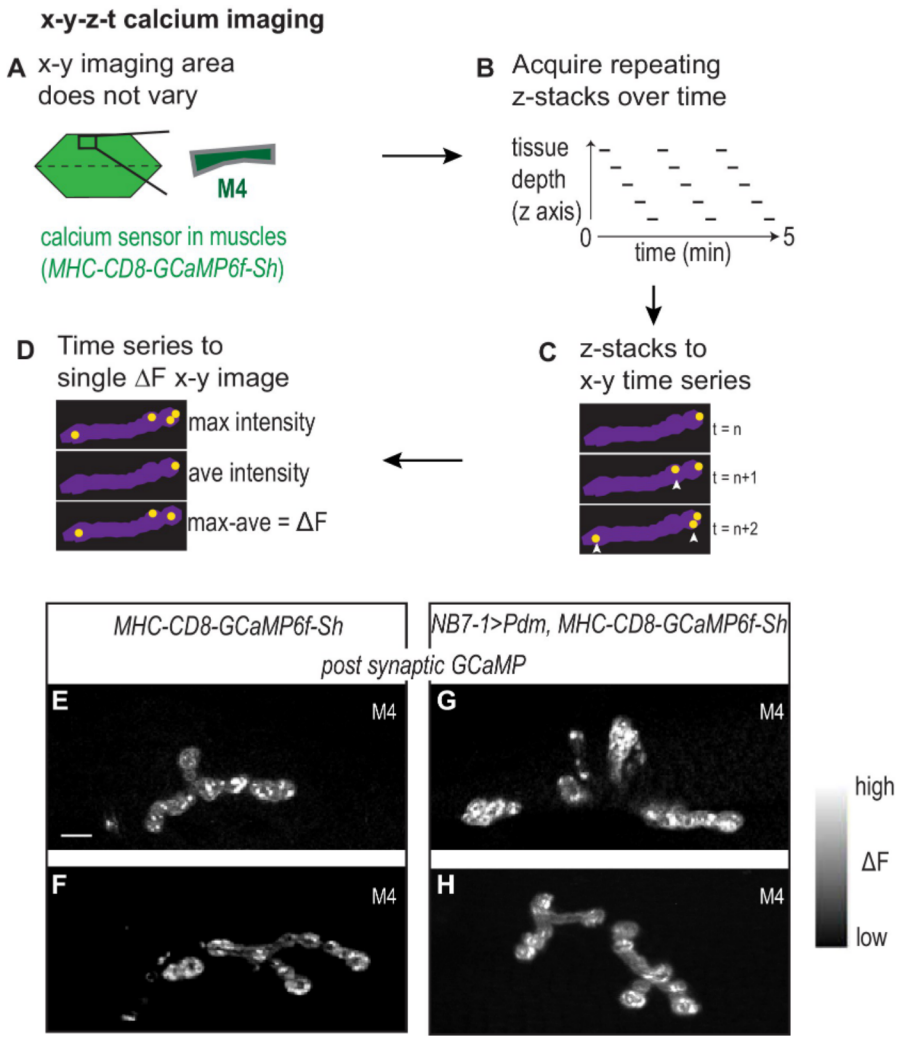


Figure 3.25: Calcium imaging protocol, analysis, and examples. (**A**–**D**) Illustration of calcium imaging protocol and analysis are shown. See Materials and methods for details. (**E**–**H**) Images of calcium signals on L3 Muscle 4. Control is NB7-1-GAL4/+; MHC-CD8-GCaMP6f-Sh/+ and NB7-1>Pdm is NB7-1-GAL4/UAS Pdm; MHC-CD8-GCaMP6f-Sh/UAS Pdm. Images are dorsal up, anterior to the left. Scale bar represents 10 microns.

abnormally late times in development, and one in which later-born U motor neurons are born at abnormally early times in development. We find a strong correlation between embryonic molecular identity and larval neuromuscular synapses. Together these data support the idea that regardless of birth time, both early-born and later-born U motor neurons can target specific dorsal muscles. They demonstrate that Hb is not the only temporal transcription that can provide enough molecular information to neuronal progeny, such that the neuronal

progeny are insensitive to time-linked environmental cues. Ultimately this supports the idea that a general feature of the temporal transcription factors is to control neuromuscular synapse formation.

3.3.4 Discussion

In this study, we address the question to what extent is control of synaptic partner selection a general feature of temporal transcription factors. Our study has two key findings. First, we find prolonged expression of the temporal transcription factor, Hunchback increases the number of RP motor neurons produced by NB3-1 and that this manipulation permanently changes the functional innervation of ventral muscles (Figures 3.15,3.18,3.19). Because we previously showed that Hunchback acts similarly in another neuroblast, NB7-1, we conclude that a general feature of Hunchback is to control motor neuron-to-muscle synaptic partnerships (Meng et al., 2019)[2]. Second, we find precocious expression of temporal transcription factors, Castor and Pdm, alter the number of U motor neurons produced by NB7-1 and permanently change the functional innervation of dorsal muscles (Figures 3.20,3.23,3.24). Together these findings provide strong support for the hypothesis that temporal transcription factors, as a class of molecules, are potent regulators of synaptic partner selection.

A general feature of the temporal transcription factor, Hunchback is to control synaptic partner selection

In Drosophila motor system development, most neuroblasts express the temporal transcription factor Hunchback early during lineage development (Pearson and Doe, 2004)[62]. In all of the multiple lineages tested so far, Hunchback is necessary and sufficient to specify early-born neuronal marker gene expression, regardless of the cell type (e.g., motor neuron, interneuron, glia) (Cleary, 2006; Isshiki et al., 2001; Kambadur et al., 1998; Novotny et al.,

2002; Pearson and Doe, 2003)[139, 68, 100, 148, 102]. Notably, the mammalian homolog of Hunchback, Ikaros, similarly regulates early-born marker gene expression in both retina and cortex (Alsiö et al., 2013; Elliott et al., 2008). In the Drosophila nerve cord, in multiple lineages, Hunchback regulates other aspects of time-linked, post-mitotic neuronal identity, including embryonic axonal trajectory (Isshiki et al., 2001; Tran and Doe, 2008; Seroka and Doe, 2019; Meng et al., 2019)[68, 70, 80, 2]. However, the extent to which Hunchback regulates terminal neuronal features is still poorly characterized. Recently, in one neuroblast, NB7-1, Hunchback was shown to regulate motor neuron-to-muscle synaptic partnerships (Meng et al., 2019)[2]. But it was unknown the extent to which this is a general feature of Hunchback.

In this study, we prolonged Hunchback expression in NB3-1. NB3-1 produces a series of ventrally-projecting, Hb9(+) RP motor neurons (Tran and Doe, 2008)[70]. Notably, NB3-1 begins dividing much later in nerve cord development than NB7-1 (Bossing et al., 1996)[57]. Prolonging the expression of Hunchback in NB3-1 dramatically increased the number of Hb9(+) motor neurons produced and caused permanent changes in neuromuscular synaptic partnerships and physiology in the ventral muscle circuit (Figures 3.15,3.18,3.19). We learn three things from these results. First, Hunchback controls muscle targeting of motor neurons consistently across two lineages. Second, muscles that are over-innervated in comparison to control can have normal synaptic transmission, but muscles that are under-innervated, in comparison to control, have impaired synaptic physiology. Third, Hunchback controls synaptic partner selection consistently across different time points in nerve cord development. This suggests that in many lineages Hunchback is likely to regulate synaptic partner selection, which has broader implications extending to Hunchback's vertebrate ortholog, Ikaros (Mattar et al., 2015)[158]. Future work will need to determine the extent to which Hunchback's function is conserved.

Precocious expression of Castor or Pdm lead to permanent changes in motor neuron-to-muscle synaptic partnerships in Drosophila locomotor circuits

Hunchback is one member of a large class of molecules termed temporal transcription factors that in the Drosophila motor system also includes Castor (Cas) and Pdm. In vertebrates, a Castor homolog, Casz1, has also been shown to be a temporal transcription factor (Mattar et al., 2015). In this study, we asked to what extent can temporal transcription factors Cas and Pdm control synaptic partner selection. Specifically, in NB7-1, precocious expression of the temporal transcription factor Castor (NB7-1 > Cas) or Pdm (NB7-1 > Pdm) leads to three different phenotypes: (1) Precocious expression of Cas in NB7-1 truncates the production of Eve(+) U motor neurons (Figure 3.20). Notably, the U motor neurons that are produced are produced at the correct time in development. (2) In NB7-1 > Pdm, in anterior segments A1-A3, there are late-born U5 motor neurons born at abnormally late times in development (Figure 3.23). (3) In NB7-1 > Pdm, in posterior segments A4-A7, there are late-born U4/U5 motor neurons born at abnormally early times in development (Figure 3.23). For reference, previous manipulations that prolonged Hunchback expression in NB7-1 generated early-born U1 motor neurons at abnormally late times in development (Meng et al., 2019)[2]. Thus, using Cas and Pdm, we probe the system to get a more comprehensive understanding of how changes in embryonic temporal identity, mediated by temporal transcription factors, impacts motor neuron-to-muscle synaptic partnerships.

In wild type, NB7-1 produces five U motor neurons, each of which can be uniquely identified by embryonic molecular markers, and each of which, in larvae, makes a unique motor neuron-to-muscle synaptic partnership. Notably, in NB7-1 > Cas, the embryonic molecular identities that are lost are U4 and U5. In larval stages, the specific dorsal muscles that are under innervated are the normal U4 and U5 target muscles. In NB7-1 > Pdm, in segments A1-A3, the U3 embryonic molecular identity is skipped, and in larval stages the normal U3 muscle is under-innervated. In NB7-1 > Pdm, in segments A4-A7, extra U5 embryonic

identities are produced, and in larval stages the normal U5 target is over-innervated. Thus, in both NB7-1 > Cas and NB7-1 > Pdm there is strong correlation between embryonic molecular identity and mature motor neuron-to-muscle synaptic partnerships. This finding is somewhat surprising given that in previous work, which prolonged Hunchback in NB7-1, there was a poor correlation between embryonic molecular identity markers and mature motor neuron-to-muscle synaptic partnerships (Meng et al., 2019)[2]. Notably the correlation between embryonic molecular identity and synaptic partnerships seen in this study using Cas and Pdm manipulation is more inline with the predominant model in the field. The predominant model states that temporal transcription factors are master regulators of entire temporal programs, and should therefore determine not just early neuronal features like marker gene expression, but also terminal neuronal features such as synaptic partner selection. Overall, our data demonstrate that there is variability in the predictive strength of molecular identity markers.

In this study, we generated 'heterochronic' mismatches between a U motor neuron's embryonic temporal identity and its birth time by precociously expressing Pdm in NB7-1. By studying heterochronic mismatches we can assess the relative contribution of intrinsic factors (e.g., neuronal gene expression) versus extrinsic factors (e.g., availability of synaptic partners or transient signaling cues) in control of synaptic partner choice. Our data in NB7-1 > Pdm, support a model in which lineage intrinsic factors determine motor neuron-to-muscle synaptic partnerships regardless of environmental cues present. This is in agreement with previous heterochronic mismatches that were induced by manipulation of Hunchback expression (Seroka and Doe, 2019; Meng et al., 2019)[80, 2]. However, there are still two unanswered questions. First, the time scale of heterochronic mismatches studied so far is on the order of one to several neuroblast divisions, or hours. So, it is unknown how heterochronic mismatches conducted at larger time scales would impact the system. Second, so far the heterochronic mismatches performed in the Drosophila motor system have focused

on neuromuscular synapses as a readout. Neuromuscular synapses are distinct from neuron-neuron synapses in the CNS, in that motor neuron-to-muscle synapses are usually one-to-one partnerships, and because motor neuron axonal targets are large, pre-existing muscles. In the future, it will be interesting to understand the extent to which intrinsic versus extrinsic factors contribute to well characterized neuron-to-neuron synaptic partnerships (Heckscher et al., 2015; Schneider-Mizell et al., 2016)[39, 28].

We note that manipulation of Pdm produces two different phenotypes (Figure 3.23). How does one manipulation give two opposing phenotypes? We find that the different phenotypes are correlated with anterior-posterior (A-P) position, raising the possibility that this difference involves factors differentially expressed along A-P axis (e.g., Hox genes). For example, in anterior segments Pdm could work with one Hox gene to promote U4 molecular identity, whereas in more posterior segments Pdm could work with a different Hox gene to promote the same fate. Already, this type of differential combinatorial use of spatial and temporal factors has been shown to converge on a common neuronal molecular identity (Gabilondo et al., 2016)[159]. Notably, in the Gabilondo study, converging mechanisms occur in different neuroblasts lineages. Our data raise the possibility that converging mechanisms leading to one molecular identity could occur within one class of stem cell (e.g., NB7-1) found at different A-P positions.

Temporal transcription factors can bi-directionally regulate the proportion of neurons from a lineage that populate specific motor circuits

The Drosophila motor system contains circuits that control synergistic groups of muscles (Clark et al., 2018)[19]. One circuit controls contraction of dorsal muscles, one circuit controls transverse muscles, and one circuit controls ventral muscles (Bate, 1993; Heckscher et al., 2012; Zarin et al., 2019)[78, 47, 30].

Early in development, NB7-1 generates motor neurons which project to dorsal muscles

and populate the dorsal muscle circuit. Later in development, NB7-1 generates interneurons, which do not project out of the CNS and do not populate the dorsal muscle circuit (Mark et al., 2021; Schmid et al., 1999)[84, 45]. Similarly, early in development, NB3-1 generates motor neurons which project to ventral muscles and populate the ventral muscle circuit, and later it generates interneurons (Schmid et al., 1999 [45]; Figure 3.26A). This leads to the question: what is the nature of the switch that controls whether neurons from a particular neuroblast populate a motor circuit versus another circuit. We suggest temporal transcription factors can be thought of as molecular switches acting in the neuroblast to regulate circuit membership of neuronal progeny. First, a pair of recent studies showed that prolonging the expression of Hunchback in NB7-1 dramatically increases the number of Eve(+) U motor neurons without changing the total number of neurons produced by the lineage (Seroka and Doe, 2019; Meng et al., 2019)[80, 2]. The extra U motor neurons form permanent, functional synapses on dorsal muscles (Meng et al., 2019)[2]. Therefore, in NB7-1, Hunchback determines what proportion of neurons from the lineage populate the dorsal muscle circuit. In our present study, we find similar effects by prolonging expression Hunchback in NB3-1 or by precociously expressing Pdm in NB7-1 in segments A1-A3 (Figure 3.26B). Also, in our present study, we find opposite effects by precociously expressing Cas in NB7-1 of by precociously expressing Pdm in NB71 in segments A4-A7 (Figure 3.26C). Thus, temporal transcription factors can bi-directionally modulate the proportion of neurons from a lineage that populate a given motor circuit.

3.3.5 Conclusion

In conclusion, our data provide support for the hypothesis that temporal transcription factors, as a class of molecules, can regulate synaptic partnerships. It is possible that temporal transcription factors in other parts of the Drosophila CNS, and vertebrate orthologs of the temporal transcription factors manipulated in this study, regulate circuit member-

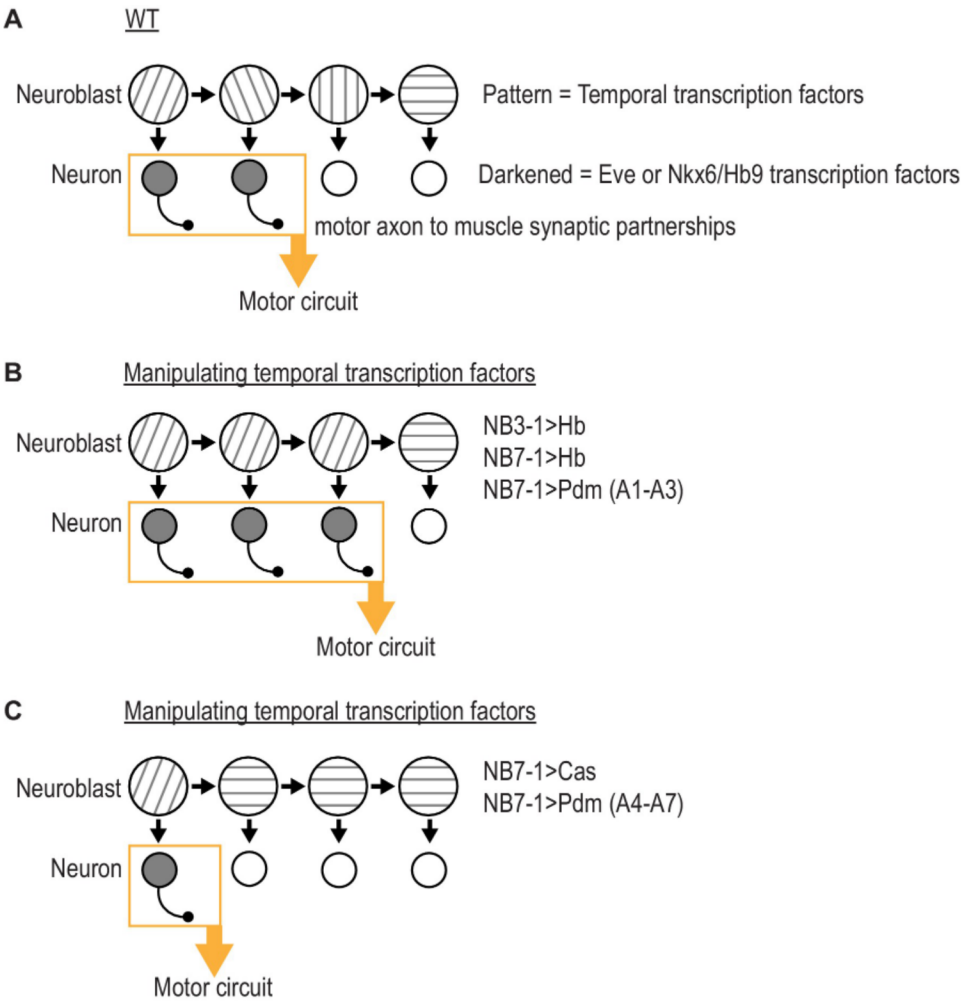


Figure 3.26: Summary of results in this study. (**A**) Illustration of WT (wildtype) neuroblast lineage progression. Different patterns in the neuroblast represent temporal transcription factor expression. Outgrowth projecting from neuron represent motor axon to muscle synaptic partnerships. Yellow box and arrow represent that these neurons are members of the same motor circuit. (**B**) Illustration of the outcome when expression of Hb (Hunchback) is prolonged in NB7-1 or NB3-1, or expression of Pdm is precocious in NB7-1 (A1-A3) (abdominal segments 1 through 3). Motor axon to muscle synaptic partnerships are altered by increased circuit membership. (**C**) Illustration of the outcome when expression of Cas (Castor) is precocious in NB7-1 or expression of Pdm is precocious in NB7-1 (A4-A7) (abdominal segments 4 through 7). Motor axon to muscle synaptic partnerships are altered by decreased circuit membership.

ship decisions in similar ways. Future studies will need to focus on downstream effectors of temporal transcription factors. Promising candidates would be transcription factors that control aspects of a neuron's anatomical features such as Morphology Transcription Factors

(Enriquez et al., 2015)[160]. Together our work provides fundamental insight into the logic of motor circuit assembly, and has implications for evolution, medicine, and the genetic basis of behavior.

3.3.6 Materials and methods

Fly genetics

Standard methods were used for propagating fly stocks. For all experiments, embryos and larvae were raised at 25 °C, unless otherwise noted. The following lines were used: DIP-alpha-GAL4 (gift of R. Carrillo), ac:VP16, gsb:v8v (aka NB7-1-GAL4) (gift of M. Kohwi), MHC-CD8-GCaMP6f-Sh (Bloomington stock center [BL] 67739), UAS-Hb; UAS-Hb/TM2 (BL 32198), 5172 J-GAL4 (aka NB3-1-GAL4, gift of H. Lacin), w1118 (BL 36005), UAS-Cas (gift of C. Doe), UAS-HA-pdm2/CyO; UAS-HA-pdm2/TM3 (gift of C. Doe), UAS-myr-GFP (BL 32198).

Tissue preparation

Three tissue preparations were used: Late stage whole mount embryos, in which antibody can still penetrate cuticle, and third instar (L3) fillet preparations, in which the neuromuscular tissue and cuticle are dissected away from other tissue and pinned open like a book, allowing for superb immuno-labeling and visualization of larval neuromuscular synapses. For all preparations, standard methods were used for fixation in fresh 3.7% formaldehyde (Sigma-Aldrich, St. Louis, MO) (Petrovic and Hummel, 2008; Pujol-Martí et al., 2012; Rossi et al., 2017)[125, 126, 108] or Bouin's fixative (RICCA, Arlington,TX) for 7 min. For detailed staining protocols see the following references: Heckscher et al., 2007; Heckscher et al., 2014 [161, 162]. For calcium imaging, L3 larvae expressing MHC-CD8-GCamp6f-Sh construct were dissected in HL3 solution containing 2 mM Ca2+ and 25 mM Mg2+, brains

removed, body walls rinsed with fresh saline, and samples imaged.

Immunostaining

Tissue was blocked for an hour at room temperature or overnight at 4 °C in phosphate buffered saline with 2% Normal Donkey Serum (Jackson ImmunoResearch), followed by 2 hr at room temperature in primary antibodies, and 1 hr at room temperature in secondary antibodies. Primary antibodies include: rabbit anti-Eve (1:1000, see Meng et al., 2019), chicken anti-GFP (1:1000, Aves GFP-1020), rat anti-Worniu (1:250 Abcam ab196362), guinea pig anti-Runt (1:500, John Rientz, UChicago), guinea pig anti-Hb (1:1000, John Rientz, UChicago), guinea pig anti-Kruppel (1:1000, John Rientz, UChicago), rat anti-Zfh2 (1:800 Chris Doe, UOregon), rabbit anti-Castor (1:1000 Chris Doe, UOregon), guinea pig anti-HB9 (1:1000 Heather Broiher, Case Western), rabbit anti-Smad3 (pMad) (1:300 Abcam 52903). The following monoclonal antibodies were obtained from the Developmental Studies Hybridoma Bank, created by the NICHD of the NIH and maintained at The University of Iowa, Department of Biology, Iowa City, IA: mouse anti-Brp (1:50, NC82), mouse anti-DLG (1:500, 4F3), mouse anti-GluRIIA (1:25, 8B4D2), mouse anti-En (1:5, 4D9), mouse anti-Eve (1:50, 3C10), mouse anti-Cut (1:50, 2B10). Secondary antibodies were from Jackson ImmunoResearch and were reconstituted according to manufacturer's instructions and used at 1:400. 647-Phalloidin (1:600, Thermofisher A22287) Rhodamine-Phalloidin (1:600, Thermofisher R415), Cy3-HRP (Jackson ImmunoResearch 123-025-021), 647-HRP (Jackson ImmunoResearch 123-605-021). Embryos were staged for imaging based on morphological criteria. Whole mount embryos and larval fillets were mounted in 90% Glycerol with 4% n-propyl gallate. Larvae brain preparations were mounted in DPX (Sigma-Aldrich, St. Louis, MO).

Image acquisition

For fixed tissue images, data were acquired on a Zeiss 800 confocal microscope with 40X oil (NA 1.3) or 63 X oil (NA 1.4) objectives, or a Nikon C2+ confocal microscope with 40X (NA 1.25) or 60X (NA 1.49) objectives. For calcium imaging, data were acquired using a Zeiss 800 confocal microscope with a 40X dipping objective (NA 1.0) using 488 nm laser power with the pinhole entirely open. Images were acquired on a Zeiss 800 confocal microscope. Images were cropped in ImageJ (NIH) and assembled in Illustrator (Adobe).

Type 1b branch counting

Third instar larval fillet preparations were stained for HRP to detect the neuronal membrane and Discs large (Dlg). Dlg allows type 1b and type 1s boutons to be distinguished. Single branches were counted as contiguous stretches of overlapping Dlg and HRP staining.

Calcium imaging

X-y-z-t stacks (Figure 3.25B-C) were converted into x-y time series images using the Maximum Intensity projection function (Fiji). X-y time series images were then registered using the Register Virtual Stack Slices plug-in (Fiji) to reduce movement artifacts. Time series images were projected into two different x-y single images using either the Maximum Intensity projection function (Fiji) or Average Intensity projection function (Fiji), and then the average intensity was subtracted from the maximum to get a change in fluorescence image.

Electrophysiology

Third instar larvae were dissected and pinned in 0.3 mM calcium modified HL3 saline (Stewart et al., 1994)[](70 mM NaCl, 5 mM KCl, 10 mM MgCl2, 10 mM NaHCO3, 5 mM

trehalose, 115 mM sucrose, 5 mM HEPES). The ventral nerve cord was dissected away and the remaining body wall muscles were perfused with modified HL3 saline containing 0.5 mM calcium. In order to access Muscle 30, Muscles 6, 7 and 13 were gently removed using a sharpened tungsten wire. Preparations were visualized by a Nikon FS microscope using a 40×/0.80 water-dipping objective. Muscles in abdominal segments A3 and A4 were impaled by sharp electrodes (electrode resistance 15–30 MΩ) filled with 3M KCl. mEPSPs were recorded, before stimulation was applied. The cut axon bundle was then stimulated by Master-9 stimulator (A.M.P.I.) at 0.2 Hz to elicit EPSPs. Signals were processed by MultiClamp 700B (Molecular Devices), Digidata 1550B (Molecular Devices), and acquired by pClamp 10 software (Molecular Devices). Data was analyzed by Mini Analysis software (Synaptosoft). Recordings were rejected if the resting potential was > 60 mV (for muscle 6) or > 50 mV (for Muscle 30). Quantal content was calculated by dividing the mean EPSP amplitude by the mean mEPSP amplitude from each muscle.

Statistics

Descriptive statistics: average and standard deviation are reported, except for behavior, where the average of average speed and standard error of the mean are reported. Every data point is plotted in figures. Test statistics: All data was assumed to follow a Gaussian distribution. If standard deviations were unmatched Welch's correction was applied. For numerical data in two populations, we used unpaired, two-tailed t tests. For numerical data in more than two populations, we used ordinary one-way ANOVAs with Dunnett or Games-Howell correction for multiple comparison. Analysis done using GraphPad Prism.

3.4 misexpression of the temporal transcription factor Kruppel

3.4.1 Introduction

My previous work explored to what extent the temporal transcription factors inform axon to motor neuron synaptic partnership decisions (Meng et al., 2019; Meng et al., 2020)[2, 3]. The following factors are temporal transcription factors and are expressed in the follwoing sequence: Hunchback (Hb), Kruppel (Kr), Nubbin/Pdm2 (Pdm), Castor (Cas), and Grainy-head (Grh) (Doe, 2017)[64]. NB7-1 is known to express the temporal sequence of the first four factors and it remains to be determined if Grh is expressed at the end of the lineage. So far, my published work focuses on manipulations of the following temporal factors: Hb, Pdm, and Cas. Here, I describe our unpublished Kruppel manipulations in NB7-1 and NB3-1 (Ellie collected and imaged all NB3-1>Kr and some NB7-1>Kr data and I collected the remaining NB7-1>Kr data). We did not publish this work because 1) at the time of data collection, other temporal factor manipulations yielded more interesting results and 2) the NB7-1>Kr results were at odds with previously published results. My goal in this section is to highlight previously published results involving Kr manipulations, present my findings, and offer possible explanations for why our data is at odds with previously published results.

3.4.2 Past studies where Kr expression is manipulated

There are a number of past studies where Kr expression is manipulated in the developing Drosophila larval nerve cord (Romani et al., 1996; Isshiki et al., 2001; Cleary and Doe, 2006; Tran and Doe, 2008)[163, 68, 139, 70] These studies offered evidence that Kr influences neural molecular identity specification. Isshiki et al., used engrailed-GAL4 to misexpress UAS-Kr in the following 8 neuroblast lineages (MNB, 1-2, 6-1, 6-2, 6-4, 7-1, 7-2, 7-4). In wildtype NB7-1, Kr is expressed during the first three divisions with expression levels peaking during the third division window when the U3 motor neuron is generated (Isshiki

et al., 2001)[68]. In *engrailed>Kr* embryos, Isshiki et al found that on average there were 5.5 extra Eve+ neurons per hemisemgnet and these extra neurons had embryonic molecular identities found in U3 and U4 Eve+ neurons (Zfh2+ Cas-). Subsequent work from the Doe lab found that the extra Eve+ neurons likely possess U3 molecular identity because they lacked Runt expression, a marker found in U4 and U5 motor neurons (Cleary and Doe, 2006)[139]. Cleary and Doe used another driver, Prospero-GAL4, which is a pan-lineage driver but only begins expressing throughout the nerve cord during NB7-1's fourth division (Pearson and Doe, 2003). Using Prospero-GAL4 to misexpress either 1x UAS-Kr or 2x UAS-Kr, on average Cleary found 2 and 6.8 extra U3-like neurons, respectively (Cleary and Doe, 2006)[139]. Cleary also misexpressed UAS-Kr using the Scabrous-GAL4, which expresses in all newly formed neuroblasts and their initial GMCs and the GMC's daughter neurons(Odden et al., 2002)[164]. Using Scabrous-GAL4, Cleary found on average 3.2 extra U3-like neurons with the range spanning 2 to 5 extras (calculated from Cleary et al's Figure 5C) [139]. Notably, these studies found evidence that misexpression of Kr did not affect the generation of U1-U2 neurons but did cause the loss of U4-U5 neurons (Isshiki et al., 2001; Cleary and Doe, 2006)[68, 139].

So far, I have summarized work that focused on characterizing the impact manipulating Kr has on the NB7-1 U motor neurons, however another study investigated the impact of Kr misexpression on NB3-1 RP motor neurons (Tran and Doe, 2008)[70]. Here, Tran used the pan-neuroblast driver Inscuteable-GAL4 to misexpress Kr. Tran and Doe reported that on average 2.3 RP3 neurons were generated, meaning that on average 1.3 extra RP3 neurons are made. They found that on average there were 0 RP5 neurons generated. Altogether, these studies reveal that ectopic expression of Kr is sufficient to specify extra neurons with the molecular identity of neurons that are normally born during the division when Kr expression is the highest within the neuroblast. Also the extra neurons are made at the expense of later born neurons.

3.4.3 Misexpression of Kruppel in NB7-1

Based on the findings from the previous studies I just described, we were eager to misexpress Kruppel to generate mismatches between birth time and embryonic molecular identity. By uncoupling birth time from inherited embryonic molecular identity, we could learn the extent to which intrinsic vs extrinsic cues specify motor neuron to muscle synaptic partnerships. We used the NB7-1 and NB3-1 specific drivers, respectively. When we misexpressed 2x UAS-Kr using NB7-1-GAL4 we found on average 1.531 U3-like (Eve+, Runt-, Hb-) neurons, meaning on average there were .5 extra U3 neurons (range between 0 and 2) (Figure 3.27E).

We found on average 0.8 U4-U5-like (Eve+, Runt+, Hb-) neurons (Figure 3.27D). Similar to previous reports the number of U1-U2 like neurons remains the same as wildtype (Figure 3.27F). Altogether, these manipulations were disappointing because they did not yield the results we expected based on the previous studies I described above. Next we wanted to know if the embryonic molecular identities observed in late stage embryos reflect the permanent motor axon to muscle synaptic decisions made at late larval stage (L3). We find evidence that for this. (Figure 3.27G-H). Compared to wildtype, we find a significant reduction of synaptic branches onto muscle 4, normally targeted by U5 (Figure 3.27I). There is a slight reduction onto muscle 3, normally target by U4 (Figure 3.27J) and a slight increase in the number of synaptic branches onto muscle 2, normally targeted by U3 (Figure 3.27K). We observed no change in the number of synaptic branches onto either muscle 9 or 10, normally targeted by U1 and U2 respectively (Figure 3.27L). Combined, our findings reveal that prolonged expression of ectopic Kr specifically in NB7-1, on average reduces the number of Eve+ neurons by 1 (from wildtype 5 to 4) (Figure 3.27C) and the lost Eve+ neuron is likely U5, based on our embryonic molecular marker and third instar larval synaptic branch count. Contrary to previous reports, we find few if any extra U3-like neurons generated.

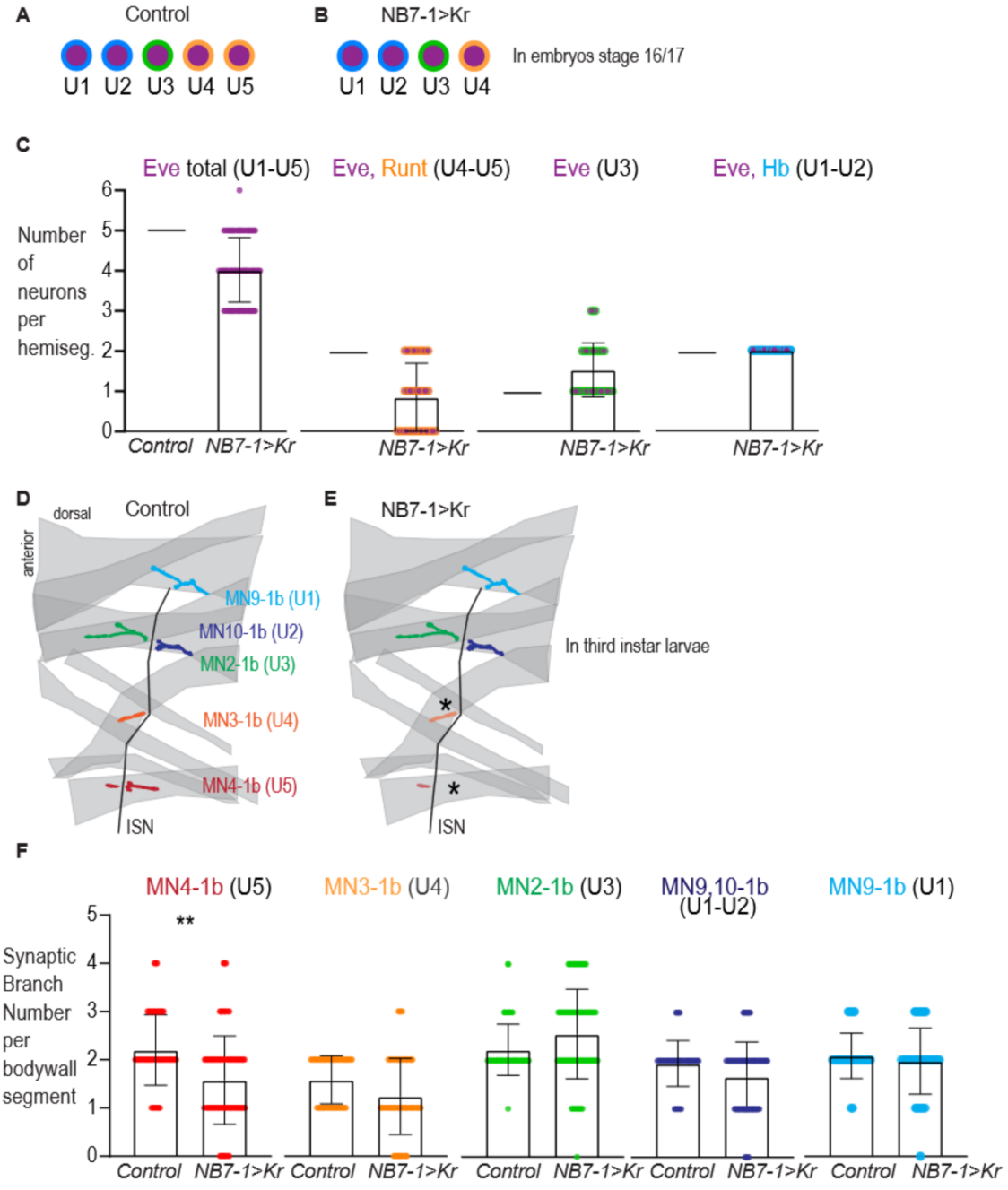


Figure 3.27: *Continued* Impact misexpression of Kruppel in NB7-1 has on motor neuron molecular identity and permanent motor neuron to muscle synaptic partnerships. (**A-B**) Illustrations of U motor neurons as circles. Purple represents Eve expression. Blue encircling represents only Hb expression, found in wildtype U1 and U2; green encircling represents no Runt or Hb expression, found in wildtype U3; and yellow encircling represents only Runt expression, found in wildtype U4 and U5. (**B**) When Kruppel is misexpressed in NB7-1, there is a reduction in the number of Eve+ neurons by 1, at the expense of a Runt+ neuron.

Figure 3.27: *Cont'd.* The impact misexpression of Kruppel in NB7-1 has on embryonic molecular identity and permanent L3 muscle synaptic partnerships of NB7-1 derived Eve+ motor neurons. (**C**) Quantification of embryonic molecular marker expression. The horizontal bars represent the number of neurons with corresponding molecular marker expression observed in wildtype. Here, we did not quantify wildtype data, hence no comparisons to control are made. On average, there are 4 Eve+ neurons per hemisegment, 1 Eve+, Runt+ neuron, 1.5 Eve+ Runt- Hb- neuron, and 2 Eve+ Hb+ neuron. (**D-E**) Illustrations of neuromuscular synapses on dorsal muscles in an L3 body wall segment (light blue = U1, dark blue = U2, green = U3, orange = U4, red = U5). In NB7-1 > Kr the number of 1b synaptic branches (in orange and red) are lost (black asterisks) onto Muscle 3 and Muscle 4 (U4 and U5 muscle targets, respectively). (**F**) Quantification of type 1b branches onto L3 muscles. Color code as in (**D**). Each dot represents the number of branches onto a single muscle. For quantifications, average and standard deviation are overlaid. Un-paired t-test with Welch's correction for unmatched standard deviations (see source datasheet for details). '**' $p<0.0001$.

3.4.4 Misexpression of Kruppel in NB3-1

We also ectopically expressed 2x UAS-Kr using the NB3-1-GAL4 driver. Disclaimer, we do not have any embryonic molecular identity data but we do have third instar larval synaptic branch counts. At the time this data was collected, we were unsure which muscle was targeted by each NB3-1 RP (RP1, RP4, RP3, RP5) motor neuron, so we only imaged the four innermost ventral longitudinal muscles: 12, 13, 6, and 7. Since then we've learned that RP1 and RP4 innervate muscles that lie behind these four muscles (Meng et al., 2020)[3]. So our data only captures muscles innervated by RP3 and RP5 (Figure 3.28A).

RP3 is the type 1b motor neuron that innervates muscles 6 and 7 (MN6/7-1b) and RP5 is the type 1s motor neuron that innervates all muscles accessible from the ISNb/d nerves (MNb/d-1s). We find that in NB3-1>Kr third instar larvae, there is a near complete loss of the type 1s branch onto these ventral muscles (see Muscle 12) (Figure 3.28B-E). We find no change in the number of type 1b branches onto muscle 6 and 7 (Figure 3.28F-H). These results suggest that NB3-1>Kr reduces the overall number of NB3-1 RPs by one. Based on our L3 bodywall data, we think that RP5 is lost. This result is reminiscent of what we find for NB7-1>Kr, namely that there is a reduction of the total number of motor neurons at the

expense of the latest born.

3.4.5 Discussion of why there may be a discrepancy between previous findings and our data

The most likely explanation for the differences in our data and previous studies is the level of ectopic Kr expression. I think the best evidence of this comes from Cleary's work where they use the same driver but express either 1x or 2x copies of the Kr transgene (Cleary and Doe, 2006)[139]. 1x copy generated 2 extra U3-like neurons while 2x copies generated 6.8 extra U3-like neurons. So our problem could be that our drivers don't drive enough ectopic Kr expression. While possible, I think it is unlikely because our lab's NB7-1 and the NB3-1 drivers drive ectopic Hb expression well. I think if there is a genetics-related issue

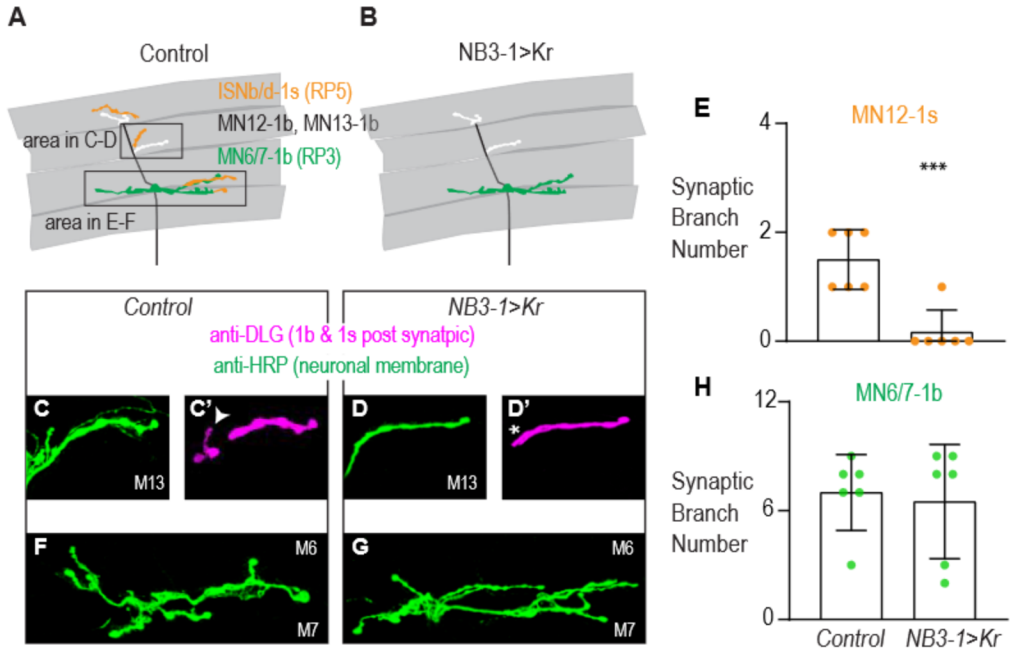


Figure 3.28: Impact misexpression of Kruppel in NB3-1 has permanent motor neuron to muscle synaptic partnerships (**A-B**). Illustrations of neuromuscular synapses on ventral muscles in a L3 body wall segment (green = RP3, orange = RP5, white = non-NB3-1 motor neurons). In NB3-1 > Kr there is loss of type 1s synaptic branches onto ventral muscles. *Continued*

Figure 3.28: *Cont'd.* Kruppel misexpression in NB3-1 causes permanent loss of type 1s branches onto ventral muscles. (**C-D,F,G**) Images of neuronal membrane, both axons and neuromuscular synapses, on ventral muscles in L3 abdominal segments. Arrowhead denotes the type 1s on muscle 13. Asterisk denotes loss of type 1s on muscle 13. (**E,H**) Quantification of type 1s branches onto L3 muscle 12 and type 1b branches onto muscle 6/7 muscles. Color code as in (A). Each dot represents the number of branches onto a single muscle. For quantifications, average and standard deviation are overlaid. Un-paired t-test with Welch's correction for unmatched standard deviations (see source datasheet for details). '***' p=0.0009.

it lies with the lab's 2x UAS-Kr stock. I believe it is the same fly line used in the Doe lab studies but it may have picked up mutations that impact transgene expression levels since then. Another possibility is the timing of the NB7-1 and NB3-1 driver onset but I think this is less likely because we know the NB7-1 driver begins driving expression within the first or second division window. In the Cleary and Doe paper they used the Prospero-GAL4 driver, which the Doe lab characterized to only begin driving during the fourth division window of NB7-1 (Pearson and Doe, 2003)[102]. Using this driver in conjunction with 2x copies of UAS-Kr they still found 6.8 extra U3-like neurons were generated (Cleary and Doe, 2006)[139]. Therefore, I think it is unlikely that the issue lies with the onset of our neuroblast specific drivers.

If someone wanted to determine whether or not our 2x UAS-Kr line is corrupted, I would recommend using driver lines from previously published studies. One of these drivers is Engrailed-GAL4, which we currently have in our fly stocks.

Source Data for Figure 3.1C

Molecular Markers	Genotype	Number of values	Mean (# of cell bodies at E16/17)	Std. Deviation	Std. Error of Mean	p value
Total Eve+	NB7-1>Kr	100	4.020	0.8038	0.08038	NA
Eve+, Runt+	NB7-1>Kr	32	0.8438	0.8466	0.1497	NA
Eve+,Runt-,Hb-	NB7-1>Kr	32	1.531	0.6713	0.1187	NA
Eve+, Hb+	NB7-1>Kr	32	2.000	0.000	0.000	NA

Source Data for Figure 3.1F

Synaptic branch	Genotype	Number of values	Mean (branch #)	Std. Deviation	Std. Error of Mean	p value
Muscle 4-1b	W1118	60	2.200	0.7318	0.09448	NA
	NB7-1>Kr	92	1.576	0.9167	0.0956	<0.0001
muscle 3-1b	W1118	60	1.583	0.4972	0.06418	NA
	NB7-1>Kr	92	1.239	0.7896	0.08232	0.2672
muscle 2-1b	W1118	58	2.224	0.5312	0.06976	NA
	NB7-1>Kr	96	2.552	0.9276	0.09467	0.0060
muscle 10-1b	W1118	58	1.948	0.4747	0.06233	NA
	NB7-1>Kr	93	1.667	0.7273	0.07542	0.0046
muscle 9-1b	W1118	58	2.086	0.4696	0.06166	NA
	NB7-1>Kr	82	1.976	0.6845	0.07559	0.2589

Unpaired t-test, with Welch's correction (for un-equal Std. Deviation)

Table 3.1: Source Data for Figure 3.27

Source Data for Figure 3.2E-H

Synaptic branch	Genotype	Number of values	Mean (branch #)	Std. Deviation	Std. Error of Mean	p value
muscle 12-1s	W1118	6	1.500	0.5477	0.2236	NA
	NB3-1>Kr	6	0.1667	0.4082	0.1667	0.0009
muscle 6/7-1b	W1118	6	7.000	2.098	0.8563	NA
	NB3-1>Kr	6	6.500	3.146	1.285	0.7537

Unpaired t-test, with Welch's correction (for un-equal Std. Deviation)

Table 3.2: Source Data for Figure 3.28

CHAPTER 4

NB7-1 INTERNEURON STORY

Around the time of our penultimate meeting, I first analyzed this data. Since then, I have mulled over the data and compiled a story that I think forms the backbone of a future publication.

4.1 Introduction

In the developing Drosophila larval nervous system, temporal transcription factors permanently alter motor neuron-to-muscle synaptic partnership decisions (Meng et al., 2019; Meng et al., 2019)[2, 3]. From these studies, we learned that lineage intrinsic cues acting at the level of neuroblasts strongly influence synaptic partnerships of motor neurons. Since motor neurons are in the peripheral nervous system, it is unclear if the principles we learned in the context of motor neurons can be applied to synaptic partnership decisions made in the central nervous system. Within the nerve cord, interneurons are the predominant neuron cell type. Thus, knowing to what extent temporal transcription factors influence circuit-relevant fate decisions of interneurons is critical to understanding the underlying logic of circuit assembly logic in the central nervous system. There are a number of culminating circuit-relevant fate decisions neurons must make before they successfully integrate into a circuit. First, neurons must extend their neurites; second, dendritic and axonal arbors must be elaborated; third, synaptic partners must be identified; and functional synapses are established and maintained between partners. To visualize these decisions at the level of single synapses requires resolution offered by electron microscopy (EM) based imaging. Serial EM volumes of complex central nervous systems are increasingly becoming available through collaborative efforts and large-scale initiatives from institutes such as Janelia. However, collecting volumes of central nervous systems in genetically perturbed backgrounds is currently

out of reach for most research groups because of high resource costs. Despite these obstacles, we explore how circuit-relevant features are specified by assessing interneuron morphologies by using a combination of experimental data collected by light microscopy and wildtype data available in an available EM dataset. The resolution offered by confocal light microscopy and sparse neuron labeling provides the overall morphology of interneurons but not synapses. Therefore, we can still learn the extent to which intrinsic cues specify interneuron neurite outgrowth decisions culminating in the establishment of arbors in a particular region of the neuropil.

To distinguish the contribution of lineage intrinsic information including temporal transcription factors and lineage extrinsic cues we need to study, at single cell resolution, interneurons known to be born during a time period when temporal transcription factors are expressed in a given neuroblast and manipulate temporal transcription factors at single neuroblast lineage resolution.These criteria make NB7-1 a good model lineage to study. Not only is there a driver specific to the NB7-1 lineage, but there is also evidence that during the Castor expression window, neuroblast '7-1' transitions from making motor neurons to generating a group of interneurons, which express Castor.

From our previous work and others we know that when Hunchback is misexpressed in NB7-1, the overall size of the lineage is not altered compared to wildtype, yet the number of Eve+ motor neurons is significantly increased [2]. Our interpretation is that Eve+ motor neurons are born at the expense of later born interneurons. However, since the entire lineage can rarely be accounted for by the extra number of Eve+ motor neurons, this strongly suggests that the remaining Eve- neurons are much later born interneurons. The question is what is the fate of these interneurons? Understanding their fate will offer insight into the impact Hunchback misexpression has on the neuroblast '7-1' and the extent to which interneuron fate is specified by lineage intrinsic vs extrinsic cues.

Here, we offer the most detailed characterization of late stage embryonic molecular iden-

tity and first instar larva morphology of NB7-1 lineage interneurons. Our characterization reveals that the NB7-1 lineage may be partitioned into three nearly equal groups of neurons generated in the following sequence: motor neurons, Cas+ interneurons that overwhelmingly project to the dorsal neuropil, and Cas- interneurons that overwhelmingly project to the ventral neuropil. We find that misexpression of Hunchback in NB7-1 impacts later-born interneuron integration into motor circuits because neurite outgrowth is arrested, meaning arbor formation is non-existent. Sometimes interneurons appear to have overall normal morphology and do form arbors. We find examples of interneurons projecting to the dorsal neuropil despite being born much later than the normal Cas+ interneuron window. The ability for interneurons to arborize can be best explained by relatively earlier neuroblast '7-1' transition from making motor neurons to interneurons. Taken together these data suggest that a combination of lineage intrinsic and birth time-linked extrinsic information are required to specify interneuron outgrowth decisions, prerequisites for circuit integration. By staining for Cas and Hb in NB7-1>Hb and misexpressing Castor in NB7-1, we find evidence for a model where Castor is dispensable for interneuron fate specification. Combined with the evidence for the contribution of lineage intrinsic information for specifying later born interneuron fate. However, since the majority of interneurons display an arrested outgrowth fate, we favor a model where Castor acts in parallel with other currently unknown factors to ensure proper interneuron outgrowth is achieved. Our work here motivates future studies to identify the factor(s) required to specify interneuron fate. While the role of temporal transcription factors in specifying fate of motor axons in the peripheral bodywall is well understood, our unexpected finding here reveals that our understanding of the role of temporal transcription factors in fate specification within the nerve cord is far from complete and warrants further investigation.

4.2 Results: Characterization of the entire NB7-1 lineage

4.2.1 Embryonic Molecular Identity

Out of the thirty hemisegmentally repeating neuroblast lineages, NB7-1 is among the most well-characterized lineages (Doe, 2017)[64]. We know that NB7-1 is a type I lineage, meaning that the neuroblast asymmetrically divides to bud off a ganglion mother cell (GMC), which then terminally divides to generate two siblings neurons, one NotchON and the other NotchOFF (Figure 1A). Previous work reported that the NB7-1 lineage generates around twenty GMCs (Schmid et al., 1999; Isshiki et al., 2001; Pearson and Doe, 2003; Grosskortenhaus et al., 2006; Cleary and Doe, 2006)[45, 68, 102, 69, 139] . In agreement, we previously found that NB7-1 generates on average forty neurons [2].The first six divisions generate the following sequence of NotchON motor neurons: Eve+ U1, Eve+ U2, Eve+ U3, Nkx5+ VO, Eve+ U4, and Eve+ U5 (Figure 1A,B). Some of the corresponding NotchOFF sibling neurons express Dbx, have small cell bodies, and stick-like neurite projections characteristic of small undifferentiated neurons (Figure 4.1A,B) [165]. After the sixth division, NB7-1 generates GMCs that go on to make interneurons (Figure 4.1B).

In contrast to our detailed understanding of the motor neuron molecular identities, the identities of interneurons are less understood. It has long been known that the temporal transcription factor Castor (Cas) is expressed in NB7-1 during the sixth division window and continues for an uncharacterized number of divisions (Grosskortenhaus et al., 2006)[69]. Since Cas expression is embryonically maintained in neurons born during the Cas expression window we can count the number of Eve- Cas+ neurons to identify the number of Cas expressing interneurons. Previously, we found that NB7-1 generates on average 13.43 Cas+ interneurons (Meng et al., 2019)[2] and is in agreement with scoring done here where we find an average of 14.35 Cas+ cells (subtract one as it corresponds to Cas+ U5) (Figure 4.1C red column). To distinguish between the possibilities that the fourteen Cas+ interneurons are

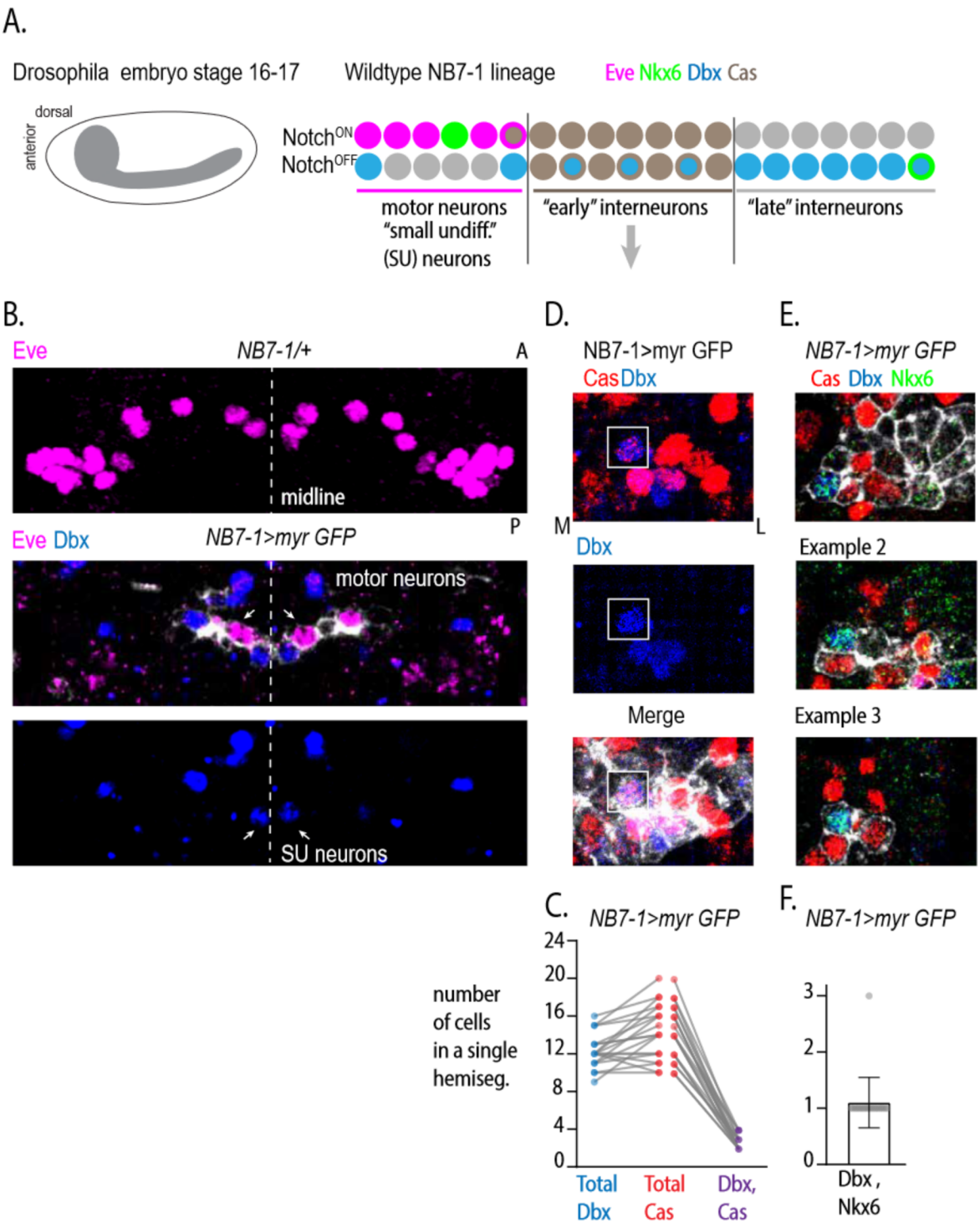


Figure 4.1: Characterization embryonic molecular identity for the entire NB7-1 lineage. (**A**) The illustration to the left represents a Drosophila embryo at stage 16-17. The illustration to the right depicts neuronal progeny from the NB7-1 lineage represented as circles. Colored circles correspond to expression of similarly colored molecular markers (magenta = Eve, green = Nkx6, blue = Dbx, brown = Cas). *Continued*

Figure 4.1: *Cont'd.* Characterization of embryonic molecular identity found within the NB7-1 lineage. The first vertical line to the left bisects the lineage at the boundary of motor neurons (left of line) and interneurons (right of the line). The second vertical line divides the interneurons into two groups. We believe the first half of the interneurons generated express Cas while the second half does not. Further experiments will need to be done to validate this assumption. (**B,D-E**) Images of embryonic molecular identity marker in cell bodies in late-stage embryonic CNSs. Images are shown in ventral view. In (D) boxes are insets from different z-planes. (**C**) Quantification of the total number of Dbx+ (blue), Cas+ (red), and Dbx+,Cas+ (purple) for single hemisegments. Note, The two vertical column of red dots represent the same data. They are duplicated for ease of comparing Dbx+ vs Cas+ counts and Cas+ vs Dbx+,Cas+ counts. (**F**) Quantification of the number of Dbx+, Nkx6+ cell bodies expressing GFP driven by the NB7-1 driver. The average and standard deviation are overlaid. (see source datasheet for more details of C, F).

from the same hemilineage (NotchON vs NotchOFF) or shared between both hemilineages, we co-stained with Dbx, a factor considered to be expressed exclusively in a single hemilineage (Lacin and Truman, 2016)[73]. Since there are a number of interneurons co-stained for Cas and Dbx (Figure 1C,D), we interpret this to mean that Cas+ interneurons populate both hemilineages. This means that NB7-1 expresses Cas+ over the course of 8 divisions, on average (Figure 4.1A). This leaves about seven divisions left. When we co-stain for Dbx and Cas, we find on average 8.6 Cas-, Dbx+ neurons (Figure 4.1C subtract Dbx,Cas column from total Dbx). Subtracting 1-2 Dbx+ small undifferentiated neurons means there are roughly 7 Dbx+ interneurons, which could represent a group of hemilineage related neurons. On average, one of these Dbx+ neurons also co-expresses Nkx6 (Figure 4.1E,F). We do not believe that the Nkx6, Dbx+ neuron is the small undifferentiated neuron belonging to the Nkx6+ VO motor neuron because the Nkx6+, Dbx+ neuron cell body is the size typically observed for interneurons and it lies extremely ventral (Seroka et al., 2020)[85]. Beyond this cell, we found no evidence for additional NB7-1 Nkx6+ interneurons. (Note for the thesis, the NB7-1 driver does sometimes hit the more dorsally positioned NB6-2 lineage (lin 19) is nearly all Nkx6+, so beware!).

Altogether, this is the most comprehensive characterization of the NB7-1 interneuron

embryonic molecular identities. While our characterization is limited by our knowledge of known molecular markers and corresponding antibodies, from our current data the NB7-1 lineage can be partitioned into nearly three equally sized groups: "motor neurons and small undifferentiated neurons", "early interneurons" marked by Cas+, and "late interneurons" (Figure 4.1A). While we have not directly shown that all the Cas+ interneurons are born contiguously, we know from several other lineages that Cas+ neurons are born nearly contiguously. Cas expression is considered to be contiguous in NB5-3A and NB5-5 (Doe, 2017)[64]. In NB3-3 in abdominal segments, there are six Cas+ EL interneurons, which are contiguously born except for one Cas- interneuron generated between the fourth and fifth Cas+ EL (Tsuji et al., 2008)[166]. This is very similar for NB5-6 in thoracic segments, where Cas is expressed in the neuroblast for six divisions and these divisions are contiguous except for the Cas- division between the third and fourth division (Doe, 2017)[64]. Considering that in all these examples Cas+ neurons are nearly contiguously born, we believe that the Cas+ interneurons are born soon after the Cas+ U5 motor neuron and do not represent the latest born interneurons. We believe instead that the latest born Cas- interneurons likely express Grainyhead, which is known to be expressed after Castor in a number of lineages (Doe, 2017)[64]. Future experiments need to be done to determine if these Cas- interneurons indeed express Grainyhead (there is an antibody but the Heckscher lab does not have it).

While this molecular marker characterization adds to our understanding of neuronal molecular diversity, understanding the extent to which molecular marker expression is correlated to morphology will begin to link molecular identity to circuit-relevant fate features. In the next section we present an atlas of the morphology of NB7-1 interneurons.

4.2.2 Morphology of NB7-1 interneurons

A long sought after goal in the field is to understand the relationship between neuroblast lineages and the vast neuronal morphology diversity found within the complex Drosophila

larval nerve cord. To this end, there have been a number of tour de force efforts characterizing morphology in lineages (Schmid et al., 1999; Chiba, 1999; Landgraf et al., 1997; Mark et al., 2021; Landgraf et al., 1997)[45, 167, 73, 84, 44]. In the past, approaches were limited to DIL labeling techniques (Schmid et al., 1999; Chiba, 1999; Landgraf et al., 1997)[45, 167, 44]. However, a major drawback to these approaches is that often clusters of lineage-related neurons are labeled, making it difficult to distinguish individual neural morphology while still capturing lineage identity. Now, with the advent of genetic tools such as MCFO, which enables sparse labeling of neurons coupled with lineage specific driver lines, we can obtain single cell morphologies with known lineage identities (Figure 4.2 4.3) [145].

In addition to light microscopy techniques, whose resolution is inherently limited, an entire first instar CNS volume obtained by serial electron microscopy is currently available to the Drosophila larval community (Schneider-Mizell et al., 2016)[28]. To date, a large fraction of the neurons in the abdominal segment 1 (A1) have been reconstructed. Using this valuable resource along with single neuron clones obtained from light microscopy, we can obtain superb resolution of interneuron morphology while also assigning lineage identity (Figure 4.2). In addition to morphology, the position of a neuron's cell body in the cortex of the nerve cord can offer insight into the relative birth time relationship of neurons within a given lineage (Figure 4.2A). This is possible because in the Drosophila larval nerve cord system, there is very little neuronal cell body migration upon birth (Schmid et al., 1999; Crew, 2019)[45, 168]. Neuroblasts delaminate from the neuroepithelium rather medially and as they divide, the neuroblast is pushed further to the lateral edge of the cortex and leave their neuronal progeny in the neuroblast's wake. Generally, cell bodies that lie closest to the neuropil (medial) are born earliest and the cell bodies that lie closest to the lateral edge of the nerve cord are born latest (Figure 4.2A) (Isshiki et al., 2001; Mark et al., 2021)[68, 84].

We first identified the constructed NB7-1 interneurons in the right hemisegment of A1 (Figure 4.2B). While we have a very limited MCFO light microscopy dataset predominantly

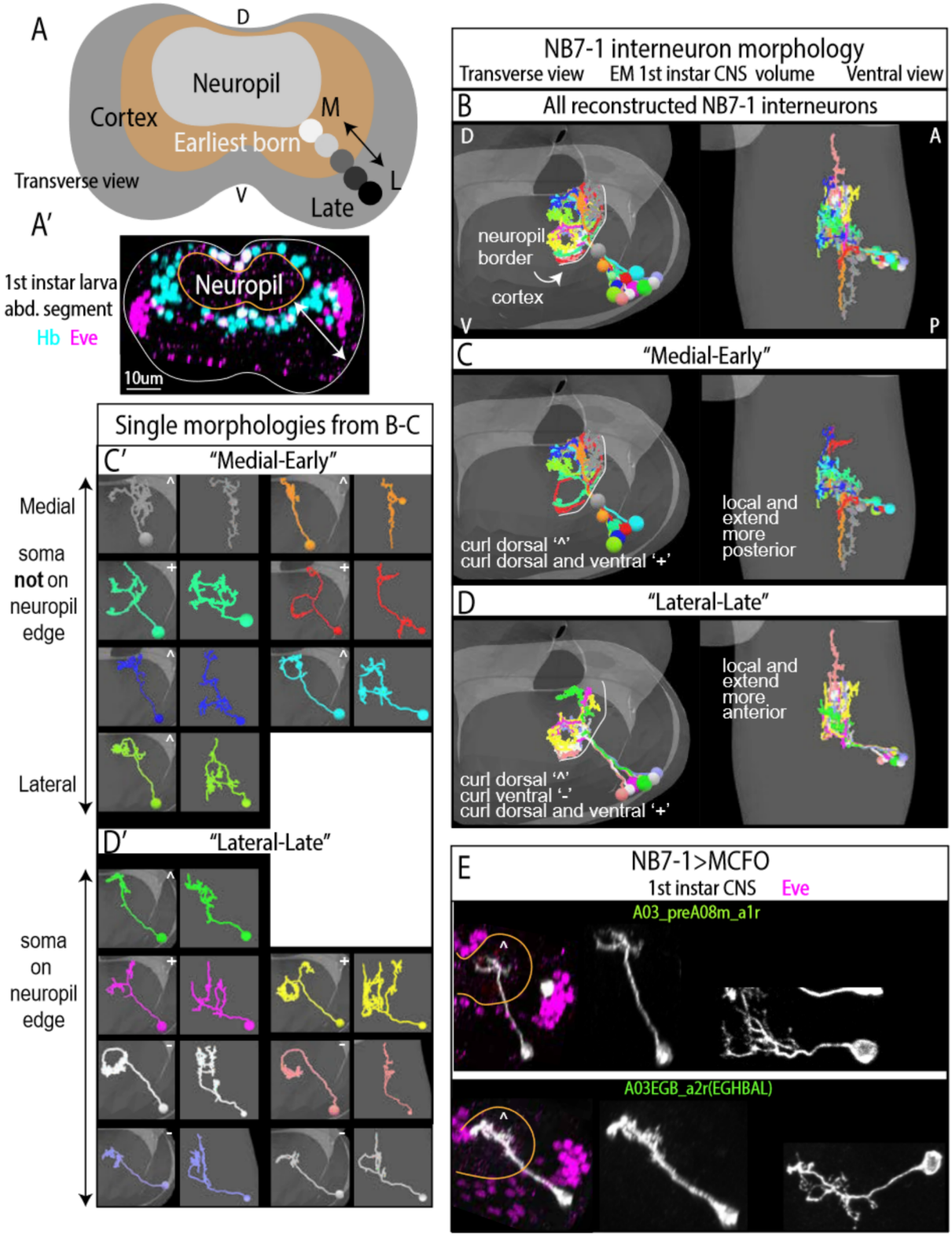


Figure 4.2: Characterization of NB7-1 interneuron morphology *Continued*

Figure 4.2: *Cont'd.* Characterization of NB7-1 interneuron morphology. (**A**) Illustration of a transverse section of the 1st instar Drosophila larval nerve cord. Circles represent neuron cell bodies. The gradient represents distance of the cell body position in the cortex to the edge of the neuropil (white = closest to the neuropil, more medial and black = furthest from the neuropil, more lateral). It is widely recognized that there is minimal cell body migration in development so the distance of the cell body from the neuropil can be a proxy for general/relative birth time. (**A'**) Image of an abdominal segment of a 1st instar Drosophila larval nerve cord in transverse view. Hb is expressed in the earliest-born neurons of lineages and these early-born neurons are positioned medially and are relatively close to the neuropil edge. (**B-D**) Images of traced/reconstructed neurons in the A1 segment of the EM volume of a wildtype 1st instar Drosophila larva. Transverse view is always on the left and the ventral view is on the right-hand side. To access these constructed neurons ask Chris Wreden in the lab. (**E-F**) Images of single-cell clones obtained from sparse labeling achieved by driving MCFO in NB7-1. The neuropil is outlined in yellow. The '∧' annotation is described in C-D

consisting of Eve+ motor neuron single cell clones, all of the NB7-1 interneuron single cell clones resemble traced NB7-1 interneurons from the 1st instar larva CNS EM volume (Figure 4.2E; Figure 4.3). We found fourteen annotated interneurons and one small undifferentiated neuron. While this is half the number of interneurons we expect from our lineage analysis done in late stage embryos, we believe this cluster of interneurons captures the earliest and latest born morphologies because the cluster spans the entire medial-lateral axis between the medial-most boundary being the edge of the neuropil and the lateral-most boundary –the outside edge of the nerve cord. However, the majority of the NB7-1 interneuron cell bodies are laterally positioned in the nerve cord (Figure 4.2B). So, we formed two general "early" or "late" clusters of interneurons based on whether or not the cell body directly borders the lateral edge of the nerve cord cortex (Figure 4.2C-C',D-D'). The most striking differences of "medial-early" versus "lateral-late" interneuron morphology in the transverse view is that the more medial interneurons curl their neurites to arborize both the dorsal and ventral portion of the neuropil (Figure 4.2C' denoted '+'), whereas more than half of the lateral interneurons curl their neurites exclusively to the ventral neuropil (Figure 4.2D' denoted '-'). When looking at these clusters in the ventral view, the most striking differences is that

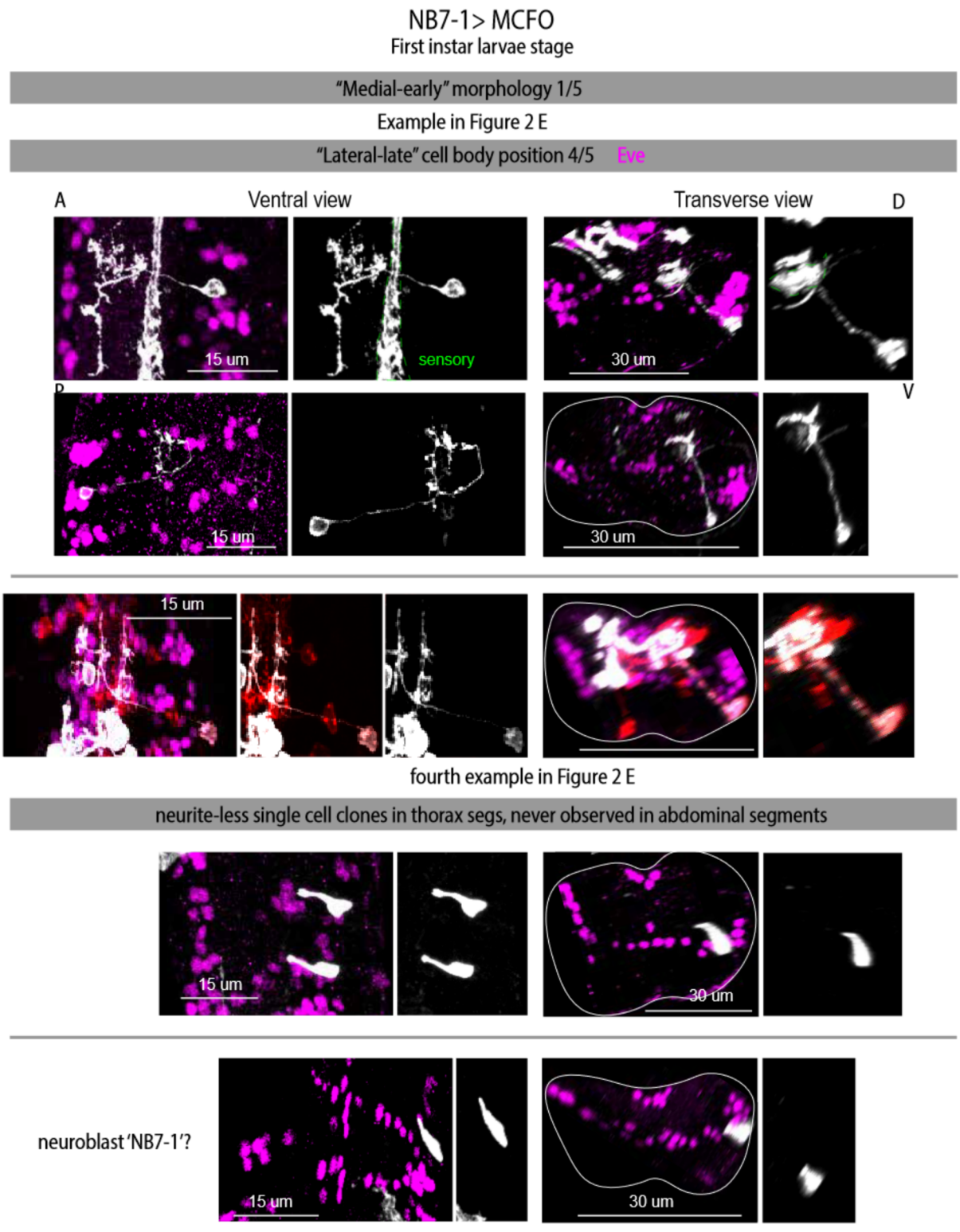


Figure 4.3: Light Microscopy of single clones of NB7-1 interneuron morphology. Images of single-cell clones obtained from sparse labeling achieved by driving MCFO in NB7-1. *Continued*

Figure 4.3: *Cont'd.* The nerve cord is outlined in white. Ventral view in on the left and Transverse view is on the right-hand side. The single-cell clone morphologies resemble traced neurons in the EM volume thought to be part of the NB7-1 lineage.

the medial most interneurons extend their neurites more posterior (orange and dark gray clones) whereas the lateral most interneurons extend their neurites more anterior (white, salmon, lilac, and light gray clones).

While we readily admit that shrinkage of the tissue caused during the EM chemical fixation process may distort the accurate position of individual cell bodies, our clustering was validated in part by previous work that stained for Cas and identified one of the neurons we call "medial-early" as Cas+, which we would expect (Mark et al., 2021)[84] (more details provided in the section entitled 'Castor is not required nor sufficient to specify interneuron outgrowth, projection, and arborization within the dorsal region of the neuropil').

4.3 In NB7-1>Hb embryos, ectopic Hunchback is expressed throughout the NB7-1 lineage

While the impact of Hunchback misexpression on U motor neuron embryonic molecular identity and motor axon to muscle synaptic partnership decisions has been explored in great detail, we know little about the impact on later born interneurons. Our previous work found that prolonged Hunchback expression in NB7-1 does not alter the size of the lineage (Meng et al., 2019)[2]. We know that extra Eve+ motor neurons are generated at much later stages in development as opposed at the expense of SU sibling neurons because we also observe nearly the same extra number of Dbx+ NotchOFF SU neurons (Figure 3A-B).

Taken together these data indicate that extra Eve+ motor neurons and small undifferentiated neurons are made at the expense of later born interneurons. We previously reported that prolonged expression of Hunchback in NB7-1 leads to a near total loss of Cas+ neurons (Meng et al., 2019)[2]. Consistently, here, we note that there is a total loss in the number of

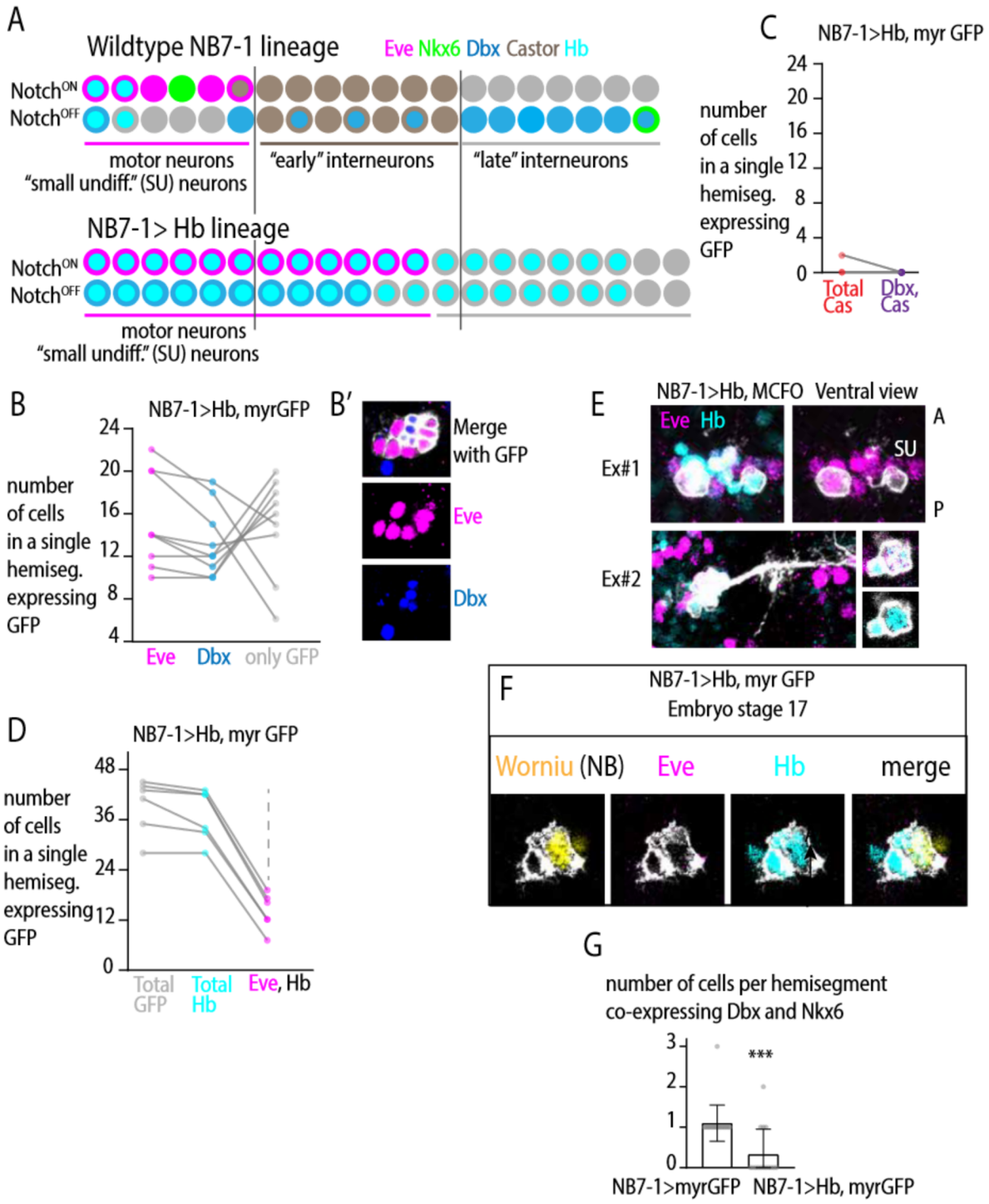


Figure 4.4: Ectopic Huncback is expressed throughout the NB7-1 lineage at late embryonic stages. (**A**) Illustrations depict neuronal progeny from the NB7-1 lineage represented as circles. Colored circles correspond to expression of similarly colored molecular markers (magenta = Eve, green = Nkx6, blue = Dbx, brown = Cas (Castor), cyan = Hb). NB7-1 > Hb increases the number of Eve+ neurons at the expense of Cas+ neurons. There is also an increase in the number of Dbx+ neurons. *Continued*

Figure 4.4: *Cont'd.* In NB7-1>Hb, ectopic Hunchback is expressed throughout the NB7-1 lineage at late embryonic stages. We believe that these extra Dbx+ neurons are the small undifferentiated sibling of the U1/U2 motor neurons. Lastly, nearly the whole lineage expresses ectopic Hb. (**B-D**) Quantifications of the number of cell bodies expressing the listed molecular markers in neurons expressing GFP and ectopic hb driven by the NB7-1 driver. (**B',E-F**) Images of embryonic molecular identity marker in cell bodies in late-stage embryonic CNSs. Images are shown in ventral view, anterior always up. (**G**) Quantification of the number of Dbx+, Nkx6+ cell bodies expressing GFP driven by the NB7-1 driver. The average and standard deviation are overlaid. Un-paired t-test with Welch's correction for unmatched standard deviations. '***' p=0.0004. (See source datasheet for more details of C-B,D,G).

interneurons co-expressing Dbx+ Cas+ (Figure 4.4C). Despite extra Eve+ motor neurons made at the expense of interneurons, there are still a number of Eve- GFP+ cells, which we interpret as interneurons generated after the motor neuron production window (Figure 3B).The majority of these interneurons express Hb+ because the total number of GFP+ cells is nearly identical to the total number of GFP+, Hb+(Figure 4.4D). We find evidence that Hb+ is ectopically expressed in the following cell types in late stage embryos: small undifferentiated neurons (Figure 4.4E), interneurons (Figure 4.4F), and the neuroblast 7-1 itself (Figure 4.4F). Taken altogether, our data reveals that even after NB7-1 transitions from making Eve+ motor neurons to Eve- interneurons, Hunchback is still misexpressed and its ectopic expression persists for at least some time in postmitotic neurons as Hb is still detectable at late embryonic stages.

4.4 Impact of Hunchback misexpression on NB7-1 interneuron morphology

The next question we wanted to ask is what impact does misexpression of Hunchback throughout the NB7-1 lineage have on the morphology of later born interneurons. I expressed MCFO in the NB7-1>Hb background and obtained 26 interneuron clones from over 20 unique 1st instar larva nerve cords. I found that Eve- interneuron morphologies fell into two classes:

wildtype-like outgrowth morphologies that resembled known wildtype NB7-1 interneuron projection and arborization patterns within the neuropil (n=8/26 30%) (Figure 4.5A-B) and arrested outgrowth morphologies that had no distinguishable arborization within the neuropil (Figure 4.5C-D) (n=18/26 70%).

In the Drosophila larval motor system, neurons form synapses at arbors and not along neurite backbones (Schneider-Mizell et al., 2016)[28]. So if a neuron does not form arbors, it is unlikely to be integrated into a motor circuit. The overwhelming percentage of the Eve- interneurons possessed an arrested outgrowth phenotype.

In wildtype animals, the neurons that most closely resemble this arrested outgrowth phenotype are the small undifferentiated (SU) neurons, which lack arbors. So one possibility is that these clones are bona fide small undifferentiated neurons. The two defining features of SU neurons is that they have a small cell body and their nucleus contains condensed chromatin (heterochromatin) (Figure 4.4B,E; Figure 4.6A, compare green to pink colored neighbors) (Andrade et al., 2019)[165].

In the A1 hemisegment, there is one SU neuron whose cell body (in mint) is adjacent to NB7-1 interneuron cell bodies (in pink) (Figure 4.6A-B). Since only the size of the cell body and not chromatin state is visible in light microscopy clones, we used this criteria to evaluate whether or not clones lacking arbors were SU neurons or not (Figure 4.7). By eye, only one of the clones has a distinguishably smaller cell body (Figure 4.7).

While this clone has an overall similar neurite structure to the wildtype SU, the distal end has a pronged morphology not observed in the wildtype SU. At most 1 out of 18 of these interneurons could be an SU neuron. Some of the arrested outgrowth interneurons lack any neurite. In the wild type first instar nerve cord, quiescent neuroblasts lack neurites, have condensed chromatin and are positioned along the lateral edge of the nerve cord cortex (Figure 4.6C, in yellow). So one possibility is that several of our clones are bona fide quiescent NB7-1 cells. While size of quiescent neuroblasts at the first instar larval stage is not

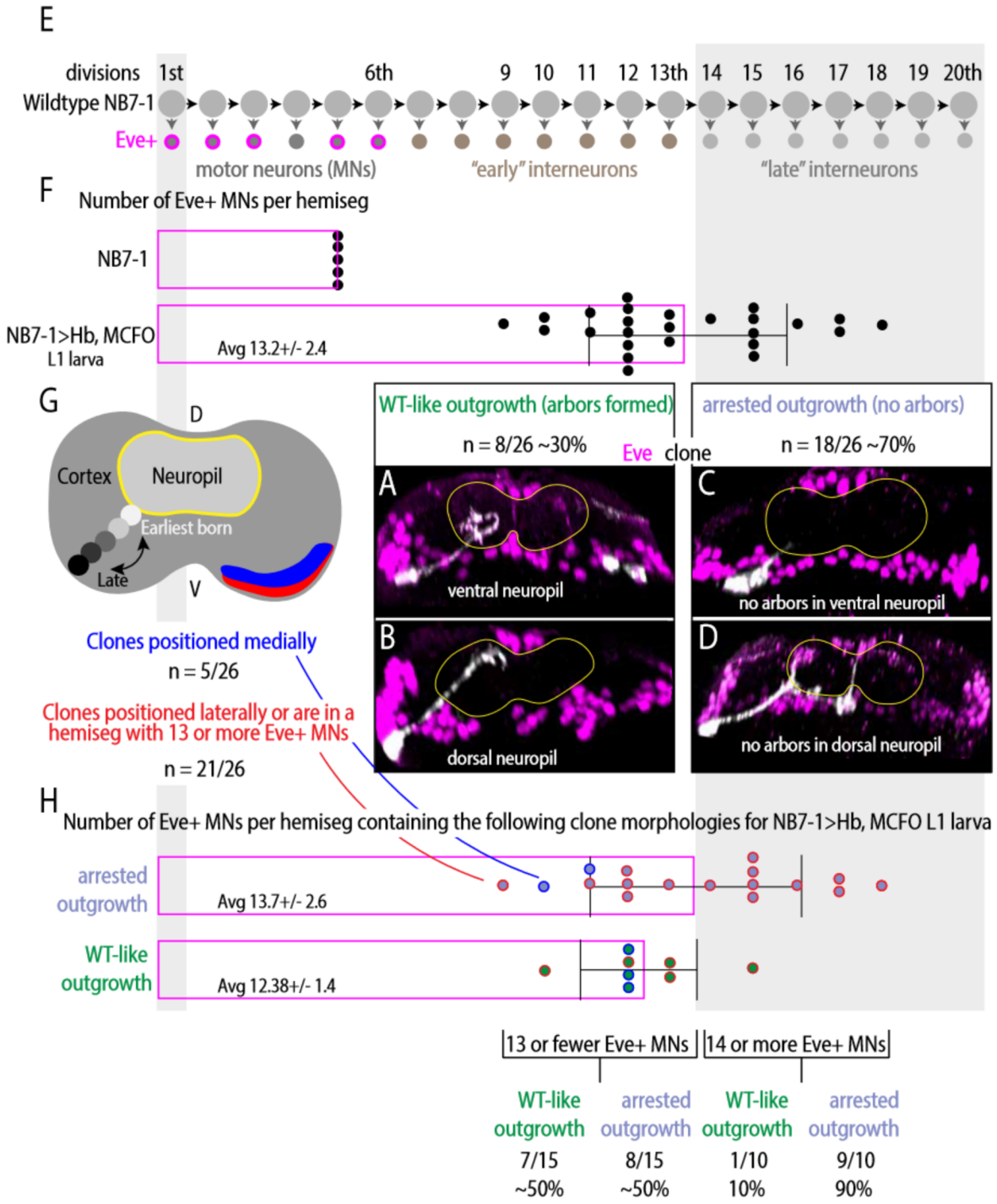


Figure 4.5: NB7-1 interneuron morphologies in 1st instar NB7-1>Hb animals. (**A-D**) Images of single-cell clones obtained from sparse labeling achieved by driving MCFO in NB7-1. The neuropil is outlined in yellow. When Hb is misexpressed in NB7-1 the majority of Eve- single-cell clones do not form arbors. (**E**) Illustration of NB7-1 lineage progression. Each arrowhead represents cell division (black = self-renewal, gray = progeny). Large circles are neuroblasts and smaller circles are neurons. *Continued*

Figure 4.5: *Cont'd.* NB7-1 interneuron morphologies in 1st instar NB7-1>Hb nerve cords. (**F**) Quantification of the number of Eve+ motor neurons per hemisegment that contains a sparsely labeled clone(s). The average and standard deviation are overlaid. The number of Eve+ motor neurons captures the number of divisions NB7-1 makes before transitioning from making Eve+ motor neurons to Eve- interneurons. (**G**) Illustration of a transverse section of the 1st instar Drosophila larval nerve cord. Circles represent neuron cell bodies. The gradient represents the distance of the cell body position in the cortex to the edge of the neuropil (white = closest to the neuropil, more medial and black = furthest from the neuropil, more lateral). The blue region corresponds to relatively medially positioned single-cell Eve- clones. The red region corresponds to relatively laterally positioned single-cell Eve- clones. (**H**) Quantification of the number of Eve+ motor neurons per hemisegment that contains a sparsely labeled clone(s) with the following phenotypes: violet = lacking arbors, arrested outgrowth, green = contain arbors, wt-like outgrowth. The average and standard deviation are overlaid.

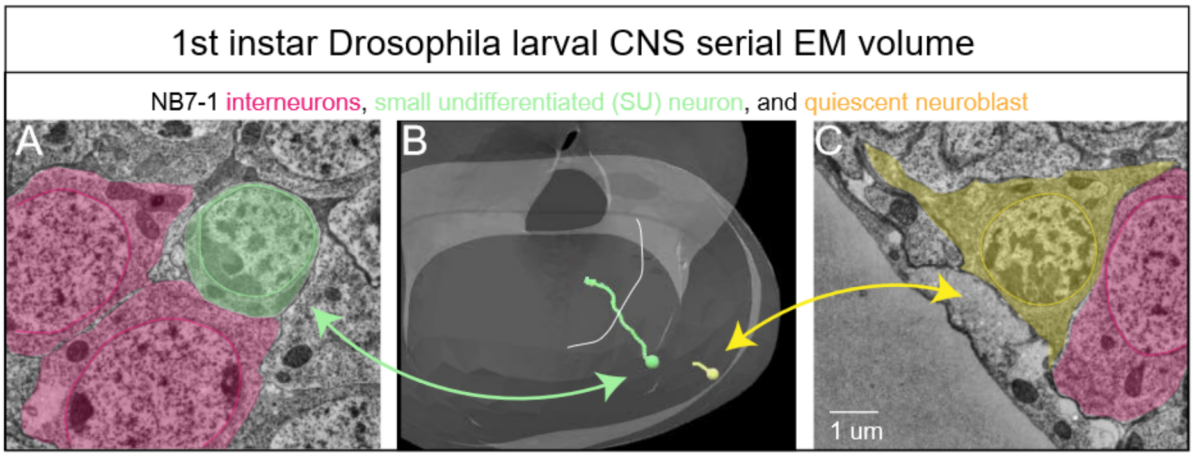


Figure 4.6: Arborless cells in the wildtype NB7-1 lineage in 1st instar larva nerve cord. (**A,C**) Images of single EM transverse slices of cell bodies of neurons belonging to the NB7-1 lineage: pink = interneurons, green = small undifferentiated neuron, yellow = quiescent neuroblast, presumably NB7-1. (**B**) Image of traced/reconstructed neurons in the A1 segment of the EM volume of a wildtype 1st instar Drosophila larva.

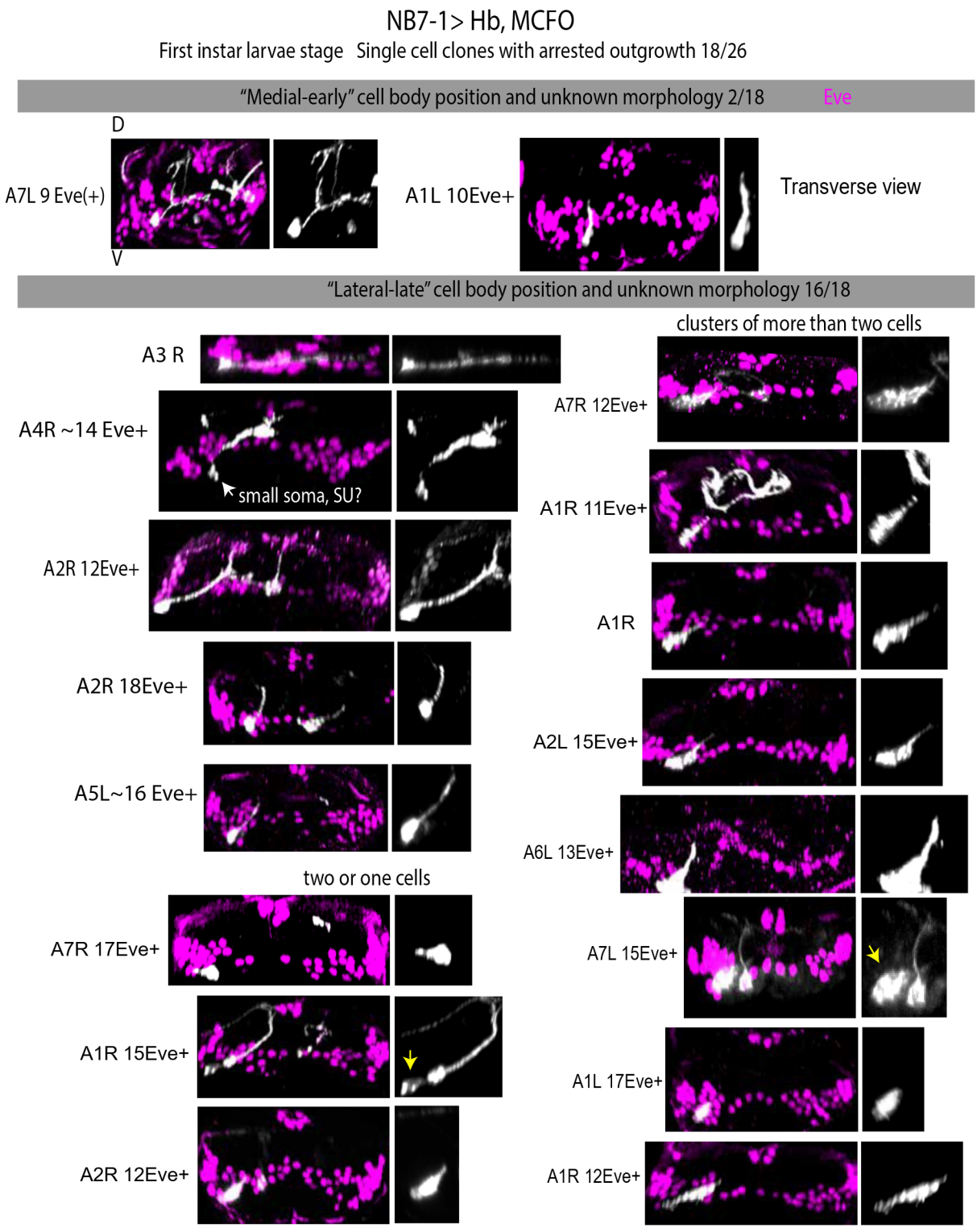


Figure 4.7: Clones of interneurons with 'arrested' outgrowth fate in 1st instar NB7-1>Hb nerve cords *Continued*

Figure 4.7: *Cont'd.* Clones of interneurons with 'arrested' outgrowth fate in 1st instar NB7-1>Hb nerve cords. Images of single-cell clones obtained from sparse labeling achieved by driving MCFO in NB7-1. All images are in transverse view. Next to each single cell clone example is the name of the abdominal hemisegment it came from and the number of Eve+ motor neurons found in the hemisegment.

distinguishable from interneuron cell bodies, our clones still offer evidence that neurite-less interneurons exist in the NB7-1>Hb background. We and others have reported that the NB7-1-GAL4 driver consistently expresses in the 7-1 neuroblast but is also known to express in the ventrally positioned 6-1 neuroblast (lin 12) (Meng et al., 2019; Lacin and Truman, 2016)[2, 73]. So it is possible that the one clone example lacking neurites and contains one or two cell bodies could be NB7-1 and NB6-1. That still leaves at a minimum, 16 clones that cannot be explained as SU neurons or neuroblasts. Additionally, I never observe this arrested outgrowth phenotype in any of the abdominal segments in my collection of 14 wildtype NB7-1>MCFO 1st instar larval nerve cords. Altogether, these arrested outgrowth morphologies are likely attributable to our Hunchback manipulation.

Since we know there is a general relationship between birth time and circuit integration decisions, I wondered if there was a relationship between birth time and the likelihood for interneurons to possess an overall wildtype-like morphology including arbors. There are several ways to assess birth time. One proxy for birth time is position along the medial-lateral axis. Under wildtype conditions, this is the only way to characterize birth time of later born interneurons (Figure 4.2). The second way to assess the relative birth time of a clone is to count the number of Eve+ motor neurons within the corresponding hemisegment. The number of Eve+ motor neurons represents the number of divisions before NB7-1 transitions to making Eve- interneurons. In wildtype, we know that the last Eve+ motor neuron is born during the sixth division window (Figure 4.5E) and the total number of Eve+ motor neurons per hemisegment is five (Figure 4.5F). For 25 out of my 26 clones, I counted the number of Eve+ motor neurons in each corresponding hemisegment and I found that on average 13.2

+/- 2.4 Eve+ motor neurons are generated (Figure 4.5F). Misexpression of Hunchback in NB7-1 does not change the overall size of the lineage, this means that NB7-1 still divides 20 times (Figure 4.5E). For any clone generated within a hemisegment containing 13 or more Eve+ motor neurons, I was confident that the clone was born during the "late" interneuron time window and thus was laterally positioned (Figure 4.5E-F,H, gray-shaded region spanning 14th-20th division). For clones generated within a hemisegment containing fewer than 13 Eve+ motor neurons (or unknown Eve+ motor neuron number), I assessed the clone's position along the medial-lateral axis. Doing so, I found 5 out of the 26 clones were positioned medially while 21 out of the 26 clones were positioned laterally (Figure 4.5G). For the two interneuron phenotype classes, I plotted the number of Eve+ motor neurons within the corresponding segment for each clone and denoted positional information by color-coding medial as blue and lateral as red (Figure 4.5H). When I did this I found that clones that had wildtype-like outgrowth fates tended to come from hemisegments with relatively fewer extra Eve+ motor neurons. In hemisegments containing 13 or fewer Eve+ motor neurons, the likelihood to have a wildtype-like outgrowth fate is nearly 50%. In hemisegments containing 14 or more Eve+ motor neurons, the likelihood to have the wildtype-like outgrowth fate plunges to 10% because I only observe 1 clone here (Figure 4.5H). I do not observe a relationship between clone position and likelihood to have wildtype-like outgrowth fate. Taken together, these observations suggest that the information required for proper outgrowth fate is dependent on the timing of NB7-1's transition from making motor neurons to generating interneurons.

4.5 Mismatch between inherited information of interneurons and birth time?

Since we found a relationship between neuroblast transition timing and proper interneuron fate, this raised the unsurprising possibility that inherited information is required to

specify proper interneuron outgrowth fate. Previously, we found that inherited information strongly influenced motor neuron synaptic partnership decisions regardless of birth time (Meng et al., 2019; 2020)[2, 3]. This means that despite a large mismatch between inherited information and birth time environment, motor neurons were able to make appropriate outgrowth decisions. What if here, for interneurons, only a small mismatch between inherited information and birth time environment can be tolerated to generate wildtype-like outgrowth fates? For animals where Hunchback is misexpressed in NB7-1, at the time of the motor neuron to interneuron transition, if NB7-1 is in a state permissible to specify the earliest born interneurons, this would mean that the sooner the transition is made, the more closely the inherited information received by an interneuron progeny matches to its normal birth time environment.

To test this model we asked what the morphology was for the two single wildtype-like outgrowth clones that were born during the "late" interneuron window. One clone (A4L 12 Eve(+)) was positioned laterally and was born from a neuroblast '7-1' parent that had generated Eve+ motor neurons during its first 12 divisions (Figure 4.8B).

Combined, we can infer this clone was born during the "late" interneuron window. The other clone (A2R 15 Eve(+)) was undeniably born during the "late" interneuron window because the first 15 divisions of its neuroblast '7-1' parent generated Eve+ motor neurons (Figure 4.8B). The most striking differences between "medial-early" vs "lateral-late" interneuron morphologies is that the former projects its arbors to the dorsal region of the neuropil and the latter to the ventral region of the neuropil (Figure 4.2). Strikingly, for both clones born during the "late" interneuron window, they extend their arbors to the dorsal region of the neuropil (Figure 4.8B). Combined, these examples reveal that it is likely neuroblast '7-1' is compatible with making the earliest interneuron fate soon after the transition between making motor neurons and interneurons. This is in agreement with the concept that misexpression of Hunchback in NB lineages maintains a young state within the neuroblast

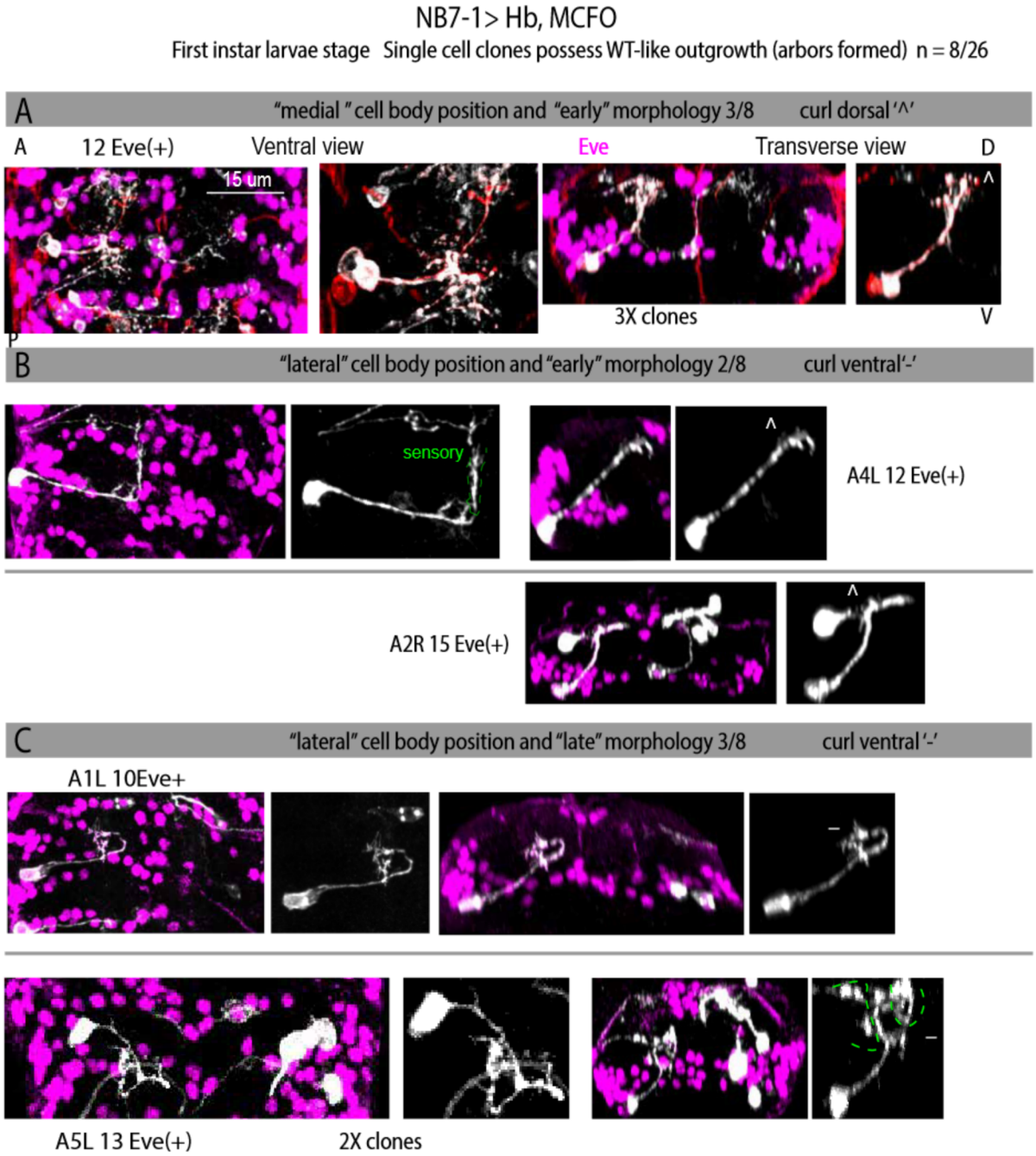


Figure 4.8: Clones of interneurons with 'wildtype-like' outgrowth fate in 1st instar NB7-1 >Hb nerve cords. Images of single-cell clones obtained from sparse labeling achieved by driving MCFO in NB7-1. All images are in transverse view. Next to each single cell clone example is the name of the abdominal hemisegment it came from and the number of Eve+ motor neurons found in the hemisegment.

(Hirono et al., 2012)[169].

4.6 Castor is not required nor sufficient to specify interneuron outgrowth, projection, and arborization within the dorsal region of the neuropil

If under misexpression of Hunchback in NB7-1 conditions, neuroblast '7-1' upon transitioning to making interneurons is compatible with making interneurons with the "early" fate, then this raises the question of what role ,if any, does Castor have in specifying the fate of the earliest born interneurons that normally express Castor under wildtype conditions. In addition to staining for Eve, in a subset of the NB7-1>Hb, MCFO nerve cords we stained for Hunchback. If any of the clones express Hb we can be certain that they do not express Cas because Hunchback strongly inhibits Castor expression (Isshiki et al., 2001; Li et al., 2014; Grosskortenhaus et al., 2006)[68, 22, 69]. Strikingly, we find three Hb+ clones possessing wildtype-like outgrowth fate positioned relatively medially within a hemisegment containing 12 Eve+ motor neurons (Figure 4.9).

This suggests that Castor expression is not required to specify interneuron outgrowth, projection, and arborization in the dorsal region of the neuropil. Next, we wanted to determine if Castor is sufficient to specify this fate, which is the predominant morphology fate found in "medial-early" interneurons.

When Cas is ectopically expressed using the NB7-1 driver, we find that all the neurons generated from the lineage express Castor (Figure 4.10A-B), including U1-U3, which despite Cas expression have otherwise wildtype-like embryonic molecular identity, morphology, and motor axon to muscle synaptic partnerships (Figure 4.10B-C" see merge) (Meng et al., 2020)[3].

We interpret this to mean that the Cas expression observed in late stage embryos and

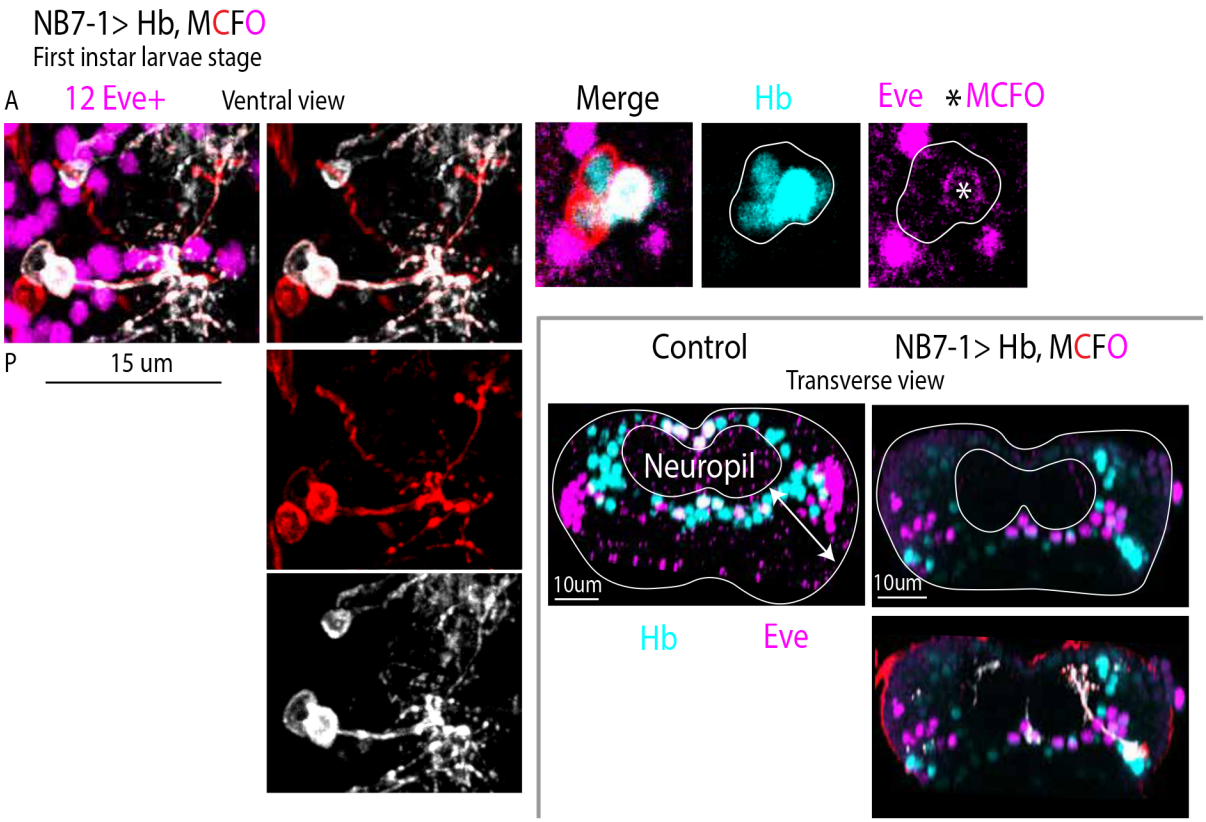


Figure 4.9: Clones of interneurons with 'wildtype-like' outgrowth fate in 1st instar NB7-1>Hb nerve cords expressing Hunchback. Images of hemisegment containing three clones with different combinations of MCFO tags. All clones express Hb in their cell bodies and lack Eve expression. Note, there is a faint ring of signal in the Eve channel because I used the same secondary fluorophore for rabbit anti-Eve and rat anti-Flag.

1st instar larval brains is likely ectopic and does not necessarily mean that Castor is being actively transcribed in the neurons (Grosskortenhaus et al., 2006; Kohwi et al., 2013)[69, 132]. So the question is can ectopic Cas influence the morphology of later born interneurons? From previous work, we know that one of single cell clones I assigned as "medial-early" born is indeed Cas+ (dark blue clone in Figure 4.2, A03a4 in Figure 4.11) (Mark et al., 2021 Figure 5F)[84]. Since Cas is normally expressed in the earlier born interneurons and not the latest born interneurons, if Cas is sufficient to specify "early" interneuron morphological fate, we would expect to only observe earlier born interneuron morphologies.

I obtained eight single cell clones of interneurons in six unique first instar nerve cords us-

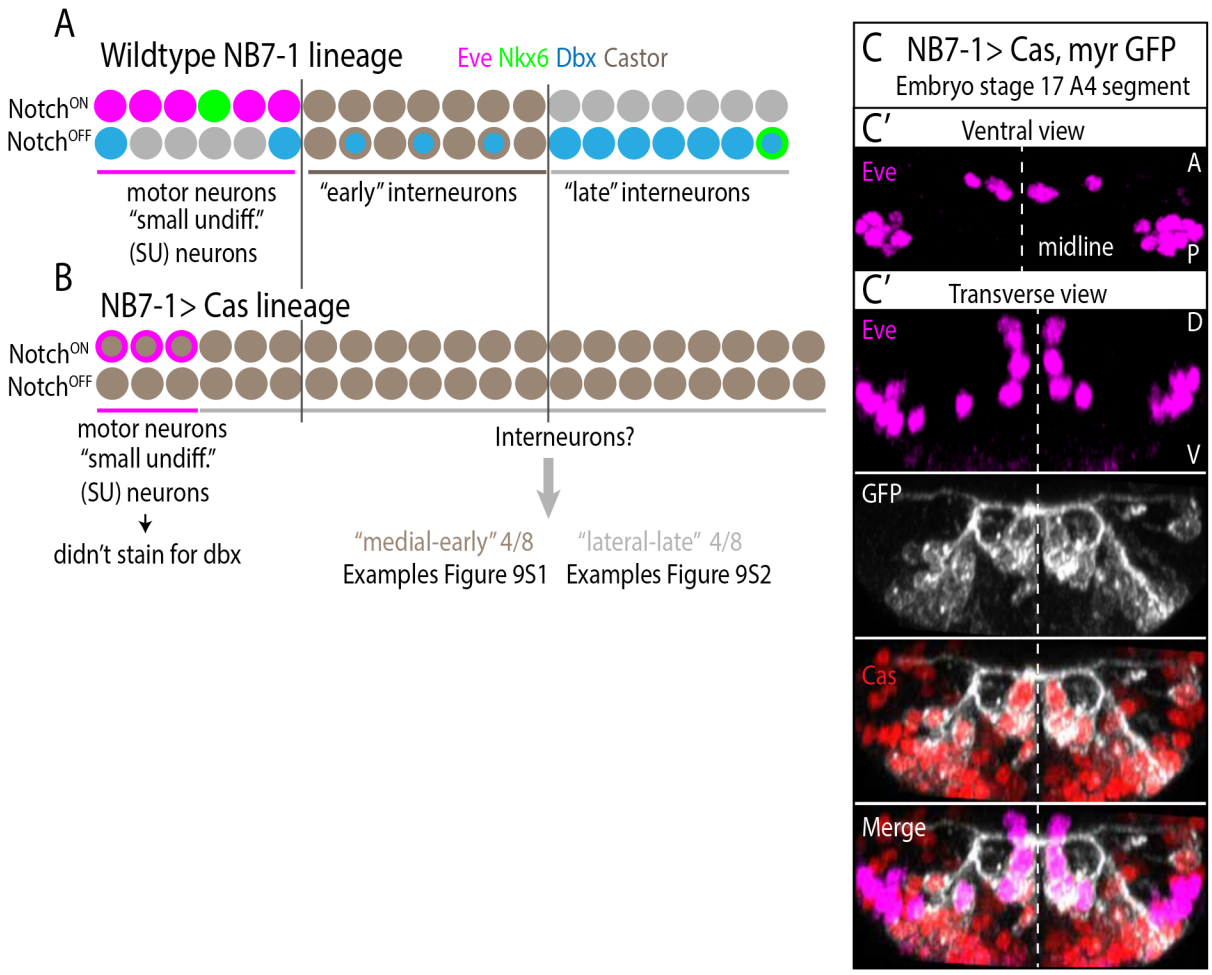


Figure 4.10: In NB7-1> Castor, ectopic Castor is expressed throughout the NB7-1 lineage at late embryonic stages. (**A-B**) Illustrations depict neuronal progeny from the NB7-1 lineage represented as circles. Colored circles correspond to expression of similarly colored molecular markers (magenta = Eve, green = Nkx6, blue = Dbx, brown = Cas (Castor)). NB7-1>Cas increases the number of Cas+ Eve- neurons at the expense of earlier-born Eve+ motor neurons and later-born Eve-, Cas+ interneurons. I did not quantify the data but by eye in (C), all GFP labeled cell bodies are expressing Cas+ including the Eve+ motor neurons. (**C**) Images of molecular marker expression and GFP within a single segment. Figures 9S1 and 9S2 are actually Figures 4.11, 4.12, respectively

ing MCFO in the Castor misexpression in NB7-1 background (NB7-1>Cas, MCFO) (Figure 4.10C,4.11,4.12). Half, 4 out of 8, of the clones resembled the "medial-early" morphologies and their cell bodies were positioned medially (Figure 4.11) while the other half of the clones

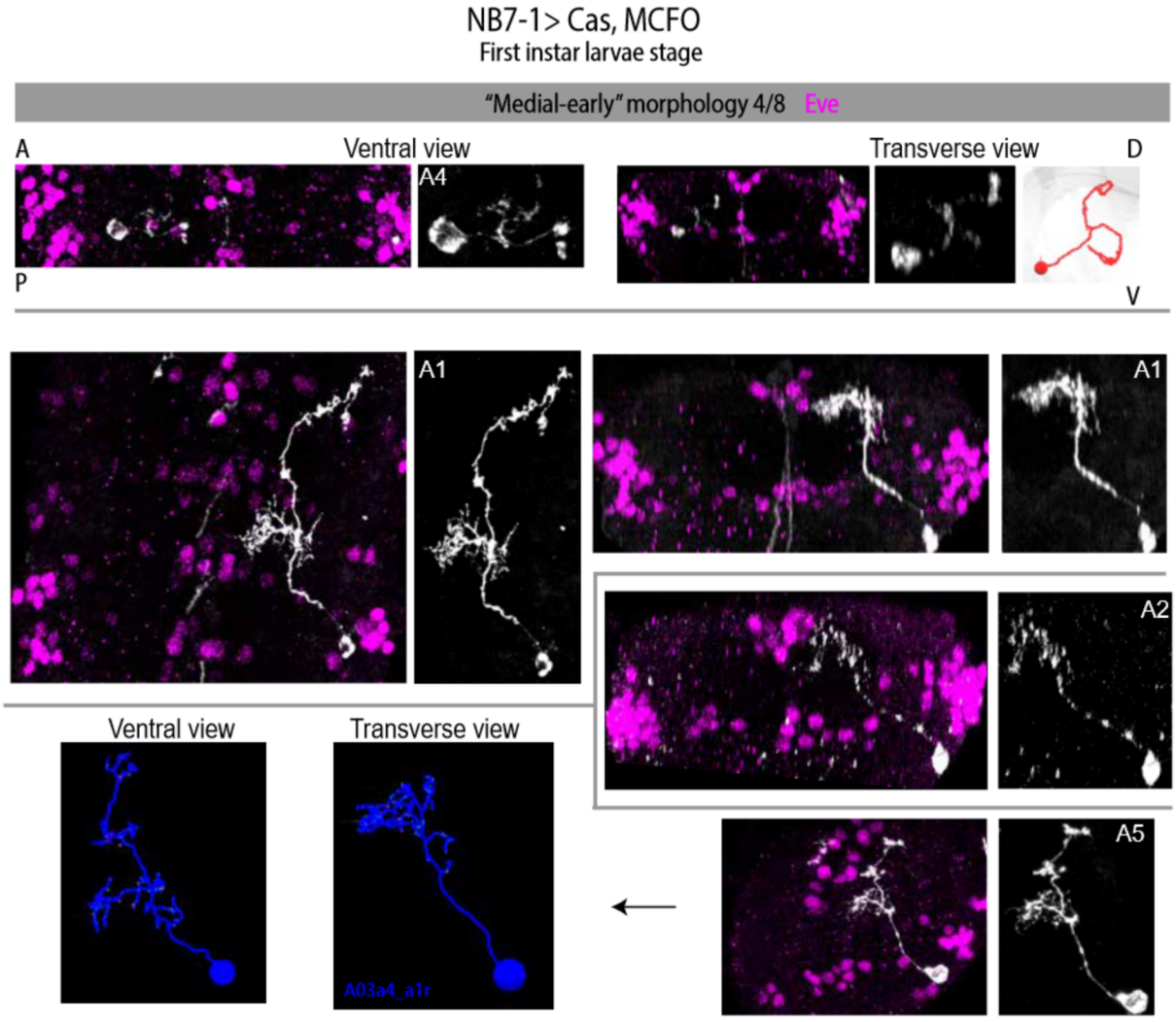


Figure 4.11: In 1st instar NB7-1>Cas, clones of interneurons with 'lateral-late' morphologies first identified in the EM volume in 1st instar. Images are in both ventral and transverse view. The single-cell clones obtained in light microscopy resemble morphologies of traced neurons in the EM volume.

resembled the "lateral-late" morphologies and consistently their cell bodies were positioned laterally (Figure 4.12). These data reveal that ectopic Cas is not sufficient to specify the "medial-early" interneuron morphology. If ectopic Cas is changing the identity of the interneurons, which is unclear from our limited understanding of NB7-1 interneuron molecular profiles, this would suggest that extrinsic birth time cues are critical determinants of in-

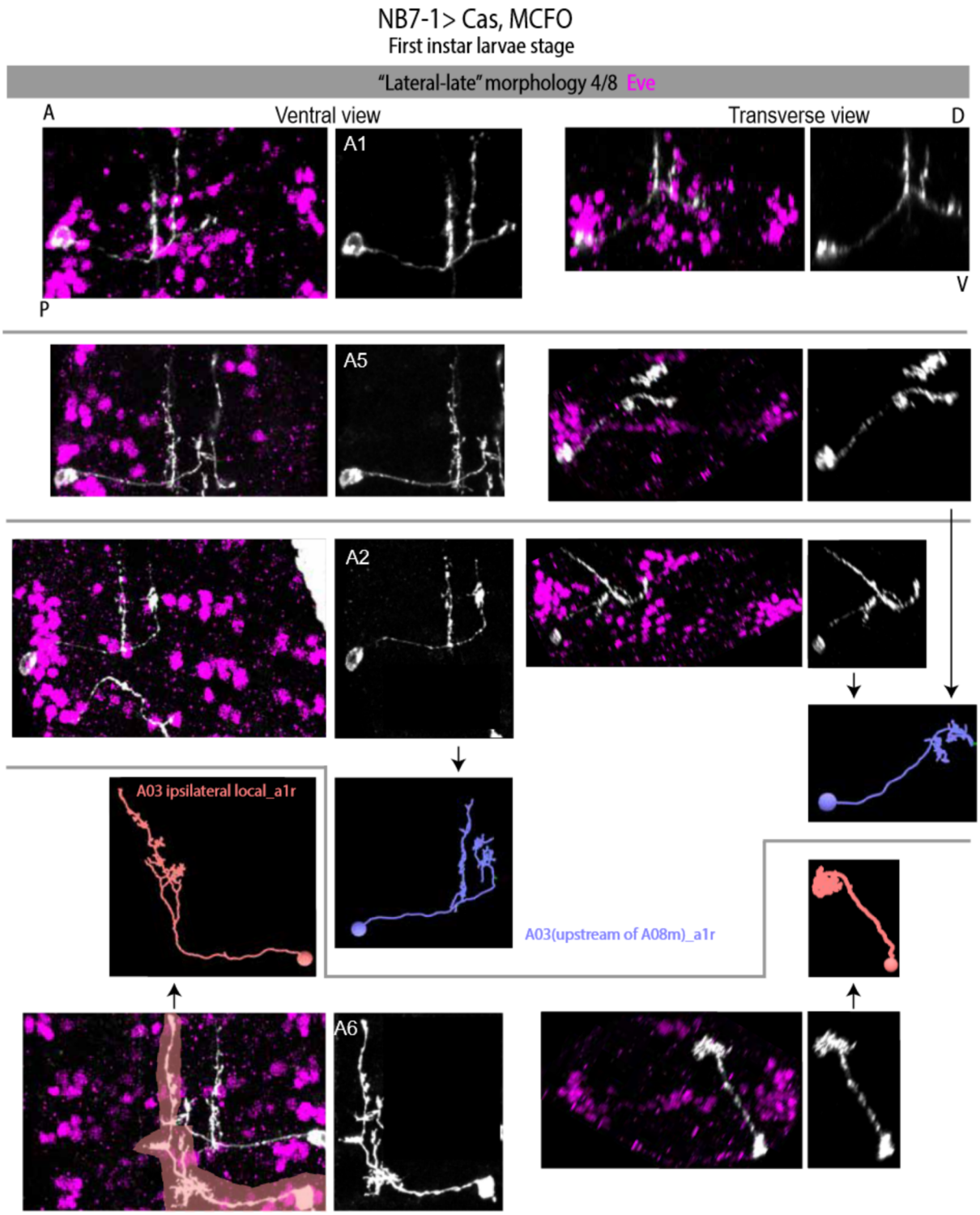


Figure 4.12: In 1st instar NB7-1>Cas, clones of interneurons with 'lateral-late' morphologies first identified in the EM volume in 1st instar. *Continued*

Figure 4.12: *Cont'd.* In 1st instar NB7-1>Cas, clones of interneurons with 'lateral-late' morphologies first identified in the EM volume in 1st instar. Images are in both ventral and transverse view. The single-cell clones obtained in light microscopy resemble morphologies of traced neurons in the EM volume.

terneuron morphology fate. Since we do not have a clear grasp of interneuron identity, it is also possible that intrinsic programs are not perturbed when Cas is ectopically expressed. The observation that U1-U3 identity and fate are not perturbed by ectopic Cas supports the latter explanation. What these results clearly rule out is that prolonged expression of Cas does not extend the window where the earliest born interneurons are generated in a comparable fashion to prolonged expression of Hunchback, which extends the window where the earliest born motor neuron fate is generated. Perhaps the difference between Hunchback and Cas is unsurprising considering that Hunchback is only expressed during the first two division windows whereas Cas is expressed for eight division windows. In fact, towards the end of development, most neuroblasts express Cas and temporal factor Grainyhead for a sizable number of divisions, raising the interesting question, how, if at all, does Cas specify neural identities? What we have come to learn from elegant work done in NB5-6 lineage is that the Cas expression window can be further subdivided by sub-temporal genes such as squeeze and nab (Stratmann and Thor, 2017)[109]. Currently, it is unknown how conserved this strategy is within the NB7-1 lineage.

4.7 Discussion

Here, we have presented evidence that when ectopic Hunchback expression is prolonged in NB7-1, interneurons are generated but the majority have an abnormal, seemingly defective outgrowth that we have been referring to as arrested outgrowth fate. Notably, no clear arbors are formed so it is unlikely synaptic connections are established. Therefore, it is unlikely these interneurons integrate into motor circuits. Overall, our work reveals that the

information NB7-1 interneurons need to successfully make their stereotyped morphologies is lost 70% of the time. So what might be happening and where does this information likely originate from? By placing our work alongside previously published studies, here we offer speculative explanations to address this question. While the majority of interneurons have an arrested outgrowth, nearly one-third of our interneuron clones possess neurites that extend into the neuropil and establish clear arborization patterns within the neuropil. We have been referring to this phenotype as wildtype-like outgrowth fate. Therefore, it is likely that these interneurons integrate into motor circuits. Our investigation found that the neuroblast '7-1' parent of these wildtype-like outgrowth interneuron progeny tend to transition from making motor neurons to interneurons earlier compared to the range of transition-timing observed across all hemisegments containing MCFO clones (Figure 4.13).

Since our data is not compatible with a model where Castor expression is essential for wildtype-like outgrowth, we favor a model where Castor acts in parallel with other currently unknown factors to ensure proper interneuron outgrowth is achieved. Lastly, our findings offer insight relevant to previously published ideas regarding 1) the regulation of the neuroblast 7-1's transition from generating motor neurons to interneuron and 2) the morphological fate of NotchON vs NotchOFF hemilineages. We discuss both of these ideas here.

Broadly, we know that developing neurons can receive information from their neuroblast stem cell parent (intrinsic) or the environment (extrinsic) and often receive cues from both sources. For example in our previous work, we found that lineage intrinsic programs involving temporal transcription factor Hunchback strongly influence motor axon outgrowth, choice of synaptic arborization field, and synaptic partnership choice, despite motor neurons being born much later in development (Meng et al., 2019; 2020)[2, 3] (Figure 4.13B-C). However, evidence suggested that the local synaptic environment likely could inform final synaptic partnership decisions. Here we find that despite misexpression of Hunchback, the neuroblast '7-1' at the time of its transition from making motor neurons to interneurons is still com-

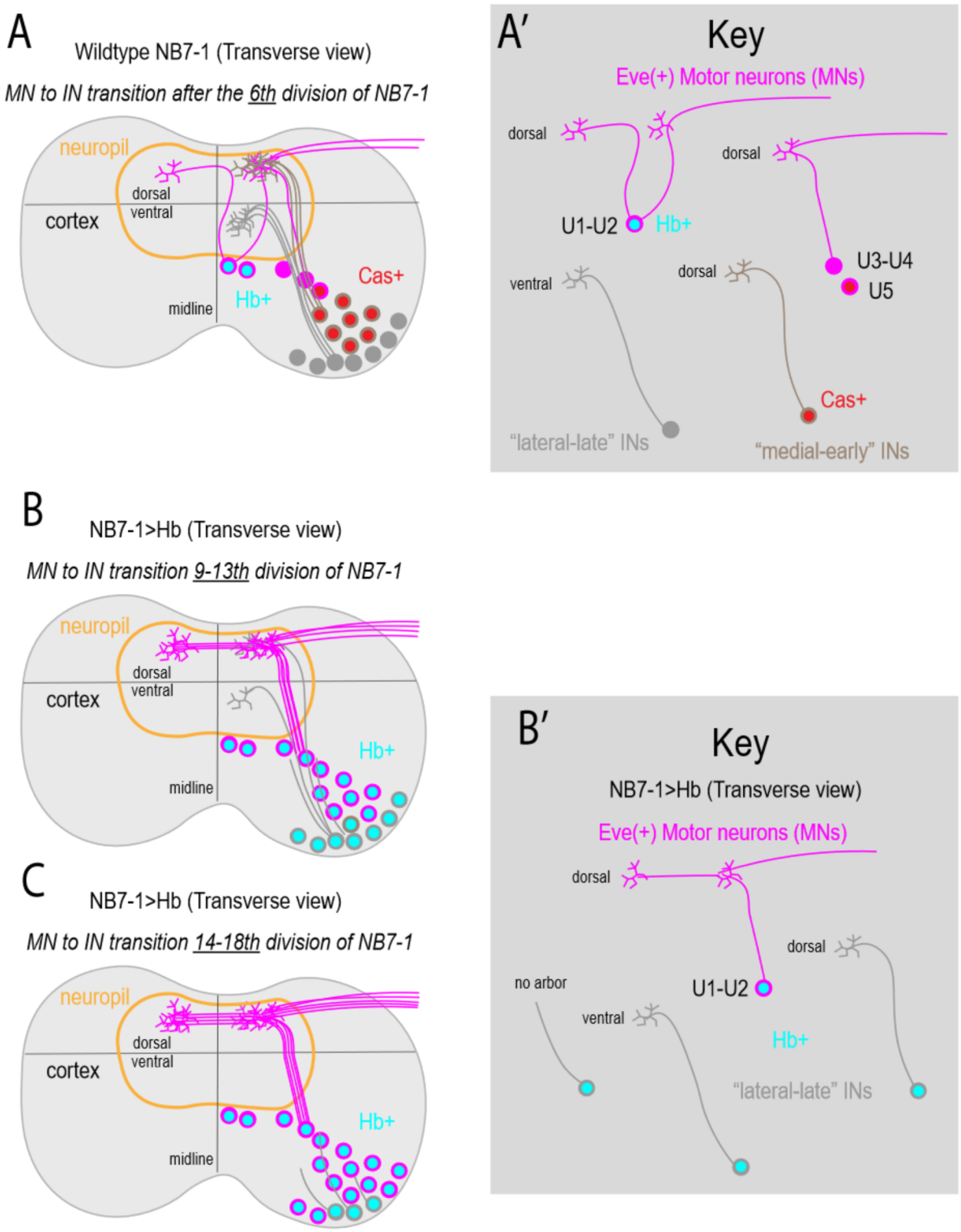


Figure 4.13: Summary (**A**) Illustration representing NB7-1 derived neuronal progeny's molecular marker expression and arborization pattern within the neuropil at around late-stage embryos and 1st instar larvae. *Cont'd*

Figure 4.13: *Cont'd.* Summary. (**B-C**) Illustrations representing NB7-1 derived neuronal progeny's molecular marker expression and arborization pattern within the neuropil when NB7-1>Hb (B) When NB7-1 transitions from making Eve+ motor neurons to Eve- interneurons during the 9-13th division there is a nearly 50% chance interneurons form arbors. (C) When NB7-1 transitions from making Eve+ motor neurons to Eve- interneurons during the 14-18th division there is almost no chance interneurons form arbors. Regardless of early or late transitions Eve+ motor neurons always form arbors in the neuropil.

patible with making early interneurons. If NB7-1 interneurons exclusively received intrinsic information to specify neurite outgrowth and arborization decisions then we would expect to see all interneurons project neurites to and establish arbors in the neuropil. Instead, we find that the majority of NB7-1 interneurons have arrested outgrowth and do not establish arbors. What best explains the ability for NB7-1 interneurons to successfully achieve wildtype-like outgrowth fate is the timing of the neuroblast 7-1's transition from making motor neurons to then generating interneurons. When the transition occurs relatively early (ie fewer extra Eve+ motor neurons are generated), the chance for interneurons to achieve wildtype-like outgrowth is 50% (Figure 4.5,4.13B). If the transition occurs relatively late the chance for interneurons to achieve wildtype-like outgrowth plummets to near zero (Figure 4.5, 4.13C). We interpret this to mean that both inherited information and extrinsic cues from the environment into which an interneuron is born are required to specify appropriate outgrowth decisions. When inherited information received by an interneuron progeny more closely matches its normal birth time environment, the greater the chance of achieving wildtype-like outgrowth is. However, even when inherited information closely matches the normal birth time, we still find that 50% of the time, interneuron clones have arrested outgrowth. So what might explain this?

We favor a model where endogenous Castor expression in the neuroblast contributes to successful outgrowth decisions. While there could certainly be other valid explanations, we favor this model in light of previously published manipulations of Castor. Early studies of Cas (previously called ming) in the Drosophila larval motor system found that loss of Cas

function led to defects in axonogenesis (Mellerick et al., 1992; Cui and Doe, 1992)[170, 171]. These studies observed that the neuropils were less dense. Interestingly, this is consistent with our phenotypes where arbors fail to elaborate within the neuropil. So even when an interneuron's inherited information closely matches its normal birth time, loss of endogenous Castor may be enough to destabilize accurate outgrowth decisions made by a given interneuron. The temporal transcription factors Grainyhead and Castor may play similar roles. We know that in other lineages where both Castor and Grainyhead are sequentially expressed, Castor promotes the expression of Grainyhead, which in turn inhibits Castor. Since ectopic Hunchback effectively inhibits endogenous Castor, if If Grainyhead is expressed later in NB7-1, Hunchback may indirectly inhibit Grainyhead expression as well.

If this model is true, it raises the question, what might be the mechanism underlying Cas's role? Mellerick et al., discovered that loss of Cas function led to CNS-specific alteration of engrailed expression and aberrant engrailed expression in laterally positioned neurons. Specifically, the number of engrailed+ neurons doubled yet neurons that normally express engrailed had reduced intensity of engrailed expression in Cas mutant backgrounds. Subsequent work revealed the importance of proper engrailed expression for axonal pathfinding in the developing nerve cord (Joly et al., 2007)[172]. We know that engrailed has a number of target genes involved in axonal guidance such as eg, con, comm, fra, ena, and trio (Solano et al., 2003)[173]. It is tantalizing to speculate that ectopic expression of Hunchback causes loss of Cas, which perturbs engrailed expression levels in the NB7-1 interneurons, which can lead to aberrant neurite outgrowth defects. In the future, engrailed expression should be assessed in Eve- interneurons in the NB7-1>Hb background.

4.7.1 What controls the timing of neuroblast's transition from generating motor neurons to making interneurons?

We learn that after generating Eve+ motor neurons, NB7-1's state is compatible with making "early"-like morphology fate at later times in development. This conclusion is consistent with previous models that suggested that prolonged expression of Hunchback keeps neuroblasts in a "young" state (Hirono et al., 2012)[169] and further supports the idea that the temporal transcription factor may be regulating the chromatin landscape of neuroblasts, to some extent (Doe, 2017; Cleary and Doe, 2006; Kohwi et al., 2013)[64, 139, 132]. While the observation that after the motor neuron to interneuron transition, interneurons express ectopic Hunchback appears incompatible with the idea that ectopic Hunchback maintains a "young" state compatible with making Eve+ U1-like motor neurons, we believe there is a simple explanation to resolve this paradox. First, we and others have shown that when Hunchback expression is high (2x UAS-Hb and 2x NB7-1-GAL4 transgenes) there is an increase in the number of extra Eve+ motor neurons generated when compared to lower levels of expression (1x UAS-Hb and 1 NB7-1-GAL4 transgenes) (Meng et al., 2019; Pearson and Doe, 2003; Cleary and Doe, 2006)[2, 102, 139]. Combined with the observation that variable numbers of Eve+ motor neurons are generated when Hunchback is misexpressed, we conclude that the transition between generating Eve+ motor neurons and Eve- interneurons is dependent on ectopic Hunchback expression. The transition is likely triggered by hunchback expression in the neuroblast dipping below some threshold. This could occur within the span of one division considering that in neuroblasts, Hb has a short half-life (Grosskortenhaus et al., 2006)[69]. Once the transition has been triggered, NB7-1 is no longer capable of responding to ectopic Hunchback expression. This loss in the ability of neuroblasts to respond to temporal transcription factors is known as loss of competency and has been an area of much research (so many Doe lab papers). This loss of competency suggests that the state of the NB7-1 after it transitions to making interneurons is not perturbed by ectopic

Hb expression.

4.7.2 Relationships between birth time and interneuron morphological fate

This detailed atlas and characterization of NB7-1 interneuron morphology build upon recent work that undertook a massive effort to understand hemilineage diversity across a handful of neuroblast lineages (Mark et al., 2021)[84]. This study presented a broad developmental framework where NotchON hemilineages predominantly project to the dorsal portion of the nerve cord whereas NotchOFF hemilineages project to the ventral portion of the nerve cord. Considering that nearly half of the "medial-early" interneurons either project to either the dorsal or the dorsal and ventral portion of the neuropil, it is tempting to speculate that these morphological differences correlate with hemilineage membership (Figure 4.2C'). However, contrary to Mark et al., we find that all of the interneurons that project their neurites to the ventral neuropil, are all lateral, meaning their cell bodies touch the edge of the nerve cord cortex. This suggests a relationship between the birth time of an interneuron and its neurite position within the neuropil. Combined, these studies highlight the rich morphological diversity found within and among neuroblast lineages, which loosely adhere to the broad classifications we assign. In the future, to confidently ascertain birth time relationships among NB7-1 interneurons and obtain more single-cell clones using light microscopy, Twin-spot MARCM lineages analysis should be employed. However, our current level of resolution is sufficient to draw valuable conclusions from our manipulations of temporal transcription factors detailed in the following sections.

Source Data for Figure 4.1C

Molecular Marker	Genotype	Number of values	Mean (number of cell bodies at E16/17)	Std. Deviation	Std. Error of Mean	p value
Total Dbx+	NB7-1>myr GFP	20	12.30	1.838	0.4110	NA
Total Cas+	NB7-1>myr GFP	20	14.35	2.889	0.6459	NA
Dbx+ Cas+	NB7-1>myr GFP	20	2.600	0.7539	0.1686	NA

Figure 4.1F

Molecular Marker	Genotype	Number of values	Mean (number of cell bodies at E16/17)	Std. Deviation	Std. Error of Mean
Dbx+ Nkx6+	NB7-1>myr GFP	20	1.100	0.4472	0.1000

Table 4.1: Source Data for Figure 4.1

Source data for Figure 4.4B

	Genotype	Number of values	Mean (# of cell bodies at E16/17)	Std. Deviation	Std. Error of Mean
Total Eve+	NB7-1>myr GFP, Hb	9	15.22	4.353	1.451
Total Dbx+	NB7-1>myr GFP, Hb	9	13.33	3.317	1.106
Only GFP+	NB7-1>myr GFP, Hb	9	14.89	4.649	1.550

Unpaired t-test Welch (for un-equal Std. Deviation)

Source data Figure 4.4C

	Genotype	Number of values	Mean (# of cell bodies at E16/17)	Std. Deviation	Std. Error of Mean
Total Cas+	NB7-1>myr GFP, Hb	15	0.2667	0.7037	0.1817
Dbx+, Cas+	NB7-1>myr GFP, Hb	15	0.000	0.000	0.0000

Unpaired t-test Welch (for un-equal Std. Deviation)

Source data Figure 4.4D

	Genotype	Number of values	Mean (# of cell bodies at E16/17)	Std. Deviation	Std. Error of Mean
Total GFP+	NB7-1>myr GFP, Hb	6	39.33	6.593	2.692
Total Hb+	NB7-1>myr GFP, Hb	6	37.00	6.197	2.530
Eve+, Hb+	NB7-1>myr GFP, Hb	6	13.83	4.355	1.778

Unpaired t-test Welch (for un-equal Std. Deviation)

Source data Figure 4.4G

	Genotype	Number of values	Mean (# of cell bodies at E16/17)	Std. Deviation	Std. Error of Mean	p value
Dbx+ Nkx6+	NB7-1>myr GFP	20	1.100	0.4472	0.1000	NA
	NB7-1>myr GFP, Hb	15	0.3333	0.6172	0.1594	0.0004*

Unpaired t-test Welch (for un-equal Std. Deviation)

Table 4.2: Source Data for Figure 4.4

CHAPTER 5

NOTCH TRANSCRIPTION FACTOR

5.1 Introduction

There are a number of transcription factors expressed early in neuronal development that have been shown to contribute to neuronal molecular identity. However, the extent to which these factors contribute to neuronal terminal features relevant for circuit wiring such as mature synaptic partnerships is only now beginning to be explored. Recently, it was found that a group of transcription factors acting in neuronal stem cells called temporal transcription factors are potent determinants of neuromuscular synaptic partner choice (Meng et al., 2020; Meng et al., 2019; Seroka and Doe, 2019)[3, 2, 80]. This work supports a model in which lineage intrinsic factors determine neuromuscular synaptic partnerships. Therefore a major question that follows from this model is to what extent do other previously defined lineage intrinsic factors expressed early in development inform neuromuscular synaptic partnership decisions? One candidate factor is Notch, a transmembrane protein, which acts early in development and plays a role in specifying neuronal molecular identity (Truman et al., 2010)[60].

In the developing Drosophila larval nerve cord, Notch is expressed in neuroblasts, ganglion mother cells (GMCs), and young postmitotic neurons (Fehon et al., 1991)[174]. Notch signaling is key for specifying cell fate across different tissues and across systems. All Drosophila larva nerve cord neuroblasts undergo type I division at some point in their life (Crew, 2019)[168]. Type I division is where neuroblast symmetrically divides to self-renew and generate a precursor cell called a ganglion mother cell (GMC) (Figure 5.1A).

Neuroblasts normally begin with type I division and either type I division persists throughout their entire division window (e.g. NB7-1) or transition to type 0 division where neuroblasts asymmetrically divide to directly generate a post mitotic neural cell. A striking

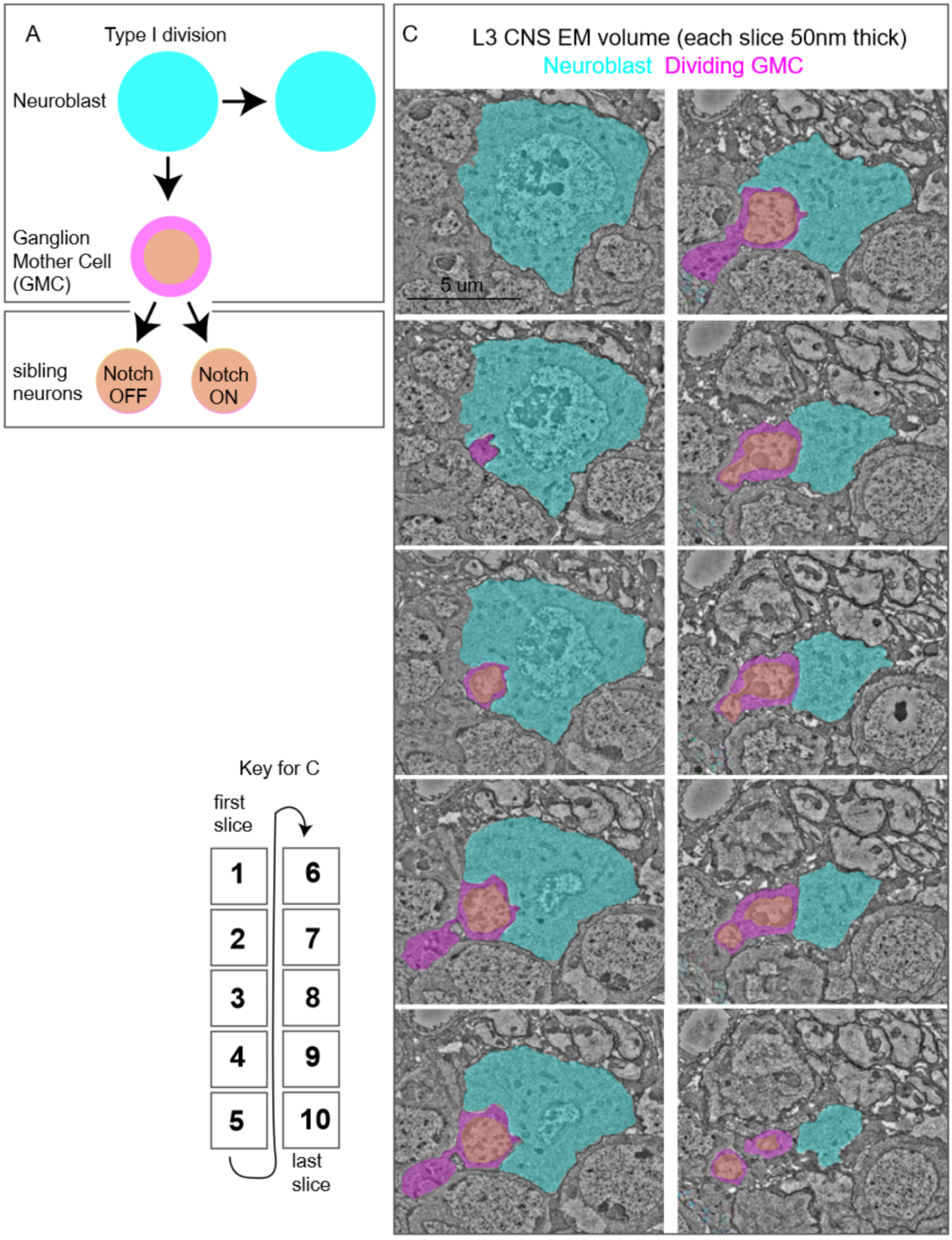


Figure 5.1: Type I division of neuroblasts within the Drosophila larval nerve cord. *Continued*

Figure 5.1: *Cont'd.* Type I division of neuroblasts within the Drosophila larval nerve cord. (**A**) Illustration of a neuroblast (cyan) dividing (arrows) to self renew (top row) and generate a neural precursor called a Ganglion mother cell (GMC) (pink, orange nucleus). (B) Unlabeled but should be the boxed region directly below (A). (**B**) Illustration of the GMC's terminal division products, two sibling neurons, one NotchOFF and the other is NotchON. (**C**) Images of single EM transverse slices of an L3 nerve cord. Slices are consecutive and begin with the first column and the second column. The last slice is in the bottom right corner. The neuroblast is overlaid with a cyan mask. The dividing GMC is overlaid with a magenta mask and the dividing GMC's nucleus is overlaid with an orange mask.

example of a swift transition from type I to 0 division mode is NB3-3 where only the first division is type I (Baumgardt et al., 2014)[175].

The GMC generated from a type I division then goes on to terminally divide to produce two post-mitotic sibling cells (Figure 5.1B-C). Despite being siblings, neurons born from the same GMC tend to have strikingly unique molecular identities and can even have different neuron cell types (interneuron vs motor neuron). This led researchers to interrogate what accounted for these differences. It was found that while the GMC expresses Notch, it also expresses Numb in a polarized fashion so that Numb is only inherited by one of the siblings. Numb is relevant because it inhibits Notch activity. In several lineages including NB1-1 (aCC/pCC), NB4-2 (RP2/RP2sib), and NB7-1 (U/Usib) the mechanism of this inhibition involves Numb inhibiting the localization of Sanpodo on the cell membrane thus blocking Notch signaling (O'Connor-Giles and Skeath, 2003)[176]. The sibling that does not inherit Numb has Notch activity, meaning that upon Notch binding to an extracellular ligand,Delta, the intracellular domain of Notch (hereafter Notch∧intra) is cleaved allowing Notch∧intra to localize to the nucleus where it often associates with other factors to form regulatory complexes and to carry out transcription factor function (Artavanis-Tsakonas et al., 1999)[177]. Intuitively, the sibling with Notch activity is referred to as NotchON whereas the sibling whose Notch activity is inhibited is referred to as NotchOFF. Another common naming scheme in the literature is that NotchON neurons are 'A' and are members of the 'A' hemilineage while NotchOFF neurons are 'B' and are members of the 'B' hemilineage

(Truman et al., 2010)[60]. Truman and colleagues found a general trend where hemilineage related neurons often share key fate features amongst themselves. For example, in the adult Drosophila nerve cord, which is made up of 34 hemilineages, hemilineage related neurons share the same neurotransmitter (Lacin et al., 2019)[178]. In another recent study involving Truman, the authors try to make the broad argue that in the Drosophila larva nerve cord 'A' hemilineage (NotchON) neurons send projections to the dorsal portion of the neuropil associated with motor function while 'B' hemilineage (NotchOFF) neurons send projections to the ventral portion of the neuropil associated with sensory function (Mark et al., 2021)[84]. Altogether, the ubiquitous highly conserved Notch signaling pathway is key for promoting neural diversity.

The early studies identifying Notch as a key promoter of GMC-derived sibling neuron diversity relied on classic genetic manipulations such as loss and gain of function strategies (Spana et al., 1995; Skeath and Doe, 1998; Buescher et al., 1998; Lear et al., 1999; Schuldt and Brand, 1999; O'Connor-Giles and Skeath, 2003)[179, 71, 180, 181, 182, 176]. At the time, a number of neurons could be identified by Even-skipped (Eve) expression. Among these neurons were the Eve+ U motor neurons (also called 'CQ' motor neurons in these older studies) from the NB7-1 lineage. In the NB7-1 lineage the Eve+ U motor neurons are in the 'A' NotchON hemilineage while the U siblings are in the 'B' NotchOFF hemilineage (Figure 5.2A).

In numb mutants on average there were 3 extra Eve+ neurons in the U motor neuron cluster (Skeath and Doe, 1998)[71]. This led the authors to conclude that in this background, the NotchOFF hemilineage transformed into the NotchON hemilineage based on Eve+ in late stage embryos. Consistently, misexpression of UAS-Notch∧intra throughout the CNS using pros-Gal4 increased the number of Eve+ neurons in embryos (O'Connor-Giles and Skeath, 2003)[176]. In Notch or Sanpodo mutants, Eve+ neurons were lost in the region where the U motor neurons are normally positioned, leading to the conclusion that in these

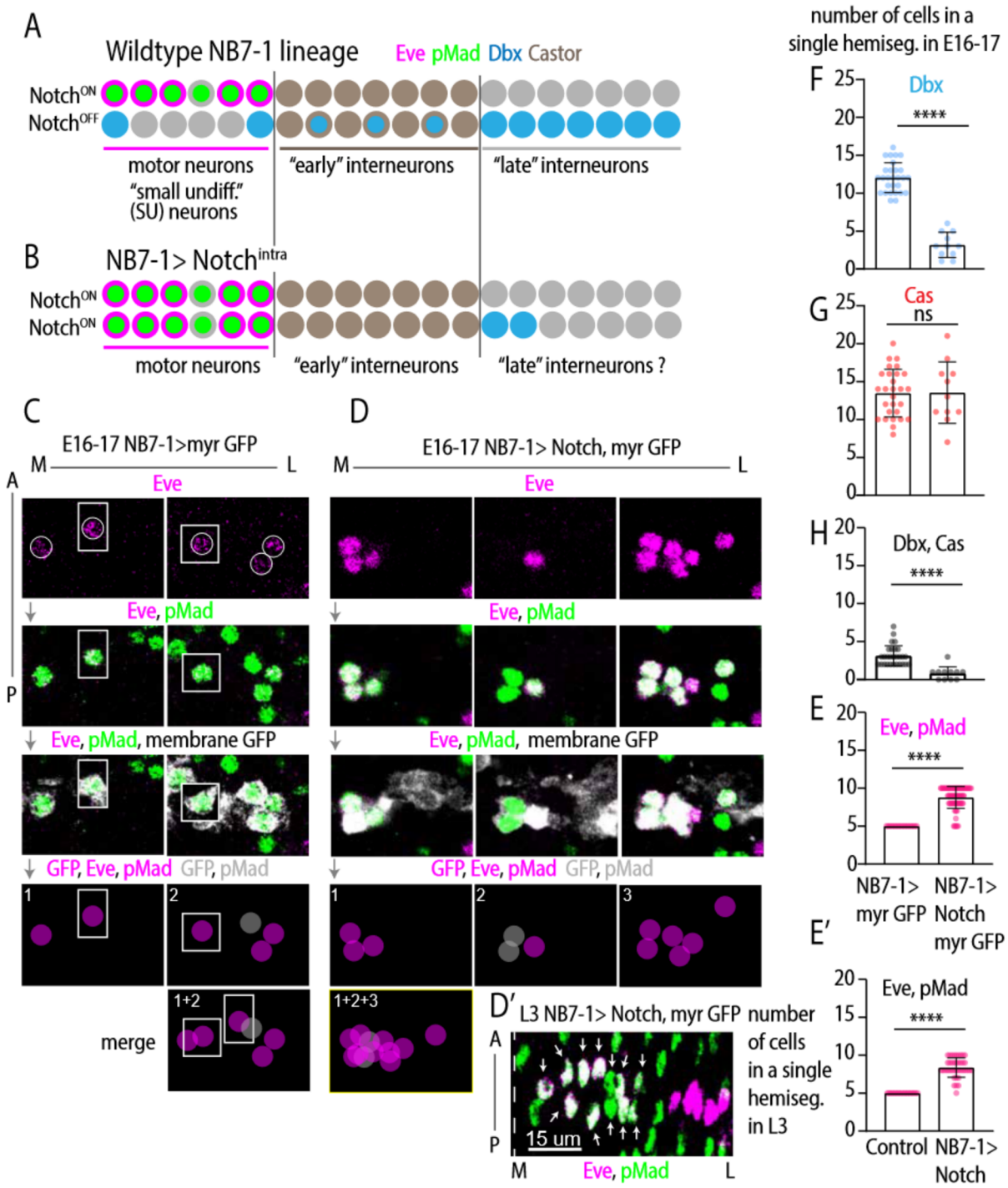


Figure 5.2: Notch∧intra misexpression in NB7-1 increases the number of neurons with NotchON molecular markers at the expense of NotchOFF molecular markers. (**A-B**) Illustrations depict neuronal progeny from the NB7-1 lineage represented as circles. Colored circles correspond to expression of similarly colored molecular markers (magenta = Eve, green = pMad, blue = Dbx, brown = Cas (Castor)). NB7-1>Notch∧intra increases the number of Eve+ pMad+ motor neurons at the expense of Dbx+ neurons. *Continued*

Figure 5.2: *Cont'd.* (**C-D**) Images of embryonic molecular identity marker in cell bodies in late-stage embryonic CNSs. Images are shown in ventral view, anterior always up. Each column is z-projection at differing z-planes along the dorsal-ventral axis for ease of visualizing the data. The bottom-most row depicts the overlaid cell bodies. In (C) boxes are insets from different z-planes. (**E-F**) Quantification of the number of cell bodies in single hemisegments with the listed molecular marker. The average and standard deviation are overlaid. Unpaired t-test with Welch's correction for unmatched standard deviations. '***' $p<0.0001$. (See source datasheet for more details of E-F).

mutant backgrounds the NotchON hemilineage containing the Eve+ U motor neurons is now transformed into the NotchOFF hemilineage containing the Eve- Usibs (Skeath and Doe, 1998; Lear et al., 1999)[71, 181]. There was evidence that misexpressing Numb could also lead to the transformation of the NotchON hemilineage to NotchOFF. While Eve+ U motor neurons were not evaluated, expression of hs-numb transformed MP2 precursor derived NotchON vMP2 neurons into NotchOFF dMP2 neurons based on axon projection (Spana et al., 1995)[179] (Note MP2 is a primary precursor, which is unique and unlike other neuroblasts in so far that MP2 only divides once to generate vMP2 and dMP2, which to my knowledge are pioneers that die prior to hatching (Gaziova et al., 2020; Miguel-Aliaga et al., 2008)[183, 184]. Combined, these studies identified the role of Notch/Numb pathways of increasing neural diversity by specifying unique sibling molecular identities.

During the pandemic as I was reading the literature in preparation to write a review with Ellie, I was inspired by these previous Notch-signaling related manipulations and I wanted to ask the straightforward question, can transforming one hemilineage to another have a permanent impact on motor neuron to muscle synaptic partnership decisions? Based on my previous work on temporal transcription factors, I hypothesized that misexpression of Notch$\wedge$intra using the NB7-1 or CQ driver would convert the NotchOFF Usibs to their NotchON U motor neuron sibling's fate. If this hypothesis is correct, we would expect the extra Eve+ neurons to express pMad (decent marker for motor neurons) beginning in late embryonic stages (Figure 5.2). We would also expect a doubling of the number of

synaptic branches onto dorsal muscles that receive innervation from the U motor neurons and the ventral oblique (VO) muscles that receive innervation from NB7-1's VO motor neuron. For the opposite manipulation where Notch expression is lost in NB7-1's motor neurons, I expected loss of synaptic branches onto muscles targeted by U1, U2, U3, VO, U4, and U5 motor neurons. At the time, I thought these experiments were straightforward since they relied on previously published fly lines and techniques I was familiar with so I gave this project off to an amazing undergraduate student I was mentoring,Yaa Asante. To summarize our findings, in the control, Notch∧intra/+, and experimental, NB7-1>Notch∧intra Yaa and I conducted parallel analysis of L3 bodywall synaptic branch count onto muscles and found consistent results that supported our hypothesis that there is a near doubling of synaptic branch numbers onto muscles innervated by NB7-1 motor neurons (Figure 3, Figure 4). Beyond the Notch∧intra manipulation, the rest did not go to plan. However, I will still present all attempted manipulations and I hope the negative results will aid future experimental design plans. I will also present glimpses of a possible sibling side story that emerged from this Notch investigation. I will offer my insights of this fledgling project with the hopes that if someone decides to carry this project forward they can benefit from my amassed knowledge.

5.2 Results: Expressing Notch∧intra in the NB7-1 lineage transforms NotchOFF to the NotchON hemilineage

This is the first study to specifically express Notch∧intra in NB7-1 and evaluate molecular marker expression in late embryonic (E16/17) and third instar larval stage (L3) at single cell resolution (Figure 5.2) and characterize permanent motor neuron to muscle synaptic partnership decisions at L3 stage (Figure 5.3, 5.4). A recent study expressed Notch∧intra using a NB7-1 specific driver but they only evaluated gross lineage morphology at the whole segment (A1) resolution (Mark et al., 2021)[84]. To characterize what happens to the NB7-1

lineage when Notch∧intra is misexpressed (NB7-1-Gal4>UAS-Notch∧intra, UAS-myr-GFP), I stained for the following: Eve, pMad, Dbx, and Castor (Figure 5.2). Under wildtype conditions, NB7-1 generates six motor neurons identifiable by pMad+ (pMad is expressed in all motor neurons and in some interneurons) and large cell body diameter, a characteristic feature of motor neurons (Figure 5.2A,C). Five of the motor neurons, U1-U5, are Eve+ and one of the motor neurons, VO, is Nkx6+ (Figure 2A). When we drive Notch∧intra and UAS-myr-GFP using the NB7-1 driver we now find up to two pMad+ neurons (Figure 2B,D') and up to ten Eve+, pMad+ motor neurons with an average of 8.8 in late stage embryos (Figure 2E). This is consistent with Skeath and Doe's observations that in late embryonic stage numb mutants, there are on average 8 Eve+ U neurons (Skeath and Doe, 1998)[71]. We find that the extra Eve+, pMad+ motor neurons persist through L3 where we find an average of 8.3 Eve+, pMad+ neurons (Figure 5.2D'-E'). So far our molecular marker data is consistent with the NotchOFF hemilineage permanently transforming to the NotchON motor neuron fate.

Next, we wanted to know if there was further evidence of this transformation by examining known NB7-1 interneuron molecular markers, Dbx and Castor, in late stage embryos (these markers do not persist until L3). Dbx+ interneurons are thought to be members of the NotchOFF hemilineage (Lacin and Truman, 2016). Consistent with this model, we find a significant decrease in the number of Dbx+ neurons generated from an average of 12 observed in wildtype to 3 observed in NB7-1>Notch∧intra (Figure 5.2F). In further support, we find that while the number of Cas+ neurons does not change (13.5 vs 13.5) there is a near total loss of Cas+ Dbx+ interneurons, average of 0.8 compared to 3 observed in our control (Figure 5.2G-H). This makes sense with my previous characterization of the NB7-1 lineage where I found that Cas+ is expressed in both NotchON and NotchOFF interneurons but only Cas+, Dbx+ interneurons to populate the NotchOFF hemilineage (see NB7-1 interneuron story chapter). Combined my data suggests that Notch∧intra transforms the NotchOFF

hemilineage beyond the first six divisions however since we find 3 Dbx+ neurons it could be that Notch∧intra expression does not persist throughout the entire NB7-1's division window.

Another explanation that is consistent with these results is that Notch∧intra expression in the neuroblast 7-1 causes NB7-1 to transition from type I to 0 division mode during the last several divisions. Previous studies have found that the Notch pathway can control the switch from Type I to Type 0 divisions within nerve cord neuroblasts (Ulvklo et al., 2012; Bivik et al., 2016)[185, 186]. Further, work in vertebrate nervous systems have identified Notch signaling to be important for neurogenesis by maintaining neural stem cells (Imayoshi et al., 2010)[187]. We wanted to further characterize the impact Notch misexpression has on the neuroblast 7-1's division modes. Unfortunately we were unable to count the total number of myr-GFP+ cell bodies when we misexpressed Notch∧intra because the myr-GFP expression was very faint, our scoring of Cas+ neurons reveals that misexpression of Notch ∧ intra in NB7-1 does not cause NB7-1 to switch from type I division (divide to generate a GMC) to type 0 division (divide to directly generate a neural progeny) during the first 13 divisions. What happens beyond the 13th division is unclear. Future work will need to resolve the impact Notch∧intra misexpression has on the size of the NB7-1 lineage.

To circumvent the potential impacts of Notch∧intra misexpression in the neuroblast 7-1 itself, we used the CQ-Gal4 driver (two tandem repeats of the U neuronal element from 3.4(BglII) to 4.3kb(MscI)) (Landgraf et al., 2003)[81]. However, we found no change in the number of Eve(+) neurons (Figure 6B) nor did we observe changes in synaptic branch counts onto NB7-1 motor neuron target muscles (data not shown). Since joining the Heckscher lab I was under the impression that the CQ-Gal4 driver was first expressed in the GMCs precursors of the U/Usibs but after the negative results I dug into the literature. A previous study reports that the CQ-Gal4 drives expression in U1-U5 and in about a third of the hemisegments it also expresses in the VO motor neuron (Mauss et al., 2009)[153]. On rare occasions the driver drives expression in up to 8 cells (Mauss et al., 2009)[153]. The

unaccounted cells are likely several of the Usibs. This means that if the CQ-Gal4 driver expresses in the GMC it is likely very weak and variable.

5.2.1 Misexpressing Notch∧intra in the NB7-1 lineage permanently transforms the NotchOFF U sib fate to NotchON U and VO motor neuron to muscle synaptic partnership fate

In the previous section, we found molecular marker evidence that the NotchOFF sibs transform into NotchON motor neurons when NB7-1>Notch∧intra. Yaa Asante imaged, scored, and analyzed L3 bodywall data for both the dorsal muscles and the ventral obliques. Prior to her analysis, I dissected, imaged, and scored synaptic branch counts onto dorsal and ventral oblique muscles but on a much smaller scale (Figure 5.3). From my dataset, I found a significant, near double increase in the number of synaptic branches onto the following muscles: 9, 2, 10, and 3 (Figure 5.3A-F, J-M).

I found a slight increase in the number of synaptic branches onto muscle 4 (Figure 5.3A-B, G-H, N). Considering that we observe nearly 9 Eve+ pMad+ neurons on average, one plausible explanation for our synaptic branch count results is that sometimes the U5 motor neuron sibling is not transformed. Consistent with this explanation, in L3 animals I found that a greater increase in the number of synaptic branch numbers onto muscle 4 in bodywall segments that correspond to nerve cord hemisegments that contain 9-10 Eve+ neurons compared to bodywall segments that correspond to hemisegments with 7-8 Eve+ neurons (Figure 3O). While I had too little data of synaptic branch counts onto the ventral oblique muscles, combining my data and Yaa's we found a significant increase in the number of branches onto VO muscle 15 (Figure 5.4A-B,C,E) and a slight increase in the number of branches onto muscle 16 (Figure 5.4A-B,D,F). NB7-1's VO motor neuron was known to innervate VO muscles but it was unclear which one, our data suggest VO innervates muscles 15 and 16. Combined, these data strongly suggest that misexpression of Notch∧intra transforms the

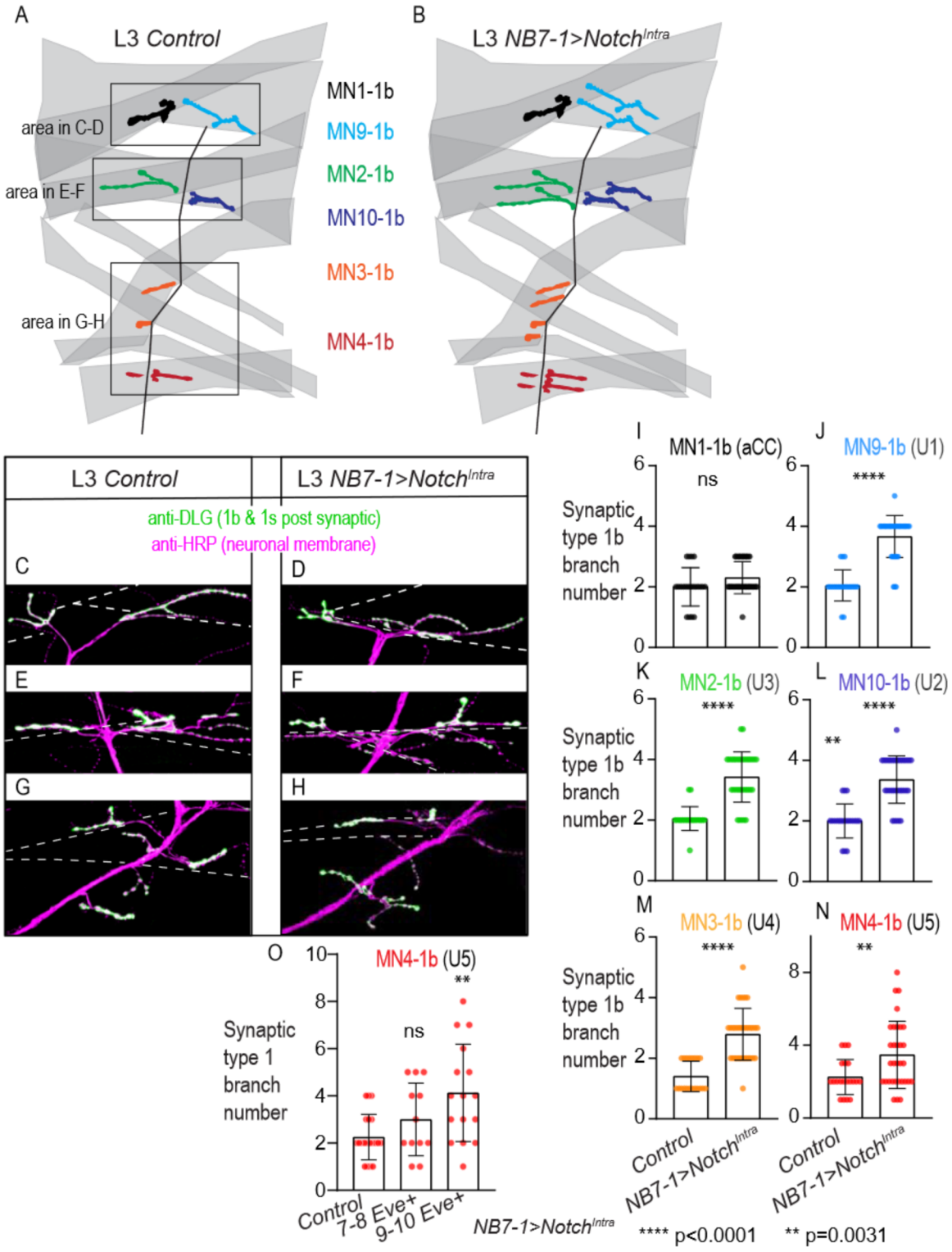


Figure 5.3: Notch∧intra misexpression in NB7-1 permanently increases the number of synaptic branches onto the NotchON U motor neuron muscle targets. *Continued*

Figure 5.3: *Cont'd.* Notch∧intra misexpression in NB7-1 permanently increases the number of synaptic branches onto the NotchON U motor neuron muscle targets. (**A-B**) Illustrations of neuromuscular synapses on dorsal muscles in an L3 body wall segment (black = aCC, light blue = U1, dark blue = U2, green = U3, orange = U4, red = U5). In NB7-1>Notch∧intra the number of 1b synaptic branches increases on all U motor neuron target muscles. (**C-H**) Images of neuronal membrane, both axons and neuromuscular synapses, on ventral muscles in L3 abdominal segments. (**I-O**) Quantification of type 1b branches onto muscles. Color code as in (A). Each dot represents the number of branches onto a single muscle. For quantifications, average and standard deviation are overlaid. Un-paired t-test with Welch's correction for unmatched standard deviations (see source datasheet for details). 'ns' not significant, '**' p=0.0031,'***' p<0.0001.

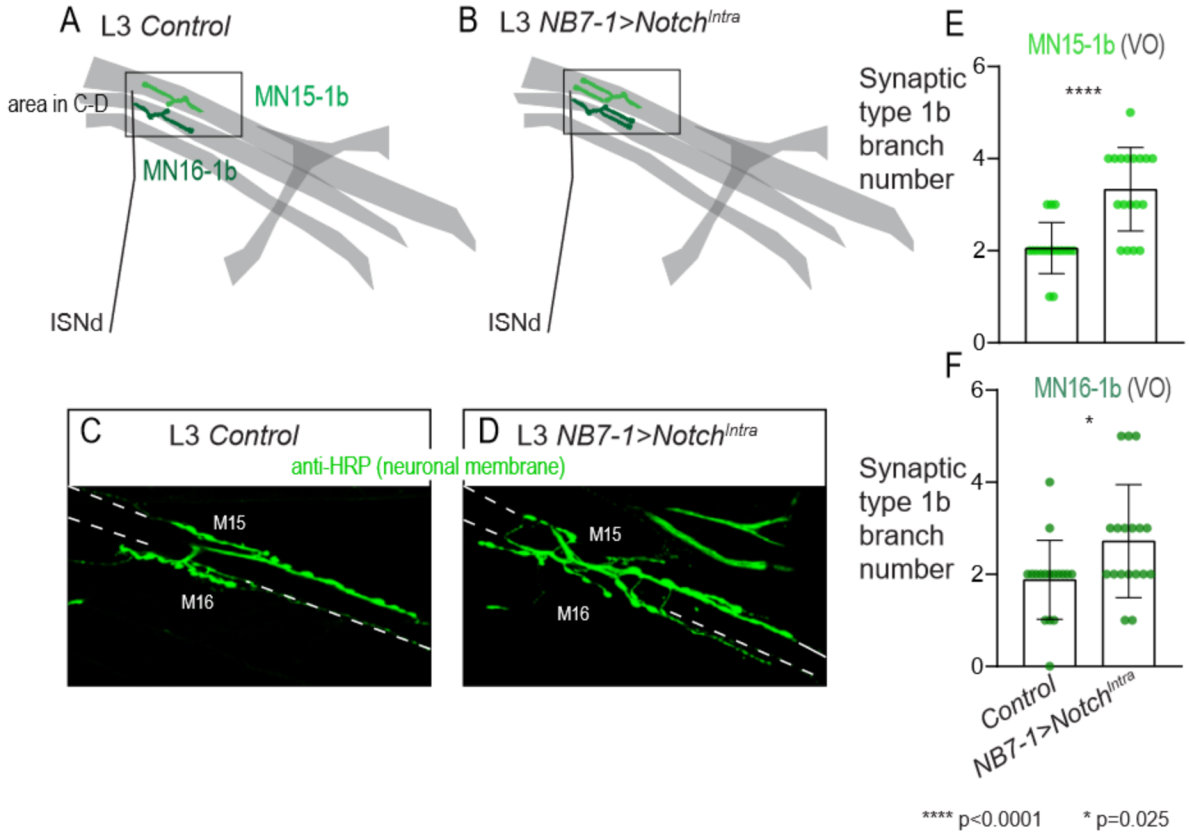


Figure 5.4: Notch∧intra misexpression in NB7-1 permanently increases the number of synaptic branches onto the NotchON VO motor neuron muscle targets. (**A-B**) Illustrations of neuromuscular synapses on dorsal muscles in an L3 body wall segment (light green = MN15-1b, dark green MN16-1b). In NB7-1>Notch∧intra the number of 1b synaptic branches increases on both putative VO motor neuron target muscles. *Continued*

Figure 5.4: *Cont'd.* Notch∧intra misexpression in NB7-1 permanently increases the number of synaptic branches onto the NotchON VO motor neuron muscle targets. (**C-D**) Images of neuronal membrane, both axons, and neuromuscular synapses, on ventral muscles in L3 abdominal segments. (**E-F**) Quantification of type 1b branches onto muscles. Color code as in (A). Each dot represents the number of branches onto a single muscle. For quantifications, average and standard deviation are overlaid. Un-paired t-test with Welch's correction for unmatched standard deviations (see source datasheet for details). 'ns' not significant, '*' p=0.025,'***' p<0.0001.

U and VO siblings into their U and VO motor neuron counterparts, respectively, causing permanent miswiring at the level of motor neuron to muscle synaptic partnerships.

5.3 Results: Misexpressing Notch∧intra in the NB3-1 lineage permanently transforms the NotchOFF RP1,4,3,5 motor neuron fates to NotchON sib.

Unlike the NB7-1 lineage where the motor neurons are NotchON and the sibs are NotchOFF, the NB3-1 lineage RP motor neurons are NotchOFF and the sibs are NotchOFF (Tran and Doe, 2008)[70]. There is evidence that the RP5 sib is a small undifferentiated neuron (Meng light microscopy data, L1 larva CNS EM volume). While we did not take any images, Yaa and I looked at L3 bodywall data of NB3-1>Notch∧intra animals. Immediately we noticed near total loss of innervation onto RP muscle targets. In the future, repeating this experiment could be helpful in a number of contexts. It could be used to study compensation mechanisms in the periphery or to study the fate transformation of the NB3-1 RP sib fates or finally to explore sibling dependent migration (see Future Projects portion in this chapter).

5.4 Results: Misexpressing Numb using the NB7-1 driver does not transform the NotchON to the NotchOFF hemilineage

Naturally after misexpressing Notch∧intra, we wanted to understand the fate transformation upon loss of Notch. The most ideal experiment is to directly knock down Notch in an NB7-1 specific manner. Therefore, Yaa and I screened through a collection of Notch RNAi lines with the following Bloomington identifiers: 33616, 33611, 31383, 27988, 35640, 35213, 31180, and 33621. Unfortunately none of these RNAi lines worked. In brief, our screening approach involved Yaa setting up small crosses between each RNAi line and our NB7-1 driver line. Next, I dissected 5 L3 larvae of each cross taking care to pull their CNS and affix them to a poly-d-lysine coated coverslip. I stained for Eve. As I was imaging, I scrolled through the nerve cord and observed the 'U' shape made up of 5 Eve+ neurons in each hemisegment. I also checked the bodywall segments and observed wildtype-like synaptic branch counts onto dorsal muscles normally innervated by U motor neurons. These results didn't surprise me because I have never been able to successfully drive an RNAi line with the NB7-1 driver. I attribute this to the fact that I know that the NB7-1 driver first turns on during the first neuroblast division. Even if we assume RNAi is first expressed during the first division, it is unclear how much is inherited by the GMC and how fast the RNAi probe associates with and degrades Notch mRNA. RNAi is especially notoriously unreliable when dealing with brief developmental time periods and I recommend against relying on it to work effectively. As a backup I had requested the following lines: UAS-numb and UAS-numb-GFP from the Bingwei Lu's lab (these lines are not available on Bloomington). I hoped that by misexpressing Numb, the inhibitor of Notch signaling activity, I could transform the NotchON siblings to NotchOFF as previously demonstrated (Spana et al., 1995)[179]. Unfortunately this strategy did not work (Figure 5.5).

Despite numb-GFP expression in the NB7-1 lineage, I consistently found 5 Eve+ neurons often co-expressing GFP+ and small Dbx+ GFP+ neurons adjacent to the Eve+ neu-

rons (Figure Figure 5.5C). This means despite ectopic Numb expression, the NotchON and NotchOFF hemilineages remain intact in the NB7-1 lineage. We could speculate that the levels of ectopic numb compared to the levels of endogenous Notch expression is key or perhaps there is another factor acting in parallel to numb required to inhibit Notch activity in NotchOFF siblings.

5.5 Discussion: Does numb exclusively inhibit Notch signaling in the context of sibling fate specification?

Revisiting Spana et al., a section of their paper is entitled "numb does not affect all sibling neuron fates" (Spana et al., 1995)[179]. They find that loss of numb expression (numb1 mutants) does not alter NB4-2's RP2/RP2 sib and NB1-1's aCC/pCC molecular markers. In a subsequent study from the Doe lab, they offer a slightly revised report that in the numb (numb1 or numb2) mutants that the U/Usib and RP2/RP2sib display partial

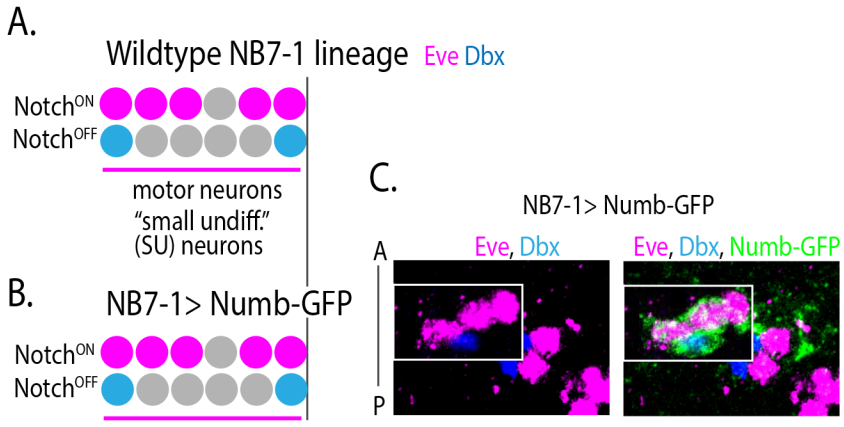


Figure 5.5: Numb-GFP misexpression in NB7-1 has no impact on molecular marker expression in late-stage embryos. (**A-B**) Illustrations depict neuronal progeny from NB7-1's first six divisions represented as circles. Colored circles correspond to expression of similarly colored molecular markers (magenta = Eve, blue = Dbx). NB7-1>Numb-GFP increases the number of Eve+ pMad+ motor neurons at the expense of Dbx+ neurons. (**C**) Image of molecular markers and Numb-GFP in cell bodies of neurons in a single hemisegment of a late stage embryo. While not quantified here, every hemisegment scored, had 5 Eve+ cell bodies and adjacent Dbx+ small cell bodies.

penetrant transformations of the NotchOFF to the NotchON lineages (Skeath and Doe, 1998)[71]. They speculate this is due to persistent maternal Numb protein. In summary ectopic numb is likely only sufficient to convert MP2's NotchON progeny to the NotchOFF sibling's fate. Loss of numb in neuroblasts has no impact on NB1-1's aCC/pCC fates and variably impact on NB4-2 and NB7-1's MN/sib fates. I think these results complicate the simplistic picture painted by the field that Numb inhibits Notch signaling during neuronal cell fate specification immediately after the GMC terminally divides. While Skeath and Doe's speculation that maternally inherited numb in the developing nerve cord complicates the numb mutant phenotypes the Doe lab in Spana et al, argue that the numb mutant phenotypes is likely not a result of maternal numb protein because they cannot detect maternal numb beginning stage 8 (data unpublished), which is just prior to nerve cord development. I want to believe Spana et al's unpublished data is accurate because I favor another explanation not previously raised, which is that notch activity can be restricted to one sibling in a numb-independent manner. Altogether, this is an area of research where more work is needed.

5.6 Notch/Numb pathway is involved in NB3-3 lineage development

One more note relevant to the Heckscher lab regarding the NB3-3 lineage is that in numb mutants there is a consistent decrease in the number of Eve+ EL neurons from 10 to about 4 in each abdominal hemisegment (Spana et al., 1995; Skeath and Doe, 1998)[179, 71]. This is interesting considering that the NB3-3 lineage swiftly transitions from type I to type 0 division mode after the first division. Is numb acting lineage autonomously? If so, when is numb acting? What is the molecular identity/morphological fate of the 4 neurons generated? I think this is a story worth exploring. This finding is vaguely reminiscent of another Doe paper focused on Notch/Numb signaling in the NB7-3 lineage (Karcavich and Doe, 2005)[188]. Here the NotchON siblings of the second and third division die so it

makes sense in the numb mutant background that largely only the neurons from the first division persist. Future Directions: strategies to knockdown Notch in the NB7-1 lineage As another potential strategy to knockdown Notch, I had ordered a line from Vienna (#341922) containing two short guide RNAs targeted against two unique sequences within the notch coding region (Port et al., 2020)[189]. After months, I believe we finally received the line but I think it has since died in a pre-quarantine stage on Chris Wreden's bench. While I totally dropped the ball, this strategy comes with its own complications. Let me explain. While the sgRNAs are expressed ubiquitously, when combined with UAS-Cas9 can mediate site-specific cleavage of DNA complementary to the sgRNA, thus effectively creating a tissue-specific mutagenesis of a gene of interest. For this strategy to work, we need to combine the following into the sgRNA (on II) background: UAS-Cas9 (on II) (also toxic so there is a newer version Port et al recommends using and can be found at Bloomington, we do not have it in our lab stocks), UAS-myrGFP (on III) (need this because we do not have a great marker for the U sibs considering only several express Dbx throughout late embryonic stages), and NB7-1-Gal4 (on II). To obtain this fly, recombination is required and before that Cas9 related toxicity issues should be explored. Furthermore even after months of building the necessary lines, ideally we would want to obtain single cell clones using MCFO. I think before this genetic task is undertaken, it would be more straightforward to repeat the notch mutant experiments from the past by requesting notch mutant (on X) lines from the Fehon lab and in the mutant background express NB7-1>myrGFP to visualize the sibs.

5.7 Results: Misexpressing Notch∧intra in NB7-1 causes Eve+ U motor neuron cell bodies to be abnormally clustered and positioned abnormally medially

The NB7-1 'U' motor neurons collectively form their namesake stereotypical 'U' shape pointing anterior (Figure 6B-E).

The 'U' shape extends from the midline to the medial border of the Eve+ EL interneurons (Figure 5.6J). When Notch∧intra is misexpressed specifically in the NB7-1 lineage this 'U' shape collapses into a medially positioned cluster (Figure 5.6A,K). While this phenotype was striking enough to visually identify, I further quantified the medial collapse using FasII to visualize landmark tracks within the neuropil of late stage embryos (E16) (Figure 5.6F-G). Notably, there is no significance in the thickness of the FasII+ region in NB7-1>Notch∧intra E16 animals compared to control (Figure 5.6I). Any Eve+ cell body that lay entirely outside of the fasII labeled regions either laterally or medially of the fasII labeled regions I categorized as 'lateral' and 'medial', respectively (Figure 5.6F-H). Any Eve+ cell body that lay fully or partially within the fasII labeled regions were labeled as 'In FasII+ region' (Figure 5.6F-H). Using this scoring strategy in control E16 animals, on average, I found one 'medial', two 'In FasII+ region', and two 'lateral' Eve+ cell bodies (Figure 5.6G-H). To better compare the averages between control and experimental, NB7-1>Notch∧intra, I created a hypothetical control which contains ten total Eve+ neurons termed 'If Control 2x' (Figure 5.6H). I simply added plus one to each value in the control column. My rationale was this hypothetical control assumed the ten total Eve+ had a distribution along the medial-lateral axis that reflects the observed control. Ideally, I would repeat this scoring analysis in the hemisegments containing 10 Eve+ neurons when ectopic Hunchback expression is prolonged in the NB7-1. However, by eye, there is no striking medial shift in NB7-1>Hb E16 animals (Figure 5.6D). In NB7-1>Notch∧intra E16 animals I find on average 3.4 'medial', 3.8 'In FasII+ region', 1.7

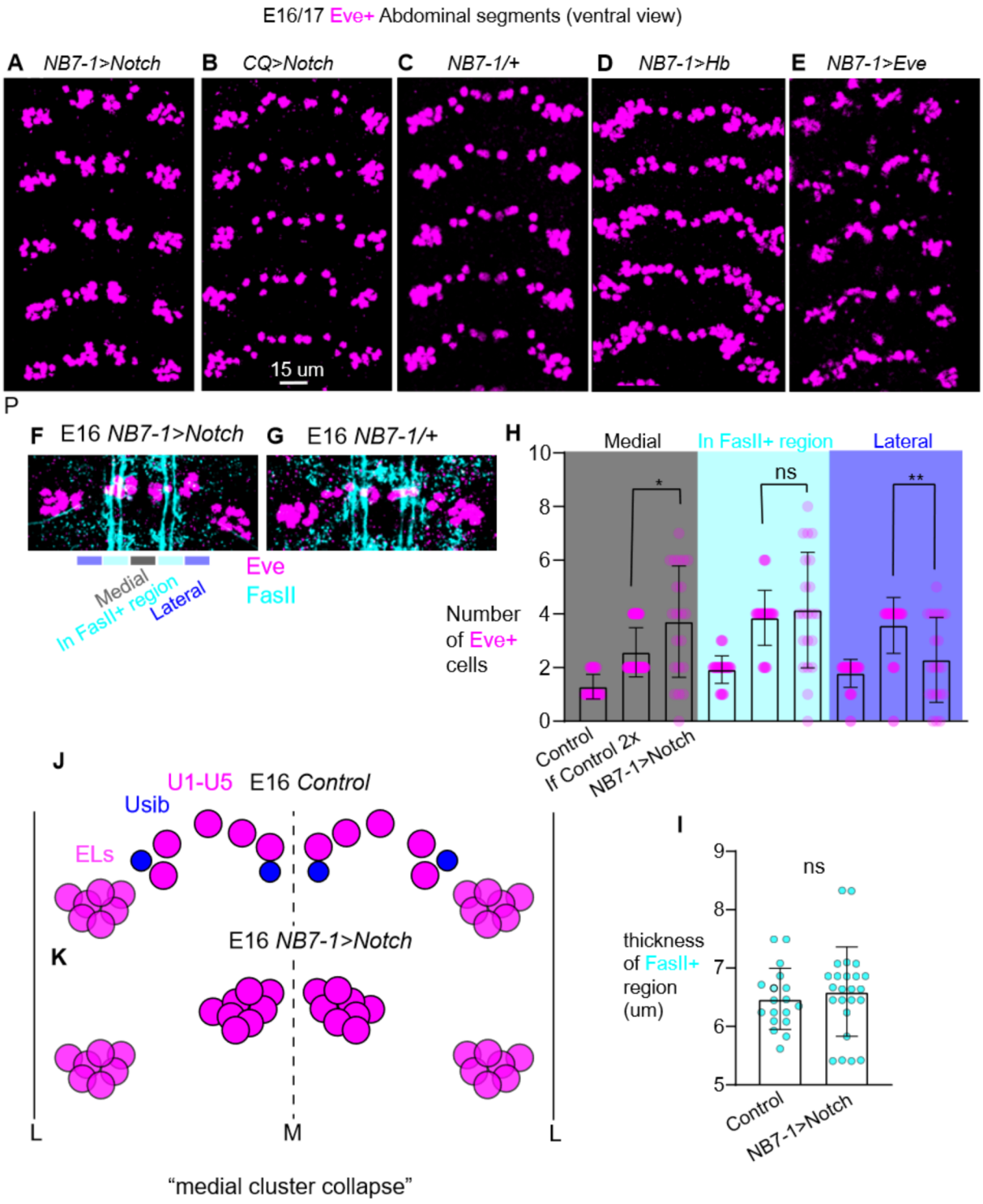


Figure 5.6: Notch∧intra misexpression in NB7-1 impacts Eve+ U motor neuron cell body position along the medial-lateral axis. *Continued*

Figure 5.6: *Cont'd.* Notch∧intra misexpression in NB7-1 impacts Eve+ U motor neuron cell body position along the medial-lateral axis. (**A-E**) Images of Eve expression throughout five abdominal segments in late-stage embryos in a variety of backgrounds. Only when Notch∧intra is misexpressed are the Eve+ cell bodies consistently clustered around the midline. All images are anterior up. (**F-G**) Images of Eve and overlaid FasII expression. Any Eve+ cell body that overlaps with FasII expression is considered to be within the FasII region. Eve+ cell bodies that lie more medial than the FasII expression region are considered to be medial. Eve+ cell bodies that lie more lateral than the FasII expression region are considered to be lateral. (**H**) Quantification of data in (F-G). The second column 'if Control 2x' is hypothetical data where the scores in Control are simply doubled. A more accurate way to do this is to score the position of Eve+ cell bodies when there are 10 Eve+ neurons as a result of Hb misexpression. The one caveat with this proposed approach is that it is not a wild-type background. However, there is no reason to believe that Hb misexpression causes Eve+ motor neurons to cluster near the midline (see D). (**I**) Quantification of the thickness of the FasII region. Each dot represents the number of branches onto a single muscle. For quantifications, average and standard deviation are overlaid. Un-paired t-test with Welch's correction for unmatched standard deviations (see source datasheet for details). 'ns' not significant. Misexpressing Notch∧intra in NB7-1 does not impact FasII expression patterns within the nerve cord of late-stage embryos. (**J**) Illustration of the phenotype I am calling "medial cluster collapse".

'lateral' Eve+ cell bodies (Figure 5.6G,H). Compared to the hypothetical control where the distribution observed remains consistent despite the number of Eve+ neurons double from five to 10, there is a slightly significant increase in the number of 'medial' Eve+ neurons, no change in the number of 'In FasII+ region' Eve+ neurons, and a significant decrease in the number of 'lateral' Eve+ neurons (Figure 5.6H). Combined, these data reveal a quantifiable collapse of the Eve+ neurons into a medial cluster when Notch∧intra is misexpressed by the NB7-1 driver.

Previous studies have manipulated Notch signaling using loss of function mutants and scored Eve+ cell bodies in embryos (Buescher et al., 1998; Skeath and Doe, 1998; O'Connor-Giles and Skeath, 2003)[180, 71, 176]. Therefore, I wanted to know if the position defect I observed in my data is obvious in old data and if anyone had noticed the phenotype in the past. First, the 'medial cluster collapse' is noticeable in published figures (see O'Connor-Giles and Skeath[176], 2003 Figure 1; Skeath and Doe, 1998[71] Figure 2; Buescher et al., 1998[180]

Figure 6 and 7) yet no comments were made. I think a major reason the phenotype went unnoticed is that either Notch∧intra was panneuronally expressed or numb loss of function mutants affecting the whole animal were used. These manipulations affected most if not all neuroblast lineages, which severely impacted development of the nerve cord. For example, misexpressing Notch∧intra panneuronally or using a numb mutant leads to near complete loss of the Eve+ EL interneurons. Loss of these interneurons leads to loss of a valuable landmark, which made the 'medial cluster collapse' visually striking. This is the first time where Notch is manipulated in a lineage specific way and Eve+ neurons were scored. This experiment revealed that mispositioning of the Eve+ U motor neurons is dependent on Notch manipulation within the NB7-1 lineage.

As this work currently stands, the biological relevance of this 'medial cluster collapse' of the Eve+ U motor neurons is unknown. We have compelling evidence that this cell body positional phenotype does not impact motor axon morphology (Figure 5.3, 5.4). However it is possible that the motor dendrite morphology or dendritic synaptic partnerships may be affected. However, from our previous work characterizing dendrite morphologies of single cell clones in NB7-1>Hb, we found that Hb+ Eve+ motor neurons whose cell bodies were abnormally lateral from midline still had a dendrite morphology characteristic of wildtype Hb+ Eve+ U motor neurons (Meng et al., 2019)[2]. This finding argues against position along the medial-lateral axis as an important factor specifying dendrite morphology fate for Eve+ neurons. However, one distinct feature of the 'medial cluster collapse' is the aggregation of Eve+ U motor neurons. They form a cluster of Eve+ cells reminiscent of the Eve+ ELs. Perhaps their close proximity impacts dendrite specification. Future experiments to obtain single cell clones in NB7-1>Notch∧intra L1 nerve cords will need to be done to determine if dendritic morphologies are impacted.

5.8 Future Directions: Could NB7-1's U motor neurons be a model system to study mechanisms underlying cell migration?

5.8.1 Introduction

Within the developing nervous system, the importance of cell motility is on full display. Neural cell bodies can migrate from their place of birth and neural cells send projections that must navigate their environments as these neurite projections extend. In insects, particularly Drosophila, much work has gone in the latter form of migration at the level of neuronal compartments such as the axon (Santiago and Bashaw, 2014)[190]. While migration at the level of cell bodies has been studied within Drosophila, it is often done in the context of glia and particularly peripheral nervous system glia (Edenfeld et al., 2007)[191]. This highlights a preference to study migration in cells that move over long distances. However, cell migration can occur over short distances. Migration over short distances is inevitable in small compact central nervous system regions such as the developing Drosophila larva nerve cord. A prevailing concept we have cited in the past is that there is minimal migration of neurons from their place of birth within the developing Drosophila larval nerve cord (Schmid et al., 1999; Crew, 2019)[45, 168]. Minimal migration means that the position of neuronal cell bodies in the nerve cord is largely dictated by birth order. Neuroblasts tend to delaminate from the epithelium relatively medially in the nerve cord and as they divide are pushed laterally by the trail of newly born neural progeny. This use of force implies that the minimal movement of neuron cell bodies in the developing nerve cord is not because of cell motility mechanisms and thus this minimal movement is not thought to be a result of migration.

Despite an underwhelming body of literature on the topic of neuronal migration within the nerve cord, there is evidence to suggest that migration sometimes occurs. The earliest

evidence of migration within the developing nerve cord comes from work done in grasshoppers (Kuwada and Goodman, 1985)[192]. The authors used live imaging to track the aCC/pCC sibling pair. They found aCC/pCC born in a thoracic segment migrate anteriorly into the next segment to assume their final stereotyped position with aCC residing adjacent but anterior to pCC (Kuwada and Goodman, 1985)[192]. They found that one cell is trailing the other during the process of migration and speculated that the leader may be aCC but they were unable to determine its identity. While aCC/pCC are conserved in Drosophila, it is currently unknown if these cells migrate along the anterior-posterior axis or if migration is dependent on nerve cord region (thorax vs abdominal). A subsequent tour de force study out of the Doe lab characterized nearly all of the larva nerve cord neuroblast lineages and noted cell migration in a number of lineages, however NB1-1, which gives rise to aCC/pCC is not among them (Schmid et al., 1999)[45]. The lineages where the authors observe that consistently one or two neurons migrate medially away from the rest of the lineage clone are: 1-2, 2-2, 2-4, 2-5, 3-4/4-4, 4-2, 5-2, 5-3, 5-5, 6-2, and 7-1. Beyond the Schmid et al study, migration of these neurons have not been explored except for one paper where the author makes a number of claims that are variably supported by their presented data (Moorthi Bhat, 2007)[193]. Here, I will outline what I believe are the most tantalizing insights from this paper.

5.8.2 First, I think there may be some general migration patterns of early born neurons, most of which are motor neurons

While the cell body position of RP2/sib was the main focus of the paper, Moorthi Bhat stained with Eve to visualize Eve+ RP2 and the sib, which transiently is Eve+. Because Eve is used, Moorthi Bhat offers some unpublished insight into other Eve+ migration patterns.They note that the first step of migration involves medial migration of the GMC-1 as it divides to generate RP2 and the sib. Since aCC/pCC are on the same dorsal-ventral axis

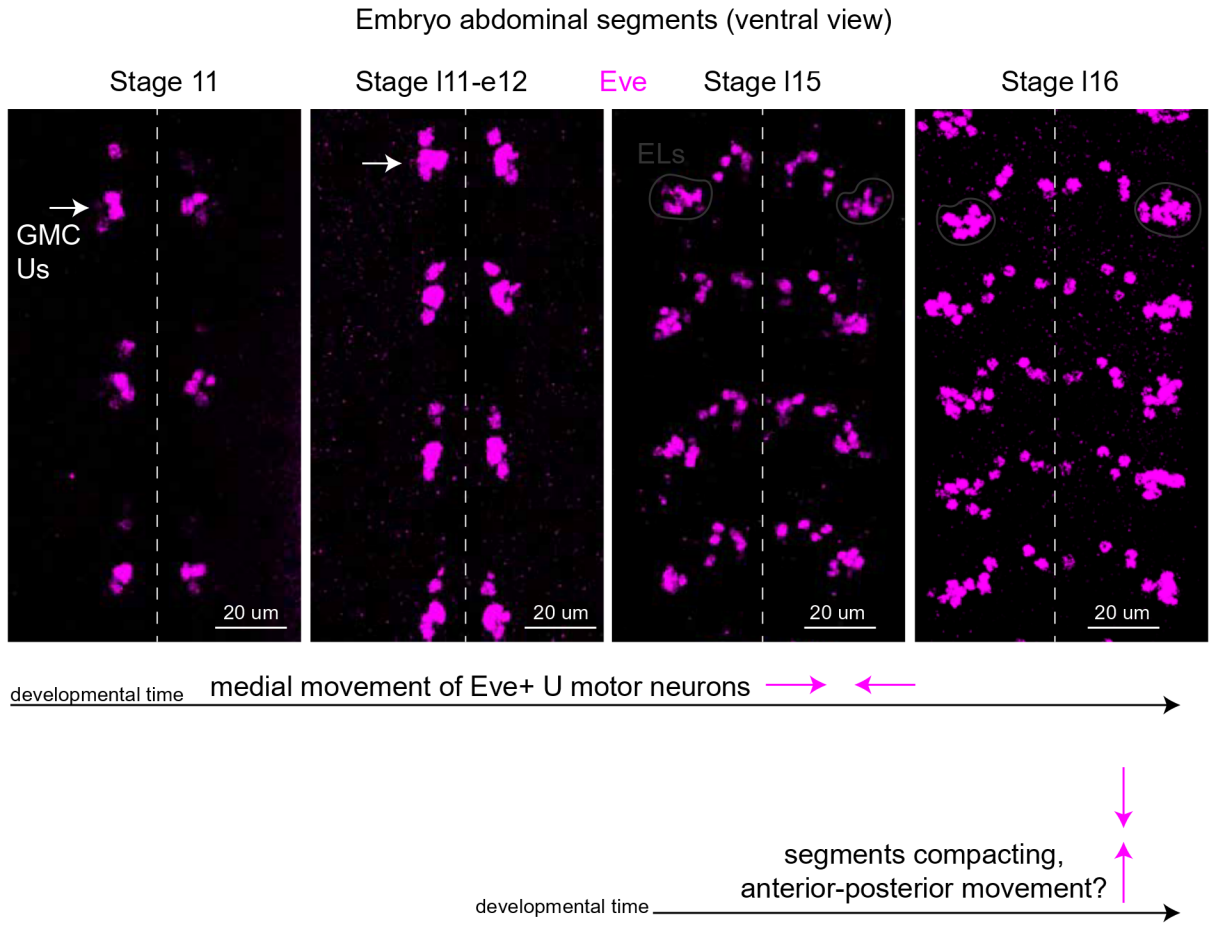


Figure 5.7: Possible Eve+ U motor neuron migration pattern during embryogenesis. Images of Eve expression throughout several abdominal segments in embryos at different developmental stages. Over time, Eve+ cell bodies from neighboring abdominal segments compact (compare stage 11 with stage 16) and Eve+ cell bodies within a single segment move closer to the midline.

plane as RP2, they say they find aCC/pCC also migrate medially (stage 11 or 8 hours post fertilization). These results are consistent with the medial migration previously observed (Schmid et al., 1999)[45]. I also notice that the Eve+ U motor neurons at earlier embryonic stages are more lateral than in later stages (Figure 7). This initial medial migration may be highly conserved and likely involves the GMC. Note the larger cell body sizes in stage 11 embryos, these likely represent GMCs (Figure 5.7). Future live imaging studies will be better able to characterize the Eve+ cell body positioning pattern over time.

Another observation Moorthi Bhat made was that the second step in the RP2/sib migration involves moving posteriorly. They also note, albeit unpublished, that they observe the CQ (aka U) motor neurons undergo a posterior-lateral migration. I find this interesting because Kuwada and Goodman back in 1985 observed aCC/pCC also undergo a posterior migration. While several embryonic stages are missing from Figure 5.7, it is unclear if there is posterior-lateral migration. However, I can clearly see anterior-posterior compaction at the level of whole abdominal segments (Figure 5.7). Comparing Eve+ U motor neuron position along the anterior-posterior axis there is a noticeable compaction of whole segments that occurs between embryonic stage 11 and 16 (Figure 5.7). Undoubtedly some of this compaction occurs during the segmentation shortening along the anterior-posterior axis of the developing embryo as it undergoes germ band contraction, which occurs from stage 11 until 13. Interestingly, even between stage 15 and 16 segments within the nerve cord may continue to experience some compaction (Figure 5.7). Combined, these data suggest that the earliest born neurons from at least three neuroblast lineages migrate posteriorly and likely occur after an initial medial migration by either the postmitotic neurons themselves or their GMC precursors.

Second, I think there may be some support for sibling-dependent migration.

Before I present Moorthi Bhat's arguments/findings I want to state that I think the sib of RP2 is a small undifferentiated neuron. We know from previous studies and Moorthi Bhat's that the RP2 sib cell bodies are much smaller than RP2 (Schmid et al., 1999; CQD's lab website)[45]. During sibs transient window of Eve expression, the sib and RP2 cell bodies are very close, often so close that Moorthi Bhat finds that the sib's cell body is obscured by the Eve+ RP2 cell body.

One of the arguments that Moorthi Bhat makes is that RP2's sib may be dependent on the migration of RP2 because they mutate genes that are only expressed at noticeable levels in RP2 and not the sib, yet migration defects are observed in both RP2 and the sib. Looking

at the figures, I can't tell what the migration defects are in the sib especially considering we can no longer see the sib after stage 13, which coincides with the transition between step 2 (migrate posterior) and step 3 (migrate anteriorly). In Figure 7I-J of Moorthi Bhat, 2007 there are arrows pointing to a cell body referred to as the sib at 12.5 and 14 hrs. The 'sib' is barely expressing Eve compared to RP2 and is more anterior then it previously was but the cell body is unexpectedly much further from the RP2 cell body. I say unexpected because small undifferentiated neurons are characteristically directly adjacent to its motor neuron sibling's cell body. Without a clear lineage marker or live imaging, I am hesitant to take Moorthi Bhat's word that this 'sib' at these later stages are indeed RP2 sibs. Note, in the 1st instar CNS volume, I cannot find a small undifferentiated sibling adjacent to RP2. The last place we indisputably see Eve+ sibs adjacent to the large Eve+ RP2 cell body is when these cells have migrated posteriorly and are positioned above aCC/pCC in the neighboring posterior segment. So it is possible that after transient Eve expression, the posteriorly positioned sib dies and then RP2 migrates anteriorly alone. In the mutant embryos, the most striking migration defect Moorthi Bhat notes is that RP2 is positioned posterior at developmental time points when RP2 is in its final anterior position in wildtype embryos. This suggests that only the final migration step (posterior to anterior) is impacted in the mutants. If the sib and RP2 migrate anteriorly together in the final migration step, then it is possible based on Moorthi Bhat's RP2 specific manipulations that the sib's migration is dependent on RP2.

Let's take a step back and compare and contrast these findings to my observations of Eve+ cell body position defects in NB7-1>Notch∧intra late stage embryos. I will remind the reader that normally the Eve+ U motor neurons form a 'U' shape pointed anteriorly and span the entire medial-lateral axis lying between the medial midline and the lateral cluster of Eve+ EL interneurons from the NB3-3 lineage (Figure 6J). In late stage embryos several of the small undifferentiated sibling neurons are Dbx+ and can be identified directly adjacent

to their U motor neuron counterparts. The U motor neurons are NotchON while the Usibs are NotchOFF. When I misexpress Notch∧intra specifically in the NB7-1 lineage I effectively convert the fate of the Usibs to the U motor neurons. I find that this manipulation also leads to an abnormally (quantifiable) medial position of the Eve+ U motor neuron cell bodies, which I have been calling a "medial cluster collapse" (Figure 6K). Considering Moorthi Bhat's work, it is clear that some GMCs from the earliest divisions of neuroblasts in the most medial column (i.e. NB1-1's aCC/pCC GMC) still undergo medial migration, it is possible that the GMCs that give rise to the U motor neurons first migrate medial before a second migratory step where the U motor neurons then migrate posterior-lateral (a migration step noted by Moorthi Bhat). So perhaps what I'm calling a "medial cluster collapse" may represent the first step of migration, something that could be determined by live imaging and/or a detailed time series of fixed tissue. If the U motor neurons are now stuck at the first migration step and if migration of one sibling can be dependent on the other, this would suggest that the second migration step of the U motor neurons is dependent on the Usibs. It is tempting to speculate that perhaps a role for small undifferentiated neurons is to aid their motor neuron sibling's final migration step.

Consistently, the most striking migration defect in Moorthi Bhat's paper is essentially RP2's migration journey arrested in the penultimate step (Figure 5.8A). If the RP2sib is required for RP's last step in migration we would expect that if we transform the fate of RP2sib into RP then RP should be stuck in a posterior position directly above the neighboring posterior segment's aCC/pCC. Since RP2 is NotchOFF and RP2sib is NotchON having a Notch or Notch dependent factor mutant background can transform the NotchON lineage to NotchOFF. Fortunately, these manipulations have already been done (Skeath and Doe, 1998)[71]. When RP2sib molecular identity (Eve-Zfh1-) NotchON is transformed to RP2 NotchOFF identity (Eve+ Zfh1+) by removal of Notch signaling by spodo or mam mutant, the anterior positioning of the RP2 cell bodies appears wildtype (Figure 5.7B-D).

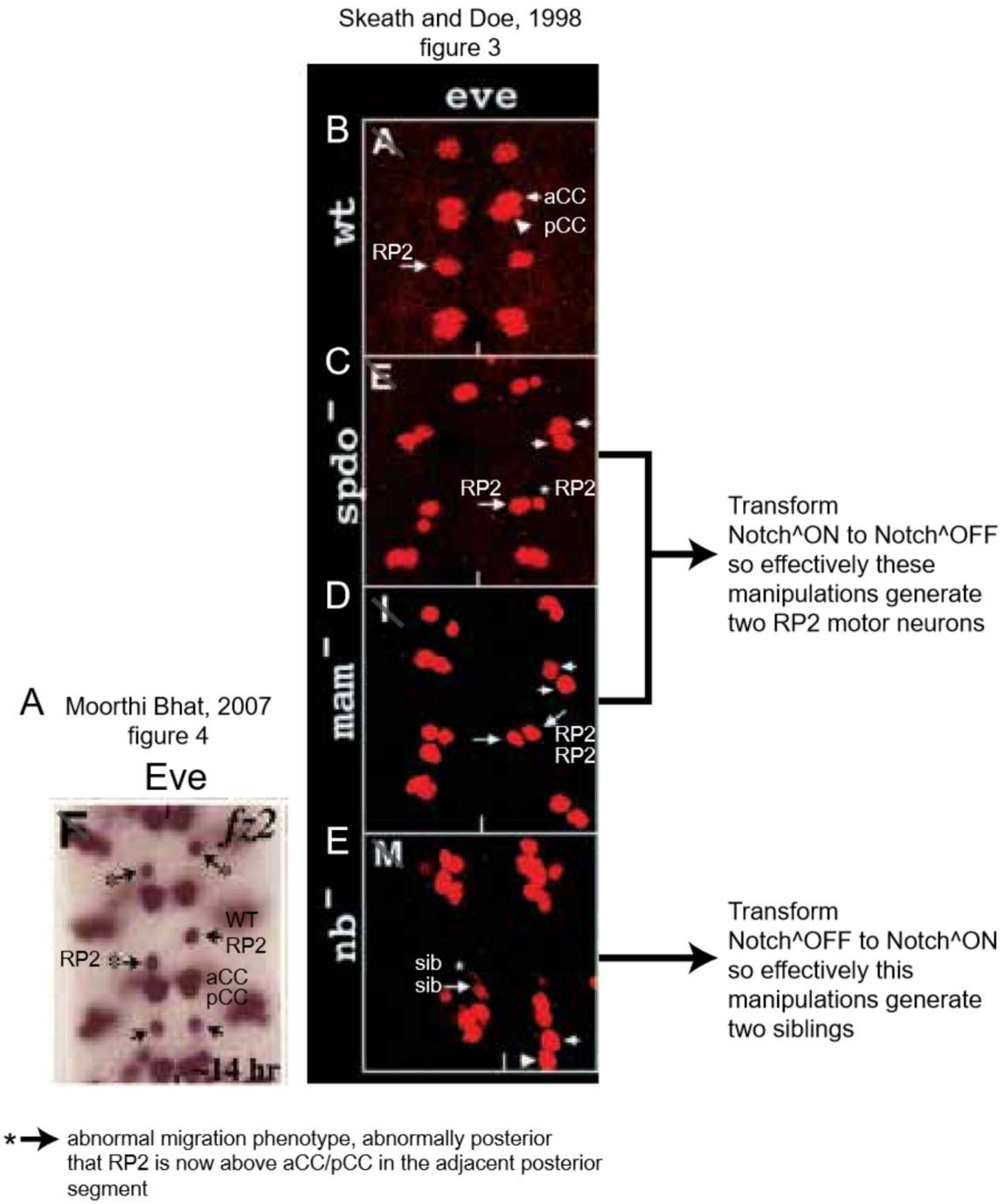


Figure 5.8: Previously published data suggesting that NotchOFF siblings may influence the migration of the NotchON sibling. In panel C and D, when NotchON hemilineage is transformed to NotchOFF, cell body migration of both NotchOFF Eve+ RP2s appear normal (compare C and D to B). When the opposite manipulation is done, and both cells are NotchON RP2 sibling, position of cell bodies is abnormal (compare C to E) and resembles migration defect observed by Moorthi Bhat (see panel A).

These data reveal that RP2 migration is not dependent on the RP2sib identity. Strikingly when NotchOFF is transformed to NotchON and now there are two small weakly Eve+, presumably both RP2sibs, their cell bodies are positioned posteriorly (Figure 5.7B,E). This suggests that either 1) the RP2sib migration is normal because this is the final position of the RP2sib fate and it never migrates anteriorly or 2) RP2sib's normal anterior migration is impaired when RP2 identity is lost and thus the sibs migration is dependent on RP2 migration (this latter model was put forth by Moorthi Bhat). Let's assume the latter is true based on the general observation that small undifferentiated siblings remain associated with each other throughout development. If we combine this observation with my data this suggests that in at least two lineages, the NotchOFF sibling, regardless of neuron type (motor neuron vs small undifferentiated neuron) controls the migration of the NotchON sibling. This model suggests that the underlying mechanisms of migration involve Notch signaling features like Notch-ligand (likely Delta) interactions as opposed to involving neuron specific features like being a motor neuron vs a small undifferentiated neuron. However this tidy model where NotchOFF siblings specify the migration of NotchON is complicated by NB1-1's aCC/pCC. When spdo or mam are mutated causing NotchON to transform to NotchOFF, essentially two aCCs based on molecular identity (aCC is Eve+ Zfh1+ 22C10+ and pCC is Eve+ Zfh1- 22C10-), the two cell bodies are strikingly lateral (Figure 5.7B-D). This suggests that aCC's medial migration may be dependent on pCC's fate. It's also worth noting that the ability for neurons to migrate in the nerve cord is likely restricted to the earliest born neurons of a lineage despite NotchOFF/NotchON siblings being generated much later in development, so there are likely time-linked intrinsic or extrinsic cues underlying regulation for medial-migration. So perhaps a more accurate model is that the underlying mechanisms of posterior/lateral-migration involve Notch signaling features like Notch-ligand (likely Delta) interactions as opposed to involving neuron specific features like being a motor neuron vs a small undifferentiated neuron.

While I can't offer a tidy model based on the currently available data, I think altogether the evidence suggests that cell migration of one of the siblings is very likely dependent on the other and the relationship depends on NotchON NotchOFF status. The extent to which this is the case and the underlying Notch-related mechanisms await future discovery.

5.8.3 Third, I think it is worthwhile to explore the extent to which circuit wiring decisions rely on proper cell body migration in the developing nerve cord

Studying the mechanisms underlying migration is a fundamental cell and developmental biological question because cell migration is paramount for assembly of complex multicellular structures at the level of tissues, organs, and whole animals. When cell migration is defective the consequences are often dire. In the Heckscher lab we care about understanding the underlying logic of circuit assembly in the developing Drosophila larval motor system housed in the nerve cord. We care about exploring mechanisms that explain circuit wiring decisions. So when it comes to impaired migration or more simply, the position of cell bodies, we want to know if there is a relationship between this cell body positional defect and synaptic partnership decisions. The classic view is that migration defects or abnormal cell body position impairs connectivity in the nervous system. Moorthi Bhat presents data to support the claim that the observed migration defects in RP2 impact neurite outgrowth decisions, however since Futsch/22C10 antibody is used to visualize RP2 neurites in a non-specific manner, I think it is difficult to draw any major conclusions about outgrowth defects and these experiments cannot tell us anything about the state of the final permanent synaptic partnerships formed by RP2 neurons whose cell bodies are misplaced. We know from our own work described earlier in this chapter on Cardinal Transcription Factors that defects in outgrowth during embryonic stages can be corrected. Past work studying the role Notch signaling plays in motor axon guidance found that loss of Notch on motor neurons or the

Delta ligand on trachea stalled nerve outgrowth but this stalling was eventually resolved and motor neurons go on to innervate muscles (Crowner et al., 2003; Giniger et al., 1993; Giniger, 1998)[194, 195, 196]. My work here supports the idea that mispositioning of Eve+ motor neurons does not perturb permanent motor neuron to muscle synaptic partnerships. When we misexpress Notch∧intra specifically in NB7-1, we find motor neuron to muscle innervation patterns consistent with all Eve+ motor neurons forming synaptic partnerships onto appropriate muscle targets (Figure 5.3). However, all of these examples are in the peripheral nervous system and not the central nervous system. Elegant work done by the Zlatic lab found that repositioning of sensory neuron dendrites in the nerve cord using Robo based manipulations led to aberrant number of synaptic partnerships formed between these sensory neurons and downstream post sensory interneurons and these wiring errors led to behavioral defects (Valdes-Aleman et al., 2020)[197]. In my own unpublished work described in the chapter on NB7-1 interneurons, I find evidence that mismatches in interneuron identity and spatial position of the cell body can impair neurite outgrowth. Arguably the most relevant piece of data when considering what consequences mis-positioned Eve+ U motor neurons may have on circuit wiring decisions between U motor neuron dendrites and premotor interneurons in the nerve cord is in my 2019 paper. Here we misexpressed hunchback in NB7-1 and found Eve+ motor neurons with U1/U2-like molecular identities born at abnormally lateral positions in the nerve cord (Meng et al., 2019)[2]. Normally U1 and U2 motor neurons are the medial-most of the U motor neurons and they, unlike the other U motor neurons, have two dendritic regions, one ipsilateral and one contralateral. We found that despite single cell clones whose cell bodies were positioned very laterally, these motor neurons still successfully formed these two dendritic regions. Future work at higher resolution will offer insight into the extent to which synaptic partnerships are aberrant. A wonderful complement to this investigation is exploring what happens to the synaptic partnerships of abnormally medially positioned U motor neurons as in NB7-1>Notch∧intra. Altogether, it is

likely that cell body migration defects are accompanied with permanent alterations to circuit wiring within the nerve cord. The question is to what extent and what are the alterations (e.g. synaptic partner, number of synapses formed, gross dendrite morphology?)

Understanding this question has implications beyond Drosophila because we have evidence to suggest that the 5 Eve+ U motor neuron's positions are remarkably conserved in other fly species such as Magaselia scalaris (coffin fly) (unpublished data, Yiqin Gao Heckscher lab). What is the role of small undifferentiated neurons in the Drosophlia larval nerve cord?

I was first introduced to this question by way of NB7-1's Usibs, which are the NotchOFF siblings of the NotchON U motor neurons (Skeath and Doe, 1998)[71]. These cells are mysterious in a number of ways. First, the Usibs variably express Dbx (Lacin et al., 2009)[198]. The U1, U5 sibs express Dbx at late embryonic stages while U2-U3sibs transiently express Dbx through stage 15, and the U4sib never expresses Dbx. Dbx expression ceases after embryonic stages because I observe no Dbx+ in small cell bodies directly adjacent to U motor neurons in first instar larvae (my unpublished data). All the Usibs express eve briefly after birth (Lacin et al., 2009)[198]. I also know that the Usibs are not glial cells because they do not express repo, the glial marker. We know that when we misexpress Hb in NB7-1, we generate extra Eve+ neurons and Usibs. If the Usibs are glia, we should find nearly a consistent ratio between Eve+ and repo+ cell bodies when we misexpress Hb but we do not (Figure 5.9).

Aside from molecular marker expression, we know that their cell bodies are small and directly adjacent to their large cell bodied motor neuron siblings. Previous work in the field suggested that these type of sibling neurons were not unique to the NB7-1 lineage (Schmid et al., 1999)[45]. There were speculations that these neurons are "axonless" and might play a role in modulating their sibling motor neuron function, however there is no evidence to support this idea (CQD lab website). Once I gained access to the 1st instar CNS volume, I

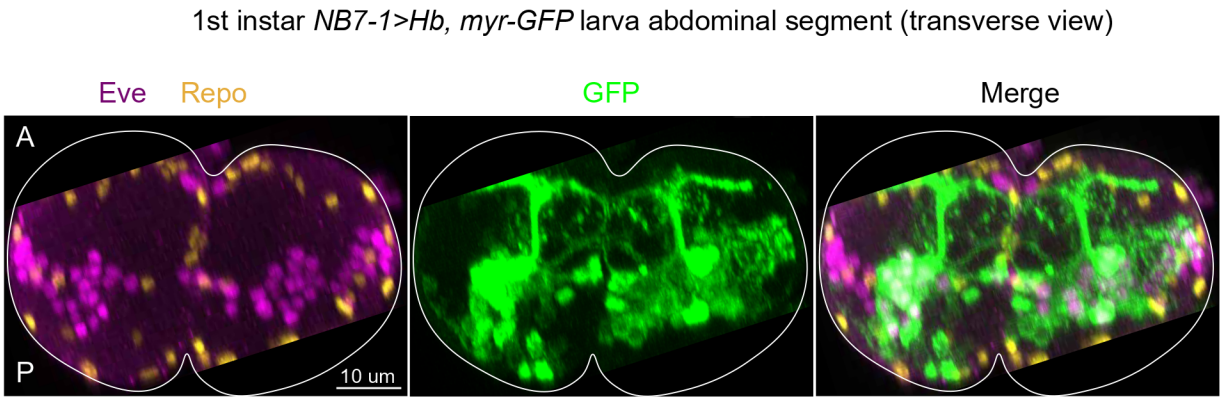


Figure 5.9: Evidence that the Dbx+ sibling neurons of the Eve+ U motor neurons are not Repo+ glial cells. Image of Eve, Repo, and GFP expression in a single abdominal segment within a NB7-1>Hb, myr-GFP 1st instar nerve cord.

wanted to find the Usibs. Like in light microscopy, the sibs are immediately adjacent to the U motor neuron cell bodies. The sibs have a very small cell body, the cell body is darker than U motor neurons suggesting there are more lipid-rich structures containing fatty acids. Within the nucleus are large dark structures, which represents compact heterochromatin. Beyond the cell body these neurons extend neurites but form no chemical synapses containing T-bars. Previously neurons with these features were found in the brain lobes and dubbed "small undifferentiated" (SU) neurons (Andrade et al., 2019)[165]. SU neurons in the Drosophila larval nerve cord have never been formally characterized and there is no published work on them.

To begin characterizing the SU neurons I wanted to know how many SU neurons are there in the A1 segment of the 1st instar larval CNS volume and relatedly where are the SU neurons positioned. First I found 62-66 SU neurons in A1 (Note, I found 66 total but when I apply the A1 volumes, 4 appear to fall directly adjacent to A1 but are in T3. I'm not sure how accurate these segment volumes are) (Figure 5.10A).

To put this value into perspective, each segment is thought to contain 600 neurons (300 each hemisegment), 64 of which are motor neurons (Ohyama et al., 2015)[15]. That means 10% of the neurons in a segment are motor neurons and that same percentage are SU neurons.

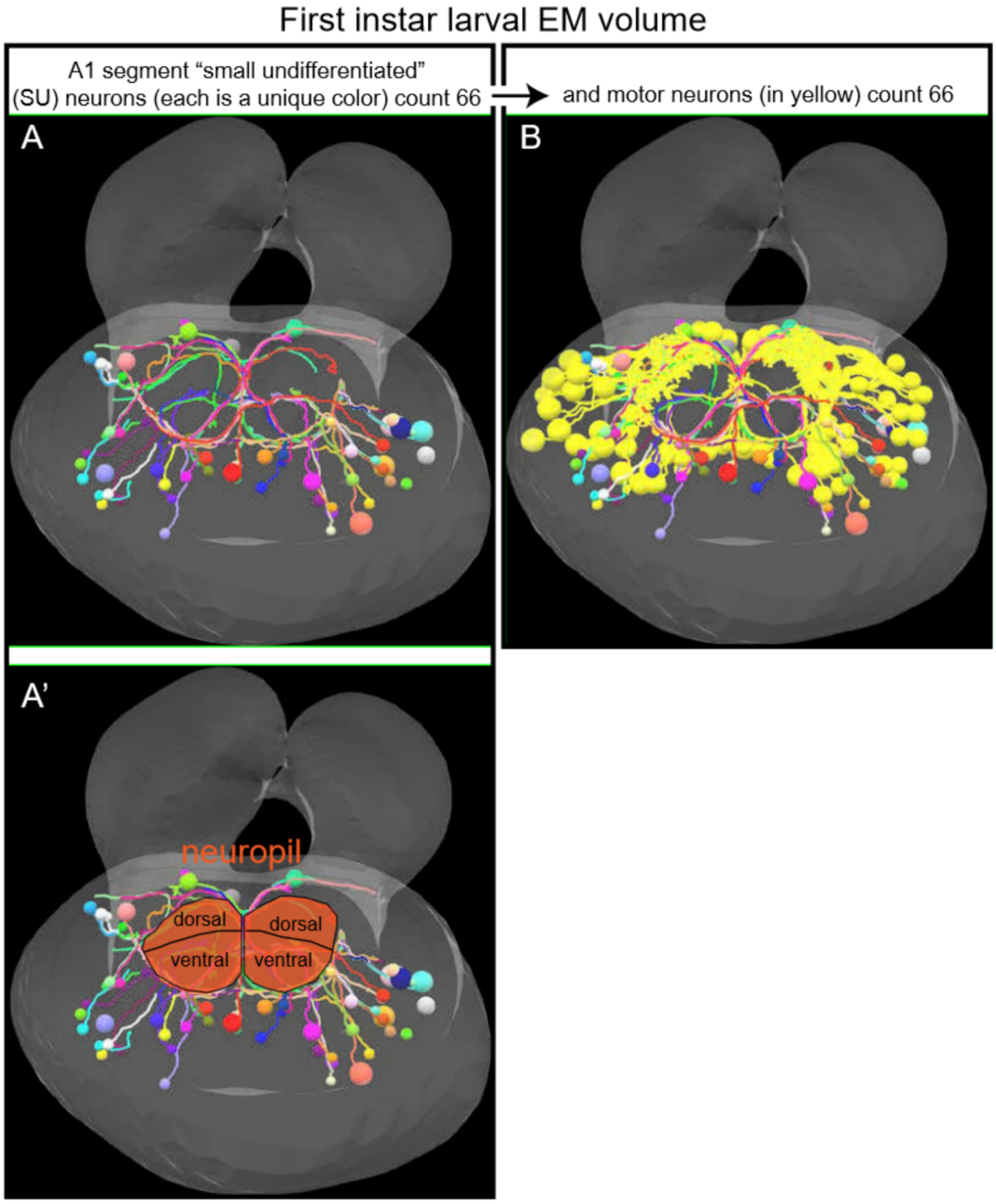


Figure 5.10: Characterization of the position of small undifferentiated neurons in the A1 segment of the 1st instar larval CNS EM volume. (**A-B**) Images of traced/reconstructed neurons in the A1 segment. Notice that the colorized cell bodies of the small undifferentiated neurons are found throughout the dorsal (up) - ventral (down) axis and their cell bodies are positioned throughout the medial-lateral axis spanning the edge of the neuropil to the edge of the nerve cord. Within the neuropil (A') undifferentiated neurons project to both the dorsal and ventral regions of the neuropil.

One attractive hypothesis is that SU are siblings of motor neurons. In opposition of this hypothesis, 1) I cannot find all of the Usibs but on average find one or two per hemisegment, 2) not all motor neuron siblings are SU neurons (e.g. NB1-1's pCC interneuron sibling of aCC motor neuron), and 3) I find one SU neuron nestled among later born NB7-1 interneurons. Consistent with these specific examples, in A1 we find SU cell bodies separate from motor neuron cell bodies (yellow) (Figure 5.10B). Looking at the position of the SU cell bodies they are scattered throughout the nerve cord cortex. Looking at the SU neurites, they project to both the dorsal and ventral regions of the nerve cord (Figure 5.10A-A'). Combined these data suggest that there are no positional preferences of SU cell bodies in the cortex or neurite projection in the neuropil. From these data it is clear that the SU neurons make up a sizable portion of the total number of neurons in the nerve cord as assessed in A1 (note, I find SUs in other segments) so this raises the question, what is their function? While I do not know what their function is, for future reference I will lay out what I do know as well as my favorite hypothesis.

One possibility along the lines of having a speculated role in cell migration, SU neurons may function only early in development. I think while this may be possible sometimes for a large number of SUs (66 SUs) I think this possibility is unlikely for several reasons. First, we know that the midline precursor cells (MPs) generate pioneer neurons that play a role in establishing the developing neuropil tracts but then die (Spana et al., 1995)[179]. Second, consistently, we find no evidence for MP neurons such as the well studied vMP2 and dMP2 in the 1st instar CNS volume (I have searched). Third, we also know that NB7-3 generates a small motor neuron, which innervates ventral muscles during embryonic stages but then dies prior to hatching. If SU neurons play a similar early developmental role then we would expect them to also die by the 1st instar CNS volume but they don't. While I admit that some SU neurons we can identify in embryonic stages I struggle to find in the first instar CNS volume. For example, I find sibs to be associated variably with different U motor

neurons from hemisegment to hemisegment. So perhaps a fraction of the SU neurons only function in the context of development and then die but this is not true for all SU neurons. To definitively characterize what fraction of SUs die or if they die during later larval stages, future experiments assaying cell cell death should be done. We have a cell death assay kit in the -20 freezer (more details to come).

A second possibility that has previously been floated in the field is that SU neurons modulate the function of U motor neurons. This hypothesis was inspired by work done in cockroaches where they found interneurons that possess dendrites but were axonless and seemed to have a role in modulating nearby motor neurons (Pearson and Fourtner, 1975)[199]. I think this possibility is unlikely for several reasons. First, SUs lack both dendrites and axons so I don't think we can compare them to the axonless interneurons observed in cockroaches. Second, SUs are not exclusively associated with motor neurons and SUs do not associate with all motor neurons. Combined, while possible SUs may play a role in modulating activity of neurons that are in close contact with SU cell bodies or neurites, I don't think there is enough evidence to strongly suggest this putative function. A third possibility is that SU neurons eventually emerge from their "undifferentiated" heterochromatin-rich state and are involved in patterning the adult nerve cord. Full disclaimer, this is my favorite hypothesis because I think there is the most support for this possibility and it raises interesting questions regarding implications for decisions made early in development on the adult nerve cord circuitry/function (I'm thinking about our NB7-1>Hb manipulation where we know we generate more U1/2sibs and our NB7-1>Notch$\wedge$intra manipulation where we lose all Usibs). First, I know that the SU neuron morphology does not persist through the L3 stage. Albert Cardona gave me access to the L3 volume encompassing several abdominal segments in the nerve cord (Gerhard et al., 2017)[200]. I quickly identified the U1 and U2 motor neurons based on their position in the nerve cord and the fact that they have bipolar cell bodies. I could not find any SU neurons near the U motor neurons. In fact, I did not observe any

SU-like neuron based on the criteria of a small cell body and condensed chromatin. This suggests that either the SU neurons die by L3 (see first possibility in this discussion section) or SU neurons emerge from their "undifferentiated" state. Second, there was a paper recently published that tracked the fate of SU neurons in the central brain and found that a group of SU neurons form the shape of the precursor fan-shaped body in larvae (Andrade et al., 2019)[165]. These SU neurons differentiate in the late larvae and pupa. They survive to adulthood where they form a class of neurons called Pontine neurons. I think the SU neurons in the nerve cord differentiate in the late larvae stage and are involved in adult Drosophila nerve cord circuitry. The major question is what do they become? To address this question, we need to permanently label SU neurons. Since we know NB7-1 generates several SU neurons we could use the NB7-1 driver to permanently label the lineage. Ideally, we would permanently label using a strategy where single cell clones can be obtained (Lee and Doe, 2021)[201]. Ideally we could drive exclusively in the SU neurons but we do not have a SU specific driver. We also do not have a strategy to convert the NotchON hemilineage to NotchOFF specifically in the NB7-1 lineage. If we did, we could use this alongside the permanent labeling strategy. If we found evidence of motor neurons in the adult nerve cord, this would suggest that the Usibs differentiate into motor neurons. In addition to a role of SU neurons in the adult perhaps some SU neurons can differentiate by 1st instar stages on need-basis. While this idea is wild, it could offer a level of plasticity for embryos based on their developmental conditions or the demands of segments that may vary at different positions along the anterior-posterior axis in different animals. I only entertain this idea as an alternative explanation to some SU neurons dying before hatching. Tracking these neurons would be very difficult because a number of SU neurons barely have neurites so their differentiation potential is great and may not resemble nor fasciculate with their lineages.

Source Data for Figure 5.2E

Molecular markers	Genotype	Number of values	Mean (# of cell bodies at E16/17)	Std. Deviation	Std. Error of Mean	p value
Eve+, pMad+	NB7-1>myr GFP	20	5.000	0.000	0.000	NA
	NB7-1>myr GFP, Notch	68	8.794	1.451	0.1760	<0.0001

Unpaired t-test Welch (for un-equal Std. Deviation)

Source Data for Figure 5.2E'

Molecular markers	Genotype	Number of values	Mean (# of cell bodies at L3)	Std. Deviation	Std. Error of Mean	p value
Eve+, pMad+	NB7-1/+	20	5.00	0.000	0.000	NA
	NB7-1> Notch	40	8.375	1.275	0.2016	<0.0001

Unpaired t-test Welch (for un-equal Std. Deviation)

Source Data for Figure 5.2F

Molecular markers	Genotype	Number of values	Mean (# of cell bodies at E16/17)	Std. Deviation	Std. Error of Mean	p value
Dbx+	NB7-1>myr GFP	28	12.04	1.972	0.3726	NA
	NB7-1>myr GFP, Notch	11	3.182	1.662	0.5012	<0.0001

Unpaired t-test Welch (for un-equal Std. Deviation)

Source Data for Figure 5.2G

Molecular markers	Genotype	Number of values	Mean (# of cell bodies at E16/17)	Std. Deviation	Std. Error of Mean	p value
Cas+	NB7-1>myr GFP	28	13.46	3.144	0.5942	NA
	NB7-1>myr GFP, Notch	11	13.55	4.059	1.224	0.9532

Unpaired t-test Welch (for un-equal Std. Deviation)

Table 5.1: Source Data for Figure 5.2

Source Data for Figure 5.3I-O

Synaptic branch	Genotype	Number of values	Mean (branch #)	Std. Deviation	Std. Error of Mean	p value
Muscle 1-1b	Notch/+	21	2.000	0.6325	0.1380	NA
	NB7-1>Notch	33	2.303	0.5294	0.09216	0.0759
muscle 9-1b	Notch/+	20	2.050	0.5104	0.1141	NA
	NB7-1>Notch	33	3.667	0.6922	0.1205	<0.0001
muscle 2-1b	Notch/+	20	2.050	0.3940	0.08811	NA
	NB7-1>Notch	33	3.424	0.8303	0.1445	<0.0001
muscle 10-1b	Notch/+	20	2.000	0.5620	0.1257	NA
	NB7-1>Notch	33	3.364	0.7833	0.1364	<0.0001
muscle 3-1b	Notch/+	20	1.400	0.5026	0.1124	NA
	NB7-1>Notch	33	2.788	0.8572	0.1492	<0.0001
muscle 4-1b	Notch/+	20	2.250	0.9665	0.2161	NA
	NB7-1>Notch	32	3.469	1.849	0.3268	0.0031
muscle 4-1b	Notch/+	20	2.250	0.9665	0.2161	NA
	NB7-1>Notch 7-8 Eve+	12	3.000	1.537	0.4438	0.1478
	NB7-1>Notch 9-10 Eve+	16	4.125	2.062	0.5154	0.0031

Unpaired t-test, with Welch's correction (for un-equal Std. Deviation)

Table 5.2: Source Data for Figure 5.3

Source Data for Figure 5.4E-F

Synaptic branch	Genotype	Number of values	Mean (branch #)	Std. Deviation	Std. Error of Mean	p value
Muscle 15-1b	Notch/+	17	2.059	0.5557	0.1348	NA
	NB7-1>Notch	18	3.333	0.9075	0.2139	<0.0001
muscle 16-1b	Notch/+	17	1.882	0.8575	0.2080	NA
	NB7-1>Notch	18	2.722	1.227	0.2893	0.0250

Unpaired t-test, with Welch's correction (for un-equal Std. Deviation)

Table 5.3: Source Data for Figure 5.4

Source Data for Figure 5.6H

Position of Eve+ cell bodies	Genotype	Number of values	Mean (# of cell bodies at E16/17)	Std. Deviation	Std. Error of Mean	p value
Medial	Notch/+	42	1.286	0.4572	0.07055	NA
	Notch/+ (hypothetical 2X)	42	2.571	0.9145	0.1411	NA
	NB7-1>myr GFP, Notch	56	3.411	1.952	0.2608	0.0058
In FasII+ region	Notch/+	42	1.929	0.5129	0.07914	NA
	Notch/+ (hypothetical 2X)	42	3.857	1.026	0.1583	NA
	NB7-1>myr GFP, Notch	56	3.750	1.909	0.2551	0.7221
Lateral	Notch/+	42	1.786	0.5196	0.08018	NA
	Notch/+ (hypothetical 2X)	42	3.571	1.039	0.1604	NA
	NB7-1>myr GFP, Notch	56	1.679	1.515	0.2024	<0.0001

Unpaired t-test Welch (for un-equal Std. Deviation)

Source Data for Figure 5.6I

Molecular markers	Genotype	Number of values	Mean (thickness of FasII+ region in um) at E16/17	Std. Deviation	Std. Error of Mean	p value
FasII+	Notch/+	18	6.471	0.5225	0.1232	NA
	NB7-1>myr GFP, Notch	24	6.596	0.7643	0.1560	0.5324

Unpaired t-test Welch (for un-equal Std. Deviation)

Table 5.4: Source Data for Figure 5.6

CHAPTER 6

CARDINAL TRANSCRIPTION FACTORS

6.1 Introduction: What role do post-mitotic transcriptional programs play in motor circuit assembly?

Since we know that factors acting in neural stem cells play a major role in controlling circuit membership, there are likely a cascade of downstream factors in neurons regulating the series of developmental events required for synaptic partnership formation. While layers of transcriptional control that determine neuron cell type molecular diversity have been uncovered to some degree (Hobert, 2008; Stratmann et al., 2019)[202, 203], this level of insight is lacking for transcriptional cascades controlling neuron synaptic partnership decisions, the key determinant for circuit membership. A class of transcription factors called cardinal transcription factors are prime candidates to be upstream regulators of circuit membership. Initially, Cardinal classes were identified in the ventral region of vertebrate spinal cords (e.g. V0, V1, V2, MN, V3). Each class comes from a unique progenitor domain positioned along the A-P axis (Jessell 2000)[63]. The domain boundaries are achieved through cross-regulatory interactions between transcription factors. Therefore, Cardinal classes of neurons are defined by expression of what we refer to as "Cardinal transcription factors". Cardinal transcription factors are highly conserved, are found across many brain regions and model systems, and include factors such as EN1/engrailed, HB9, EVX1/Eve, SIM1/Sim (Lu et al., 2015; Arber 2012; Briscoe et al., 2000; Jessell 2000; Pierani et al., 2001; Gribble et al., 2007)[204, 205, 206, 63, 207, 127].

Cardinal transcription factors are distinguished from temporal transcription factors in several ways. First, temporal transcription factors are thought to specify the temporal identity of a neuron (e.g., first-born, second-born), regardless of stem cell origin (e.g., NB7-1, NB3-1), and regardless of cell type (e.g., motor neuron, glia), whereas cardinal transcription

factors are thought to specify cell type (e.g., dorsal motor neuron, ventral motor neuron, commissural interneuron, glia, etc.). Second, temporal transcription factors act in neuronal stem cells, whereas cardinal transcription factors act in newly-formed, post-mitotic neurons. Third, temporal transcription factors are thought to be nested in complex loops of activation and inhibition (Nakajima et al., 2010)[208], whereas cardinal transcription factors have cross-repressive interactions (Briscoe and Ericson, 2001; Broihier et al., 2002; Broihier et al., 2004; Landgraf and Thor, 2006)[209, 210, 211, 212]. Cardinal transcription factors have been shown to regulate axon guidance in maturing motor neurons (Landgraf et al., 1999; Broihier et al., 2002; Broihier et al., 2004)[136, 210, 211]. These data demonstrate that in motor neurons, cardinal class transcription factors regulate the early decisions that contribute to circuit assembly. An attractive hypothesis is that cardinal transcription factors are downstream effectors of temporal transcriptions acting as key regulators of circuit membership (Seroka et al., 2020)[85]. To test this idea, cardinal transcription factors must be manipulated and circuit membership (i.e., synaptic connectivity) in mature circuits must be assayed.

Prolonged expression of the temporal transcription factor, Hunchback increases the number of Eve(+) motor neurons that make functional synapses onto dorsal muscles at late larval stages (Meng et al., 2019).[2] Eve is a cardinal transcription factor proposed to specify dorsal motor neuron fate including motor axon targeting to dorsal muscles (Labrador et al., 2005)[213]. Together this raises the possibility that the cardinal transcription factor Eve is a major downstream effector of Hunchback. If this is the case, then any manipulation that increases the number of Eve(+) motor neurons should lead to an increased number of synaptic branches on dorsal muscles at larval stages. From previous studies, we learned that we could ectopically generate Eve(+) motor neurons by removing the cardinal transcription factors Nkx6 and Hb9. Nkx6 and Hb9 are normally expressed in motor neurons that project to ventral muscles (Broihier et al., 2002; Broihier et al., 2004)[210, 211]. In Nkx6 Hb9 double mutant embryos, Eve repression in ventral motor neurons is lost, leading to an

increase in the total number of Eve(+) motor neurons (Broihier et al., 2004)[211]. Additionally, in Nkx6 and Hb9 double mutants there is a loss of axons in the ISNb nerve roots, which project to ventral muscles, and increased thickness of the ISN nerve (projects dorsally) root as it passes over the ventral muscle field (Broihier et al., 2004[211], Figure 4C). Thus, we entered this project thinking Nkx6 Hb9 double mutants would be an excellent genetic background in which to test the following hypotheses: 1) increasing Eve(+) motor neurons leads to alterations in muscle innervation in larval stages. 2) Cardinal transcription factors are required for specifying permanent motor neurons to muscle synaptic partnership choice. We find that loss of the cardinal transcription factors, nkx6 and hb9, does not change motor neuron-to-muscle synaptic partnerships at larval stages, and contrary to what was reported in Broihier et al., 2004[211], we do not observe a dramatic increase in Eve+ neurons nor do we find evidence for dramatically altered axon guidance in late embryonic stages. These data reveal cardinal transcription factors do not have the same potency to regulate circuit membership compared to the temporal transcription factor, Hunchback acting in NB7-1.

6.2 Results

6.2.1 Introduction to the Drosophila motor system

The Drosophila motor system is organized into anterior-posterior repeated, left-right symmetrical hemisegements (Figure 6.1D-E). Each bodywall segment contains 30 muscle cells, which are organized into three main groups—dorsal, transverse, and ventral (Figure 6.1E). Each muscle group is controlled by a unique circuit (Heckscher et al., 2012)[47], and populating each circuit are non-overlapping sets of motor neurons. Importantly, by late larval stages Drosophila motor neuron-to-muscle synapses are large, experimentally-accessible, and extremely well-characterized. Furthermore, in the Drosophila motor system, cardinal transcription factors–Eve, Hb9 and Nkx6–have been characterized at embryonic

stages (Briscoe and Ericson, 2001; Broihier and Skeath, 2002; Broihier et al., 2004; Landgraf and Thor, 2006; Landgraf et al., 1999)[209, 210, 211, 212, 136]. In general, manipulation of these transcription factors leads to alterations in marker gene expression and changes in axonal trajectories. However, the impact on synaptic partner choice at larval stages has not been documented.

6.2.2 Loss of Nkx6 and Hb9 has no impact on third instar larval motor neuron-to-muscle synaptic connectivity

The Nkx6 mutant is NKx6∧D25, is a null allele of the Nkx6 locus and the Hb9 mutant is Hb9∧KK30, a nonsense mutation(Broihier et al., 2004)[211]. Similar to previous reports, in the double hb9 and nkx6 mutant embryos we observed loss of Nkx6 and Hb9 expression (Figure 6.1I-L). However, we only observed a slight increase in Eve(+), 2 extra per hemisegment (Figure 1G-H). This differs from Broihier et al's observation that loss of Nkx6 and Hb9 expression led to an increase in 6 extra Eve+ neurons per hemisegment (Broihier et al., 2004)[211]. The position of the 2 extra Eve(+) neurons is reminiscent of previous work published by Broihier where they found that loss of only Hb9 led to two ectopic Eve+ neurons, which were determined to come from the NB1-1 lineage (Broihier and Skeath, 2002)[210]. The NB1-1 lineage normally first generates the Eve+ aCC motor neuron and sibling pCC interneuron followed by subsequent Hb9+ interneurons (Lacin and Truman, 2016)[73]. So we hypothesized that perhaps the extra Eve+ neurons may assume the aCC and pCC fates, respectively.

Next, we raised Nkx6 and Hb9 double mutants until late larval stages. The increase in Eve(+) motor neurons in embryos is maintained in late larvae (Figure 6.1M). We assayed muscle innervation in dissected fillet preparations by visualizing muscles (phalloidin) and neuronal membrane (anti-HRP) and scoring the number of synaptic branches per muscle (Figure 6.1N-Q). In Nkx6 Hb9 double mutants, the number of synaptic branches onto dorsal

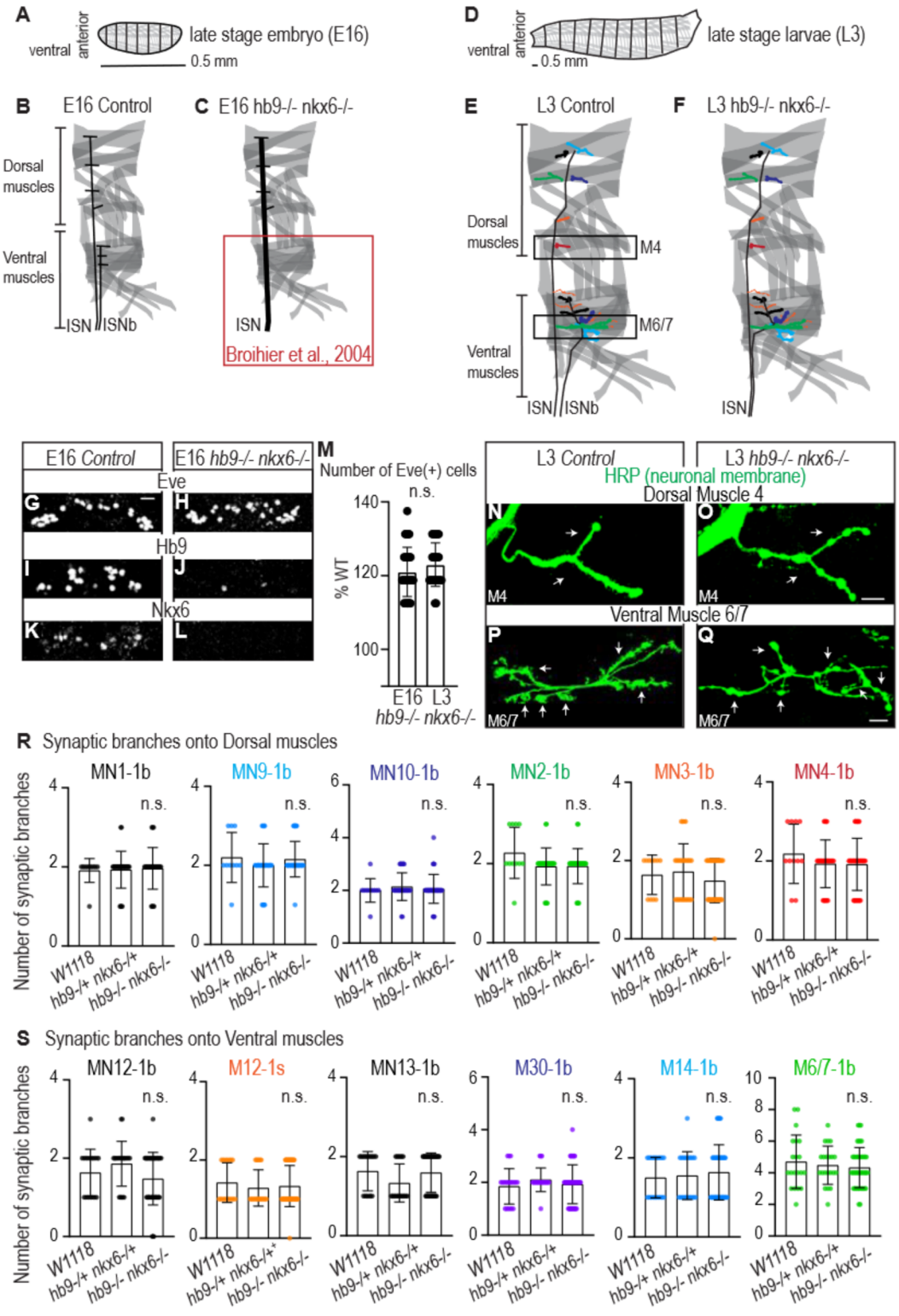


Figure 6.1: Loss of Hb9 and Nkx6 does not impact permanent motor neuron to muscle synaptic partnership decisions. *Continued*

Figure 6.1: *Cont'd.* Loss of Hb9 and Nkx6 does not impact permanent motor neuron to muscle synaptic partnership decisions. Nk6 Hb9 double mutant does not impact neuromuscular synaptic formation inlate stage larvae. (**A**) Illustration of the late stage embryo, body is organized into repeated left-right, mirror image hemisegments. Muscles (in gray) have a stereotyped pattern. (**B-C**) Illustration of muscles, ISN nerve that contact dorsal muscles, and ISNb nerve that contact ventral muscles in abdominal bodywall hemisegments at stage 16 in embryos (E16).(**C**) Illustration representing findings from Broihier et al., 2004. Hb9 nkx6 double mutants lack motor axons of the ISNb nerve and the ISN is thicker than normal. (**D**) Illustration is the same as in (A), except the body is of a late stage larvae (L3). (**E-F**) Illustration is the same as in (B-C), except at L3 and synaptic branches are shown. Color code matches axon synapse names in (Q, R). Note, 1s (yellow on ventral muscles) is only scored on Muscle 12 as M12-1s. (**E**) Illustration of normal synaptic branch pattern at late larval stage (L3). (**G**) Illustration of L3 synaptic branch pattern seen in hb9 nkx6 mutants, there is no change from normal, wildtype conditions. (**G-L**) Images of nerve cord segments in stage 16 embryos. In hb9 nkx6 mutants, extra Eve(+) motor neurons are produced while Hb9(+) and Nkx6(+) motor neurons are absent. These findings have been previously published in Broihier et al., 2004. Images are shown anterior up, scale bar represents 15 microns. (**M**) Quantification of the number of Eve(+) cells represented as a percentage of Control numbers. There is no difference in the number of Eve(+) cells at embryonic stage 16 (E16) or late larval stage (L3). (**N-Q**) Images of neuronal membrane, both axons and neuromuscular synapses, on ventral muscles in L3 abdominal segments. There is no change in branch number onto each RP muscle target. Data quantified in (I-L). Images are shown dorsal up, anterior left, scale bar represents 10 microns. (**R-S**) Quantification of the number of 1b or 1s branches on L3 muscles. Color code as in (A) Each dot represents the number of branches onto a single muscle. There is no significant change in synaptic branch number compared to W1118. (R) For w1118 n=11; nkx6-/+, hb9-/+ n=14; nkx6-/-, hb9-/- n=15. (S) For w1118 n=35; nkx6-/+, hb9-/+ n=9; nkx6-/-, hb9-/- n=12. Control is W1118. hb9-/- nkx6-/- is hb9(KK30), Nkx6 (D25)/ hb9(KK30), Nkx6 (D25). hb9-/+ nkx6-/+ is hb9(KK30), Nkx6 (D25)/+. For quantifications average and standard deviation are overlaid. ANOVA, corrected for multiple samples 'ns' not significant.

or ventral muscles are unchanged compared to wild-type or heterozygous controls (Figure 6.1F,R-S). Thus, Nkx6 and Hb9 are not required for normal, stable motor neuron-to-ventral muscle partner choice. Since aCC normally innervates the dorsal muscle 1, our observations that there is no increase in the number of synaptic branches onto muscle 1 refutes our hypothesis that ectopic Eve(+) transforms the fate of normally Hb9(+) NB1-1 lineage interneurons into Eve(+) aCC/pCC neurons.

In conclusion our data show that changes in the expression of motor neuron cardinal

transcription factors Hb9, and Nkx6 do not lead to permanent alterations in motor neuron-to-muscle synaptic partnerships. This raises the question of possible compensatory mechanisms in place to restore the motor system to the expected pattern of wiring. But before we can conclude that compensation is indeed occurring we need to rule out another possible non-compensatory explanation–a delayed outgrowth defect in the Hb9 and Nkx6 loss of function mutants. The reason I do not consider a delayed outgrowth phenotype to support a compensatory mechanism is that under delay conditions there is no initial miswiring that is sensed and corrected.

6.2.3 Loss of hb9 and nkx6 delays ISNb outgrowth?

In late stage embryos (E17) in double hb9 and nkx6 mutants I find that the ISNb nerve is significantly shorter compared to control (Figure 6.2).

I measured both the length of the ISN from the ventral base of the bodywall segment to a distinct branch point in the dorsal muscle region (Figure 6.2A, gray line). I did not measure the entire length of the ISN because the dorsal most portion was obscured in a number of my embryos. I then measured the length of the ISNb (Figure 6.2A, orange line) and found that the average length was significantly shorter compared to the control (Figure 6.2C). Since there may be segment to segment variability in the length of the ISN, I also calculated the fraction of the ISNb length versus the ISN in the same segment as a percentage (Figure 6.2D). Consistently, there is a significant difference compared to controls. This suggests that the aberrant outgrowth phenotype for the double hb9 and nkx6 mutants is characterized by delayed neurite outgrowth. While there is a significant difference in the averages, when looking at the fraction of ISNb/ISN percentages, nearly two thirds (10 out of 17) segments resemble wildtype-like ISNb outgrowth lengths (Figure 6.2D). I interpret this as the delayed outgrowth is nearly caught up to wildtype levels by late stage embryos. This is fairly consistent with what Broihier et al reported where they noted that by stage 16 the

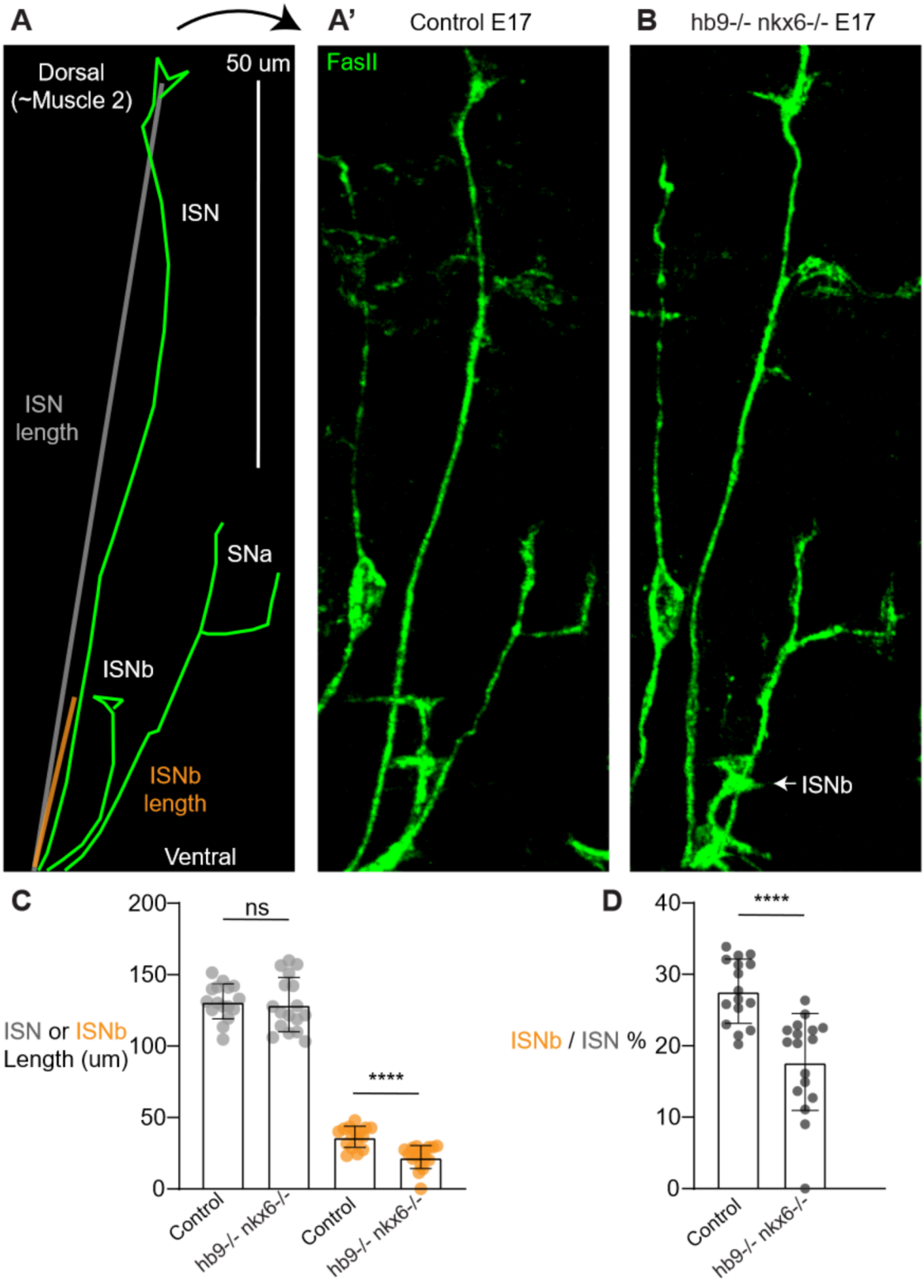


Figure 6.2: ISNb nerve outgrowth in late-stage embryos. (**A'-B**) Images of single bodywall segments in stage 17 embryos. In hb9 nkx6 mutants, the ISNb is significantly shorter compared to control. *Continued*

Figure 6.2: *Cont'd.* ISNb nerve outgrowth in late-stage embryos. (**A**) Illustration representing the nerves seen in (A) and the measurements quantified in (C). (**C**) Quantification of ISN and ISNb lengths represented in (A-B). (**D**) Quantification of the fraction of ISNb/ISN expressed as a percentage. Each dot represents a single measurement. For quantifications, average and standard deviation are overlaid. Un-paired t-test with Welch's correction for unmatched standard deviations (see source datasheet for details). 'ns' not significant, '***' $p<0.0001$.

ISNb axons appeared to be extending along the ISN in the ventral muscle region (Broihier et al., 2004)[211]. Since they also used FasII, which makes it difficult to distinguish between overlapping nerves, their data is also consistent with the conclusion that the ISNb nerve is indeed present but runs closer to the ISN nerve. Combined, these data suggest that hb9 and nkx6 are required for timely ISNb outgrowth however by late embryonic stages, the delayed outgrowth observed in double hb9 and nkx6 loss of function mutants is nearly resolved. While obviously more data should be collected, I think future effort dedicated to the characterization of the exact outgrowth timing of the ISNbs could be better served elsewhere. One area of interesting future directions that would not require much effort beyond tracking the age of embryos and dissecting 1st instar larvae, is to determine the extent to which ISNb nerves for a given animal are at the proper length at the time of hatching. In other words, could the double hb9 and nkx6 mutants cause a delay in hatching? If so, identifying the mechanisms underlying the delay will be challenging because Hb9 and Nkx6 are not exclusively expressed in the developing nervous system of the embryo. Hb9 is known to be expressed in the midgut invaginations (Broihier and Skeath, 2002)[210]. Beyond the nervous system, Nkx6 (also known as Nk6) is also expressed in the hindgut and internal head structure (Uhler et al., 2002)[214].

6.3 Discussion: An update view on the cross-repressive relationships between cardinal factors

I entered this project with the general assumption that cardinal transcription factors have cross-repressive interactions (Briscoe and Ericson, 2001; Broihier et al., 2002; Broihier et al., 2004; Landgraf and Thor, 2006)[209, 210, 211, 212]. For example, if Hb9 and Nkx6 expression is lost then Eve expression is no longer repressed, meaning neurons now express Eve. This example was a model favored by Broihier et al because at stage 15 embryos they observed 6 extra Eve+ neurons per hemisegment in the double hb9 and nkx6 mutants. This study hypothesized that several of these ectopic Eve+ neurons are the NB3-1 derived RP motor neurons, aside from noting that the extra Eve+ neurons lie relatively medially in nerve cord segments, no direct evidence was presented to support this hypothesis. While cross-repressive interactions do exist, I favor a model where cross-repressive interactions largely occur within neuroblast lineages that normally express both Eve and at least one of the following: hb9, nkx6. There are a number of examples to support this model. First, NB1-1 generates Eve+ aCC and pCC neurons as well as Hb9+ interneurons (Lacin and Truman, 2016)[73]. Loss of Hb9 causes two extra Eve+ neurons per hemisegment (Broihier and Skeath, 2002)[210]. Since these extra Eve+ neurons were positioned next to the aCC/pCC neurons and expressed an Eve-beta-gal reporter gene unique to Eve+ aCC/pCC and RP2, the authors concluded these extra Eve+ neurons are bona fide NB1-1 lineage neurons. When Eve is lost in aCC and pCC, Hb9 can be derepressed in aCC but not pCC (Fujioka et al., 2003)[215], which suggests there are further criteria beyond a lineage's ability to generate both neurons that express either Eve or the cross repressible hb9/Nkx6. Second, NB4-2 generates the Eve+ RP2 and three Hb9+ coR motor neurons (Lacin et al., 2009)[198]. Loss of Eve in RP2 depresses Hb9 expression, thus RP2 motor neurons now express Hb9 (Fujioka et al., 2003)[215]. Third, loss of Nkx6 by RNAi in the NB7-1 lineage generates one extra Eve+ neuron per hemisegment (NB7-1 normally generates the Eve+ motor neurons) (Seroka et al., 2020)[85]. When ectopic

cardinal transcription factor expression is supplied, now lineages that never express one or the other repressive counterpart can but do not always exhibit the cross-repressive interactions. For example, pan-neuronal expression of nkx6 (elav-GAL4>UAS-nkx6) leads to loss of Eve expression in the NB3-3 derived EL interneurons, which normally do not express Nkx6 but at the same time this same manipulation does not impact endogenous Eve expression in the NB1-1 lineage (Broihier et al., 2004)[211]. In summary, while it is attractive to make the broad claim that cardinal transcription factors are cross repressive, I believe that this relationship is context-dependent.

From these data, I am confident that none of the 6 extra Eve+ neurons Broihier et al reported in their double hb9 and Nkx6 mutants are NB3-1 derived RPs. A large fraction of all Drosophila larval motor neurons express hb9 and/or nkx6, so if the NB3-1 derived RPs indeed express Eve as predicted by Broihier et al then we would expect to see a much larger increase in the number of extra Eve expressing neurons. However, only 6 extra Eve+ neurons were reported. I believe these 6 extra Eve+ neurons came from 3 lineages: +2 from NB1-1, +3 from NB4-2, and +1 from NB7-1. As further support, if the RP motor neurons did express Eve, the expectation is that these neurons would be misrouted to the dorsal muscle field (Landgraf et al., 1999)[136]. Based on the phenotypes observed in late stage embryos in both Brohier et al and data I collected (Figure 6.2), there is no evidence that the ISN nerve is thicker as it passess over the transverse and dorsal muscles (Figure 6.2A-B).

6.4 Further characterization of the double loss of hb9 and nkx6 mutant larvae

I want to take this opportunity to offer an important side comment on the double hb9 and nkx6 animals. Upon hatching these larvae grow slowly. Normally the larval instar stage takes several days before pupal formation. It takes the double hb9 and nkx6 mutant larvae around 7-10 days to grow to comparable wildtype-sized third instar larvae. If these larvae

co-habitat with heterozygotes, the homozygous larvae will be out-competed. It is best to pick out 1st instar larvae (select against green balancers) and place them in a separate vial housing only homozygous larvae. In addition to growing slowly, I noticed that long stringy-like structures that run along anterior-posterior along the sides of the larvae and I believe are associated with the gut, are much darker in color (purple) compared to wildtype.

Another striking feature of these larvae is I found very little evidence of digging in the food substrate. Despite housing at least a dozen larvae in each vial, I found no upturned substrate, commonly observed in vials that contain only several wildtype-like larvae. I hypothesized that perhaps these animals struggled to dig because of miswiring of motor neurons onto mouthpart-associated muscles. I went to Lacin and Truman, 2016[73], a wonderful resource to identify what Cardinal transcription factors are expressed in which neuroblast lineage. In addition to NB3-1, two other lineages express both Hb9 and Nkx6, NB1-2 and NB2-2 (Lacin and Truman, 2016)[73]. The next resource I used was the neuroblast tool on Chris Doe's lab website. Interestingly in the thoracic segments NB1-2 generates motor neurons (2 but up to 4) that innervate the mouthpart-associated muscles (muscles 33-35). While there is no explicit evidence in the literature that the motor neurons of NB1-2 express Hb9 and Nkx6, it is likely they do because these motor neurons innervate ventral muscles. Following from this assumption, my hypothesis was perhaps Hb9 and Nkx6 are required for outgrowth of these motor neurons. If so, this could open up an interesting area to explore possible anterior-posterior or region specific differences for the requirement of cardinal factors, hb9 and nkx6 in specifying motor neuron to muscle synaptic partnerships.

Alas, the limited data I collected does not support any of these ideas, rather the data is consistent with my previous observations that Hb9 and Nkx6 cardinal transcription factors do not impact the final wiring decisions of motor axon to muscles. Right before the fateful week of March 16th, 2020 as the world seemingly turned upside down with the stay at home order, I dissected several 3rd instar sized double hb9 and nkx6 mutant larvae and focused

on preserving the thoracic regions, which are very close to the head (Figure 6.3).

While I only had one good example from wildtype and one decent example from the double mutant, in both genotypes, I find evidence of innervation onto the mouthpart-associated muscles (M33-35) thought to be innervated by NB1-2 motor neurons (Figure 6.3). While more data needs to be collected before any substantial conclusion can be drawn, from my one experimental example, revealing that innervation of type 1-b onto M33-35 persists,this is suggestive that if NB1-2 motor neurons normally express Hb9 and Nkx6 in wildtype, expression of these cardinal transcription factors is not required for motor neuron to muscle synaptic partnership decisions.

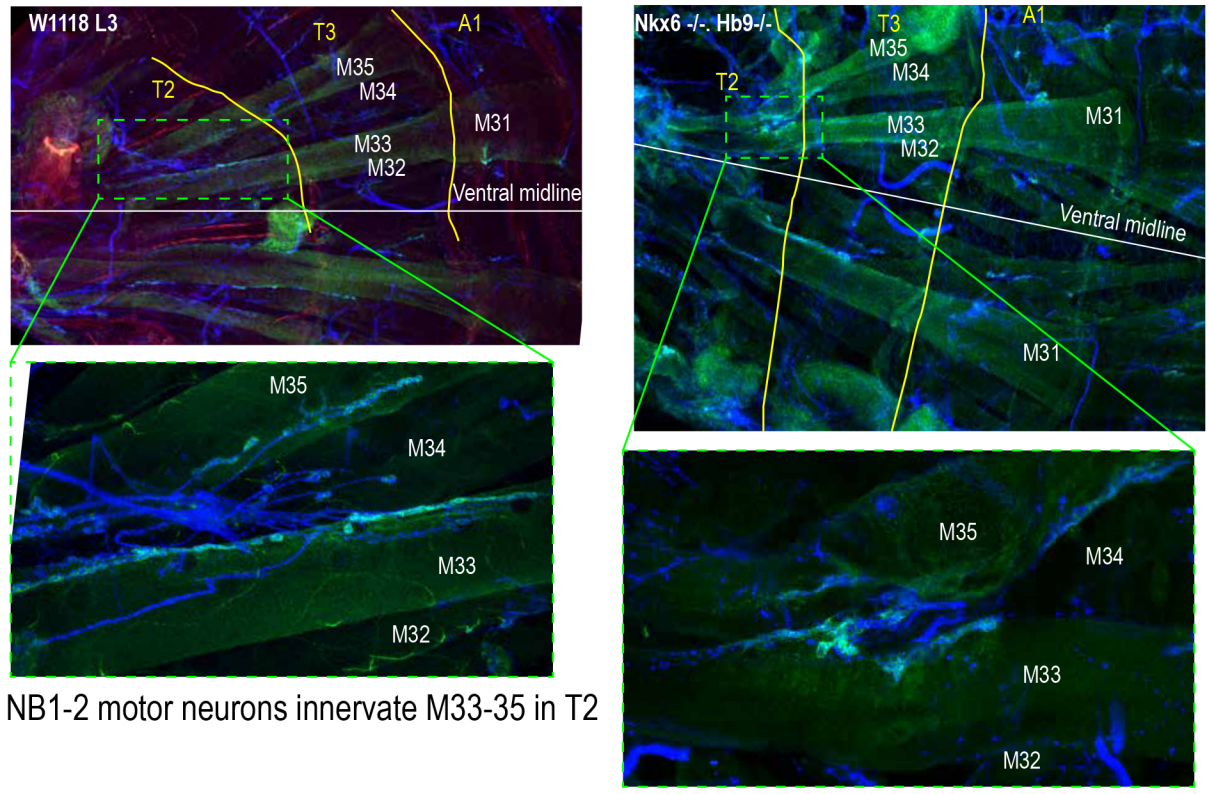


Figure 6.3: In hb9 nkx6 mutants, there is no change in the permanent synaptic partnership decisions of thoracic motor neurons onto mouthook-related muscles. Images of thoracic segments in L3 larvae. Yellow lines mark the borders between segments. HRP is in blue and DLG is in green.

6.5 Eve misexpression manipulation

6.5.1 Background

In the last section, I had initially introduced the double loss of hb9 and nkx6 mutants as a way to generate extra Eve+ motor neurons. While we had little success replicating previously published approaches (Broihier et al., 2004)[211], we still learned that loss of endogenous hb9 and nkx6 expression in motor neurons does not impair their ability to make permanent synaptic partnerships with ventral muscles. In this section, we take a more direct approach to generating extra Eve+ motor neurons by expressing ectopic Eve using a transgene.

This manipulation was previously done by mis-expressing Eve panneuronally (Elav GAL4>UAS Eve) (Landgraf et al., 1999)[136]. This means motor neurons that normally express cardinal transcription factors Hb9 and Nkx6, now experience repression of these factors because of ectopic Eve expression. The authors of this study found evidence that the dorsally projecting nerve was thicker than in wildtype and ventrally projecting nerves were diminished in stage 16 embryos. However, in late stage embryos (stage 17) immediately prior to hatching they found evidence that motor axons that misrouted dorsally could reroute to the ventral muscle field and form synapses onto ventral muscles. This was done by injecting Dil into the ventral muscles 6 and 7 to retrogradely label synaptically connected motor neurons. Using this technique they were able to learn if these ventral muscles receive innervation and if so, what is the morphology of the innervating motor neurons? Interestingly they found that an "RP-like" motor neuron (based on morphology) extended its axon into the dorsal muscle field and near muscle 4, the axon looped back down to the ventral muscle field to form a stable synapse onto muscles 6 and 7. Presumably they injected Dil into other ventral muscles but no other experiments were described. Thus, we asked to what extent can rerouting occur? Perhaps Landgraf et al., observed an intermediate phenotype where only some of the motor neurons have fully rerouted by E17 but eventually all motor neurons are rerouted. Alternatively,

perhaps only specific motor neurons like RP3 can reroute. Because of the embryonic lethal nature of elav-GAL4 >UAS-eve, these questions could not be fully addressed. However, now that we have more specific driver lines available, we can finally understand whether or not cardinal transcription factors can affect permanent synaptic partnership decisions.

6.5.2 Results

The goal was to misexpress Eve in the NB3-1 RP motor neurons. We can drive UAS-Eve using either our NB3-1 specific driver or the Hb9 driver. As the names imply, NB3-1 will only misexpress Eve in the NB3-1 derived RP motor neurons: RP1, RP4, RP3, and RP5. The Hb9 driver will misexpress Eve in all Hb9+ neurons, meaning all Hb9+ motor neurons including the NB3-1 RP motor neurons. From work done characterizing Hb9 and eve expression patterns in the developing Drosophila embryo, these cardinal transcription factors are thought to be only expressed in ganglion mother cells and postmitotic neurons, so we wanted to use the Hb9 driver line to avoid driving ectopic Eve expression in the 3-1 neuroblast. While the Hb9 driver drives GFP in nearly all Hb9(+) neurons by late embryonic stages (E15-17) there are a number of labeled Hb9(-) neurons (Figure 6.5). This suggests that perhaps the Hb9 driver may be expressed in neuroblasts. This is possible because the enhancer trap Hb9-Gal4 was made by transposon-mediated random insertion of the Gal4. The Gal4 insertion mapped close to the Hb9 locus however we know that there are enhancer elements surrounding the Hb9 locus that are expressed in neuroblasts (Lacin et al., 2014)[216]. In fact, the NB3-1 driver is a DNA fragment proximal to the Hb9 locus. In the future, if this project is carried forward it will be essential to carefully characterize the Hb9-Gal4 driver and see if there is evidence of expression in worniu+ large cell bodied neuroblasts.

When I misexpressed eve using the NB3-1 driver and dissected third instar larvae to characterize the permanent motor neuron to muscle synaptic partnership decisions, I found

no change in type 1b synaptic branch count onto the ventral muscles that do not receive innervation from NB3-1 type 1b RP motor neurons – muscles 12 and 13 (Figure 6.4A-B,D-F, H, I).

I did however find significant loss of the type 1s onto the ventral muscles (data only for type 1s innervation onto muscle 12 (Figure 6.4A-B, D, J). I saw a reduction of type 1b innervation onto muscle 14, compared to wildtype (Figure 6.4A-B,K). While I sometimes observed a decrease in the synaptic branches onto muscle 30, 6 and 7, the average branch number is not significantly different compared to wildtype (Figure 6.4A-B, L-M). I also observed that there were instances of ectopic innervation onto muscles 30 (5% of all scored segments) and muscles 6/7 (12% of all scored segments) (Figure 6.4A-B, D-F, Table 1). I observed no ectopic innervation onto any other ventral muscles. When I misexpressed Eve using the Hb9 driver, compared to NB3-1>Eve I found consistent but more extreme results. The synaptic branch counts onto all ventral muscles are significantly reduced except for muscles 6/7 (Figure 6.4G, H-M). I only observed ectopic type 1b innervation onto muscles 6/7 (17% of all scored segments) (Table 6.1 1).

Combined, these findings reveal that ectopic Eve can alter the wiring of motor neurons that normally project to the ventral muscles. Next, I wanted to know if ectopic Eve is sufficient to permanently misroute these ventrally projecting motor neurons to the dorsal muscle field.

Landgraf et al sketched out an example of a Dil labeled motor neuron whose axons extend to the dorsal muscle field as far as the muscle 4 and 3 region before then looping towards the ventral muscle field (Landgraf et al., 1999). So I asked if there was increased innervation onto these dorsal muscles. I observed that muscle 4 is the only muscle that has increased synaptic branches of both type 1b and 1s identity (Figure 6.6).

Once again, the NB3-1 and Hb9 driver offer comparable results with the Hb9 driver data being more extreme (Figure 6.6). This is consistent with the observation that when Eve

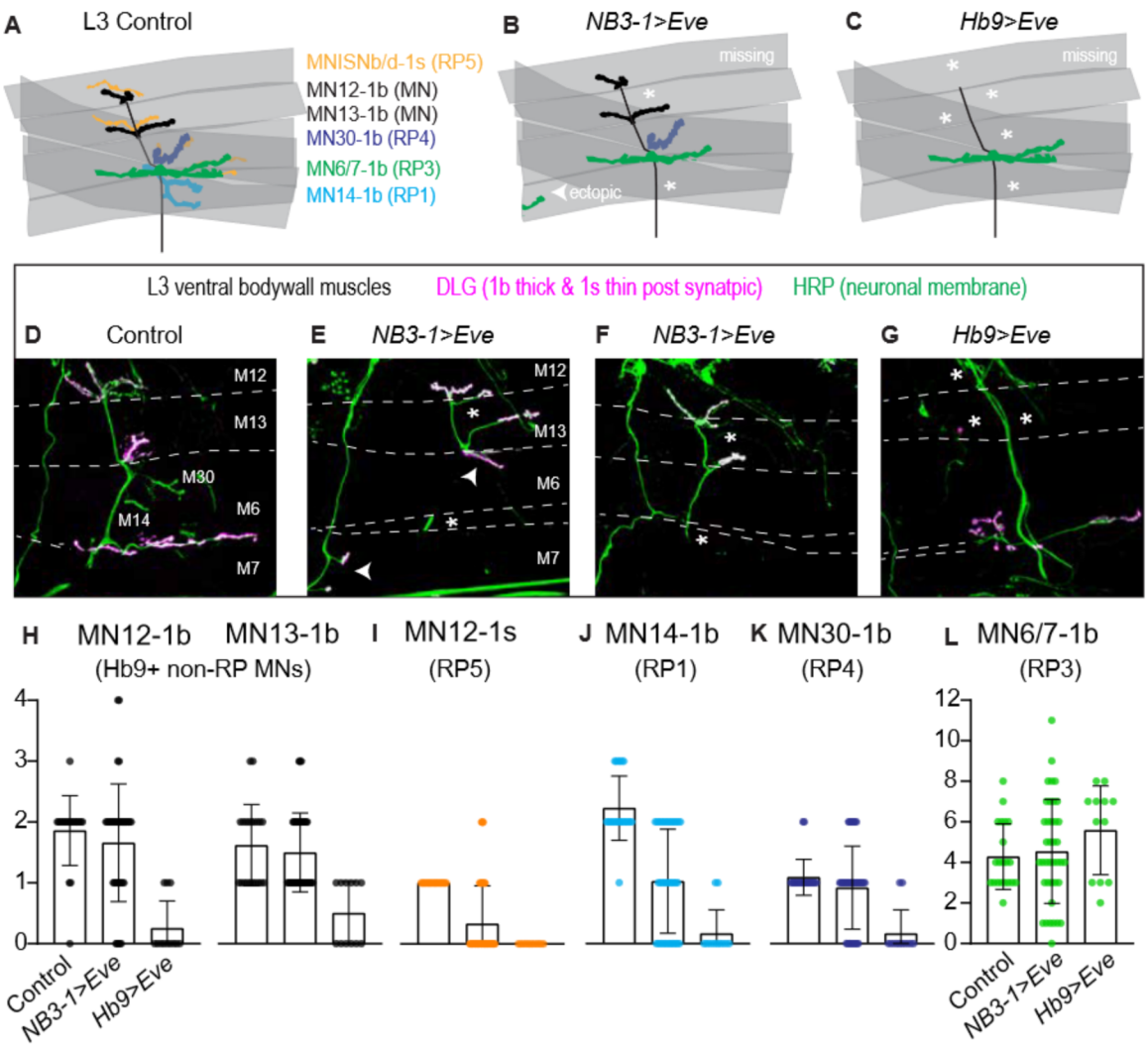


Figure 6.4: Misexpression of Eve in Hb9+ motor neurons permanently reduces the number of type 1b and 1s motor neuron-to-muscle synaptic branches onto ventral muscles. (**A-C**) Illustrations of neuromuscular synapses on ventral muscles in an L3 body wall segment (black = MN12-1b and MN13-1b not from the NB3-1 lineage, blue = RP1/4, green = RP3, orange = RP5). In NB3-1>Eve the number of synaptic branches is reduced (white asterisks) but not entirely abolished onto NB3-1 RP motor neuron muscle targets except for RP3's muscle targets, muscles 6/7. Denoted by an arrowhead, there is evidence for ectopic innervation onto muscles6/7. In Hb9>Eve the number of synaptic branches is severely reduced (white asterisks) onto Hb9+ motor neuron muscle targets (i.e. all ventral muscles) except for muscles 6 and 7 continued. *Continued*

Figure 6.4: *Cont'd.* (**D-G**) Images of neuronal membrane, both axons and neuromuscular synapses, on ventral muscles in L3 abdominal segments. Arrowhead indicates ectopic innervation onto muscles 6/7. An asterisk * indicates missing synapses. Data quantified in (K-P). (**K-P**) Quantification of the number of 1b or 1s branches on L3 muscles. Color code as in (A). Each dot represents the number of branches onto a single muscle. All images are shown dorsal up, anterior left. For quantifications average and standard deviation are overlaid. Un-paired t-test with Welch's correction for unmatched standard deviations. (NB3-1>Eve in I-J is '****'; Hb9>Eve in H-K is '****') '****' $p<0.0001$ (For more details see Source datasheet)

is misexpressed by Hb9-Gal4, there is a more extreme loss of synaptic branch count onto ventral muscles compared to NB3-1>Eve. These data reveal that ectopic expression of Eve can permanently misroute ventrally projecting motor neurons to the dorsal muscle field.

The data so far reveals two major takeaways. First, the two drivers yield different phenotypes where ectopic expression of Eve using the Hb9 driver generates more extreme loss of innervation onto ventral muscles normally innervated by NB3-1's RP1, RP4, and RP5 compared to the NB3-1 driver (Figure 6.4J-L). Second, ectopic expression of Eve irrespective of driver does not significantly impact type 1b innervation onto muscles 6/7, normally innervated by type 1b RP3. To understand the extent to which differences in Eve expression between driver lines and across unique RP motor neurons underlie these observed phenotypes we characterized cardinal transcription factor expression. Since cardinal transcription factors are expressed only during development meaning they do not persist until the third instar larval stage, we need to characterize cardinal factor expression in late stage embryos.

Under normal, wildtype conditions, the NB3-1 RP motor neurons express Hb9 and Nkx6 but here we only use an antibody against Hb9. While the RP motor neurons are in a stereotyped position within the nerve cord, we drove myr-gfp for two reasons: 1) to unambiguously identify the RP motor neurons and 2) identify if during development, myr-GFP+ Eve+ motor axons route dorsally earlier in development (E15) (Broadie et al., 1993)[217]. As I was preparing to do these experiments, our current rotation student at the time, Anali Migueles Lozano was interested in this work so for her rotation project she stained and imaged

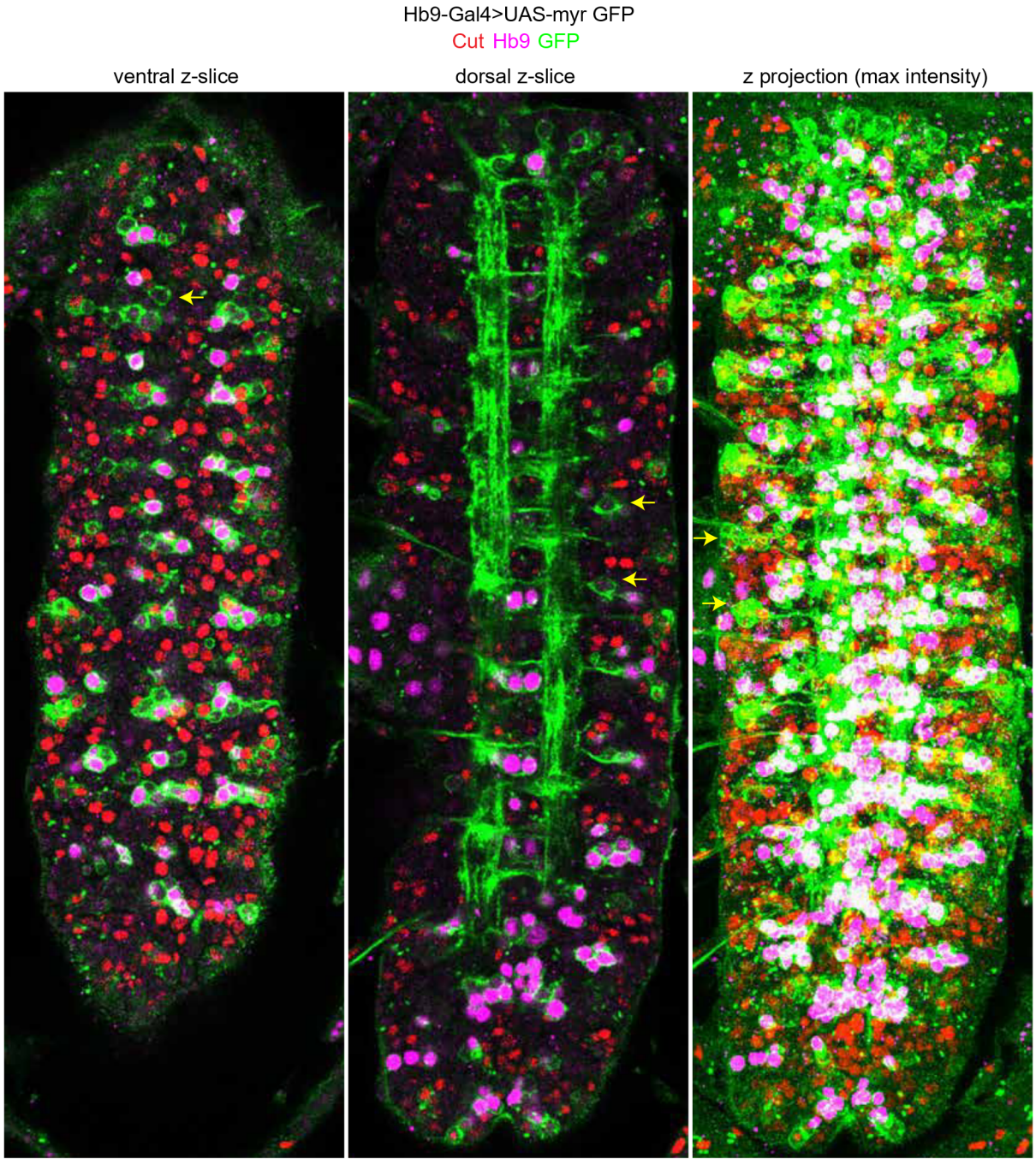


Figure 6.5: Characterization of the Hb9 driver. The image is of the full length of a nerve cord in a late-stage embryo (E16/17). Anterior is up, ventral view imaged.

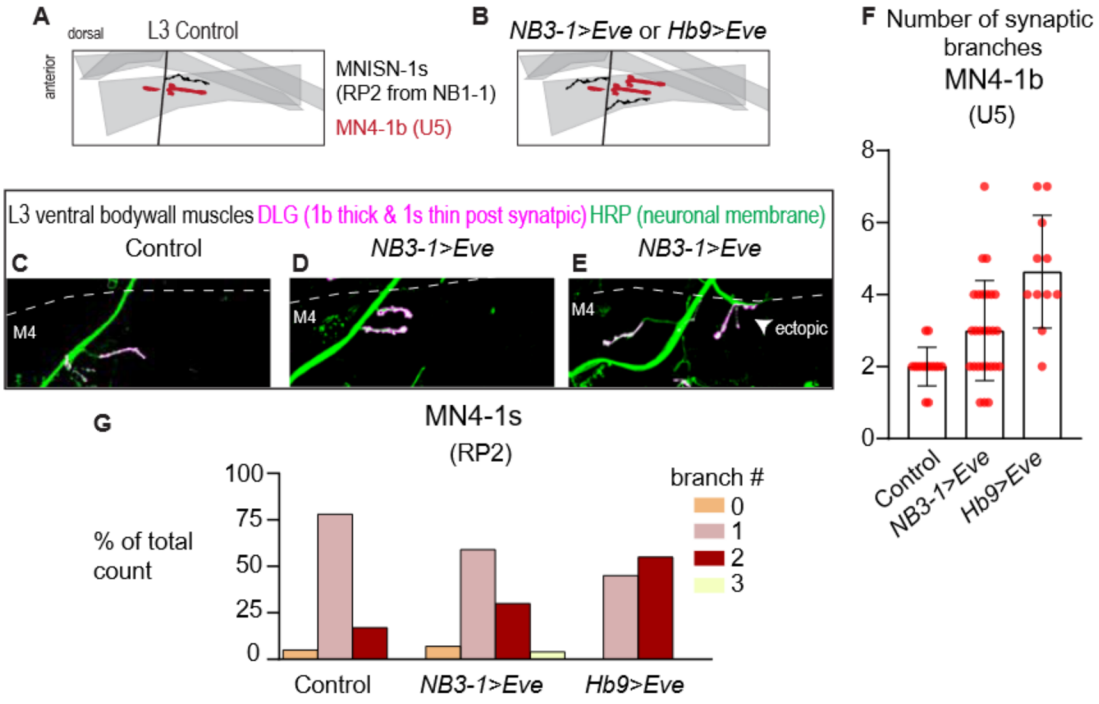


Figure 6.6: Misexpression of Eve in Hb9+ motor neurons permanently increases the number of type 1b and 1s motor neuron-to-muscle synaptic branches onto dorsal muscle 4. (**A-B**) Illustrations of neuromuscular synapses on dorsal muscle 4 in an L3 body wall segment (black = MNISN-1s, red = MN4-1b). (**C-E**) Images of neuronal membrane, both axons and neuromuscular synapses, on dorsal muscle 4 in L3 abdominal segments. Arrowhead indicates ectopic type 1b and 1s innervation onto muscle 4. All images are shown dorsal up, anterior left. (**F**) Quantification of the number of 1b branches on L3 muscle 4. Each dot represents the number of branches onto a single muscle. For quantifications average and standard deviation are overlaid. Un-paired t-test with Welch's correction for unmatched standard deviations. There is an increase in synaptic branch count when Eve is misexpressed by NB3-1 and Hb9 drivers, p=0.002 and p=0.0002, respectively (**G**) Quantification of the number of 1s branches on L3 muscle 4 is expressed as a percentage of the total number of scored segments. There is an increase in the number of type 1s branches when Eve is misexpressed by NB3-1 and Hb9 drivers.

embryos. Unfortunately the myr-GFP on the 2nd chromosome expression was variable but often weak so it was not of much help. However, I was still able to identify RP-like motor neurons based on their position (Figure 6.7).

For both genotypes (NB3-1>Eve and Hb9>Eve) we found the following expression in RP motor neurons: exclusively expressing Eve "transformed" (Figure 6.7, see 6F as an

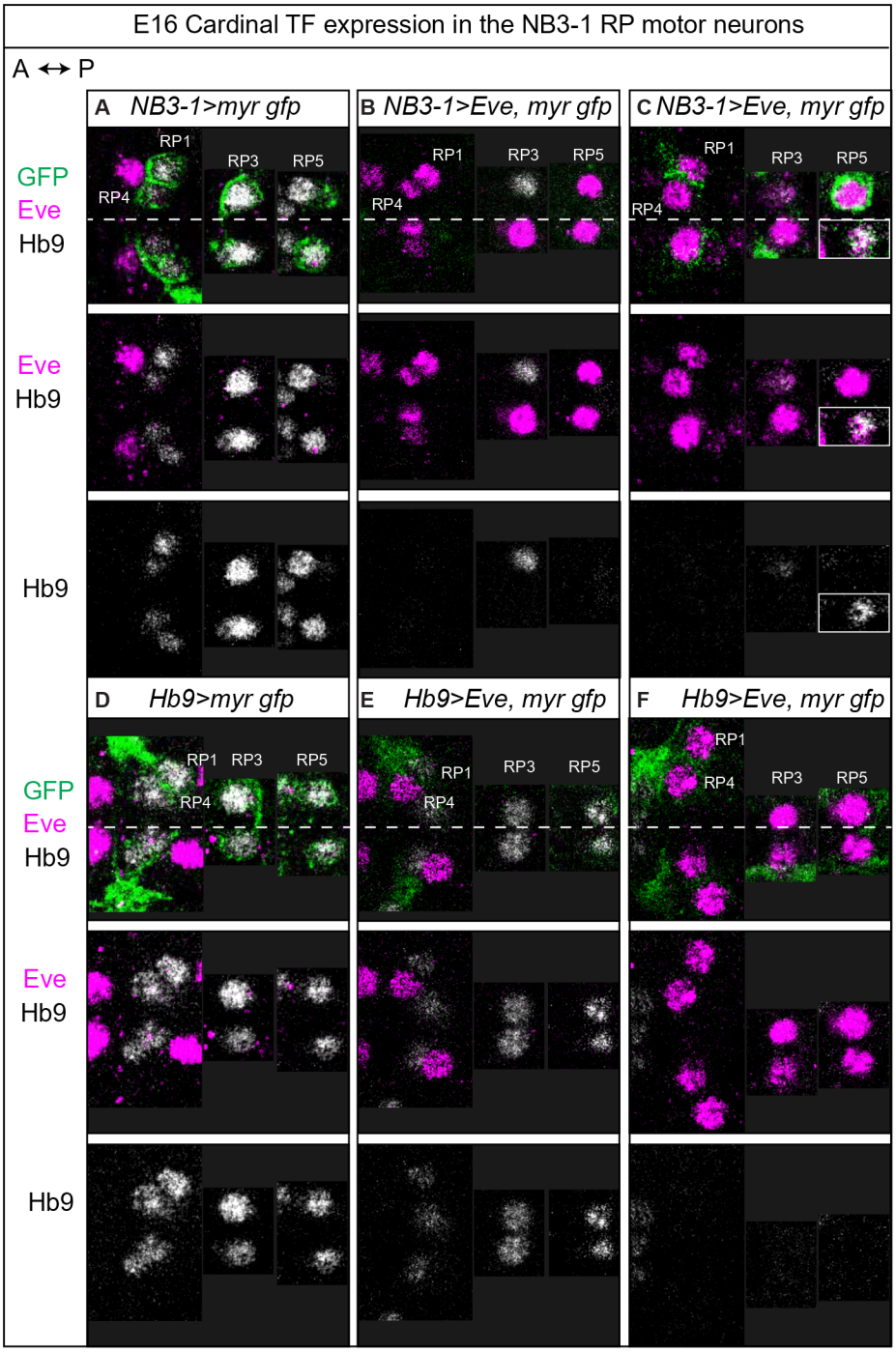


Figure 6.7: Misexpressing Eve in neurons that are normally Hb9+ variably represses endogenous Hb9+ expression. (**A-F**) Images of molecular markers in nerve cord hemisegments of late-stage embryos (E16). White boxes are insets from different z-planes. Note, the myr-GFP used was on the II chromosome and was much weaker than the myr-GFP on the III (used for all past NB7-1 related experiments).

example), exclusively expressing Hb9 "untransformed" (Figure 6.7, see 6.7E as an example), and co-expressing Eve and Hb9 "partially transformed" (Figure 6.7, see 6.7C as an example). Overall, NB3-1>Eve has a higher percentage of "untransformed" or "partially transformed" hemisegments compared to Hb9>Eve (Table 6.1 2). Do these differences in cardinal factor expression explain the difference we observe in the synaptic branch count phenotypes at L3?

Strikingly, we find a strong correlation between cardinal transcription factor expression and the RP5 type 1s phenotypes (Table 6.1 1,2, yellow highlighted boxes). The percentage value for the number of L3 bodywall segments where the type 1s innervation onto muscle 12 appears "wildtype" is nearly similar to the percentage value for the number of E16 nerve cord hemisegments where RP5 is expressing Hb9, "untransformed" (Table 6.1 1,2, yellow highlighted boxes). This suggests that when RP5 motor neurons co-express Eve and Hb9, ectopic Eve can still permanently misroute RP5. So what about the other RP motor neurons? First, I do find a general trend where there are more Eve+ "transformed" hemisegments and more misrouted L3 phenotypes when Eve is misexpressed by the Hb9 driver versus the NB3-1 driver. This suggests that higher levels of ectopic Eve expression increases the odds that permanent misrouting occurs. Second, I don't find a striking correlation between RP1, RP4, and RP3's cardinal transcription factor expression and their type 1b synaptic branch phenotypes (Table 6.1 1,2). Namely, there is a greater percentage of "wildtype-like" type 1b synaptic branch phenotypes than Hb9+ "untransformed" hemisegments. This suggests that there are Eve+ RP motor neurons that eventually give rise to permanent "wildtype-like" type 1b phenotypes.

When we misexpress Eve irrespective of driver choice the most consistent "wildtype-like" example in L3 bodywall data is the type 1b innervation onto muscles 6/7. While the type 1b innervation is undoubtedly an RP motor neuron, it is unclear if it is consistently RP3 (our NB3-1 specific manipulation data, Landgraf et al., 1999)[136]. Perhaps RP3 is unique in its ability to be rerouted ventrally upon initially being misrouted dorsally (note, this is

the only example Landgraf et al reported) or there is something unique about muscles 6/7 necessity to be innervated and any type 1b RP can meet this need. I think the latter model that any type 1b RP can innervate muscle 6/7 can be ruled out by data I have collected. First, I find two examples (one from each driver) where there is innervation onto muscle 14 and 30, normally innervated by RP1 and RP4, respectively and the innervation onto muscle is ectopic and appears to come from the TN (transverse nerve) (as in Figure 6.4E). If muscles 6/7 were a priority and could be innervated by any type 1b RP, we would expect "wildtype-like" innervation onto muscles 6/7 before muscles 14 and 30. In further support that RP1 and RP4 cannot assume RP3 fate, my previously published work showing that ectopic expression of Hunchback increased the number of synaptic branches onto muscle 14 and 30 while branch number was significantly reduced onto muscles 6/7 (Meng et al., 2020)[3]. If RP3 was unique in that its ability to consistently reroute to generate a "wildtype-like" synaptic branch phenotype then why do we observe on average 15% of all innervation onto muscles 6/7 as ectopic? These ectopic type 1b branches most often come from the TN but I have also observed them coming from the vicinity of ISNd, muscle 13 and 14. I think these data reveal local compensatory mechanisms whereby nearby type 1b motor neurons can extend a synaptic branch to innervate muscles 6/7, despite compensatory branch number is far reduced from the wildtype branch count from RP3. The question is what accounts for the diversity in how muscles 6/7 receive innervation? Compensation can occur and Landgraf et al reported rerouting by what we concluded above is likely the bona fide RP3 motor neuron, so what are the mechanisms by which compensation or rerouting occur? Is there a logic driving these decisions or is it largely random? To what extent is the function driving the system to find a workable solution? These are important questions to address if we want to understand the underlying logic of motor circuit assembly.

There are several previous studies focused on ectopic innervation particularly from the TN motor neurons onto muscles 6/7. Ablation of RP3 leads to physiologically functional ectopic

innervation onto muscles 6/7 from transverse nerve motor neurons (Chang and Keshishian, 1996)[104]. During development, off-target contacts are made but during an early critical period (late embryonic to first instar stage) these ectopic contacts are pruned. This refinement is dependent on neural activity whereby silencing electrical activity of motor neurons leads to ectopic innervation persisting (Vonhoff and Keshishian, 2017)[218]. This suggests that when ectopic innervation is observed on muscles 6/7 this permanency is likely a result of no RP3 rerouting back to muscles 6/7. This suggests that the choice to ectopically innervate muscles 6/7 is dependent on the lack of "wildtype-like" innervation onto these muscles.

Our data raises the possibility that perhaps RP3 is unique in its ability to reroute ventrally upon being initially misrouted dorsally. If so, the question is what makes RP3 unique? Here I offer several suggestions. First, the type 1b innervation of RP3 is rather unique in comparison to other type 1b innervation patterns in a given bodywall segment. Not considering the narrow ventral oblique muscle region, the RP3 is the only type 1b to be positioned at the cleft between two muscles and innervate both of them. RP3 is arguably the most well studied motor neuron in the Drosophila larvae so there is a large body of RP3-related work. We know that RP3 receives signals from its target (Broadie et al., 1993)[217]. While the idea of muscle target derived cues is not unique to RP3s perhaps it is a very strong specific cue that despite RP3 initially misrouted dorsally because of Eve expression once its motor axon exists the ISN nerve near muscle 4 it searches or is drawn to the unique molecular signature of muscles 6/7. There are ongoing efforts in labs including our neighbors, the Carrillo lab to understand the identity of the neuromuscular codes whereby motor axon to muscle synaptic partners are recognized.

Future experiments to push this project forward will require single cell motor axon neurite morphology to determine the extent to which RP1, RP4, and RP3 misroute dorsally and then reroute ventrally. This could be done using a multi color flip out approach I used in my 2019 paper. To do so, the NB3-1 GAL4 driver or UAS Eve must be moved to the II chro-

mosome. I used a gateway cloning strategy to place the NB3-1 specific sequence upstream to a GAL4 and LexA sequence on destination vectors. These plasmids are ready to be sent off for injections. The Hb9 GAL4 driver is on the third chromosome too but since it is not a transgene but rather was made using a random transposon-mediated insertion strategy, unless we characterize the precise DNA sequence associated with the GAL4 expression pattern, we cannot simply move Hb9 Gal4 to the second chromosome. Ideally this single cell analysis would be done at late embryonic stages because both morphology and molecular marker expression can be obtained for single RP motor neurons. In wildtype RP motor neurons, Hb9 and Nkx6 expression do not persist until L3 stages but Eve expression persists in the U motor neurons, so I was hoping Eve expression would persist when I ectopically express Eve using the Hb9 and NB3-1 drivers but Eve expression does not persist until L3 stages. This also tells us that ectopic Eve does not cause RP motor neurons to maintain endogenous Eve expression.

6.6 Discussion for the whole section on cardinal TFs

For years cardinal transcription factors have been studied in the context of axon pathfinding, where they have been shown to be required for proper motor axon outgrowth in the developing Drosophila larvae. Cardinal transcription factors act early in newly born motor neurons, making these factors attractive downstream candidates linking temporal transcription factors to synaptic partnership decisions (Seroka et al., 2020; Landgraf and Thor, 2006)[85, 212]. Considering previous studies and the data I present here, the extent to which cardinal transcription factors specify permanent motor neuron to muscle synaptic partnership decisions and thus likely lie downstream of the temporal transcription factors is dependent on individual cardinal transcription factors, therefore I think we must re-evaluate whether we should assign the following factors to the same category: eve, hb9, and nkx6. Let me explain. First, there is evidence in the field that eve controls nerve cord exit. For

example in NB1-1's aCC motor neuron eve is upstream to grn and zfh-1, genes that regulate axon guidance (Garces and Thor, 2006)[219]. Consistently work from our own lab finds that loss of eve expression in NB7-1's U motor neurons inhibits their exit from the nerve cord (personal communication with Zarion Marshall and Ellie Heckscher). If hb9 and nkx6 collaborate to have a similar role to eve we would expect that loss of hb9 and nkx6 in motor neurons should inhibit motor axon exit from the nerve cord. While there is evidence to suggest that loss of hb9 and nkx6 delay ISNb motor neuron exit (Figure 6.2) (Broihier et al., 2004; Broihier and Skeath, 2002)[211, 210], these factors are not required for motor neuron outgrowth (Figure 6.1). This means that in NB3-1 there must be another factor that either works either in combination with hb9 and nkx6 or independently to control nerve cord exit. Identifying this factor will be key to understanding the transcriptional cascade linking temporal transcription factors to NB3-1's RP motor neuron to muscle synaptic partnership decisions.

Table 1. Comparing the percentage of WT-like innervation pattern at third instar larvae with the percentage of WT-like cardinal transcription factor expression in late stage embryos						
NB3-1>Eve	Permanent motor axon to muscle innervation pattern in third instar larval (L3) stage			Cardinal transcription factor expression in late stage embryos (E)		
Motor axon at L3 Motor neuron cell body at E	WT-like	Abnormal innervation (ectopic)	Loss (misrouted)	Hb9 (WT)	Eve	Hb9 & Eve
14-1b, RP1	72% (23/32)	0%	28% (9/32)	19% (6/31)	71% (22/31)	10% (3/31)
30-1b, RP4	68% (25/37)	5% (2/37)	27% (10/37)	3% (1/32)	87% (28/32)	10% (3/32)
6/7-1b, RP3	76% (26/34)	12% (4/34)	12% (4/34)	12% (4/33)	79% (26/33)	9% (3/33)
12-1s, RP5	26% (10/39)	0%	74% (29/39)	30% (9/30)	50% (15/30)	20% (6/30)

Table 1. Comparing the percentage of WT-like innervation pattern at third instar larvae with the percentage of WT-like cardinal transcription factor expression in late stage embryos						
Hb9>Eve Expressed in RPs & other Hb9+ MNs	Permanent motor axon to muscle innervation pattern in third instar larval (L3) stage			Cardinal transcription factor expression in late stage embryos (E)		
Motor axon at L3 Motor neuron cell body at E	WT-like	Abnormal innervation (ectopic)	Loss (misrouted)	Hb9 (WT)	Eve	Hb9 & Eve
14-1b, RP1	16% (2/12)	0%	84% (10/12)	0%	100% (22/22)	0%
30-1b, RP4	16% (2/12)	0%	84% (10/12)	0%	96% (21/22)	4% (1/22)
6/7-1b, RP3	83% (10/12)	17% (2/12)	0%	4% (1/22)	64% (14/22)	32% (7/22)
12-1s, RP5	0%	0%	100% (12/12)	0%	77% (17/22)	23% (5/22)

Table 6.1: Correlation between molecular marker expression and synaptic connectivity decisions. Note, both tables are sub-tables within this table

Source Data for Figure 1M

Age	Genotype	Number of values	Mean (% WT)	Std. Deviation	Std. Error of Mean	p value
E16	Nkx6-/-, hb9-/-	41	121.0	6.667	1.041	NA
L3	Nkx6-/-, hb9-/-	28	123.0	5.906	1.116	0.2051

Unpaired t-test, with Welch's correction (for un-equal Std. Deviation)

Source Data for Figure 1R

Synaptic branch	Genotype	Number of values	Mean (branch #)	Std. Deviation	Std. Error of Mean	p value
Muscle 1-1b	W1118	11	1.909	0.3015	0.09091	NA
	Nkx6-/+, hb9-/+	28	1.929	0.4658	0.08802	0.9981
	Nkx6-/-, hb9-/-	26	1.962	0.5277	0.1035	0.9735
muscle 4-1b	W1118	11	2.182	0.7508	0.2264	NA
	Nkx6-/+, hb9-/+	28	1.929	0.6042	0.1142	0.6888
	Nkx6-/-, hb9-/-	35	1.914	0.6585	0.1113	0.6493
muscle 3-1b	W1118	11	1.636	0.5045	0.1521	NA
	Nkx6-/+, hb9-/+	28	1.714	0.7127	0.1347	0.9728
	Nkx6-/-, hb9-/-	35	1.486	0.5621	0.09501	0.7860
muscle 2-1b	W1118	11	2.273	0.6467	0.1950	NA
	Nkx6-/+, hb9-/+	28	1.929	0.4658	0.08802	0.3278
	Nkx6-/-, hb9-/-	31	1.935	0.4424	0.07945	0.3338
Muscle 10-1b	W1118	11	2.000	0.4472	0.1348	NA
	Nkx6-/+, hb9-/+	28	2.143	0.5245	0.09913	0.7778
	Nkx6-/-, hb9-/-	34	2.059	0.5472	0.09385	0.9775
Muscle 9-1b	W1118	10	2.200	0.6325	0.2000	NA
	Nkx6-/+, hb9-/+	28	2.000	0.5443	0.1029	0.7572
	Nkx6-/-, hb9-/-	32	2.156	0.4479	0.07918	0.9956

Source Data for Figure 1S

Synaptic branch	Genotype	Number of values	Mean (branch #)	Std. Deviation	Std. Error of Mean	p value
muscle 12-1b	W1118	19	1.632	0.5973	0.1370	NA
	Nkx6-/+, hb9-/+	21	1.857	0.5732	0.1251	0.5399
	Nkx6-/-, hb9-/-	42	1.476	0.6713	0.1036	0.7459

Table 6.2: Source Data for Figure 6.1

Source Data for Figure 6.2C

Nerve name	Genotype	Number of values	Mean (nerve outgrowth length um at E17)	Std. Deviation	Std. Error of Mean	p value
ISN	Nkx6-/+, hb9-/+	16	131.3	12.27	3.067	NA
	Nkx6-/-, hb9-/-	17	129.0	18.98	4.604	0.6846
ISNb	Nkx6-/+, hb9-/+	16	36.47	7.402	1.851	NA
	Nkx6-/-, hb9-/-	17	22.32	8.066	1.956	<0.0001

Unpaired t-test, with Welch's correction (for un-equal Std. Deviation)

Source Data for Figure 6.2D

Genotype	Number of values	Mean (ratio of ISNb/ISN % at E17)	Std. Deviation	Std. Error of Mean	p value
Nkx6-/+, hb9-/+	13	26.37	3.917	1.086	NA
Nkx6-/-, hb9-/-	16	18.09	3.881	.9703	<0.0001

Unpaired t-test, with Welch's correction (for un-equal Std. Deviation)

Table 6.3: Source Data for Figure 6.2

Source Data for Figure 6.4H-L

Synaptic branch	Genotype	Number of values	Mean (branch #)	Std. Deviation	Std. Error of Mean	p value
Muscle 13-1b	W1118	21	1.619	0.6690	0.1460	NA
	NB3-1>Eve	38	1.500	0.6472	0.1050	0.5117
	Hb9>Eve	12	0.5000	0.5222	0.1508	<0.0001
muscle 12-1b	W1118	21	1.857	0.5732	0.1251	NA
	NB3-1>Eve	38	1.658	0.9664	0.1568	0.3247
	Hb9>Eve	12	0.2500	0.4523	0.1306	<0.0001
muscle 12-1s	W1118	21	1.000	0.000	0.000	NA
	NB3-1>Eve	39	0.3333	0.6213	0.09948	<0.0001
	Hb9>Eve	12	0.000	0.000	0.000	<0.0001
muscle 14-1b	W1118	22	2.227	0.5284	0.1127	NA
	NB3-1>Eve	38	1.026	0.8538	0.1385	<0.0001
	Hb9>Eve	12	0.1667	0.3892	0.1124	<0.0001
muscle 30-1b	W1118	22	1.091	0.2942	0.06273	NA
	NB3-1>Eve	37	0.9189	0.6823	0.1122	0.1865
	Hb9>Eve	12	0.1667	0.3892	0.1124	<0.0001
muscle 6/7-1b	W1118	21	4.286	1.617	0.3528	NA
	NB3-1>Eve	39	4.538	2.563	0.4105	0.6423
	Hb9>Eve	12	5.583	2.193	0.6332	0.0903

Unpaired t-test, with Welch's correction (for un-equal Std. Deviation)

Table 6.4: Source Data for Figure 6.4

Source Data for Figure 6.6F

Synaptic branch	Genotype	Number of values	Mean (branch #)	Std. Deviation	Std. Error of Mean	p value
Muscle 4-1b	W1118	15	2.000	0.5345	0.1380	NA
	NB3-1>Eve	27	3.000	1.387	0.2669	0.002
	Hb9>Eve	11	4.636	1.567	0.4724	0.0002

Unpaired t-test, with Welch's correction (for un-equal Std. Deviation)

Source Data for Figure 6.6G

Muscle 4-1s branch number	Genotype	Number of values	% of total
0	W1118	1	5%
1		14	78%
2		3	17%
3		0	0%
0	NB3-1>Eve	2	7%
1		16	59%
2		8	30%
3		1	4%
0	Hb9>Eve	0	0%
1		5	45%
2		6	55%
3		0	0%

Table 6.5: Source Data for Figure 6.6

CHAPTER 7

ELECTRON MICROSCOPY

In this chapter, I lay out our labeling approach, which may need to be re-evaluated, and lay out our protocol, which in my hands has yielded clean, precipitate-free transmission EM data (see 7.5).

7.1 Comparative EM connectomics project of nerve cord volumes containing APEX labeled neurons

EM reconstruction is the gold standard for visualizing synaptic connectivity of neurons in the CNS. To gain insight into the underlying logic of circuit wiring we can compare and contrast the wiring morphology for motor neuron and interneurons produced from the NB7-1 lineage under wildtype conditions and prolonged expression of Hb. The overarching goal was to compare synaptic partnership and NB7-1 interneuron morphology in NB7-1>Hb animals compared to wildtype. This approach would allow us to assess the following: (1) number of synaptic contacts between each premotor interneuron and NB7-1 motor neurons, (2) monitor differences in synaptic number for NB7-1 motor neurons with regards to birth time because cell body distance from the midline is a proxy for birth order, and (3) the morphology of later born interneurons to those found in wildtype NB7-1 lineages. Ultimately, this approach would allow me to draw conclusions regarding lineage intrinsic temporal factor Hb's control of circuit wiring decisions within the CNS. In addition to this manipulation, more recently I wanted to understand how manipulating Notch in NB7-1 impacts presynaptic partnerships made within the nerve cord. When we misexpress Notch, based on our current findings, I think we are converting the Notch∧off sibling to its corresponding Notch∧on U motor neuron sibling, meaning we effectively double the number of U motor neurons. So this manipulation offers a platform to ask what happens to the synaptic partnership decisions between premotor

interneurons and the NB7-1 motor neurons. Undoubtedly establishing the tools needed to conduct comparative studies at EM resolution would be valuable in other lineage contexts and comparing between different species.

Here, are a number of questions I had previously brainstormed when thinking about the extra Eve+ motor neurons and their dendrites when we misexpress Hunchback using the NB7-1 driver. They may be helpful for someone who wants to carry this project forward:

Question: What impact does prolonged hunchback expression have on circuit wiring for the extra motor neuron dendrite synaptic connections to pre motor neuron interneurons?

More specific questions that stem from the main question:

For the motor neurons possessing a contralateral branch, does this region of the dendrite contain sites of synaptic input?

For the contralateral branch, do pre motor interneuron synaptic partners resemble those found uniquely onto U1, U2, a combination of U1 and U2, or novel?

For the contralateral branch, if pre motor interneuron synaptic partners resemble those found onto U1, U2, or are a combination of U1 and U2, do the synaptic partners contact each motor neuron with the same number of synapses or is there variability in synaptic connections?

For the motor neurons lacking a contralateral branch, does the dendritic region that extends close to the midline contain sites of synaptic input? Do these motor neurons form synapses with pre motor interneuron partners known to synapse to U motor neurons?

Regardless the outcome of these questions, the answers will provide insight into the extent of hunchback's control of circuit wiring between motor neurons and the pre-motor interneurons within the CNS.

7.2 EM protocol background

A major limitation of comparative studies at EM resolution is quickly identifying cells of interest. Tracing out neurons is non-trivial. To put this task into perspective, the single 1st instar CNS EM volume published in 2016 (Schneider-Mizell et al., 2016)[28] and accessible by many groups has yet to have all neurons fully traced out. A comparative connectomics project by definition already doubles the number of samples from one to at least two. So we wanted to expedite the process by labeling neurons of interest. A classic labeling approach is to use HRP, an enzyme which catalyzes a reaction involving hydrogen peroxidase and 3-3' diaminobenzidine (DAB). The reaction product is electron-dense meaning the reaction product is strikingly dark and resembles the lipid rich cell membranes, which osmium tetroxide, a heavy metal, reacts with adding density and contrast. Older studies labeling neurons in insect nervous systems simply injected HRP intracellularly by passing a current (Watson and Burrows, 1981)[220]. Next, the tissue was fixed and exposed to reaction substrates (DAB and hydrogen peroxide or a glucose oxidase reaction mixture involving ammonium chloride, glucose, and glucose oxidase. Many of these early studies were done in non-genetically amenable but relatively large insects like locusts. Fortunately, in Drosophila, genetic labeling strategies have been employed to specifically express HRP in a subset of neurons (Watts et al., 2004)[221]. While HRP activity is the most sensitive enzyme, active HRP is dependent on subcellular environments (Martell et al., 2012)[222]. For example HRP is inactive when expressed in mammalian cytosol. To this end, our initial collaboration with the Kasthuri lab recommended using APEX (enhanced APX, which stands for ascorbate peroxidase), which essentially catalyzes the same reaction HRP does. We have been using a UAS-NES(nuclear export signal)-APEX-GFP line (Chen et al., 2015)[223]. Based on staining against GFP in fixed tissue, APEX-GFP is driven well by the NB7-1 driver and persists in 1st instar larva (Figure 7.11).

While there is some evidence from our previous collaborator Gregg Wildenberg that

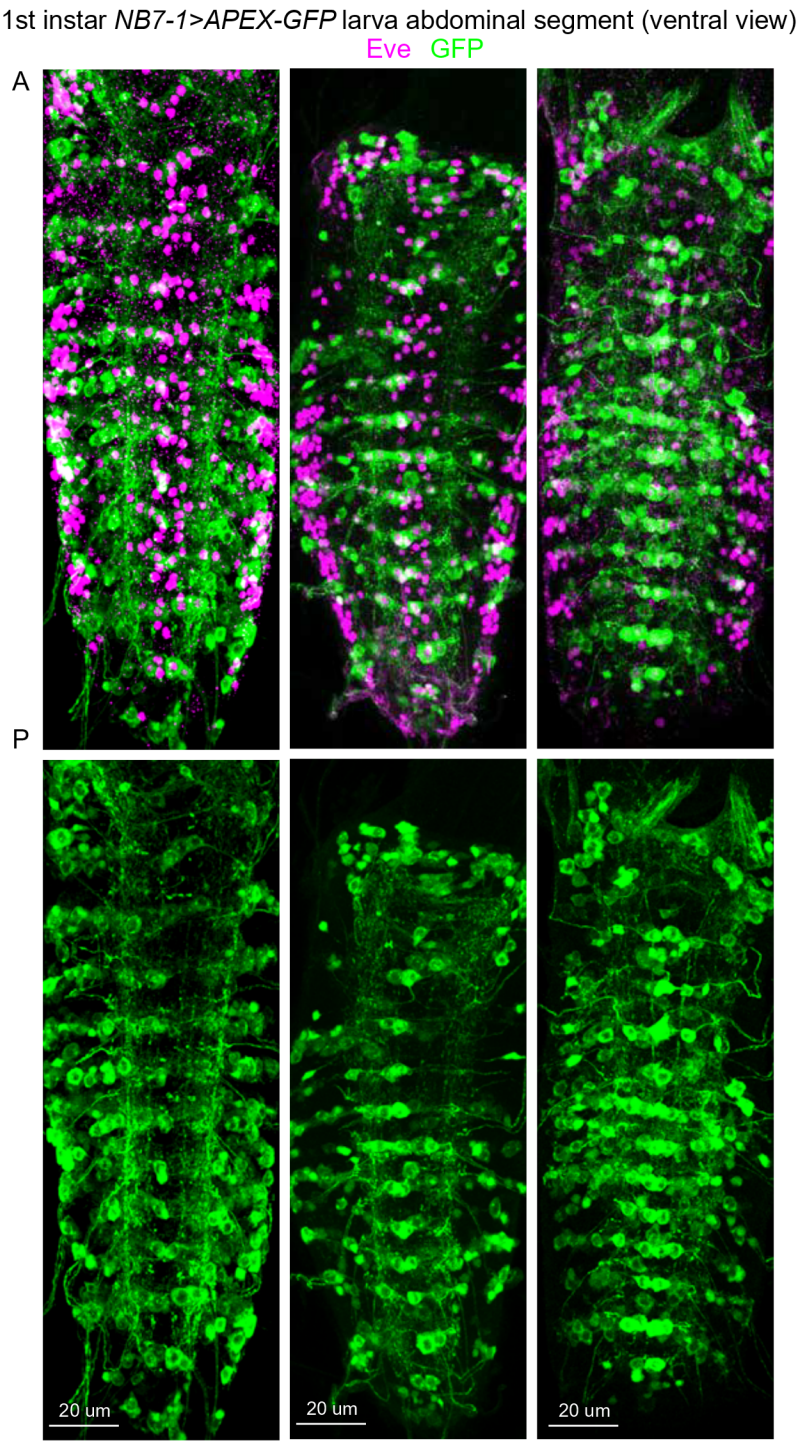


Figure 7.1: APEX-GFP expression in 1st instar larval nerve cords when driven by the NB7-1 driver

APEX can catalyze the reaction to produce electron-dense products (Figures 7.2 7.3), we still have not established a successful protocol where the APEX mediated reaction is successful (ie reaction product is present) and the nerve cord is undamaged or littered with precipitates. Precipitates are contamination that are electron-dense aggregates that obscure the underlying biological membranes, which is a major issue if we want to go in and accurately trace neurites.

One of the reaction substrates, hydrogen peroxide, easily damages tissue, so Gregg Wildenberg recommended using very small concentrations of hydrogen peroxide but on the flipside, we need enough hydrogen peroxide, reaction substrate, for the reaction to work. Future experiments will need to test a range of hydrogen peroxide concentrations. Fortunately the reaction product can be visualized using light microscopy. So I recommend optimizing this step in the Heckscher lab space instead of running through the whole EM fix protocol. If we find that the reaction only works with hydrogen peroxide concentrations that are damaging to the issue, we will want to explore HRP-based approaches. An alternative is to use an HRP based approach that Tim Sander's lab has had success with. We received plasmid DNA from them so I can clone the HRP downstream of a UAS sequence.

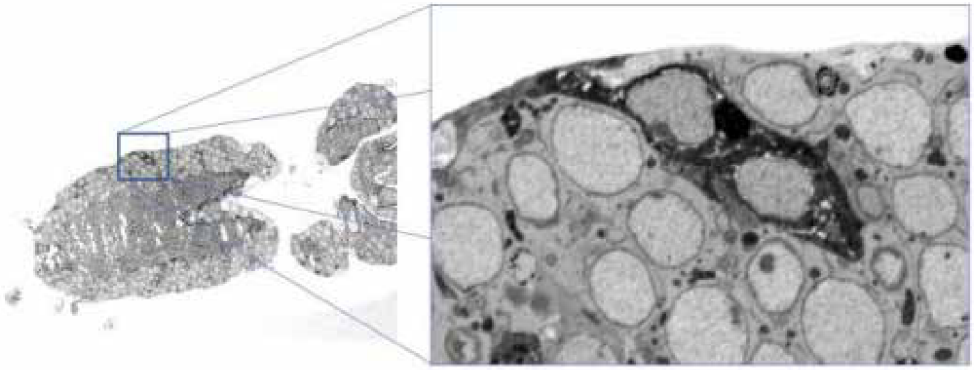
A must-read for anyone desiring to learn the EM chemical fixation process is Electron Microscopy by Bozzola and Russell (the Heckscher lab has a copy in the "library" outside of Ellie's office). Note, Jotham (Joe) Austin, UChicago's EM Facility Director strongly urges folks from non-EM backgrounds to read this book before conducting any EM chemical fixation-related experiments.

7.3 EM protocol

Updated protocol (adapted from Gregg Wildenberg. Joe Austin, UChicago EM Facility Director, recommended more wash steps and a different resin to embed tissue in. I developed the resin infiltration protocol from skimming widely through previous published EM

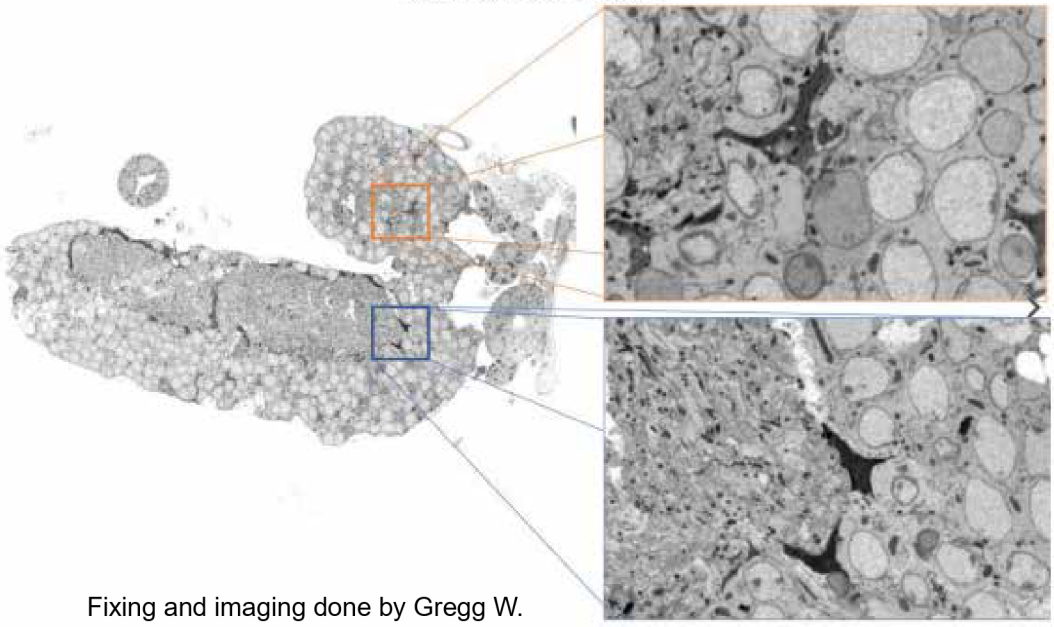
Here we are looking at the nerve cord top down (D-V). In the box are cell bodies, positioned adjacent to the neuropil. We believe the precipitate in these cell bodies is APEX. We are driving APEX in a stem cell lineage that generates ~40 neurons

12/2019_Control Image 1/2



Here we are looking at another brain. The yellow box highlights cell bodies in the brain lobes. It looks like we have some precipitate here but I'm unsure if this is indeed a cell body labeled by APEX because the shape looks more deformed compared to the surrounding cell bodies. It could be glia based on the shape and the higher electron density (higher concentration of vesicles etc). The blue box shows similarly shaped darker regions, which look like they are surrounding the nerve cord. This is likely glial and not APEX labeled neurites/cell bodies.

12/2019_Control Image 2/2



Fixing and imaging done by Gregg W.

Figure 7.2: Possible APEX-mediated reaction product accumulation in neuronal cell bodies

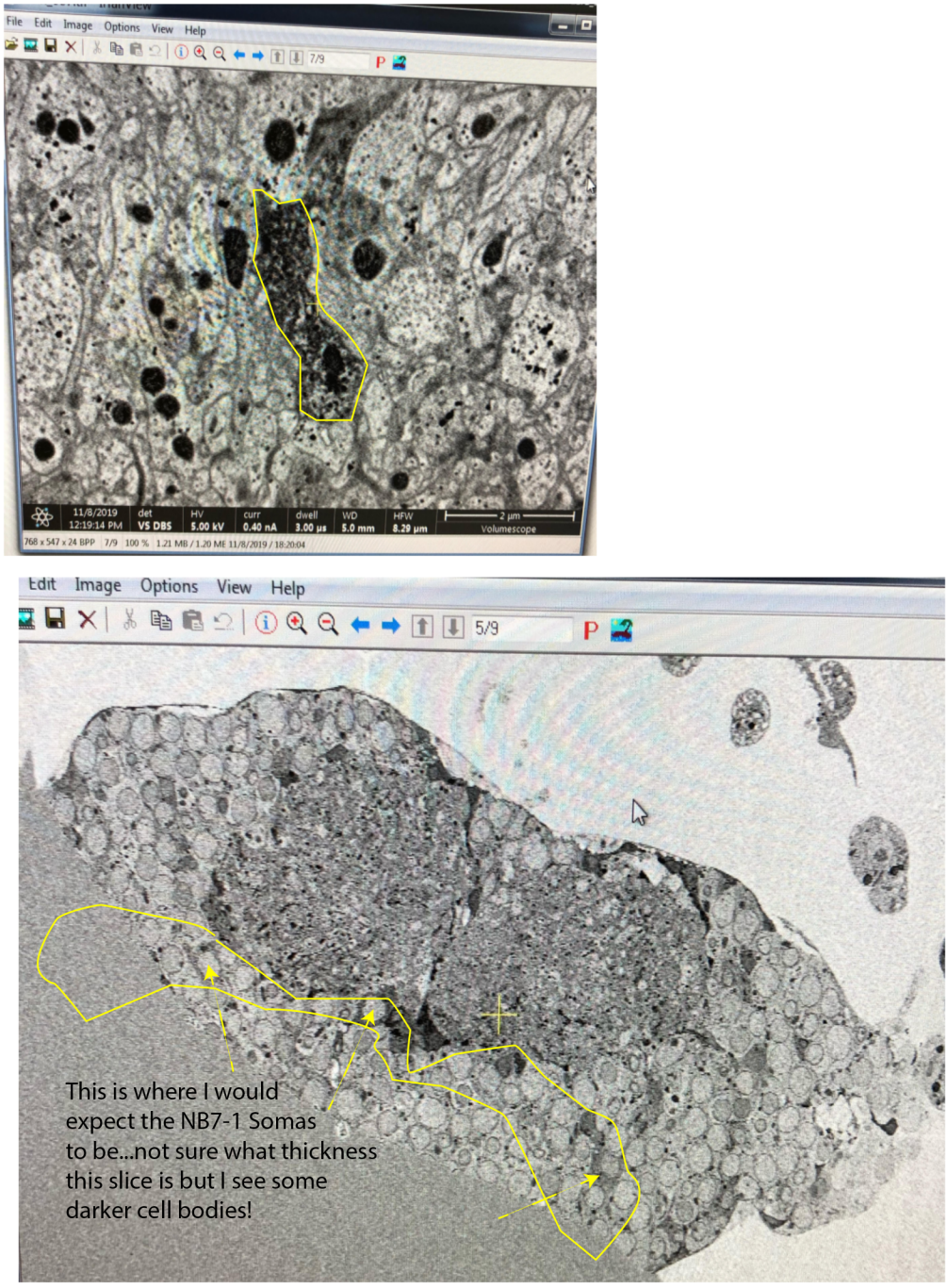


Figure 7.3: Possible APEX-mediated reaction product accumulation in neuronal cell bodies of serial section taken by Gregg Wildenberg

protocols and talking with Yimei Chen, UChicago EM Associate Technical Director).

Day 1.

For 7 minutes pull as many 1st instar brains in 0.1 M ice cold Cacodylate buffer Place brains in a tissue basket (70um cell strainer Fisherbrand cat no. 22363547) submerged in 0.1 M ice cold Cacodylate buffer (Figure 7.4A)

Note: Must place pulled brains into Cacodylate buffer, if you attempt to place pulled brains straight into fixative, brains will deform upon contact to the fixative solution.

Note: Use a fresh tissue basket for each experiment. I attempted to "clean" the baskets and reuse them but unfortunately no cleaning will remove all contaminants (e.g. oxidized Osmium).

After 7 minutes transfer the the basket with brains to the fix solution

Fixation: 2% paraformaldehyde, 2.5% gluteraldehyde, 0.1 M Cacodylate pH 7.4

Dilute stocks for 10 ml of fix

0.2 M pH 7.4 Na Cacodylate: 5 ml

25% Gluteraldehyde: 1 ml

20% Paraformaldehyde: 1 ml

MilliQ water: 3 ml

Incubate for 2 hours at RT with agitation (use a small stir bar placed in the container holding the brain basket(s).

Note: For each step where a new chemical is introduced, use a fresh plastic container.

Note: Incubation time can be flexible. I have done overnight at 4c. I found an article where adult Drosophila brains were fixed for 2 hours at RT (Hayworth et al., 2015)[224]. Considering that Drosophila larvae brains are much smaller they can likely be fixed within 1 hour at RT.

After fixation, transfer basket to a fresh container containing ice cold 0.1 M Cacodylate

buffer, wash 4x for 10 minutes each.

Incubate in 1x DAB in 0.1 M Cacodylate for 30 minutes at 4c

10x DAB recipe:

35 mg (0.035g) of DAB

10.0 ml of 0.1 M HCI

Add H202 to the 1x DAB solution and incubate for 5-10 minutes at RT or until dark precipitate is visible.

Dilute H202 by adding 1ul 30% H202 into 1ml of MilliQ water

Try the following dilutions:

1:1000 (e.g. 10 ul of dilution into 10 ml of 1x DAB solution

1:10,000 (e.g. 1 ul of dilution into 10 ml of 1x DAB solution

Note: I did 1:1000 and 1:5000 dilutions and I didn't really see a dark precipitate (I was using black baskets so that made it difficult to see a color change). I ended up waiting 40 minutes before moving to the next step.

Transfer, wash in ice cold 0.1 M Cacodylate buffer, 4x for 10 minutes each

Transfer to ice cold 1% Osmium in 0.1 Cacodylate buffer for 30 minutes at 4c

Transfer to Potassium ferrocyanide (no wash in between): (0.0085 g/ml K Ferro in 0.1 M Na Cacodylate), incubate for 30 minutes at RT, agitate Transfer, wash in MilliQ water 5x for 20 minutes each

Transfer to 4% pyrogallol in MilliQ water, filter 4% pyrogallol with 0.22 um syringe filter, incubate for 30 minutes, agitate

Transfer, wash in MilliQ water 5x for 20 minutes each

Transfer to 2% Osmium in water for 30 minutes at RT

Transfer, wash in MilliQ water 5x for 20 minutes each

Transfer to 1% UA overnight at 4c.

Day 2.

Incubate in 1% UA for 30 minutes at 50c

Transfer, wash in MilliQ water 5x for 20 minutes each

Add aspartic acid buffered PB(II) nitrate for 30 minutes at 50c

Recipe:

0.03 M Aspartic Acid: dissolve 0.1 g of Aspartic Acid in 25 ml water, adjust pH to 3.84 by adding 250 ul of KOH

Add 0.066 g lead(II) nitrate/10 ml to 0.03 M Aspartic Acid and adjust pH to 5.0 by adding 235 ul 1N KOH/10 ml

Vortex to fully dissolve

Filter solution through 0.22 um syringe filter

Note: I came across an article (Tapia et al., 2012)[225] where they heat up the solution to 50-60c for stain stability, heating greatly aided dissolving.

Transfer, wash in MilliQ water 4x for 15 minutes each

Note: This is a safe stopping point where brains are stored in 4c overnight

At this point, transfer brains from the baskets to eppendorf tubes, use a chopped off plastic pipette.

Dehydration in acetone, agitate, sequence:

25% acetone in milliQ water for 10 minutes

50% acetone in milliQ water for 10 minutes

75% acetone in milliQ water for 10 minutes

95% acetone in milliQ water for 10 minutes

95% acetone in milliQ water for 10 minutes

100% acetone in milliQ water for 10 minutes

100% acetone in milliQ water for 10 minutes

100% acetone in milliQ water for 10 minutes

2:1 acetone in Durcupan resin for 30 minutes at RT

2:1 acetone in Durcupan resin for 30 minutes at RT

1:1 acetone in Durcupan resin overnight at RT

Durcupan recipe, volumes (by weight) I used and had success:

'A/M' bottle 17.1 g

'B' bottle 15.1 g

'C' bottle 0.46 g

'D' bottle 0.16 g

Note: Do not follow the Durcupan instructions for curing sequence. They recommend applying heat to an incubation step once the Durcupan resin has the accelerator. I followed these directions and my resin semi-cured (think soft candy viscosity) in the eppendorf tube. It was a disaster. The resin infiltration must be slow and gentle to ensure that resin fully infiltrates the tissue.

Day 3.

100% Durcupan resin for 6 hours at RT

Place brains in molds, cure in oven 60c for 2-3 days (Figure 7.4B). Take care to position the brains at the tapered end of the mold because this the resin block is cut first.

Notes: I chopped off the tip of a plastic pipette to transfer the brains from the eppendorf to the molds. Bubbles are your enemy. If there are some, remove/pop them. To position the brains I used a metal pick (used to dechorionate) to gently swirl the resin to move the brains. Do not touch the metal to the brains. This action will destroy the extremely fragile tissue.

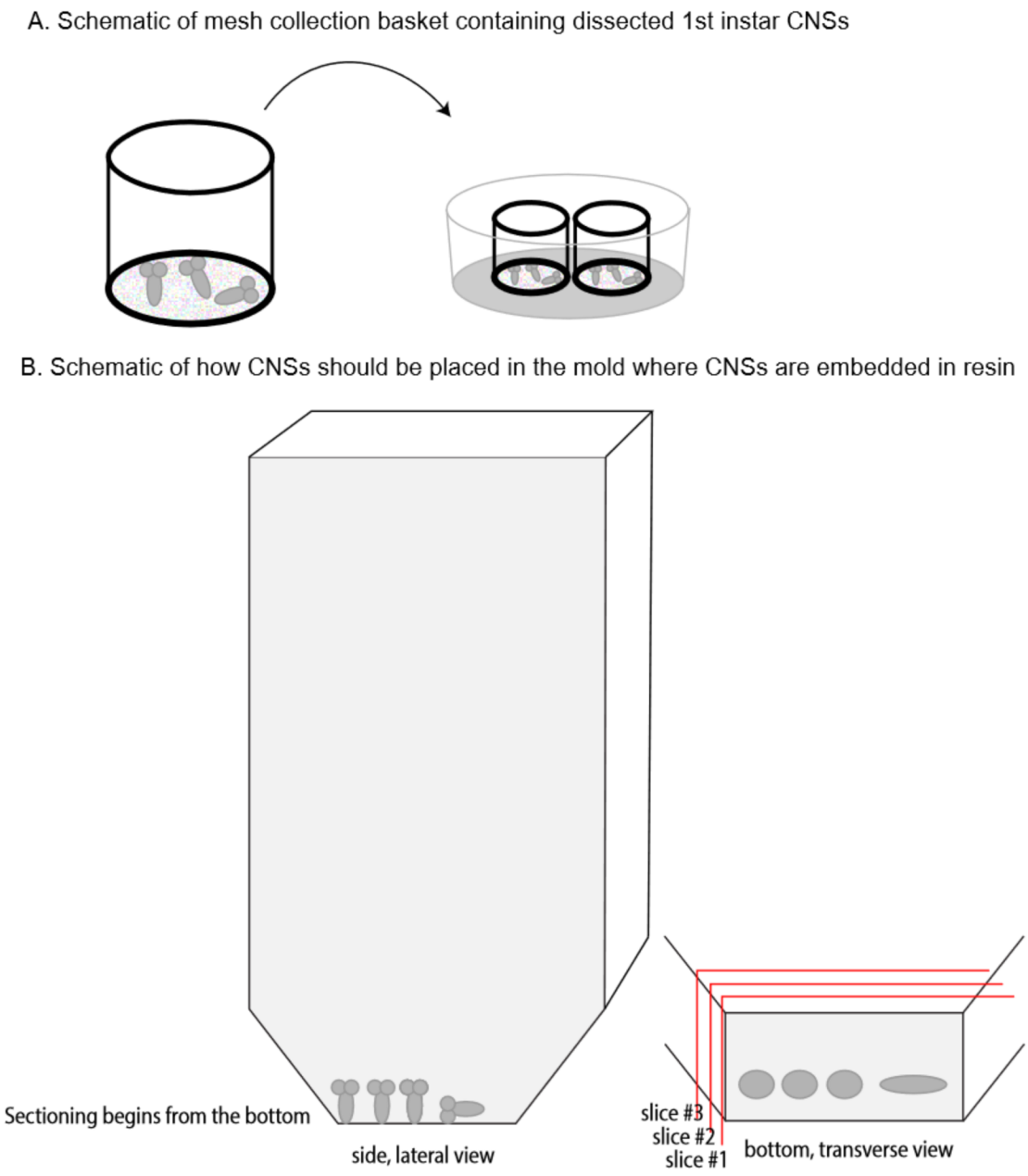


Figure 7.4: Schematics for EM protocol

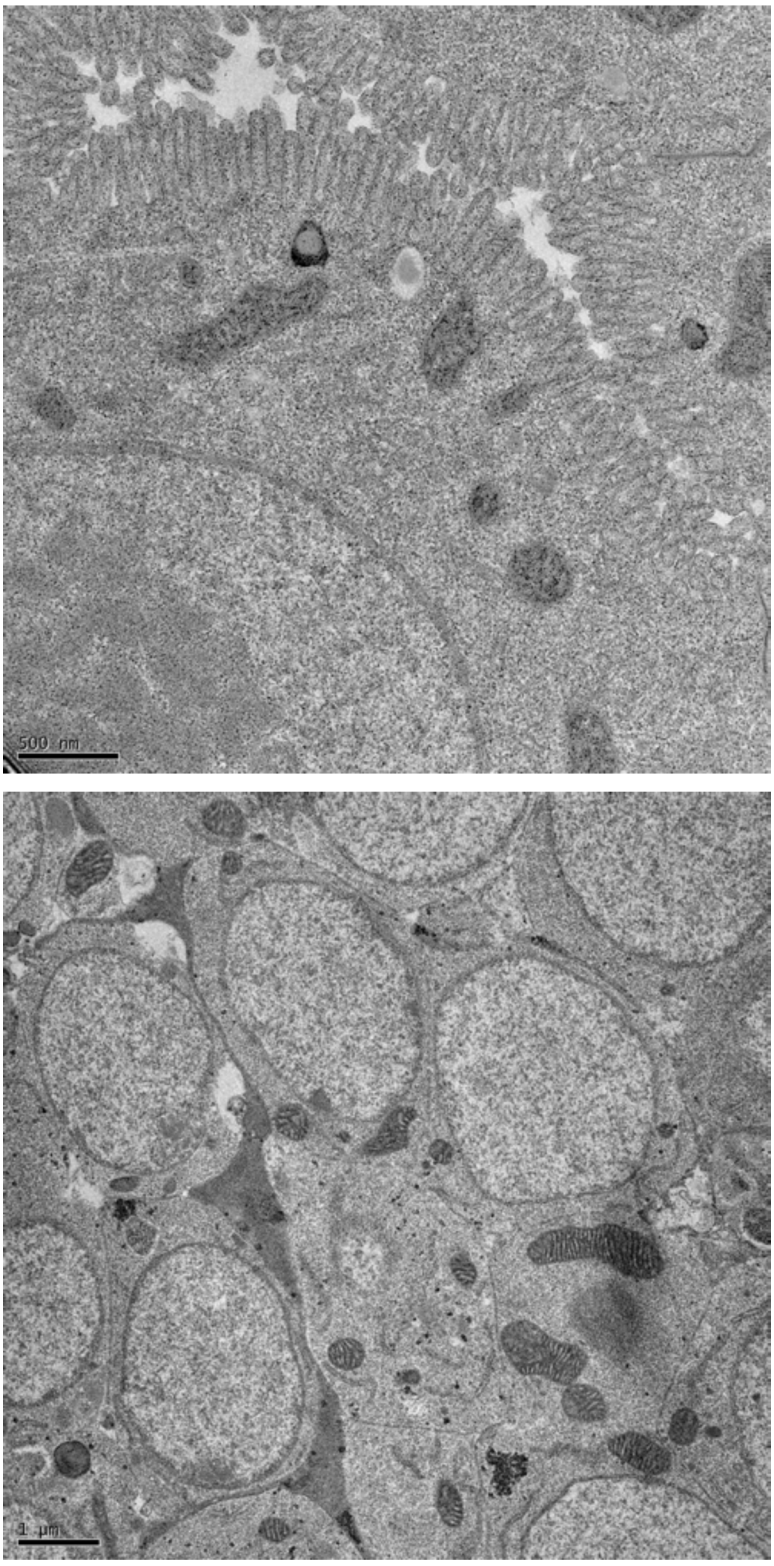


Figure 7.5: EM images obtained when Julia prepared samples using the provided protocol

CHAPTER 8

APPENDIX

8.1 Misexpressing Hunchback in NB7-1 reduces larval crawling speed

When we misexpress Hunchback using the NB7-1 driver (*NB7-1>Hb*), we find dramatic and permanent rewiring of NB7-1 lineage Eve+ motor neurons onto dorsal muscles in the dorsal muscle field (Meng et al., 2019)[2]. Specifically, we find an increase in the number of synaptic branches onto some dorsal muscles (M9, M10, M2) and a decrease onto other dorsal muscles (M3, M4). Early on, we wondered what impact this manipulation of Hunchback has on the larval crawling behavior. Specifically we wanted to know what impact if any this manipulation had on larval crawling speed during each larval stage (L1-L3). To address this question, I imaged and tracked larvae using our lab's behavior-imaging set-up and the open-source FIMTrack software (Risse et al., 2017)[226]. For analysis, I used custom written MATLAB code created previously in the Heckscher lab (I obtained the code from Zarion Marshall).

Each column in (Figure 8.1A-B) was compiled from data collected in four independent trials. Each column in (Figure 8.1C) was compiled from data collected in three independent trials. For the first instar larval stage (L1), I found no significant differences in the crawling speed of *NB7-1>Hb* larvae compared to my two controls: *NB7-1/+* and *W1118* (Figure 8.1A). By the second instar larval stage (L2), I found a slight significant decrease in the crawling speed of *NB7-1>Hb* larvae compared to my *W1118* control but not my *NB7-1/+* control (Figure 8.1B). Finally, at the last larval stage (L3) before pupal formation, I found a significant decrease in the crawling speed of *NB7-1>Hb* larvae compared to my *W1118* control (Figure 8.1C). Combined, these data reveal that misexpressing Hunchback in NB7-1 can reduce larval crawling speed but only at later larval stages, particularly the last, L3.

Since I only measured crawling speed, it is possible that manipulating Hunchback expression in NB7-1 may impact other larval behaviors such as hunching, head-sweeps, escape rolling, c-bending, etc.

While the question of behavior is one I often get asked when presenting my published data, the reason this data is unpublished and subjected to the appendix of my thesis is because the underlying basis for the behavioral phenotype is not readily obvious from my these behavioral data. Let me explain. We know that misexpressing Hunchback in NB7-1 increases the number of Eve+ motor neurons that are generated at the expense of later born interneurons. This means that the underlying basis of the observed behavioral phenotype could be a result of increased motor neurons or loss of later born interneurons, or a combination of the two. From the onset of doing the behavioral experiments, I knew that if I did observe a phenotype, I wouldn't know what caused it but if on the other hand no phenotype was observed, it would have allowed me to conclude that despite gross rewiring of permanent motor neuron to muscle synaptic connectivity, the motor system is somehow able to compensate. What my

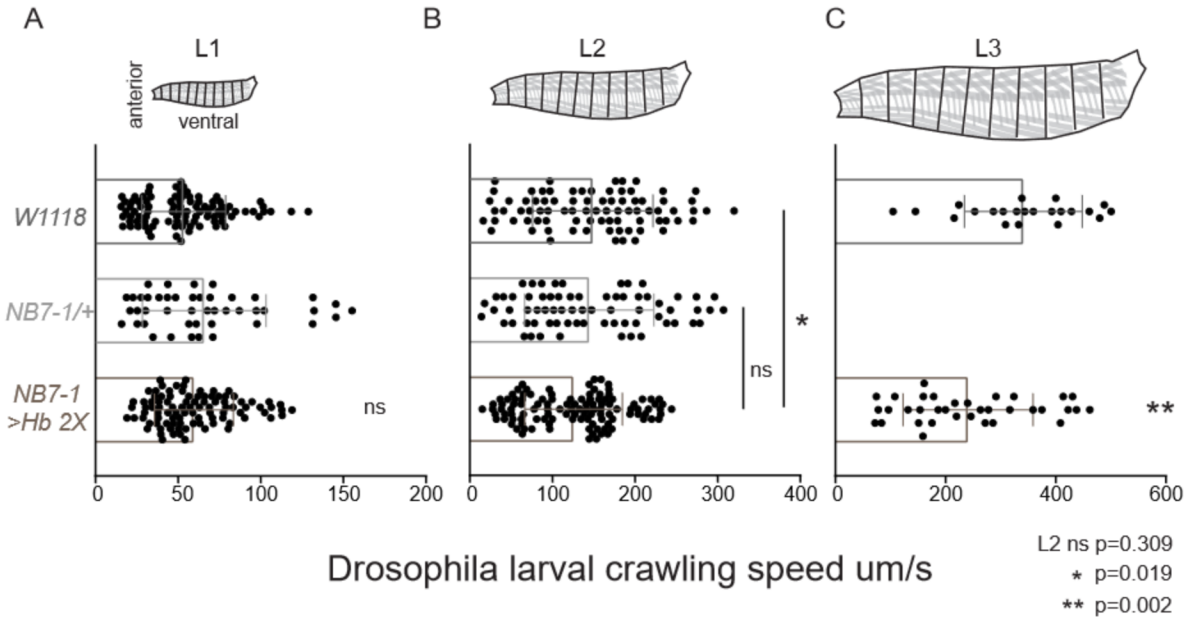


Figure 8.1: larval crawling speed behavior

data suggests is that there is something about earlier larval stages that might compensate for the perturbed NB7-1 lineage.

Since doing these experiments, we have learned a few more things. Supported by bits of data here and there and some speculation, I offer my current perspectives on what may be causing the behavioral phenotype we observe and recommendations for future experiments.

First, we have evidence that muscles still have a wildtype-like response to nerve stimulation even if these muscles are contacted by an increased number of synaptic branches from extra motor neurons . We learned this from electrophysiological recordings done by Yupu Wang [3] on ventral muscles when Hunchback is misexpressed in the NB3-1 lineage, which generates the ventrally projecting RP motor neurons. Conceptually this manipulation is nearly identical to when we misexpress Hunchback in the NB7-1 lineage, which generates the dorsally projecting U motor neurons. In both manipulations there is a dramatic rewiring pattern where there is an increase of synaptic branches onto some muscles and loss of synaptic branches onto other muscles within the same muscle region (i.e. dorsal vs ventral).

Second, we have unpublished data in the lab from Zarion Marshall that loss of U motor neurons in development does not alter first instar larval crawling speed. Zarion ablated the U motor neurons by driving hid, rpr with the CQ driver CQ-GAL4>UAS-hid,rpr. From Zarion's data alone, we cannot rule out the possibility that reduced innervation on two of the dorsal muscles (M3 and M4) does not impact crawling speed at later larval stages. Ideally, his ablation manipulation should be repeated and third instar larval crawling speed should be measured.

Third, we now know that when interneurons are born after the extra Eve motor neurons generated in NB7-1>Hb animals, the majority of these interneurons fail to make arbors. Effectively this means that nearly all NB7-1 interneurons do not integrate into their normal motor circuits either because they were never born or because they do not form arbors. From the Heckscher lab's experience with NB3-3 EL interneurons, from a behavioral standpoint, we

often find that loss of interneurons in development is less deleterious for an animal compared to when interneuorns are born but project aberrantly. Allow me to speculate. I think this reveals that as motor circuits are first assembling within the nerve cord, there is a degree of plasticity where loss of some synaptic partnerships is more easily compensated than the formation of some aberrant synaptic partnerships. If we apply this concept from NB3-3, this would suggest that loss of NB7-1 interneuron integration into their respective motor circuits is likely compensated, so this is not the underlying basis of the crawling speed phenotype we observe. So what is left? What could be the basis for the phentoype we observe? I think the answer lies with the increased number of early-like motor neuron dendritic arbors in the nerve cord. When we misexpress Hunchback, we find that around 70% of the motor neurons have dendritic arbors that resemble the earliest born motor neurons (U1 and U2). So the question is how many synaptic partnerships do these extra motor neurons form and with whom (presumably pre-motor interneurons)? To address this question, we need to do comparative EM connectomics that offer single-synaptic resolution.

Here, I will layout a hypothetical situation, which may explain the phenotype and why crawling speed defects are only manifest in late larval stages. There is evidence that between first instar and third instar larvae the synaptic partnerships remain the same but the number of synapses formed between partners increases by five-fold (Gerhard et al., 2017)[200]. When we misexpress Hunchback in NB7-1, what if the extra motor neurons are contacting and forming synapses with premoter interneurons that normally contact the early born U1 and U2 motor neurons but there is an issue with scaling the number of synapses as the larva ages? During L1, when the number of synapses is relatively similar to the number of synapses initially made, the motor circuits may function relatively normal. However as the the larva grows perhaps these synaptic connections, which would normally be strengthened, now no longer are strengthened, meaning the number of synaptic connections does not change from L1 to L3. We know that in the 1st instar nerve cord many one-off connections are present.

	Genotype	Number of values	Mean (speed um/s)	Std. Deviation	Std. Error of Mean	p value
L1	W1118	94	53.40	25.37	2.617	NA
	NB7-1/+	45	65.82	37.40	5.575	0.0229*
	NB7-1>Hb	95	59.57	23.88	2.450	0.0869*
L2	W1118	82	148.9	72.91	8.052	NA
	NB7-1/+	69	144.6	78.17	9.410	0.7269
	NB7-1>Hb	114	125.7	59.13	5.538	0.0149*
L3	W1118	22	341.4	107.0	22.81	NA
	NB7-1>Hb	35	240.9	118.0	19.95	0.0020*

*Unpaired t-test Welch (for un-equal Std. Deviation)

Table 8.1: Source Data for Behavior data in 8.1

By one-off connections, I mean a given interneuron only forms one synaptic connection with another interneuron. Could it be that one-off synaptic connections are not strengthened as the larva grows? Could there be some thresh-hold value for the number of synaptic connections between two partners that will go on to be strengthened versus pruned away? If so, it might be possible that when there are extra early-like motor neurons, each motor neuron makes fewer synapses with premotor interneurons and the reduction in synapse number may fall under the threshhold value required for synaptic partnerships to be strengthened.

I think a large black box in our understanding of functional motor circuit assembly lies with the "functional" part. While I wouldn't say our understanding of anatomical integration is anywhere near to complete, what I have learned from my thesis is that integration is largely driven by inherited information the neuronal progeny receives from the neuroblast parent. Once a neuron is integrated into a motor circuit, how is its integration maintained functionally? To what extent can functional changes occur at the level of altered synaptic strengths between partners? If these changes occur, how are they changing over the larval lifespan? I know obtaining single synaptic resolution within the nerve cord is really hard but we need to push forward with developing approaches (expansion microscopy, EM) in the lab to achieve the necessary resolution to begin to address these questions.

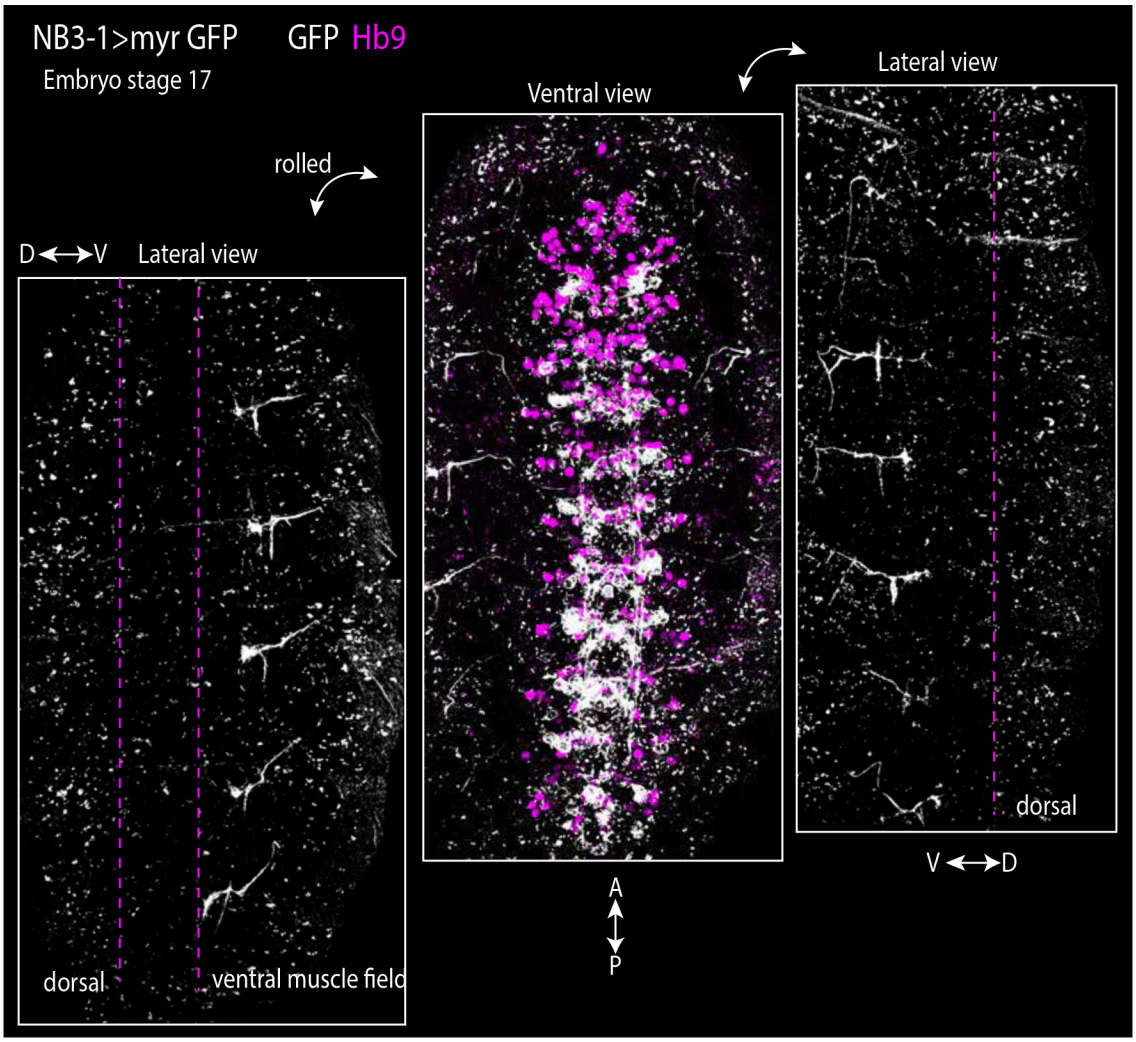


Figure 8.2: NB3-1 driver

8.2 Characterization of the NB3-1 driver and lineage

I include this in the appendix as a resource and evidence that the NB3-1 driver hits motor neurons that innervate ventral muscles. However, sometimes I think I see a motor axon extend to the transverse muscle field (Figure 8.2 left-most panel, second segment from the top). Could NB3-1 also generate a transverse-projecting motor neuron? If someone wants to follow this up, I'd recommend driving membrane-bound GFP to identify cells hit by the NB3-1 driver and stain for worniu (neuroblast marker) and pMad (all motor neurons are pMad but not all pMad+ neurons are motor neurons).

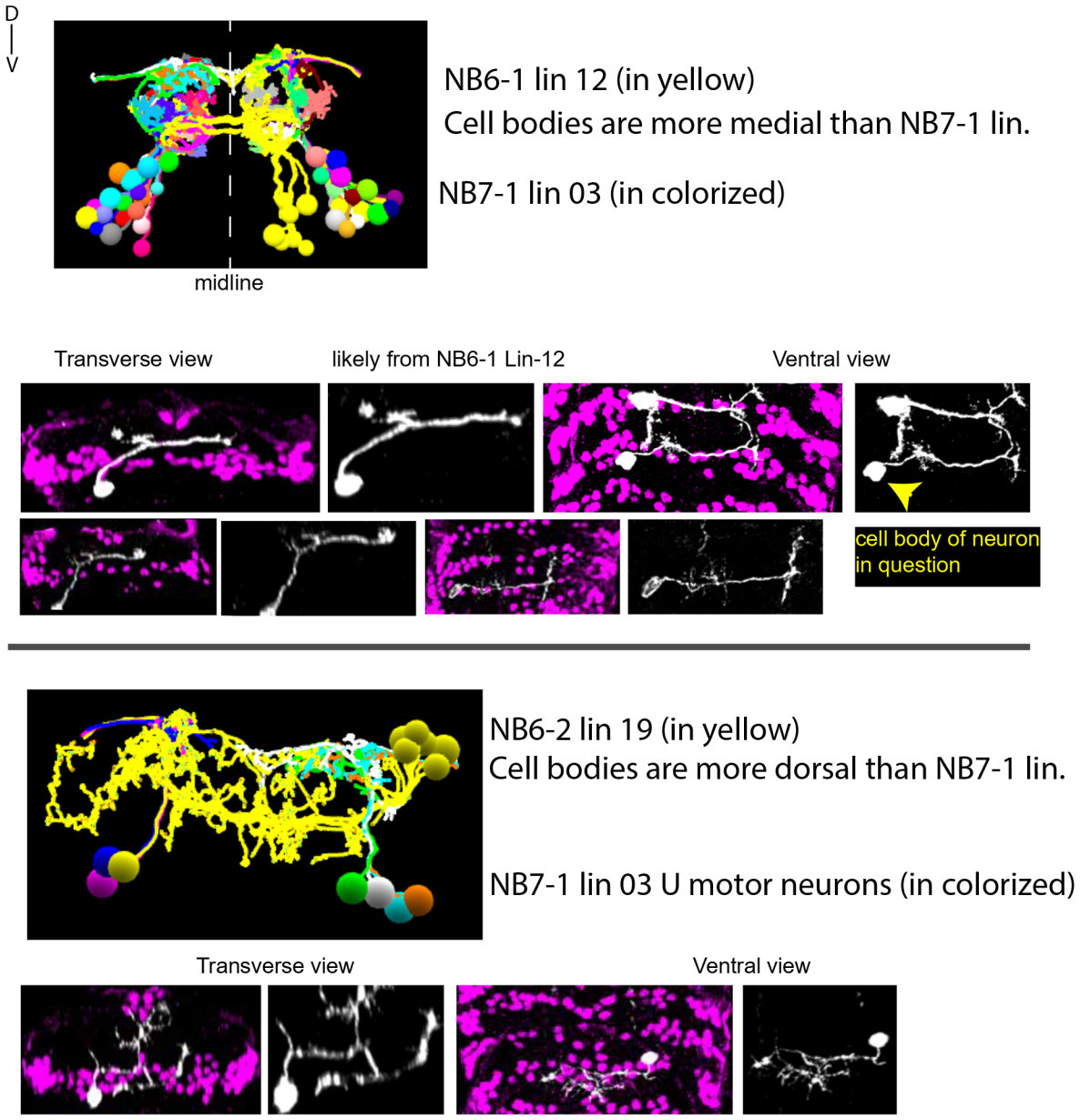


Figure 8.3: NB7-1 driver

8.3 Characterization of the NB7-1 driver and lineage

I include this in the appendix as a resource and evidence that the NB7-1 driver frequently hits the NB6-1 and NB6-2 lineage in addition to NB7-1.

8.4 Unpublished VP16::Hb related experiments

Full disclaimer, my fly line containing two copies of VP16::Hb on the II and III chromosomes died in my stocks during 2021. I recommend if someone wants to do future VP16::Hb related experiments, they request the VP16::Hb 2x line from the Doe lab.

The temporal factor, Hunchback is a zinc-finger transcription factor. Among its other capabilities, Hunchback can directly activate or repress target gene expression. To begin to distinguish the role of Hunchback's activator vs repressive capabilities, we turned to a consecutively activate form of Hunchback (Tran et al., 2010)[131]. Here, VP16, the potent transcriptional activator is tethered to Hunchback (VP16::Hb). Characterization of VP16::Hb found that this construct can activate gene targets of Hunchback that are known to normally be activated and repressed by Hunchback (Tran et al., 2010)[131]. We found that prolonging the expression of the activating Hunchback (tethered to the vp16 transcription factor) cannot increase the number of motor neurons produced but it can lead to an increase in both U1/U2 molecular identity (assessed by being Eve+ and Hb+) at L3 and notably, increased synapse formation onto the U1 muscle target rather than on the U2 muscle target (Figure 8.4A-C,F)(Meng et al., 2019)[2].

At the time of this discovery, I was eager to misexpress VP16::Hb in two different contexts. First, I wanted to misexpress VP16::Hb and the normal Hb transgene to test if the inability of the VP16::Hb to increase the number of Eve+ motor neurons was limiting the number of motor neurons with U1/U2 molecular identity and terminal features. Second, I wanted to misexpress VP16::Hb only in the U motor neurons to test if inherited Hunchback has an activating role in the post-mitotic neuron and if this activating role is sufficient to specify a given post-mitotic motor neuron's identity and synaptic partnership fate. In the subsections, I present my unpublished findings.

	Genotype	Number of values	Mean (# of cell bodies at L3)	Std. Deviation	Std. Error of Mean	p value
Total Eve+	NB7-1>VP16::Hb-2x	71	5.042	0.6853	0.08133	NA
	NB7-1>VP16::Hb-2x, Hb-1x	14	10.57	2.652	0.7088	<0.0001*
Eve+ Hb+	NB7-1>VP16::Hb-2x	71	3.690	1.316	0.1562	NA
	NB7-1>VP16::Hb-2x, Hb-1x	14	5.071	1.592	0.4254	0.0074*

*Unpaired t-test Welch (for un-equal Std. Deviation)

Table 8.2: Source Data for Figure 8.4

8.4.1 Impact misexpressing VP16::HB2x and Hb1x using the NB7-1 GAL4 driver

When I expressed both the activating hunchback and regular hunchback in NB7-1 (*NB7-1>VP16::Hb 2x and Hb 1x*), I assessed both the molecular identity and motor neuron to dorsal muscle synaptic partnerships at L3. Here, I only present molecular identity data at L3 because these results negate the need to check the synapses onto the U motor neuron muscle targets (I did check but I did not feel like it added anything to the conclusion so I left it out of the figure). First, as expected, I find that the number of motor neurons is on average 11 Eve+ motor neurons (Figure 8.4D) (Table 8.2), which is what we observe when we drive only 1 copy of the Hb transgene (Meng et al., 2019) [2]. Second, somewhat unexpectedly, I find that on average only 5 of the Eve+ motor neurons express Hb+ at third instar larval stages (Figure 8.4E,G-H). This means that the inability for the VP16::Hb construct to increase the number of Eve+ and Hb+ motor neurons is not limited by the number of Eve+ motor neurons generated. Rather, this result suggests that VP16::Hb's ability to lead to permanent Hb expression in Eve+ motor neurons is limited to the number of divisions it takes to generate the five U motor neurons.

At the time of this discovery I was reminded of M. Kohwi's observation that after the fifth division, the endogenous Hunchback locus is positioned at the nuclear Lamin, thus

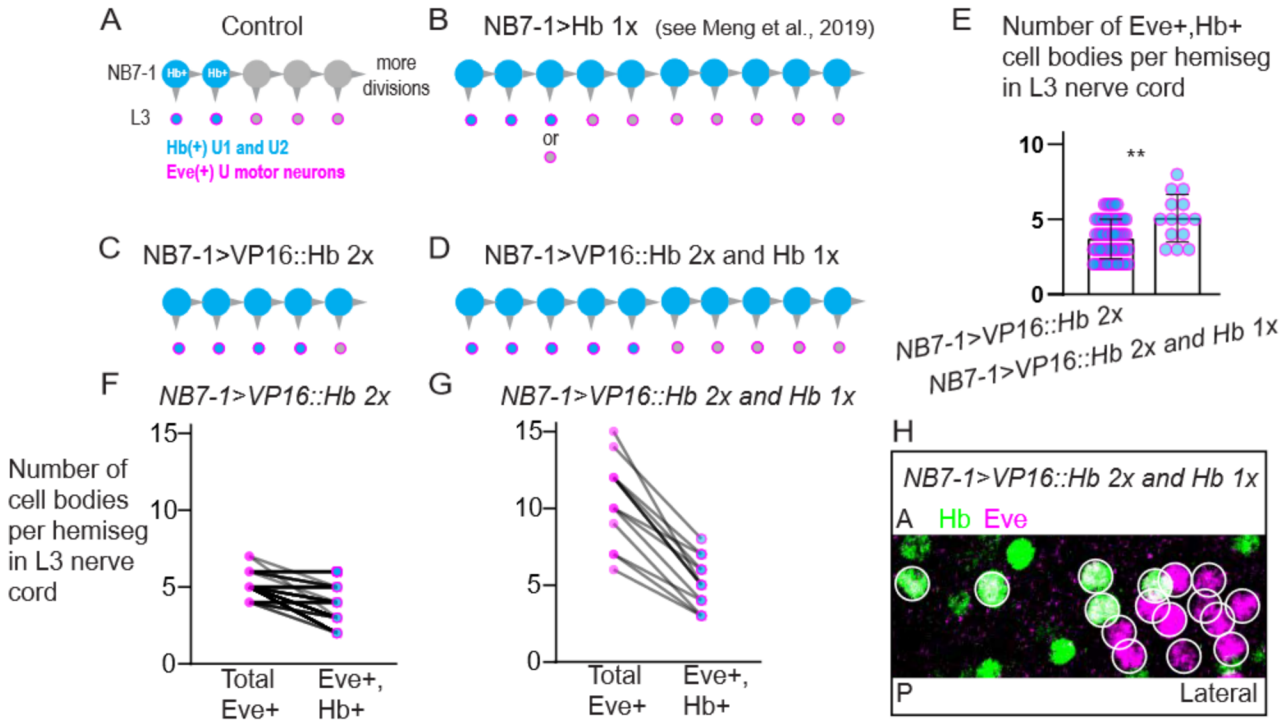


Figure 8.4: Misexpressing constitutively activated form of Hunchback, VP16::Hb can only lead to an average of 5 Hb+, Eve+ neurons at L3 regardless of the number of Eve+ neurons generated. (**A-D**). Illustrations of the divisions in NB7-1 in Control, NB7-1>Hb 1x, NB71>VP16::Hb 2x, and NB71>VP16::Hb 2x, Hb 1x. Each gray arrowhead represents cell division, large circles represent NB7-1. The rows of small circles represent U motor neuron identity at L3. In Control, two Eve+ (magenta) neurons are Hb+ (blue), in NB7-1>Hb 1x often two but sometimes three Eve+ (magenta) neurons are Hb+ (blue), in NB71>VP16::Hb 2x most of the five Eve+ (magenta) neurons are Hb+ (blue), and in NB71>VP16::Hb 2x, Hb 1x on average five out of eleven Eve+ (magenta) neurons are Hb+ (blue). (**E**) Quantification of Eve(+) Hb(+) U motor neuron (magenta and blue) neuron number at L3. Expressing an activated form of Hb in NB7-1 (NB71>VP16::Hb) alongside Hb can slightly increase the number of Hb+, Eve+ neurons compared to when VP16::Hb is misexpressed alone in NB7-1. (**F-G**) Quantification of the proportion of the number of total Eve+ and Eve+, Hb+ cell bodies in a single hemisegment in L3 nerve cords. Despite the increase in Eve+ neurons when Hb is misexpressed, VP16::Hb can only promote endogenous Hb expression in half of the total Eve+ neurons. (**H**) Image of Hb and Eve expression in a single L3 nerve cord hemisegment. Eve(+) U motor neurons from NB7-1 are circled in white. For quantification in (E), average and standard deviation are overlaid. Un-paired t-test with Welch's correction for unmatched standard deviations (see source datasheet for details).'**' $p = 0.0074$.

effectively silencing hunchback (Kohwi et al., 2013)[132]. Therefore, I wanted to know if chromatin restructuring inhibits the ability of the activated form of hunchback to extend the number of neurons possessing U1/U2 molecular identity at L3. M. Kohwi found that prolonging Dan (Pip-squeak domain protein, Distal antenna) expression prevents hunchback repositioning to the nuclear lamina and Dan extends the window of time in which hunchback is inducible but not transcribed. However, prolonged hunchback and dan expression led to an increase in the number of neurons expressing endogenous hunchback. Kohwi et al also found if in addition to prolonged hunchback expression, the nuclear lamina was disrupted with lamin RNAi, the number of neurons expressing endogenous hunchback increased.

Full disclaimer, I never actually did these experiments because my committee members encouraged me to be more bold and take on a riskier project. Looking back, I acknowledge I was very "in the weeds" with this project, so it was helpful to have my committee nudge me out of the weeds. It is also crazy that we were about six months away from the start of the ongoing pandemic, which curbed my ability to go bold and do a risky project.

Below, I include the relevant portion of my progress report from my 2019 committee meeting.

Working hypothesis: Since the average number of motor neurons possessing U1/U2 molecular identity at L3 is consistently 5 when I express the activating Hb, even though if I increase the overall number of Eve(+) U motor neurons using Hb, I hypothesize the activated form of hunchback is dependent on the chromatin structure present in NB7-1 during the first five divisions.

Experimental Approach: I can address my question with two manipulations. First, I will prolong expression of hunchback, dan, and the activated form of hunchback. Second, I can prolong Hb expression, lamin RNAi, and the active form of hunchback. If animals survive until L3, I will assess synapse morphology at this stage. If the animals do not survive past embryogenesis, I will express myr-GFP transgene and see where the axons project in

late stage 17 embryos (myr-GFP; NB7-1/vp16::Hb; Hb/dan or myr-GFP; NB7-1/vp16::Hb; Hb/lamin RNAi) or I will fillet late stage 16/early stage 17 embryos. Although I have never had to fillet embryos for my previous work, I am familiar with the technique and am confident that I will learn the technique quickly. With regards to scoring innervation patterns in embryos, my previous experience with embryos expressing myr-GFP in the NB7-1 lineage, I am able to distinguish innervation onto M9, M10/M2, M3/M4. This level of resolution, will allow for comparison to the following controls: *NB7-1>myr-GFP* in a wildtype background; *NB7-1>myr-GFP, VP16::Hb* in a wildtype background; and *NB7-1>myr-GFP, Hb*.

Possible outcomes: Outcome (1) Almost all Eve(+) neurons are Hunchback(+) at L3 for both manipulations. I will conclude that the activated form of hunchback is dependent on endogenous Hb repositioning and maintenance at the nuclear periphery. Based on M Kohwi's work, that would suggest that the activated form of hunchback can only function to bring about stable hunchback expression until L3 with the chromatin architecture that exists during structure the first five divisions of NB7-1.

Outcome (2) Only five Eve(+) neurons are hunchback(+) at L3, and the rest of the Eve(+) neurons are Hb(-) for both manipulations. I will conclude that the activated form of hunchback is not dependent on Dan expression or lamina integrity. Based on M Kohwi's work, that would suggest that the activated form of hunchback is dependent on another possible chromatin structure related factor unrelated to huncback re-positioning and maintenance at the nuclear lamina.

Outcome (3) Almost all Eve(+) neurons are Hunchback(+) at L3 for the dan manipulation but only five Eve(+) neurons are hunchback(+) at L3 for the lamin RNAi manipulation. I would conclude that activation by hunchback is dependent on Dan but not dependent on lamina integrity. This would suggest that another factor not involved in permanently silencing Hb to the nuclear lamina, yet related to Dan expression is required for the activated form of hunchback to function.

Outcome (4) Almost all Eve(+) neurons are Hunchback(+) at L3 for the lamin RNAi manipulation but only five Eve(+) neurons are hunchback(+) at L3 for the dan manipulation. I would conclude that activation by hunchback is dependent on lamina integrity and not dependent on dan. This would suggest another factor that is permanently silenced to the nuclear lamina and not endogenous Hb silencing is required for the activated form of Hb to function.

8.4.2 Impact misexpressing VP16::HB using the CQ GAL4 driver

Past work found that selective removal of Hunchback in the U motor neurons using the CQ GAL4 driver did not abolish early born molecular identity (i.e. U1 is still Zfh2(-)) (Hirono et al., 2017)[227]. Consistently, we previously found that misexpressing Hunchback using the CQ GAL4 driver does not impact the final permanent synaptic partnership fates of the U motor neurons (Meng et al., 2019)[2]. Since we found that driving VP16::Hb in NB7-1 increases the number of Eve+ motor neurons expressing Hb at L3 (Figure 4.4A,C) and increases the number of synaptic branches onto U1's muscle target (M9) (Meng et al., 2019)[2], I wanted to know if VP16::Hb could act in the postmitotic U motor neurons to alter their molecular identity and ultimately their fate. First, for three *CQ-GAL4>VP16::Hb 2x* L3 animals, I fixed and stained their bodywalls and corresponding CNSs. I stained the separated CNS, on a poly-d-lysine coated coverslip, for Eve and Hb. As a reminder, in wildtype, only U1 and U2 are Eve+ and Hb+ (Figure 4.5A,D).

Surprisingly, I found in addition to the expected two Eve+, Hb+ number of cell bodies in a hemisegment, I also sometimes found three (Figure 4.5B,C,D). Note, these three Eve+, Hb+ cell bodies are always in the position of U1, U2, and U3. If the molecular identity matches the synaptic fate, I expected U3 to be transformed into either U1 or U2. In one of the animals, I observed all abdominal hemisegments had three Eve+,Hb+ cell bodies, except for one hemisegment, so I imaged this animal's bodywall segments. I found no change in the number of synaptic branches onto muscles 9, 10, and 2 compared to my control (Figure 4.5E-G). It is important to remind the reader that the CQ-GAL4 driver turns off by L30. So it is very likely that U3 is now abnormally expressing Hunchback endogenously. If this is true, this means that despite endogenous Hunchback expression in U3, this motor neuron still assumes its normal synaptic partnership fate. The results here, offer further evidence that temporal transcription factors are acting IN the neuroblast and NOT the neuron to specify circuit-relevant fate features.

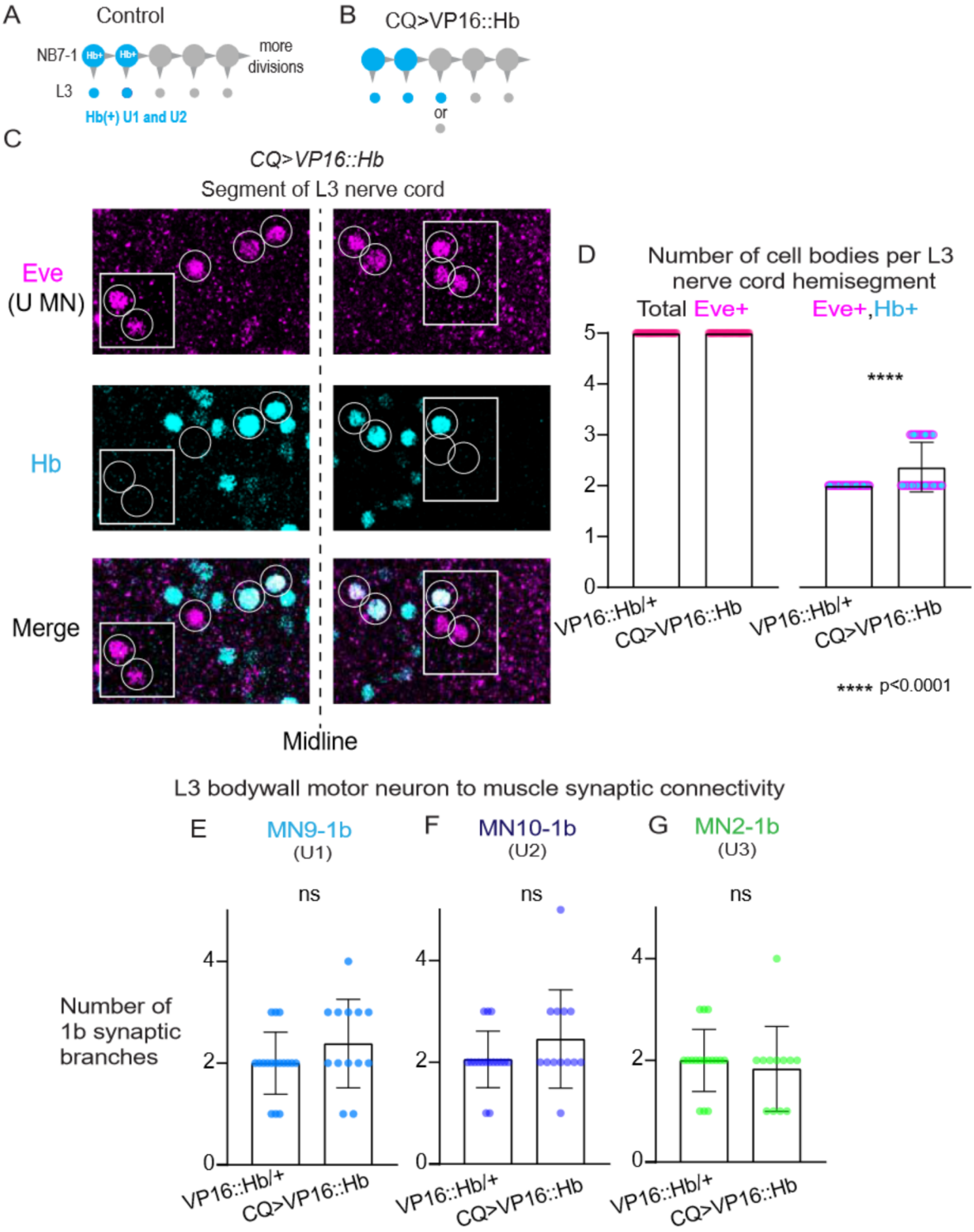


Figure 8.5: Misexpressing constitutively activated form of Hunchback, VP16::Hb transiently in U motor neuron GMC precursor and U motor neurons during early development can lead to endogenous expression of Hb in 'U3' but not impact permanent synaptic partnership with dorsal muscle targets. *Continued*

Figure 8.5: (*Cont'd.* Misexpressing constitutively activated form of Hunchback, VP16::Hb transiently in U motor neuron GMC precursor and U motor neurons during early development can lead to endogenous expression of Hb in 'U3' but not impact permanent synaptic partnership with dorsal muscle targets. (**A-B**). Illustrations of the divisions in NB7-1 in Control and CQ>VP16::Hb 2x. Each gray arrowhead represents cell division, large circles represent NB7-1. The rows of small circles represent U motor neuron identity at L3. In Control, two neurons are Hb+ (blue), in CQ>VP16::Hb 2x two but sometimes three neurons are Hb+ (blue). **C**) Images of Hb and Eve expression in a single L3 nerve cord hemisegment. White boxes are insets from different z-planes. Eve(+) U motor neurons from NB7-1 are circled in white. (**D**) Quantification of data in (C). (**E-G**) Quantification of the number of 1b branches onto muscle 9, muscle 10, and muscle 2. Un-paired t-test with Welch's correction for unmatched standard deviations (see source datasheet for details). 'ns' (not significant).

	Genotype	Number of values	Mean (number of cell bodies at L3)	Std. Deviation	Std. Error of Mean	p value
Eve+ Hb+	VP16::Hb/+	42	2.000	0.0000	0.0000	NA
	CQ>VP16::Hb	41	2.366	0.4877	0.0762	<0.0001*

*Unpaired t-test Welch (for un-equal Std. Deviation)

	Genotype	Number of values	Mean (1b branch number)	Std. Deviation	Std. Error of Mean	p value
M9	VP16::Hb/+	17	2.000	0.6124	0.1485	NA
	CQ>VP16::Hb	13	2.385	0.8697	0.2412	0.1892*
M10	VP16::Hb/+	17	2.059	0.5557	0.1348	NA
	CQ>VP16::Hb	13	2.462	0.9674	0.2683	0.1966*
M2	VP16::Hb/+	17	2.000	0.6124	0.1485	NA
	CQ>VP16::Hb	12	1.833	0.8348	0.2410	0.5629*

*Unpaired t-test Welch (for un-equal Std. Deviation)

Table 8.3: Source Data for Figure 8.5

CHAPTER 9

CONCLUSION

9.1 Historical overview of the field of neurobiology's major goals

The unifying goal of neurobiology is to understand how the nervous system functions. The nervous system is wildly complicated and incredibly necessary for life. The nervous system connects our bodies to the world. Through sensory organs and musculature we can experience and react to what is happening around us. By forming memories, thinking, and synthesizing concepts we can shape the world around us. If we can understand how the nervous system functions this means we will know its developmental blueprints as well as its anatomical and functional architecture. Ideally, when errors arise as a result of disease or age we will be equipped to successfully repair broken nervous systems. To this end, an incredible amount of work has been done. This work has been enabled by techniques that allow us to peer into the nervous system. The first comprehensive insight into nervous system organization and anatomy came from Ramon Cajal's application of Golgi staining. This breakthrough opened the way for cell biologists to focus on particular brain regions and carefully capture static Golgi preparations over developmental time. In parallel yet independently, scientists such as Alan Hodgkin and Andrew Huxley were beginning to describe the functional basis of neurons using electrophysiological techniques whereby current could be applied to nerves or large single axons and voltage could be measured The discovery that neurons are electrically active spurred the careful mapping of functional neural circuits in accessible systems such as lamprey, leach, cats, and crustaceans. Having an anatomical and functional framework as well as advances in microscopy were crucial to interpret the impact of single gene perturbations in C. elegans, mice, and flies. Genetically amenable model systems coupled with cutting-edge molecular tools that burst forth from our discovery of the Central Dogma revealed molecular diversity that matched Cajal's cataloged morphological

diversity.

9.2 Historical overview of developmental neurobiology's approaches and goals

The field of developmental neurobiology threw itself into the task of understanding the mechanisms underlying how neural diversity is achieved. Soon parallel work in vertebrates,mainly mice, and invertebrates, mainly Drosophila, revealed that a number of genes are highly conserved. Around this time, groundbreaking work in grasshoppers/locusts in labs including Corey Goodman's group were identifying and describing neural stem cells, their formation, division, and neural lineages. From the Goodman lab, Chris Doe carried this work into the genetically amenable Drosophila system. The Doe lab identified all the Drosophila larva motor system neural stem cells, called neuroblasts, and their lineages. While neural stem cells have subsequently been studied in vertebrate systems, the developing Drosophila larva motor system within the nerve cord is arguably one of the best systems to study neural stem cells because this system offers single cell resolution. Over a decade ago, Janelia pledged to advance tool development in Drosophila. Subsequently, there was an explosion of high resolution tools to genetically manipulate specific subsets of neurons, and improved sensitivity in calcium imaging indicators as well as optogenetics. Last but not least, Janelia funded projects to develop, collect, and compile whole CNS volumes composed of serial sections imaged using transmission electron microscopy. This staggering effort offered for the first time a platform to chart out connectivity at single synaptic resolution. Altogether, these tools made it feasible for the first time ever to link early developmental events involving neural stem cells to neural circuit assembly decisions at single cell resolution. Understanding this link at single cell resolution is critical to understand the mechanisms employed to form functional circuits that allow animals to move.

9.3 My PhD thesis's contribution to the field of developmental neurobiology

So far I have offered a broad-stroke, condensed historical overview leading up to and setting the stage onto which I accidentally stumbled upon (my undergraduate research dealt with understanding how an infectious bacteria's cell cycle is regulated by its symbiotic plant host). When I first joined Ellie Heckscher's lab, my goal was to expand upon the observation that at the level of a single neural stem cell lineage containing functionally similar interneurons, there was a relationship between birth time and circuit membership (Wreden et al., 2017)[1]. These findings were consistent with previous studies done in both vertebrates and invertebrates that collectively pointed to time as an important axis for establishing diversity and circuit membership. However, this was the first example of this birth time/circuit membership relationship at single neural stem cell resolution. This resolution offered us the opportunity to make very specific perturbations to interrogate the contribution of lineage intrinsic vs extrinsic cues for circuit membership decisions. I believe that the synaptic partnerships of a given neuron not only informs its function within a circuit but ultimately determines its circuit membership. The most accessible synaptic partnerships in the Drosophila larva nervous system are those formed between motor neuron and muscles, so to address the question of lineage intrinsic vs extrinsic cues driving synaptic partnerships and thus circuit membership, I studied neuroblast lineages known to generate motor neurons. While I also hoped we would obtain EM-resolution of synaptic partnerships within the larva nerve cord, I did not have the chance to do so. Fortunately, I had the opportunity to interrogate interneuron morphologies, whose neurites had a striking arrested outgrowth phenotype. This meant I didn't need synaptic resolution to draw conclusions regarding the role of lineage intrinsic vs extrinsic cues influencing interneuron outgrowth decisions.

9.4 My PhD thesis's major takeaway points

While in each main-bodied chapter of my thesis, I have stated conclusions and future directions, in this chapter I lay out what I believe are the overarching conclusions that can be drawn from my work. I hope to offer an eagle's eye view unifying the collection of projects I call my thesis.

All of my projects can be unified in their goal to address the broad question to what extent can lineage intrinsic vs extrinsic information specify circuit relevant fate features such as synaptic partnership decisions?

The first takeaway is that temporal cohorts are a general developmental strategy linking neural stem cell lineage organization to motor circuit membership and motor neuron temporal cohort borders are regulated by temporal transcription factors acting in neuroblasts.

Takeaway is supported by: My published work manipulating temporal transcription factors in neuroblasts to generate motor neuron progeny with extreme mismatches between birth time/spatial environment and inherited molecular information. Synaptic partnership decisions reflect inherited molecular information and not birth time (Meng et al., 2019; 2020)[2, 3].

The second takeaway is that lineage intrinsic programs inherited from neural stem cell parents strongly influence permanent motor neuron-to-muscle synaptic partnership decisions.

This takeaway draws into question a previous model where motor neuron to muscle synaptic partnership decisions are made through a stepwise series of decisions that build upon one another.

Takeaway is supported by: My published work manipulating temporal transcription factors in neuroblasts to generate motor neuron progeny with extreme mismatches between birth time/spatial environment and inherited molecular information. Synaptic partnership decisions reflect inherited molecular information and not birth time (Meng et al., 2019; 2020)[2, 3]. Manipulating Notch leads to NotchOFF siblings to fully adopt their NotchON

motor neuron sibling to muscle synaptic partnership fate. This manipulation also causes later born motor neuron cell bodies to be abnormally medially positioned in the nerve cord, yet synaptic partnership decisions are still made onto later born motor neuron muscle targets (Notch Chapter). Manipulating factors acting early in postmitotic motor neurons leads to abnormal motor axon outgrowth in late embryonic stages that can be corrected by late larval stages (Cardinal factor Chapter). Loss of hb9 and nkx6 affects normal ventral motor axon outgrowth in late stage embryos but by third instar stages, the innervation pattern onto ventral muscles is indistinguishable from wildtype. If we misexpress Eve in NB3-1's ventrally projection muscles or all Hb9+ motor neurons we have evidence to suggest that Eve+ Hb9- motor neurons are misrouted dorsally but can sometimes reroute to appropriate ventral muscle targets. This means that factors classically known to be required for motor axonogenesis can be dispensable for establishing correct, permanent synaptic partnerships.That being said, endogenous Eve in Eve+ motor neurons is required to establish correct, permanent synaptic partnerships because loss of Eve in the U motor neurons causes U motor axons to never exist in the nerve cord (Zarion Marshall and Ellie Heckscher data). Combined, the question is to what extent and under what conditions are cardinal factors like Eve, Hb9, Nkx6 required for synaptic partnership decisions? I favor a model where Eve acts alone and is positioned downstream of temporal transcription factors whereas Hb9 and Nkx6 act combinatorially with other factor(s). All these factors lie downstream of temporal transcription factors.

The third takeaway is that local motor neuron-to-muscle synaptic environments can impact final synaptic partnership decision and synaptic strength.

Takeaway is supported by: In NB7-1>Hb manipulation, when late born U motor neuron identity is lost, I see evidence of local compensation onto de-innervated muscles that normally form synaptic partnerships with late born U motor neurons (Meng et al., 2019)[2]. In NB3-1>Hb manipulation, despite a significant increase in the number of synaptic branches

onto M30, the muscle's response to nerve stimulation resembles wildtype despite an increase in the number of vesicles released during nerve stimulation. This suggests that the muscle is desensitized to increased neurotransmitter release. From a homeostatic plasticity perspective, this is interesting because this suggests that the homeostatic set point is established independent of the synaptic partnerships formed in development. This means that the set point establishment is likely a property of the muscle. This raises the question of how does the muscle know to set the set point? Perhaps there is an upper limit threshold that cannot physically be breached.

The fifth takeaway is that lineage intrinsic and spatial environment are required for successful interneuron outgrowth decisions in the developing nerve cord

Takeaway is supported by: When I misexpress Hunchback in NB7-1, I find that the likelihood that interneurons successfully establish wildtype-like arborization patterns in the neuropil is greatest when the neuroblast 7-1 transitions from generating motor neuron to interneurons relatively early. Since we find evidence that once 7-1 transitions, despite at abnormally later times in development, 7-1 is compatible with making interneurons that resemble the earliest born interneurons, this suggest that when inherited information of an interneuron progeny most closely matches its normal birth environment, the outgrowth success rate is increased (NB7-1 interneuron chapter, unpublished data).

Altogether, my thesis work reveals a common principle where the inherited information a neuronal progeny receives contributes to circuit-relevant fate features. I find that inherited information controlled by temporal transcription factor expression within the neuroblasts strongly influences motor axon to muscle synaptic partnership choices. While we do not have synaptic resolution within the nerve cord using light microscopy we can identify overall morphologies using single-cell labeling approaches. Doing so has revealed that the U motor neurons' dendritic arborization pattern within the neuropil is strongly influenced by inherited information (Meng et al., 2019)[2]. More recent analysis and characterization of single-cell

clones of NB7-1 interneurons reveals that when Hunchback is misexpressed, the majority of interneurons fail to properly extend neurites and fail to establish arbors within the nerve cord and when interneurons do establish arbors, they tend to come from neuroblast 7-1 parents that transitioned from making motor neurons to interneurons at relatively earlier times in development. Taken together, this suggests that the decisions interneurons make to integrate into circuits relies on both inherited and environmental cues. An avenue for future research is to begin to interrogate the relationship between inherited information and environmental cues. For example, we know that receptors on developing neurites can impact outgrowth decisions in response to the receptor's ligands (i.e. Slit-Robo repulsive signaling). Undoubtedly, to advance our understanding of the role intrinsic and extrinsic cues play in regulating circuit-relevant fate features of interneurons within the nerve cord, we need to achieve synaptic resolution. The reason I focused on motor axon to muscle synaptic partnerships is that these synapses are easy to access in dissected larvae using confocal light microscopy. If we can establish with high confidence an accessible synaptic partnership model between specific interneurons (or even sensory dendrite to sensory processing interneuron axon) in the nerve cord neuropil, then we effectively have the same resolution offered currently in the peripheral nervous system. In the short term, it is worthwhile pursuing 1) expansion microscopy techniques, which rely on a gel matrix to expand fixed tissue in every plane. Recent improvements have led to 8X expansion of Drosophila central nervous systems (Lillvis et al., 2021)[228] (Note, I highly recommend reading this recent article and setting alerts for future citations of this paper. I think the methods described in the paper, if broadly applicable will be a key tool to access single synaptic resolution within the CNS of genetically manipulated animals). In tandem, 2) we need to keep pursuing comparative connectomic approaches using electron microscopy available to us in UChicago's EM core.

CHAPTER 10

METHODS

10.1 Julia Meng's Gateway Cloning Protocol

Goal: Clone an endogenous enhancer fragment and place upstream of a GAL4 and LexA on a destination vector to then be sent off for injection into embryos.

Workflow

1. Isolate genomic DNA

2. Amplify endogenous enhancer fragment sequence using PCR

3. A-tailing with Taq Polymerase

4. Insert PCR product into entry TOPO vector

5. Perform L/R reaction to transfer region of interest to destination vector

1. Isolate genomic DNA Protocol (From Janelia Farms Genomic DNA preps)

Make Buffer A (5ml) Store at room temperature (RT) *solutions are on the shelf above Chris's bench

100 mM Tris-CI (pH 7.5)—.5 mL 1M

100 mM EDTA—1 mL 0.5M

100 mM NaCI—100 uL 5M

0.5 % SDS—250 uL 10% SDS

Molecular grade water—Until total vol 5 mL

Make Buffer B (700 ul) Store at 4 C

Potassium acetate (5M)—200 uL

Lithium chloride (6)—500 uL

TE Buffer (25 mL) Store at RT

Tris-CI (pH 7.5)—250 uL 1M

EDTA—50 uL 0.5M

Molecular grade water—25 mL

1. Collect 30 adult flies in a 1.5 microcentrifuge tube and place on ice

2. Grind flies using the blue plastic pestles (on shelf above Meng's bench) in 200uL Buffer A, add additional 200uL Buffer A grind for 1-2 minutes.

3. Incubate samples at 65 C for 30 minutes (use water bath or heat block)

4. Add 800uL Buffer B, mix well inverting the tube several times incubate on ice for at least 10 minutes and up to a few hours (I incubated for 1 hour).

5. Centrifuge @ 14,000xg for 15 minutes @ RT

6. Transfer 1 mL of the supernatant into a new microcentrifuge tube

7. Add 500 uL isopropanol and mix well by inverting tube several times

8. Centrifuge @ 12,000rpm for 15 minutes @ RT (you should see a clear pellet at the bottom)

9. Discard the supernatant, wash pellet with 70% EtOH

10. Air dry upside down (1-2 hours)

11. Resuspend in 100uL TE buffer

12. Measure DNA concentration using the nanodrop on the 8th floor

13. Store @ -20 C

2. PCR endogenous sequence

1. Design and order Primers (email Chris primer sequences)

2. Once Primers arrive, resuspend in TE buffer and follow the directions on the Oligo Data Sheet included with your Primers.

3. Store at -20 C

4. In the -20 C there are several tubes of Invitrogen Platinum SuperFi Green PCR Master Mix (google to find manufactures' user documents)

Reaction Mixture 50 uL Total

Master Mix—25 uL

DNA template 50 ng/uL

Reverse primer 10 uM—2.5 uL

Forward primer 10 uM—2.5 uL

Nuclease free water

Total 50 uL

5. Set PCR reaction settings

1. 98 C for 30 seconds
2. 30 cycles of: 98 C for 10 s, Tm temp for 30 s, 72 C for ext time
3. 72 C for 5 minutes
4. 4 C forever

To calculate ext time (expected product length bp)/(1000) X 30 gives you the value in seconds

6. Run PCR reaction product on a 1% agarose gel

7. Use UV gel box from Carrillo lab to view band to cut out. You want to be quick here because you don't want the UV to damage your DNA fragment.

8. Gel purify the band using the kit on the shelf above the water bath in lab

3. A-Tailing with Taq Polymerase (Do this step on the same day of the TOPO Cloning Reaction)

Set-up the reaction by adding the following components:

PCR-amplified DNA (200 ng/uL)—10 uL

10X Taq buffer in blue box in -20C—5 uL

MgCI2 (impt cofactor forTaq pol)—1 uL

1mM dATP in blue box in -20C—10 uL

Taq polymerase—0.2 uL

Nuclease free water

Total—30 uL (can scale up for 50 uL)

Incubate the reaction at 72 C for 20 minutes (do this step in the pcr machine)

Store on ice or 4C

4. Insert PCR product into entry TOPO vector

Use the pCR 8/GW/TOPO TA Cloning kit manual (starting on page 8 with the header Set Up the TOPO Cloning Reaction)

Below are added notes to point out important steps and where reagents are stored in our lab.

Reagents:

- We don't have the salt solution (1.2 M NaCI; 0.06 M MgCI2) provided with the TOPO Cloning reaction but you can make it!
- A vial of S.O.C. medium sits on Chris's bench's shelf where the formaldehyde was. I (Julia) also have a vial of S.O.C. medium sitting on my bench's shelf.
- Jars of Spectinomycin and ampicillin are stored in the large 4C fridge on the door.
- To autoclave the LB agar you need to go to the basement. If you haven't been trained to use the autoclaves see if a staff member is in the room or email the individual listed on the

autoclaves that can help you.

- Glass beads for spreading the bacteria are stored on Chris's bench

- The One Shot TOP10 chemically competent E. coli are stored in the -80C freezer

Tips on steps:

- You want to use a 2:1 ratio of PCR product to TOPO vector (5-10 ng/uL)

- The TOPO cloning reaction incubation time can vary from 30 seconds to 30 minutes. 5 minutes is probably okay but I went with 30 minutes.

- When incubating the TOPO Cloning reaction with the One Shot chemically competent cells I incubate on ice for 15 minutes (range they recommend is 5-30 minutes).

- The protocol recommends spreading 2 different volumes of transformed cells to ensure that at least one plate will have well-spaced colonies. I recommend spreading the remaining volume onto a third plate.

5. Perform L/R reaction to transfer region of interest to destination vector

Use the Gateway Technology with Clonase II manual

https://tools.thermofisher.com/content/sfs/manuals/gateway_clonaseii_man.pdf

Below are added notes to point out important steps and where reagents are stored in our lab.

Reagents:

- Use One Shot ccdB E coli cells stored in the -80 C freezer

- Gateway LR Clonase II enzyme is in the -20 C freezer

Tips on steps:

- Use 1:1 to 2:1 ratio of the TOPO vector + PCR product (in the correct orientation) to the Destination vector (150 ng/uL). (I used 1:1 ratio and had success)

10.2 HL3 recipe for calcium imaging of the MHC tethered GCaMP6f

This protocol applies to calcium imaging of the SynapGCaMP6f (MHC-CD8-GCaMP6f-Sh) published in Newman et al., 2017.

This is the Saline 'HL3' recipe I used

NaCI 70mM

KCI 5mM

Hepes 5mM

NaHCO3 10mM

Trehalose 5 mM

Sucrose 115 mM

Store aliquots at 4C

Right before use add

MgCI2 20-25 mM

CaCI2 0.5 mM

CaCI 1.0 mM

CaCI 1.5 mM // I used 1.5 mM in my Meng et al., 2019 and 2020 papers

Artificial Hemolymph Recipe (shared by Kayly Lembke from Seth Tomchik's CSHL protocol) Kayly said she was getting nice signal using this protocol. Disclaimer, I always just used the Saline 'HL3' recipe above because it was simpler and worked.

Total volume: 400 mL

NaCI (103 mM): 2.4 g

KCI (3 mM): 0.089 g

Hepes (5 mM): 0.4766 g

NaHCO3 (26mM): 0.8736 g

NaH2PO4 (1 mM): 0.0552 g

Trehalose (10 mM): 1.5132 g

Sucrose (7 mM): 0.95844 g

Glucose (10 mM): 0.72064 g

H2O for total volume: 400 mL

Aliquot 25 mL for storage at 4C

Right before use add

MgCI2 (10 mM): 250 uL

CaCI2 (0.5 mM): 12.5 uL

(1.0 mM): 25 uL

(1.5 mM): 37.5 uL

// range from 0.5-2 mM is used for Ca imaging. From my experience, more calcium higher rate of spontaneous release events. If too much calcium is added, muscles will spasm.

1. Dissect, remove guts and CNS and a L3 in a small sylgard dish and use bent pins so that the top of the pin is parallel and flush with the sylgard dish. We do not want the pins to scratch the 40x dipping objective. FYI James Ashley from the Carrillo lab was horrified we even use pins. He uses a system based on magnets. I promise that if you bend the pins such that they are parallel and flush with the sylgard dish and pointed away from the region of the bodywall you desire to image, you will not scratch the lens. If you don't bend the pins

and the bent portion is not flush with the sylgard dish or the pins are overlaying the region of the bodywall you want to image then there is a chance you may scratch the precious very costly 40x dipping objective.

10.3 live imaging protocol

Live imaging preparations: Rich et al., 2020 //what I learned from her when I rotated Preparation of Drosophila tissues for live imaging Drosophila embryos were collected on apple juice agar plates for 90 min and aged for 90-120 min at 25∘C such that a majority of embryos were completing cellularization at the time of mounting. Embryos were dechorionated in 30% bleach for 1 min, rinsed in water, aligned on an apple juice agar pad, and mounted on a coverslip with embryo glue (adhesive from double sided tape dissolved in heptane). The imaged surface (dorsal or ventral) was mounted on the coverslip. This coverslip was affixed via petroleum jelly to a metal slide with a hole in the center. Embryos were covered with halocarbon oil 200 immediately after mounting; they were not compressed.

Glue-coated coverslips: Incubate 10 pieces of adhesive tape (5x1cm2) in 10 mLs of Heptane for several days at Room temperature

Siebert et al., 2009 ([229]) methods details an agarose mounting approach.

10.4 Illustrations of the adult Drosophila thoracic muscles

I included these reference sheets because there was a time when I dissected adult Drosophila thorax in an attempt to see if I could find evidence of increased synaptic innervation onto flight muscles when Hb is misexpressed in NB7-1. Full disclaimer, I found it difficult to identify innervation onto the muscles within the thorax.

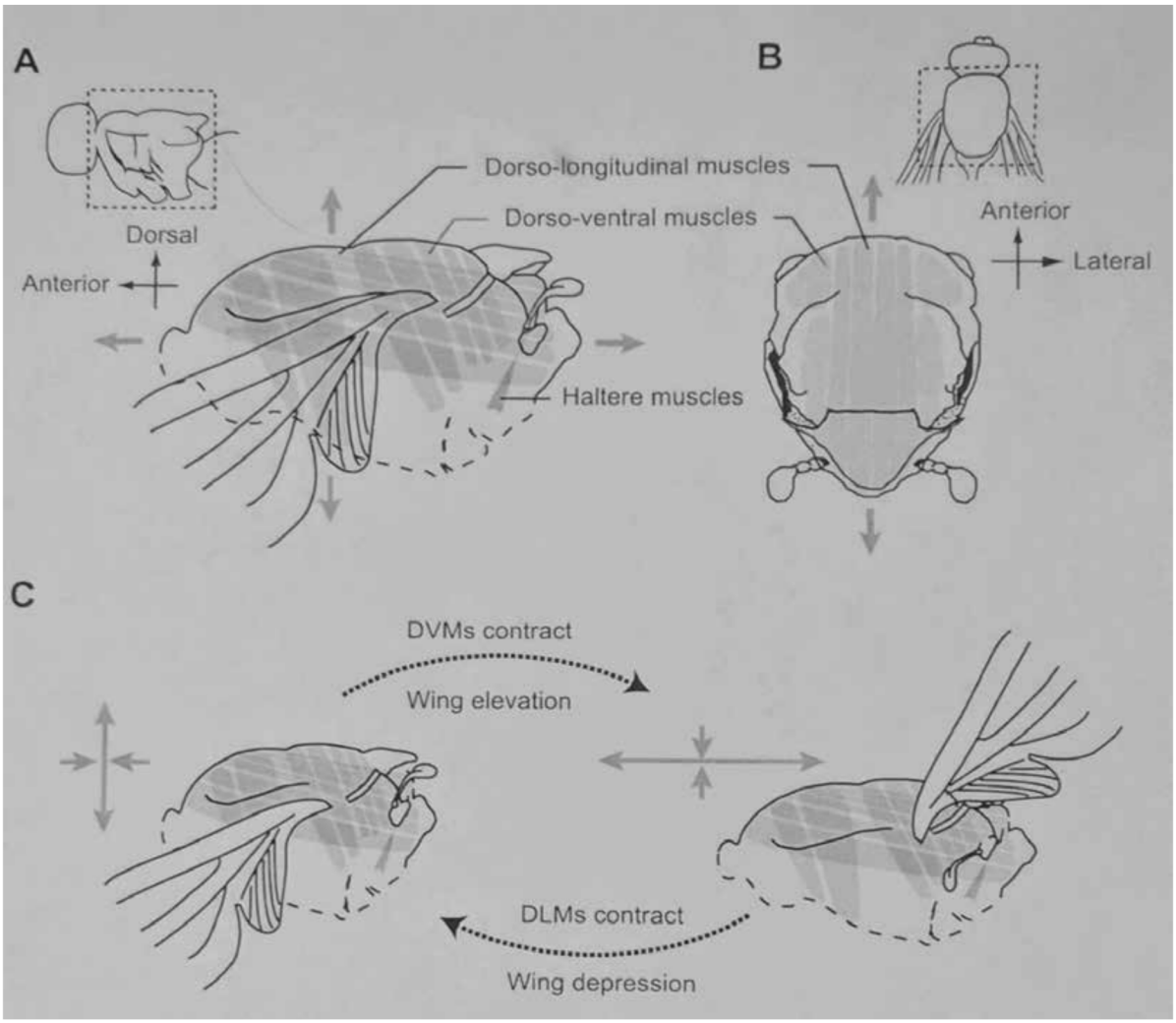


Figure 10.1: Diagram of adult flight muscles part I

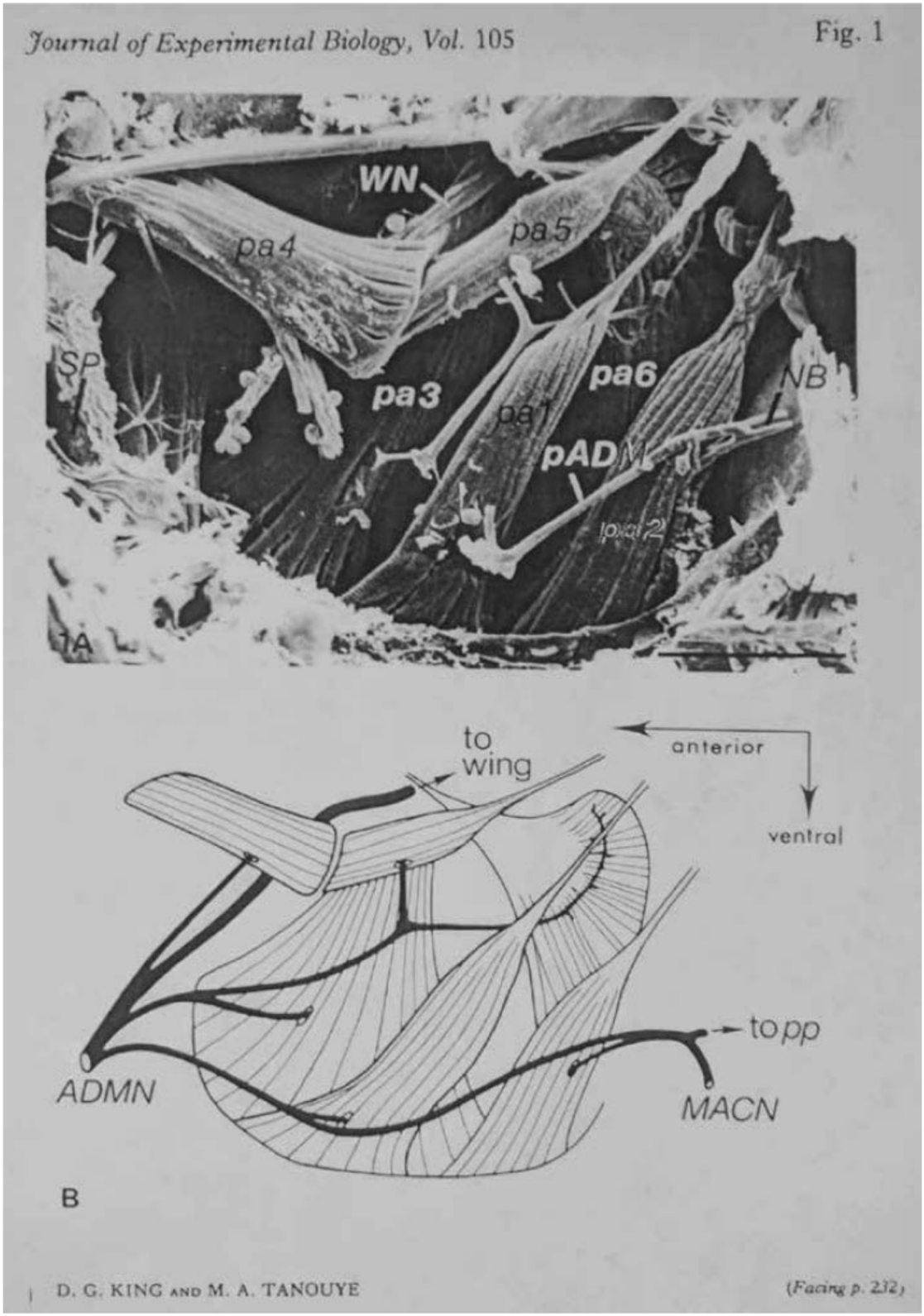


Figure 10.2: Diagram of adult flight muscles part II

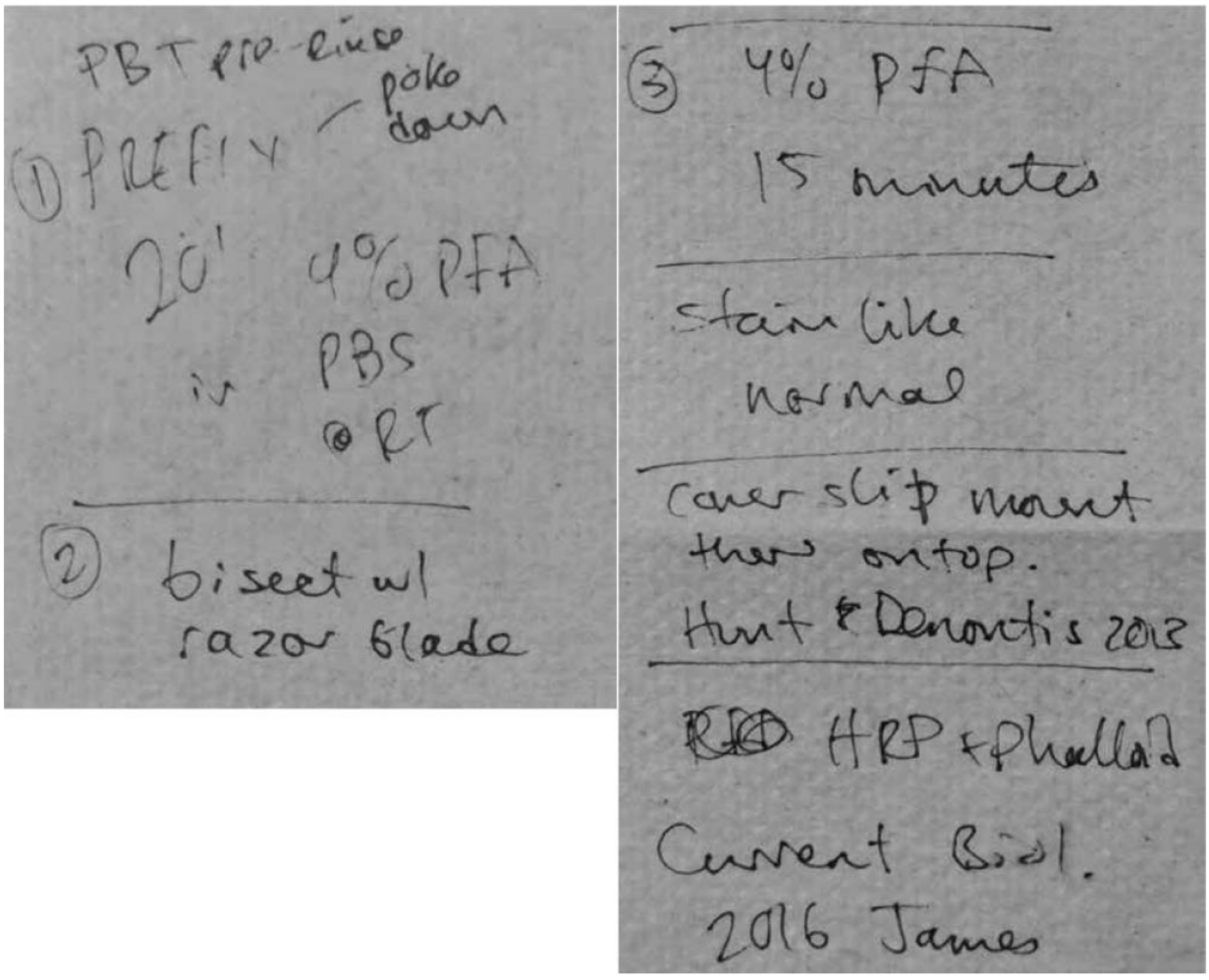


Figure 10.3: Protocol for dissecting, fixing, and staining the adult thorax

10.5 Matching L3 bodywall segments to nerve cord hemisegments

I have included a step-by-step schematic to aid in the successful matching of nerve cord hemisegments to bodywall segments.

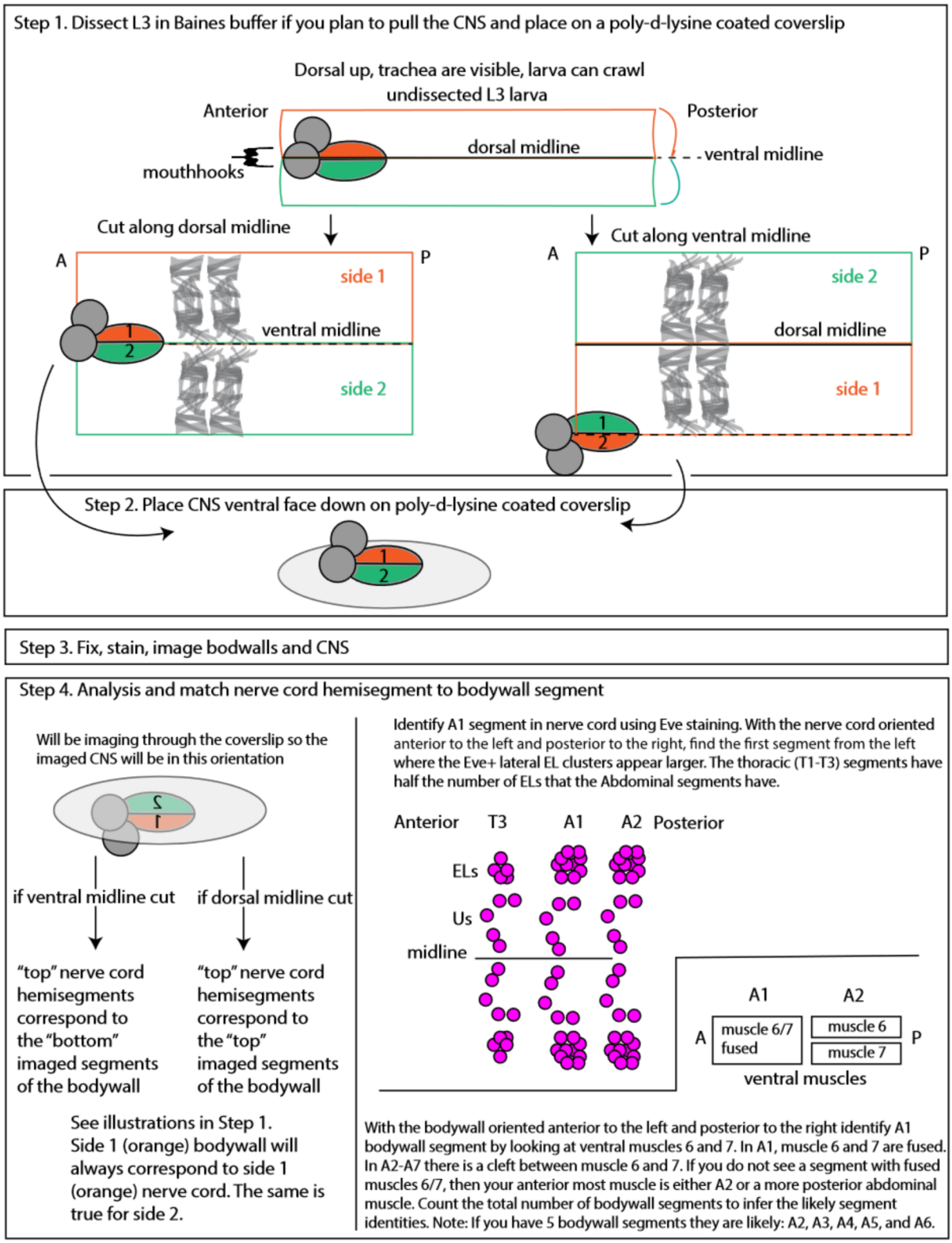


Figure 10.4: Matching L3 bodywall segments to nerve cord hemisegments

REFERENCES

[1] Christopher C. Wreden, Julia L. Meng, Weidong Feng, Wanhao Chi, Zarion D. Marshall, Ellie S. Heckscher, S. Preibisch, C. Rueden, S. Saalfeld, B. Schmid, and et al. Temporal Cohorts of Lineage-Related Neurons Perform Analogous Functions in Distinct Sensorimotor Circuits. *Current Biology*, 27(10):1521–1528, 5 2017.

[2] Julia L. Meng, Zarion D. Marshall, Meike Lobb-Rabe, and Ellie S. Heckscher. How prolonged expression of hunchback, a temporal transcription factor, re-wires locomotor circuits. *eLife*, 8, 9 2019.

[3] Julia L. Meng, Yupu Wang, Robert A. Carrillo, and Ellie S. Heckscher. Temporal transcription factors determine circuit membership by permanently altering motor neuron-to-muscle synaptic partnerships. *eLife*, 9:1–23, 5 2020.

[4] Julia L. Meng and Ellie S. Heckscher. Development of motor circuits: From neuronal stem cells and neuronal diversity to motor circuit assembly. *Current topics in developmental biology*, 142:409–442, 1 2021.

[5] Gabi Zeilig, Shavit Enosh, Deborah Rubin-Asher, Benjamin Lehr, and Ruth Defrin. The nature and course of sensory changes following spinal cord injury: Predictive properties and implications on the mechanism of central pain. *Brain*, 135:418–430, 2 2012.

[6] Stephanie C. Koch, David Acton, and Martyn Goulding. Spinal circuits for touch, pain, and itch. *Annual Review of Physiology*, 80:189–217, 2 2018.

[7] Hiroshi Kohsaka, Pierre A. Guertin, and Akinao Nose. Neural Circuits Underlying Fly Larval Locomotion. *Current Pharmaceutical Design*, 23(12):1722–1733, 5 2017.

[8] Seol Hee Im and Michael J. Galko. Pokes, sunburn, and hot sauce: ¡i¿Drosophila¡/i¿ as an emerging model for the biology of nociception. *Developmental Dynamics*, 241(1):16–26, 1 2012.

[9] Nicolas Stifani. Motor neurons and the generation of spinal motor neuron diversity. 8(OCT), 10 2014.

[10] Victoria E. Abraira and David D. Ginty. The sensory neurons of touch. 79(4):618–639, 8 2013.

[11] Jay B. Bikoff. Interneuron diversity and function in the spinal motor system. 8:36–43, 4 2019.

[12] Peter J. Osseward and Samuel L. Pfaff. Cell type and circuit modules in the spinal cord. *Current Opinion in Neurobiology*, 56:175–184, 6 2019.

[13] Matt Q. Clark, Stephanie J. McCumsey, Sereno Lopez-Darwin, Ellie S. Heckscher, and Chris Q. Doe. Functional genetic screen to identify interneurons governing behaviorally distinct aspects of Drosophila larval motor programs. *G3: Genes, Genomes, Genetics*, 6(7):2023–2031, 7 2016.

[14] Jean Baptiste Masson, Francois Laurent, Albert Cardona, Chloe Barre, Nicolas Skatchkovsky, Marta Zlatic, and Tihana Jovanic. Identifying neural substrates of competitive interactions and sequence transitions during mechanosensory responses in Drosophila. *PLoS Genetics*, 16(2):e1008589, 2020.

[15] Tomoko Ohyama, Casey M. Schneider-Mizell, Richard D. Fetter, Javier Valdes Aleman, Romain Franconville, Marta Rivera-Alba, Brett D. Mensh, Kristin M. Branson, Julie H. Simpson, James W. Truman, Albert Cardona, and Marta Zlatic. A multilevel multimodal circuit enhances action selection in Drosophila. *Nature*, 520(7549):633–639, 4 2015.

[16] Dawn M. Blitz and Michael P. Nusbaum. Modulation of circuit feedback Specifies motor circuit output. *Journal of Neuroscience*, 32(27):9182–9193, 7 2012.

[17] Eve Marder and Dirk Bucher. Central pattern generators and the control of rhythmic movements. *Current Biology*, 11(23):R986–R996, 11 2001.

[18] W. O. Friesen, M. Poon, and G. S. Stent. An oscillatory neuronal circuit generating a locomotory rhythm. *Proceedings of the National Academy of Sciences of the United States of America*, 73(10):3734–3738, 1976.

[19] Matthew Q. Clark, Aref Arzan Zarin, Arnaldo Carreira-Rosario, and Chris Q. Doe. Neural circuits driving larval locomotion in Drosophila. 13(1), 4 2018.

[20] Ibrahim Tastekin and Matthieu Louis. Manipulation of neural circuits in drosophila larvae. In *Decoding Neural Circuit Structure and Function: Cellular Dissection Using Genetic Model Organisms*, pages 171–189. Springer International Publishing, 7 2017.

[21] Laurina Manning, Ellie S. Heckscher, Maria D. Purice, Jourdain Roberts, Alysha L. Bennett, Jason R. Kroll, Jill L. Pollard, Marie E. Strader, Josh R. Lupton, Anna V. Dyukareva, Phuong Nam Doan, David M. Bauer, Allison N. Wilbur, Stephanie Tanner, Jimmy J. Kelly, Sen Lin Lai, Khoa D. Tran, Minoree Kohwi, Todd R. Laverty, Joseph C. Pearson, Stephen T. Crews, Gerald M. Rubin, and Chris Q. Doe. A Resource for Manipulating Gene Expression and Analyzing cis-Regulatory Modules in the Drosophila CNS. *Cell Reports*, 2(4):1002–1013, 10 2012.

[22] Hsing Hsi Li, Jason R. Kroll, Sara M. Lennox, Omotara Ogundeyi, Jennifer Jeter, Gina Depasquale, and James W. Truman. A GAL4 driver resource for developmental and behavioral studies on the larval CNS of Drosophila. *Cell reports*, 8(3):897–908, 8 2014.

[23] Arnim Jenett, Gerald M. Rubin, Teri T.B. Ngo, David Shepherd, Christine Murphy, Heather Dionne, Barret D. Pfeiffer, Amanda Cavallaro, Donald Hall, Jennifer Jeter, Nirmala Iyer, Dona Fetter, Joanna H. Hausenfluck, Hanchuan Peng, Eric T. Trautman, Robert R. Svirskas, Eugene W. Myers, Zbigniew R. Iwinski, Yoshinori Aso, Gina M. DePasquale, Adrianne Enos, Phuson Hulamm, Shing Chun Benny Lam, Hsing Hsi Li, Todd R. Laverty, Fuhui Long, Lei Qu, Sean D. Murphy, Konrad Rokicki, Todd Safford, Kshiti Shaw, Julie H. Simpson, Allison Sowell, Susana Tae, Yang Yu, and Christopher T. Zugates. Annotated embryonic CNS expression patterns of 5,000 GMR GAL4 lines: a resource for manipulating gene expression and analyzing cis-regulatory modules. *Cell Rep.*, 2(4):991–1001, 10 2012.

[24] Barret D. Pfeiffer, Arnim Jenett, Ann S. Hammonds, Teri T.B. Ngo, Sima Misra, Christine Murphy, Audra Scully, Joseph W. Carlson, Kenneth H. Wan, Todd R. Laverty, Chris Mungall, Rob Svirskas, James T. Kadonaga, Chris Q. Doe, Michael B. Eisen, Susan E. Celniker, and Gerald M. Rubin. Tools for neuroanatomy and neurogenetics in Drosophila. *Proceedings of the National Academy of Sciences*, 105(28):9715–9720, 7 2008.

[25] Hod Dana, Yi Sun, Boaz Mohar, Brad K. Hulse, Aaron M. Kerlin, Jeremy P. Hasseman, Getahun Tsegaye, Arthur Tsang, Allan Wong, Ronak Patel, John J. Macklin, Yang Chen, Arthur Konnerth, Vivek Jayaraman, Loren L. Looger, Eric R. Schreiter, Karel Svoboda, and Douglas S. Kim. High-performance calcium sensors for imaging activity in neuronal populations and microcompartments. *Nature Methods*, 16(7):649–657, 7 2019.

[26] Rebecca D. Vaadia, Wenze Li, Venkatakaushik Voleti, Aditi Singhania, Elizabeth M.C. Hillman, and Wesley B. Grueber. Characterization of Proprioceptive System Dynamics in Behaving Drosophila Larvae Using High-Speed Volumetric Microscopy. *Current Biology*, 29(6):935–944, 3 2019.

[27] Julie H. Simpson and Loren L. Looger. Functional imaging and optogenetics in drosophila. *Genetics*, 208(4):1291–1309, 4 2018.

[28] Casey M. Schneider-Mizell, Stephan Gerhard, Mark Longair, Tom Kazimiers, Feng Li, Maarten F. Zwart, Andrew Champion, Frank M. Midgley, Richard D. Fetter, Stephan Saalfeld, and Albert Cardona. Quantitative neuroanatomy for connectomics in Drosophila. *eLife*, 5(MARCH2016):1–36, 2016.

[29] Hiroshi Kohsaka, Maarten F. Zwart, Akira Fushiki, Richard D. Fetter, James W. Truman, Albert Cardona, and Akinao Nose. Regulation of forward and backward locomotion through intersegmental feedback circuits in drosophila larvae. *Nature Communications*, 10:1–11, 12 2019.

[30] Aref Arzan Zarin, Brandon Mark, Albert Cardona, Ashok Litwin-Kumar, and Chris Q. Doe. A multilayer circuit architecture for the generation of distinct locomotor behaviors in Drosophila. *eLife*, 8, 12 2019.

[31] Suguru Takagi, Benjamin Thomas Cocanougher, Sawako Niki, Dohjin Miyamoto, Hiroshi Kohsaka, Hokto Kazama, Richard Doty Fetter, James William Truman, Marta Zlatic, Albert Cardona, and Akinao Nose. Divergent Connectivity of Homologous Command-like Neurons Mediates Segment-Specific Touch Responses in Drosophila. *Neuron*, 96(6):1373–1387, 12 2017.

[32] Akira Fushiki, Maarten F Zwart, Hiroshi Kohsaka, Richard D Fetter, Albert Cardona, and Akinao Nose. A circuit mechanism for the propagation of waves of muscle contraction in Drosophila. *eLife*, 5, 2 2016.

[33] Hiroshi Kohsaka, Satoko Okusawa, Yuki Itakura, Akira Fushiki, and Akinao Nose. Development of larval motor circuits in Drosophila. *Development Growth and Differentiation*, 54(3):408–419, 2012.

[34] Jimena Berni, Stefan R. Pulver, Leslie C. Griffith, and Michael Bate. Autonomous circuitry for substrate exploration in freely moving drosophila larvae. *Current Biology*, 22(20):1861–1870, 10 2012.

[35] Stefan R Pulver, Timothy G Bayley, Adam L Taylor, Jimena Berni, Michael Bate, and Berthold Hedwig. Imaging fictive locomotor patterns in larval Drosophila. *J Neuro-physiol*, 114:2564–2577, 2015.

[36] William C. Lemon, Stefan R. Pulver, Burkhard Höckendorf, Katie McDole, Kristin Branson, Jeremy Freeman, and Philipp J. Keller. Whole-central nervous system functional imaging in larval Drosophila. *Nature Communications*, 6, 8 2015.

[37] Arnaldo Carreira-Rosario, Aref Arzan Zarin, Matthew Q. Clark, Laurina Manning, Richard D. Fetter, Albert Cardona, and Chris Q. Doe. MDN brain descending neurons coordinately activate backward and inhibit forward locomotion. *eLife*, 7, 8 2018.

[38] Shigehiro Namiki, Michael H. Dickinson, Allan M. Wong, Wyatt Korff, and Gwyneth M. Card. The functional organization of descending sensory-motor pathways in drosophila. *eLife*, 7, 6 2018.

[39] Ellie S. Heckscher, Aref Arzan Zarin, Serge Faumont, Matthew Q. Clark, Laurina Manning, Akira Fushiki, Casey M. Schneider-Mizell, Richard D. Fetter, James W. Truman, Maarten F. Zwart, Matthias Landgraf, Albert Cardona, Shawn R. Lockery, and Chris Q. Doe. Even-Skipped+ Interneurons Are Core Components of a Sensorimotor Circuit that Maintains Left-Right Symmetric Muscle Contraction Amplitude. *Neuron*, 88(2):314–329, 10 2015.

[40] H. Babski, T. Jovanic, C. Surel, S. Yoshikawa, M. F. Zwart, J. Valmier, J. B. Thomas, J. Enriquez, P. Carroll, and A. Garcès. A gabaergic maf-expressing interneuron subset regulates the speed of locomotion in drosophila. *Nature Communications*, 10:1–17, 12 2019.

[41] Tihana Jovanic, Michael Winding, Albert Cardona, James W. Truman, Marc Gershow, and Marta Zlatic. Neural substrates of drosophila larval anemotaxis. *Current Biology*, 29:554–566.e4, 2 2019.

[42] Anton Miroschnikow, Philipp Schlegel, Andreas Schoofs, Sebastian Hueckesfeld, Feng Li, Casey M. Schneider-Mizell, Richard D. Fetter, James W. Truman, Albert Cardona, and Michael J. Pankratz. Convergence of monosynaptic and polysynaptic sensory paths onto common motor outputs in a drosophila feeding connectome. *eLife*, 7, 12 2018.

[43] Anita Burgos, Ken Honjo, Tomoko Ohyama, Cheng Sam Qian, Grace Ji Eun Shin, Daryl M. Gohl, Marion Silies, W. Daniel Tracey, Marta Zlatic, Albert Cardona, and Wesley B. Grueber. Nociceptive interneurons control modular motor pathways to promote escape behavior in drosophila. *eLife*, 7, 3 2018.

[44] Matthias Landgraf, Torsten Bossing, Gerd M. Technau, and Michael Bate. The Origin, Location, and Projections of the Embryonic Abdominal Motorneurons of Drosophila. *Journal of Neuroscience*, 17(24), 1997.

[45] Aloisia Schmid, Akira Chiba, and Chris Q. Doe. Clonal analysis of Drosophila embryonic neuroblasts: neural cell types, axon projections and muscle targets. *Development*, 126(21):4653–4689, 11 1999.

[46] Kaushiki Menon, Robert Carrillo, and Kai Zinn. Development and Plasticity of Drosophila Larval Neuromuscular Junction. *Wiley interdisciplinary reviews. Developmental biology*, 2(5):647–670, 2013.

[47] E. S. Heckscher, S. R. Lockery, and C. Q. Doe. Characterization of drosophila larval crawling at the level of organism, segment, and somatic body wall musculature. *Journal of Neuroscience*, 32:12460–12471, 9 2012.

[48] Juergen A. Knoblich. Asymmetric cell division: Recent developments and their implications for tumour biology. 11(12):849–860, 12 2010.

[49] Volker Hartenstein and Angelika Stollewerk. The evolution of early neurogenesis. 32(4):390–407, 2 2015.

[50] Oliver Birkholz, Christof Rickert, Julia Nowak, Ivo C. Coban, and Gerhard M. Technau. Bridging the gap between postembryonic cell lineages and identified embryonic neuroblasts in the ventral nerve cord of Drosophila melanogaster. *Biology Open*, 4(4):420–434, 2015.

[51] Oliver Birkholz, Olaf Vef, Ana Rogulja-Ortmann, Christian Berger, and Gerhard M. Technau. Abdominal-B and caudal inhibit the formation of specific neuroblasts in the Drosophila tail region. *Development*, 140(17):3552–3564, 9 2013.

[52] Julie Broadus, James B. Skeath, Eric P. Spana, Torsten Bossing, Gerhard Technau, and Chris Q. Doe. New neuroblast markers and the origin of the aCC/pCC neurons in

the Drosophila central nervous system. *Mechanisms of Development*, 53(3):393–402, 11 1995.

[53] Corey S Goodman and Carla J Shatz. Developmental Mechanisms That Generate Precise Patterns of Neuronal Connectivity. Technical report, 1993.

[54] Gerhard M. Technau, Ana Rogulja-Ortmann, Christian Berger, Oliver Birkholz, and Christof Rickert. Composition of a neuromere and its segmental diversification under the control of Hox genes in the embryonic CNS of drosophila. 28(3-4):171–180, 12 2014.

[55] C. Q. Doe. Molecular markers for identified neuroblasts and ganglion mother cells in the Drosophila central nervous system. *Development*, 116(4):855–863, 12 1992.

[56] Hartmut Schmidt, Christof Rickert, Torsten Bossing, Olaf Vef, Joachim Urban, and Gerhard M Technau. The Embryonic Central Nervous System Lineages of Drosophila melanogaster II. Neuroblast Lineages Derived from the Dorsal Part of the Neuroectoderm. *DEVELOPMENTAL BIOLOGY*, 189:186–204, 1997.

[57] Torsten Bossing, Gerald Udolph, Chris Q. Doe, and Gerhard M. Technau. The Embryonic Central Nervous System Lineages ofDrosophila melanogaster: I. Neuroblast Lineages Derived from the Ventral Half of the Neuroectoderm. *Developmental Biology*, 179(1):41–64, 10 1996.

[58] Christof Rickert, Thomas Kunz, Kerri Lee Harris, Paul M. Whitington, and Gerhard M. Technau. Morphological characterization of the entire interneuron population reveals principles of neuromere organization in the Ventral nerve cord of Drosophila. *Journal of Neuroscience*, 31(44):15870–15883, 11 2011.

[59] Torsten Bossing and Gerhard M. Technau. The fate of the CNS midline progenitors in Drosophila as revealed by a new method for single cell labelling. *Development*, 120(7):1895–1906, 7 1994.

[60] James W. Truman, Wanda Moats, Janet Altman, Elizabeth C. Marin, and Darren W. Williams. Role of Notch signaling in establishing the hemilineages of secondary neurons in Drosophila melanogaster. *Development*, 137(1):53–61, 1 2010.

[61] Robin M. Harris, Barret D. Pfeiffer, Gerald M. Rubin, and James W. Truman. Neuron hemilineages provide the functional ground plan for the Drosophila ventral nervous system. *eLife*, 4(JULY2015), 7 2015.

[62] Bret J. Pearson and Chris Q. Doe. Specification of temporal identity in the developing nervous system. *Annual Review of Cell and Developmental Biology*, 20:619–647, 2004.

[63] Thomas M. Jessell. Neuronal specification in the spinal cord: Inductive signals and transcriptional codes. 1(1):20–29, 2000.

[64] Chris Q Doe. Temporal patterning in the drosophila cns. *Annual Review of Cell and Developmental Biology Annu. Rev. Cell Dev. Biol*, 33:219–40, 2017.

[65] Alicia Estacio-Gómez and Fernando J. Díaz-Benjumea. Roles of Hox genes in the patterning of the central nervous system of Drosophila. *Fly*, 8(1):26, 2014.

[66] James B. Skeath and Stefan Thor. Genetic control of Drosophila nerve cord development. 13(1):8–15, 2 2003.

[67] James B. Skeath. At the nexus between pattern formation and cell-type specification: the generation of individual neuroblast fates in the drosophila embryonic central nervous system. *BioEssays*, 21(11):922–931, 1999.

[68] Takako Isshiki, Bret Pearson, Scott Holbrook, and Chris Q Doe. Drosophila Neuroblasts Sequentially Express Transcription Factors which Specify the Temporal Identity of Their Neuronal Progeny. *Cell*, 106:511–521, 2001.

[69] Ruth Grosskortenhaus, Kristin J Robinson, and Chris Q Doe. NB7-1 lineage Pdm and Castor specify late-born motor neuron identity in the. 2007.

[70] Khoa D Tran and Chris Q Doe. Pdm and Castor close successive temporal identity windows in the NB3-1 lineage. *Development (Cambridge, England)*, 135(21):3491–9, 11 2008.

[71] James B. Skeath and Chris Q. Doe. Sanpodo and Notch act in opposition to Numb to distinguish sibling neuron fates in the Drosophila CNS. *Development*, 125(10):1857–1865, 5 1998.

[72] Christof Rickert, Karin Lüer, Olaf Vef, and Gerhard M. Technau. Progressive derivation of serially homologous neuroblast lineages in the gnathal CNS of Drosophila. *PLOS ONE*, 13(2):e0191453, 2 2018.

[73] Haluk Lacin and James W. Truman. Lineage mapping identifies molecular and architectural similarities between the larval and adult Drosophila central nervous system. *eLife*, 5(MARCH2016), 3 2016.

[74] Douglas W. Allan and Stefan Thor. Transcriptional selectors, masters, and combinatorial codes: Regulatory principles of neural subtype specification. *Wiley Interdisciplinary Reviews: Developmental Biology*, 4(5):505–528, 2015.

[75] Miki Fujioka, Yukiko Emi-Sarker, Galina L. Yusibova, Tadaatsu Goto, and James B. Jaynes. Analysis of an even-skipped rescue transgene reveals both composite and discrete neuronal and early blastoderm enhancers, and multi-stripe positioning by gap gene repressor gradients. *Development*, 126(11):2527–2538, 6 1999.

[76] Liping He, Sarun Gulyanon, Mirna Mihovilovic Skanata, Doycho Karagyozov, Ellie S. Heckscher, Michael Krieg, Gavriil Tsechpenakis, Marc Gershow, and W. Daniel Tracey.

Direction Selectivity in Drosophila Proprioceptors Requires the Mechanosensory Channel Tmc. *Current Biology*, 29(6):945–956, 3 2019.

[77] R.E Snodgrass. Principles of insect morphology. 1935.

[78] Martinez Arias Bate. The mesoderm and its derivatives. 1993.

[79] James C Choi, Demian Park, and Leslie C Griffith. Electrophysiological and Morphological Characterization of Identified Motor Neurons in the Drosophila Third Instar Larva Central Nervous System. 2004.

[80] Austin Q. Seroka and Chris Q. Doe. The hunchback temporal transcription factor determines motor neuron axon and dendrite targeting in drosophila. *Development (Cambridge)*, 146(7), 4 2019.

[81] Matthias Landgraf, Natalia Sánchez-Soriano, Gerd M Technau, Joachim Urban, and Andreas Prokop. Charting the Drosophila neuropile: a strategy for the standardised characterisation of genetically amenable neurites. *Developmental Biology*, 260(1):207–225, 8 2003.

[82] Claire Bertet, Xin Li, Ted Erclik, Matthieu Cavey, Brent Wells, and Claude Desplan. Temporal patterning of neuroblasts controls Notch-mediated cell survival through regulation of Hid or Reaper. *Cell*, 158(5):1173, 8 2014.

[83] Maria Monastirioti, Nikolaos Giagtzoglou, Konstantinos A. Koumbanakis, Evanthia Zacharioudaki, Myrto Deligiannaki, Irmgard Wech, Mara Almeida, Anette Preiss, Sarah Bray, and Christos Delidakis. Drosophila Hey is a target of Notch in asymmetric divisions during embryonic and larval neurogenesis. *Development*, 137(2):191–201, 1 2010.

[84] Brandon Mark, Sen Lin Lai, Aref Arzan Zarin, Laurina Manning, Heather Q. Pollington, Ashok Litwin-Kumar, Albert Cardona, James W. Truman, and Chris Q. Doe. A developmental framework linking neurogenesis and circuit formation in the drosophila cns. *eLife*, 10, 5 2021.

[85] Austin Seroka, Rita M. Yazejian, Sen Lin Lai, and Chris Q. Doe. A novel temporal identity window generates alternating Eve+/Nkx6+motor neuron subtypes in a single progenitor lineage. *Neural Development*, 15(1):9, 7 2020.

[86] M. Baek and R. S. Mann. Lineage and Birth Date Specify Motor Neuron Targeting and Dendritic Architecture in Adult Drosophila. *Journal of Neuroscience*, 29(21):6904–6916, 2009.

[87] A. Benito-Gonzalez and F. J. Alvarez. Renshaw Cells and Ia Inhibitory Interneurons Are Generated at Different Times from p1 Progenitors and Differentiate Shortly after Exiting the Cell Cycle. *Journal of Neuroscience*, 32(4):1156–1170, 2012.

[88] Floor J. Stam, Timothy J. Hendricks, Jingming Zhang, Eric J. Geiman, Cedric Francius, Patricia A. Labosky, Frederic Clotman, and Martyn Goulding. Renshaw cell interneuron specialization is controlled by a temporally restricted transcription factor program. *Development*, 139(1):179–190, 1 2012.

[89] Hans Hultborn. Spinal reflexes, mechanisms and concepts: From Eccles to Lundberg and beyond.

[90] Marco Tripodi, Anna E. Stepien, and Silvia Arber. Motor antagonism exposed by spatial segregation and timing of neurogenesis. *Nature*, 479(7371):61–66, 11 2011.

[91] Mollie B. Woodworth, Kelly M. Girskis, and Christopher A. Walsh. Building a lineage from single cells: Genetic techniques for cell lineage tracking. 18(4):230–244, 4 2017.

[92] Joshua R. Sanes and Jeff W. Lichtman. Development of the vertebrate neuromuscular junction. *Annual review of neuroscience*, 22:389–442, 1999.

[93] Andrew M. Ravanelli and Bruce Appel. Motor neurons and oligodendrocytes arise from distinct cell lineages by progenitor recruitment. *Genes and Development*, 29(23):2504–2515, 12 2015.

[94] Svend Sparre Geertsen, Maria Willerslev-Olsen, Jakob Lorentzen, and Jens Bo Nielsen. Development and aging of human spinal cord circuitries. 118(2):1133–1140, 8 2017.

[95] J. I. P. de Vries and B. F. Fong. Normal fetal motility: an overview. *Ultrasound in Obstetrics and Gynecology*, 27(6):701–711, 6 2006.

[96] Sarah Crisp, Jan Felix Evers, André Fiala, and Michael Bate. The development of motor coordination in Drosophila embryos. *Development*, 135(22):3707–3717, 2008.

[97] David L. McLean and Joseph R. Fetcho. Spinal interneurons differentiate sequentially from those driving the fastest swimming movements in larval zebrafish to those driving the slowest ones. *Journal of Neuroscience*, 29(43):13566–13577, 10 2009.

[98] Joseph R. Fetcho and David L. McLean. Some principles of organization of spinal neurons underlying locomotion in zebrafish and their implications. *Annals of the New York Academy of Sciences*, 1198:94–104, 2010.

[99] Michael Jay and David L. McLean. Reconciling the functions of even-skipped interneurons during crawling, swimming, and walking. 8:188–192, 4 2019.

[100] Ravi Kambadur, Keita Koizumi, Chad Stivers, James Nagle, Stephen J. Poole, and Ward F. Odenwald. Regulation of pou genes by castor and hunchback establishes layered compartments in the drosophilacns. *Genes Development*, 12:246, 1 1998.

[101] Thomas Ward F. Brody and Odenwald. Programmed transformations in neuroblast gene expression during drosophila cns lineage development.

[102] Bret J. Pearson and Chris Q. Doe. Regulation of neuroblast competence in Drosophila. *Nature*, 425(6958):624–628, 10 2003.

[103] C. Andrew Frank, Thomas D. James, and Martin Müller. Homeostatic control of drosophila neuromuscular junction function. *Synapse*, 74, 1 2020.

[104] Te Ning Chang and Haig Keshishian. Laser Ablation of Drosophila Embryonic Motoneurons Causes Ectopic Innervation of Target Muscle Fibers. *Journal of Neuroscience*, 16(18):5715–5726, 9 1996.

[105] Polyxeni Philippidou and Jeremy S. Dasen. Hox genes: Choreographers in neural development, architects of circuit organization. *Neuron*, 80:12–34, 10 2013.

[106] Andreas Sagner and James Briscoe. Establishing neuronal diversity in the spinal cord: A time and a place. *Development (Cambridge)*, 146, 11 2019.

[107] Luis F. Sullivan, Timothy L. Warren, and Chris Q. Doe. Temporal identity establishes columnar neuron morphology, connectivity, and function in a drosophila navigation circuit. *eLife*, 8, 2 2019.

[108] Anthony M Rossi, Vilaiwan M Fernandes, and Claude Desplan. Timing temporal transitions during brain development. *Current Opinion in Neurobiology*, 42:84–92, 2017.

[109] Johannes Stratmann and Stefan Thor. Neuronal cell fate specification by the molecular convergence of different spatio-temporal cues on a common initiator terminal selector gene. *PLoS Genetics*, 13(4), 4 2017.

[110] James W. Truman and Eldon E. Ball. Patterns of embryonic neurogenesis in a primitive wingless insect, the silverfish, ctenolepisma longicaudata: Comparison with those seen in flying insects. *Development Genes and Evolution*, 208:357–368, 1998.

[111] D. Shepherd and C. M. Bate. Spatial and temporal patterns of neurogenesis in the embryo of the locust (schistocerca gregaria). *Development*, 108:83–96, 1 1990.

[112] Ressouches A. Tamarelle M, Haget A. Segregation, division, and early patterning of lateral thoracic neuroblasts in the embryo of carausius morosus br. (phasmida: Lonchodidae). *Int. J. Insect Morphol. Embryol.*, page 307–317, 1985.

[113] C. Q. Doe, J. Y. Kuwada, and C. S. Goodman. From epithelium to neuroblasts to neurons: the role of cell interactions and cell lineage during insect neurogenesis. *Philosophical transactions of the Royal Society of London. Series B, Biological sciences*, 312:67–81, 1985.

[114] Jeremy E. Niven, Christopher M. Graham, and Malcolm Burrows. Diversity and evolution of the insect ventral nerve cord. *Annual Review of Entomology*, 53:253–271, 1 2008.

[115] Lucia Biffar and Angelika Stollewerk. Conservation and evolutionary modifications of neuroblast expression patterns in insects. *Developmental Biology*, 388:103–116, 4 2014.

[116] Yuichi Deguchi, Flavio Donato, Ivan Galimberti, Erik Cabuy, and Pico Caroni. Temporally matched subpopulations of selectively interconnected principal neurons in the hippocampus. *Nature Neuroscience*, 14:495–504, 2011.

[117] Punita Bhansali, Ilana Rayport, Alexandra Rebsam, and Carol Mason. Delayed neurogenesis leads to altered specification of ventrotemporal retinal ganglion cells in albino mice. *Neural Development*, 9:11, 2014.

[118] Eerdunfu, Naoki Ihara, Bao Ligao, Yuji Ikegaya, and Haruki Takeuchi. Differential timing of neurogenesis underlies dorsal-ventral topographic projection of olfactory sensory neurons. *Neural Development*, 12:2, 2017.

[119] Marie R. Greaney, Ann E. Privorotskiy, Kristen P. D'Elia, and David Schoppik. Extraocular motoneuron pools develop along a dorsoventral axis in zebrafish, ¡i¿danio rerio¡/i¿. *Journal of Comparative Neurology*, 525:65–78, 1 2017.

[120] Gregory S.X.E. Jefferis, Elizabeth C. Marin, Reinhard F. Stocker, and Liqun Luo. Target neuron prespecification in the olfactory map of drosophila. *Nature 2001 414:6860*, 414:204–208, 11 2001.

[121] Abhishek Kulkarni, Deniz Ertekin, Chi Hon Lee, and Thomas Hummel. Birth order dependent growth cone segregation determines synaptic layer identity in the drosophila visual system. *eLife*, 5:1–22, 2016.

[122] David L. McLean, Jingyi Fan, Shin Ichi Higashijima, Melina E. Hale, and Joseph R. Fetcho. A topographic map of recruitment in spinal cord. *Nature*, 446:71–75, 3 2007.

[123] Eric M Morrow, C-M Amy Chen, and Constance L Cepko. Temporal order of bipolar cell genesis in the neural retina. *Neural Development*, 3:2, 1 2008.

[124] Jessica A Osterhout, Rana N El-Danaf, Phong L Nguyen, and Andrew D Huberman. Birthdate and outgrowth timing predict cellular mechanisms of axon-target matching in the developing visual pathway. 2014.

[125] Milan Petrovic and Thomas Hummel. Temporal identity in axonal target layer recognition. *Nature 2008 456:7223*, 456:800–803, 11 2008.

[126] Jesús Pujol-Martí, Andrea Zecca, Jean-Pierre Baudoin, Adè Le Faucherre, Kazuhide Asakawa, Koichi Kawakami, and Hernán López-Schier. Development/plasticity/repair neuronal birth order identifies a dimorphic sensorineural map. 2012.

[127] Suzanna L. Gribble, O. Brant Nikolaus, and Richard I. Dorsky. Regulation and function of Dbx genes in the zebrafish spinal cord. *Developmental Dynamics*, 236(12):3472–3483, 12 2007.

[128] Jessica M. Alsiö, Basile Tarchini, Michel Cayouette, and Frederick J. Livesey. Ikaros promotes early-born neuronal fates in the cerebral cortex. *Proceedings of the National Academy of Sciences*, 110(8):E716–E725, 2013.

[129] Jimmy Elliott, Christine Jolicoeur, Vasanth Ramamurthy, and Michel Cayouette. Ikaros confers early temporal competence to mouse retinal progenitor cells. *Neuron*, 60:26–39, 10 2008.

[130] Makoto I. Kanai, Masataka Okabe, and Yasushi Hiromi. Seven-up controls switching of transcription factors that specify temporal identities of drosophila neuroblasts. *Developmental Cell*, 8:203–213, 2 2005.

[131] Khoa D. Tran, Michael R. Miller, and Chris Q. Doe. Recombineering hunchback identifies two conserved domains required to maintain neuroblast competence and specify early-born neuronal identity. *Development*, 137:1421–1430, 5 2010.

[132] Minoree Kohwi, Joshua R. Lupton, Sen Lin Lai, Michael R. Miller, and Chris Q. Doe. Developmentally regulated subnuclear genome reorganization restricts neural progenitor competence in Drosophila. *Cell*, 152(1-2):97–108, 1 2013.

[133] Zachary L Newman, Adam Hoagland, Krishan Aghi, Kurtresha Worden, Sabrina L Levy, Jun Ho Son, Luke P Lee, and Ehud Y Isacoff. Input-specific plasticity and homeostasis at the drosophila larval neuromuscular junction. *Neuron*, 93:1388–1404.e10, 3 2017.

[134] Chand J. Desai, Joseph G. Gindhart, Lawrence S.B. Goldstein, and Kai Zinn. Receptor tyrosine phosphatases are required for motor axon guidance in the drosophila embryo. *Cell*, 84:599–609, 2 1996.

[135] Neil X. Krueger, David Van Vactor, Hong I. Wan, William M. Gelbart, Corey S. Goodman, and Haruo Saito. The transmembrane tyrosine phosphatase dlar controls motor axon guidance in drosophila. *Cell*, 84:611–622, 2 1996.

[136] Matthias Landgraf, Sudipto Roy, Andreas Prokop, K Vijayraghavan, and Michael Bate. even-skipped Determines the Dorsal Growth of Motor Axons in Drosophila for such a system of combinatorial specification comes from studies of vertebrate embryos where it has been possible (in the chick and the zebrafish) to establish a. *Neuron*, 22:43–52, 1999.

[137] Akinao Nose, Masatoshi Takeichi, and Corey S Goodman. Ectopic expression of connectin reveals a repulsive function during growth cone guidance and synapse formation. *Neuron*, 13:525–539, 1994.

[138] John Jacob, Cédric Maurange, and Alex P Gould. Temporal control of neuronal diversity: common regulatory principles in insects and vertebrates? *Development (Cambridge, England)*, 135:3481–9, 11 2008.

[139] Michael D Cleary and Chris Q Doe. Regulation of neuroblast competence: multiple temporal identity factors specify distinct neuronal fates within a single early competence window. 2006.

[140] Hua Tai Xu, Zhi Han, Peng Gao, Shuijin He, Zhizhong Li, Wei Shi, Oren Kodish, Wei Shao, Keith N. Brown, Kun Huang, and Song Hai Shi. Distinct lineage-dependent structural and functional organization of the hippocampus. *Cell*, 157:1552–1564, 6 2014.

[141] Yong Chun Yu, Ronald S. Bultje, Xiaoqun Wang, and Song Hai Shi. Specific synapses develop preferentially among sister excitatory neurons in the neocortex. *Nature*, 458:501–504, 3 2009.

[142] Sijun Zhu, Ann Shyn Chiang, and Tzumin Lee. Development of the drosophila mushroom bodies: elaboration,remodeling and spatial organization of dendrites in the calyx. *Development*, 130:2603–2610, 6 2003.

[143] Thomas Kunz, Karoline F. Kraft, Gerhard M. Technau, and Rolf Urbach. Origin of drosophila mushroom body neuroblasts and generation of divergent embryonic lineages. *Development*, 139:2510–2522, 7 2012.

[144] Kathleen T. Walsh and Chris Q. Doe. Drosophila embryonic type ii neuroblasts: Origin, temporal patterning, and contribution to the adult central complex. *Development (Cambridge)*, 144:4552–4562, 12 2017.

[145] Aljoscha Nern, Barret D Pfeiffer, Gerald M Rubin, Thomas R Clandinin, Claude Desplan, Chris Q Doe, and Joshua R Sanes. Optimized tools for multicolor stochastic labeling reveal diverse stereotyped cell arrangements in the fly visual system.

[146] Takumi Suzuki, Masako Kaido, Rie Takayama, and Makoto Sato. A temporal mechanism that produces neuronal diversity in the drosophila visual center. 2013.

[147] Marta Moris-Sanz, Alicia Estacio-Gómez, Javier Álvarez Rivero, and Fernando J. DÍaz-Benjumea. Specification of neuronal subtypes by different levels of hunchback. *Development (Cambridge)*, 141:4366–4374, 11 2014.

[148] T Novotny, R Eiselt, and J Urban. Hb specifies early nb7-3 sublineage fates. 2002.

[149] Magnus Baumgardt, Daniel Karlsson, Javier Terriente, Fernando J. Díaz-Benjumea, and Stefan Thor. Neuronal subtype specification within a lineage by opposing temporal feed-forward loops. *Cell*, 139:969–982, 11 2009.

[150] Akinao Nose. Generation of neuromuscular specificity in drosophila: novel mechanisms revealed by new technologies. *Frontiers in molecular neuroscience*, 5:62, 2012.

[151] Bao Hoang and Akira Chiba. Single-cell analysis of drosophila larval neuromuscular synapses. 2001.

[152] Helen Sink and Paul M. Whitington. Location and connectivity of abdominal motoneurons in the embryo and larva of drosophila melanogaster. *Journal of Neurobiology*, 22:298–311, 4 1991.

[153] Alex Mauss, Marco Tripodi, Jan Felix Evers, and Matthias Landgraf. Midline signalling systems direct the formation of a neural map by dendritic targeting in the Drosophila motor system. *PLoS Biology*, 7(9), 2009.

[154] James Ashley, Violet Sorrentino, Meike Lobb-Rabe, Sonal Nagarkar-Jaiswal, Liming Tan, Shuwa Xu, Qi Xiao, Kai Zinn, and Robert A. Carrillo. Transsynaptic interactions between igsf proteins dip- and dpr10 are required for motor neuron targeting specificity. *eLife*, 8, 2 2019.

[155] Juan J. Pérez-Moreno and Cahir J. O'Kane. Gal4 drivers specific for type ib and type is motor neurons in drosophila. *G3 Genes—Genomes—Genetics*, 9:453–462, 2 2019.

[156] C. Andrew Frank, Matthew J. Kennedy, Carleton P P. Goold, Kurt W. Marek, and Graeme W W. Davis. Mechanisms underlying the rapid induction and sustained expression of synaptic homeostasis. *Neuron*, 52:663–677, 11 2006.

[157] Pragya Goel and Dion Dickman. Distinct homeostatic modulations stabilize reduced postsynaptic receptivity in response to presynaptic dlk signaling. *Nature Communications*, 9, 12 2018.

[158] Pierre Mattar, Johan Ericson, Seth Blackshaw, and Michel Cayouette. A conserved regulatory logic controls temporal identity in mouse neural progenitors. *Neuron*, 85:497–504, 2 2015.

[159] Hugo Gabilondo, Johannes Stratmann, Irene Rubio-Ferrera, Irene Millán-Crespo, Patricia Contero-García, Shahrzad Bahrampour, Stefan Thor, and Jonathan Benito-Sipos. Neuronal cell fate specification by the convergence of different spatiotemporal cues on a common terminal selector cascade. *PLOS Biology*, 14:e1002450, 5 2016.

[160] Jonathan Enriquez, Lalanti Venkatasubramanian, Myungin Baek, Meredith Peterson, Ulkar Aghayeva, and Richard S. Mann. Specification of individual adult motor neuron morphologies by combinatorial transcription factor codes. *Neuron*, 86:955–970, 5 2015.

[161] Elizabeth S. Heckscher, Richard D. Fetter, Kurt W. Marek, Stephanie D. Albin, and Graeme W. Davis. Nf-b, i-b and irak control glutamate receptor density at the drosophila nmj. *Neuron*, 55:859, 9 2007.

[162] Ellie S. Heckscher, Fuhui Long, Michael J. Layden, Chein Hui Chuang, Laurina Manning, Jourdain Richart, Joseph C. Pearson, Stephen T. Crews, Hanchuan Peng, Eugene Myers, and Chris Q. Doe. Atlas-builder software and the eneuro atlas: resources for developmental biology and neuroscience. *Development*, 141:2524–2532, 6 2014.

[163] Susana Romani, Fernando Jimenez, Michael Hoch, Nipam H. Patel, Heike Taubert, and Herbert Jäckle. Krüppel, a Drosophila segmentation gene, participates in the specification of neurons and glial cells. *Mechanisms of Development*, 60(1):95–107, 11 1996.

[164] Joanne P. Odden, Scott Holbrook, and Chris Q. Doe. Drosophila HB9 is expressed in a subset of motoneurons and interneurons, where it regulates gene expression and axon pathfinding. *Journal of Neuroscience*, 22(21):9143–9149, 11 2002.

[165] Ingrid V. Andrade, Nadia Riebli, Bao Chau M. Nguyen, Jaison J. Omoto, Albert Cardona, and Volker Hartenstein. Developmentally Arrested Precursors of Pontine Neurons Establish an Embryonic Blueprint of the Drosophila Central Complex. *Current Biology*, 29(3):412–425, 2 2019.

[166] * Takuya Tsuji1, Eri Hasegawa1 and † Takako Isshiki1, 2. Neuroblast entry into quiescence is regulated intrinsically by the combined action of spatial Hox proteins and temporal identity factors. *Development*, 135:3859–3869, 2008.

[167] Akira Chiba. Early Development of the Drosophila Neuromuscular Junction: A Model for Studying Neuronal Networks in Development. *International Review of Neurobiology*, 43:1–24, 1 1999.

[168] Stephen T. Crews. Drosophila embryonic CNS development: Neurogenesis, gliogenesis, cell fate, and differentiation. *Genetics*, 213(4):1111–1144, 12 2019.

[169] Keiko Hirono, Jonathan S Margolis, James W Posakony, and Chris Q Doe. Identification of hunchback cis-regulatory DNA conferring temporal expression in neuroblasts and neurons. *Gene Expression Patterns*, 12:11–17, 2012.

[170] Dervla M. Mellerick, Judith A. Kassis, Shang Ding Zhang, and Ward F. Odenwald. castor encodes a novel zinc finger protein required for the development of a subset of CNS neurons in drosophila. *Neuron*, 9(5):789–803, 1992.

[171] X Cui and C Doe. ming is expressed in neuroblast sublineages and regulates gene expression in the Drosophila central nervous system. *Development (Cambridge, England)*, 952:943–952, 1992.

[172] Willy Joly, Bruno Mugat, and Florence Maschat. Engrailed controls the organization of the ventral nerve cord through frazzled regulation. *Developmental Biology*, 301(2):542–554, 1 2007.

[173] Pascal Jean Solano, Bruno Mugat, David Martin, Franck Girard, Jean Marc Huibant, Conchita Ferraz, Bernard Jacq, Jacques Demaille, and Florence Maschat. Genome-wide identification of in vivo DrosophilaEngrailed-binding DNA fragments and related target genes. *Development*, 130(7):1243–1254, 4 2003.

[174] R. G. Fehon, K. Johansen, I. Rebay, and S. Artavanis-Tsakonas. Complex cellular and subcellular regulation of notch expression during embryonic and imaginal development of Drosophila: implications for notch function. *The Journal of cell biology*, 113(3):657–669, 1991.

[175] Magnus Baumgardt, Daniel Karlsson, Behzad Y Salmani, Caroline Bivik, Ryan B Macdonald, Erika Gunnar, and Stefan Thor. Developmental Cell Article Global Programmed Switch in Neural Daughter Cell Proliferation Mode Triggered by a Temporal Gene Cascade. *Developmental Cell*, 30:192–208, 2014.

[176] Kate M. O'Connor-Giles and James B. Skeath. Numb Inhibits Membrane Localization of Sanpodo, a Four-Pass Transmembrane Protein, to Promote Asymmetric Divisions in Drosophila. *Developmental Cell*, 5(2):231–243, 8 2003.

[177] Spyros Artavanis-Tsakonas, Matthew D. Rand, and Robert J. Lake. Notch signaling: Cell fate control and signal integration in development. *Science*, 284(5415):770–776, 4 1999.

[178] Haluk Lacin, Hui Min Chen, Xi Long, Robert H. Singer, Tzumin Lee, and James W. Truman. Neurotransmitter identity is acquired in a lineage-restricted manner in the Drosophila CNS. *eLife*, 8, 3 2019.

[179] E. P. Spana, C. Kopczynski, C. S. Goodman, and C. Q. Doe. Asymmetric localization of numb autonomously determines sibling neuron identity in the Drosophila CNS. *Development*, 121(11):3489–3494, 11 1995.

[180] Marita Buescher, Su Ling Yeo, Gerald Udolph, Michael Zavortink, Xiaohang Yang, Guy Tear, and William Chia. Binary sibling neuronal cell fate decisions in the Drosophila embryonic central nervous system are nonstochastic and require inscuteable-mediated asymmetry of ganglion mothercells. *Genes & Development*, 12(12):1858, 6 1998.

[181] Bridget C. Lear, James B. Skeath, and Nipam H. Patel. Neural cell fate in rca1 and cycA mutants: the roles of intrinsic and extrinsic factors in asymmetric division in the Drosophila central nervous system. *Mechanisms of Development*, 88(2):207–219, 11 1999.

[182] Alison J. Schuldt and Andrea H. Brand. Mastermind Acts Downstream of Notch to Specify Neuronal Cell Fates in theDrosophilaCentral Nervous System. *Developmental Biology*, 205(2):287–295, 1 1999.

[183] Ivana Gaziova, Michael Gazi, Jordan Mar, and Krishna Moorthi Bhat. Restriction on self-renewing asymmetric division is coupled to terminal asymmetric division in the Drosophila CNS. *PLOS Genetics*, 16(9):e1009011, 9 2020.

[184] Irene Miguel-Aliaga, Stefan Thor, and Alex P. Gould. Postmitotic Specification of Drosophila Insulinergic Neurons from Pioneer Neurons. *PLoS Biology*, 6(3):0538–0551, 3 2008.

[185] Carina Ulvklo, Ryan MacDonald, Caroline Bivik, Magnus Baumgardt, Daniel Karlsson, and Stefan Thor. Control of neuronal cell fate and number by integration of distinct daughter cell proliferation modes with temporal progression. *Development*, 139(4):678–689, 2 2012.

[186] Caroline Bivik, Ryan B. MacDonald, Erika Gunnar, Khalil Mazouni, Francois Schweisguth, and Stefan Thor. Control of Neural Daughter Cell Proliferation by Multilevel Notch/Su(H)/E(spl)-HLH Signaling. *PLOS Genetics*, 12(4):e1005984, 4 2016.

[187] Itaru Imayoshi, Masayuki Sakamoto, Masahiro Yamaguchi, Kensaku Mori, and Ryoichiro Kageyama. Essential Roles of Notch Signaling in Maintenance of Neural Stem Cells in Developing and Adult Brains. *Journal of Neuroscience*, 30(9):3489–3498, 3 2010.

[188] Rachel Karcavich and Chris Q Doe. Drosophila Neuroblast 7-3 Cell Lineage: A Model System for Studying Programmed Cell Death, Notch/Numb Signaling, and Sequential Specification of Ganglion Mother Cell Identity. *J. Comp. Neurol*, 129:240–251, 2002.

[189] Fillip Port, Claudia Strein, Mona Stricker, Benedikt Rauscher, Florian Heigwer, Jun Zhou, Celine Beyersdörffer, Jana Frei, Amy Hess, Katharina Kern, Laura Lange, Nora Langner, Roberta Malamud, Bojana Pavlović, Kristin Rädecke, Lukas Schmitt, Lukas Voos, Erica Valentini, and Michael Boutros. A large-scale resource for tissue-specific CRISPR mutagenesis in Drosophila. *eLife*, 9, 2 2020.

[190] Celine Santiago, Juan Pablo Labrador, and Greg J. Bashaw. The homeodomain transcription factor Hb9 controls axon guidance in drosophila through the regulation of robo receptors. *Cell Reports*, 7(1):153–165, 10 2014.

[191] Gundula Edenfeld, Benjamin Altenhein, Ariane Zierau, Diana Cleppien, Karin Krukkert, Gerhard Technau, and Christian Klämbt. Notch and Numb are required for normal migration of peripheral glia in Drosophila. *Developmental Biology*, 301(1):27–37, 1 2007.

[192] John Y. Kuwada and Corey S. Goodman. Neuronal determination during embryonic development of the grasshopper nervous system. *Developmental biology*, 110(1):114–126, 1985.

[193] Krishna Moorthi Bhat. Wingless activity in the precursor cells specifies neuronal migratory behavior in the Drosophila nerve cord. *Developmental Biology*, 311(2):613–622, 11 2007.

[194] Daniel Crowner, Maude Le Gall, Michael A. Gates, and Edward Giniger. Notch steers Drosophila ISNb motor axons by regulating the AbI signaling pathway. *Current Biology*, 13(11):967–972, 5 2003.

[195] E. Giniger, L. Y. Jan, and Y. N. Jan. Specifying the path of the intersegmental nerve of the Drosophila embryo: a role for Delta and Notch. *Development*, 117(2):431–440, 2 1993.

[196] Edward Giniger. A role for Abl in Notch signaling. *Neuron*, 20(4):667–681, 1998.

[197] Javier Valdes-Aleman, Richard D. Fetter, Emily C. Sales, Emily L. Heckman, Lalanti Venkatasubramanian, Chris Q. Doe, Matthias Landgraf, Albert Cardona, and Marta Zlatic. Comparative Connectomics Reveals How Partner Identity, Location, and Activity Specify Synaptic Connectivity in Drosophila. *Neuron*, 10 2020.

[198] Haluk Lacin, Yi Zhu, Beth A Wilson, and James B Skeath. dbx mediates neuronal specification and differentiation through cross-repressive, lineage-specific interactions with eve and hb9. *Development (Cambridge, England)*, 136(19):3257–66, 10 2009.

[199] K. G. Pearson and C. R. Fourtner. Nonspiking interneurons in walking system of the cockroach. *Journal of neurophysiology*, 38(1):33–52, 1975.

[200] Stephan Gerhard, Ingrid Andrade, Richard D. Fetter, Albert Cardona, and Casey M. Schneider-Mizell. Conserved neural circuit structure across drosophila larval development revealed by comparative connectomics. *eLife*, 6, 10 2017.

[201] Kristen Lee and Chris Q. Doe. A locomotor neural circuit persists and functions similarly in larvae and adult drosophila. *eLife*, 10, 7 2021.

[202] Oliver Hobert. Regulatory logic of neuronal diversity: Terminal selector genes and selector motifs. 2008.

[203] Johannes Stratmann, Helen Ekman, and Stefan Thor. A branching gene regulatory network dictating different aspects of a neuronal cell identity. *Development (Cambridge)*, 146(6), 3 2019.

[204] Daniel C. Lu, Tianyi Niu, and William A. Alaynick. Molecular and cellular development of spinal cord locomotor circuitry. *Frontiers in Molecular Neuroscience*, 8(June), 6 2015.

[205] Silvia Arber. Motor Circuits in Action: Specification, Connectivity, and Function. *Neuron*, 74(6):975–989, 2012.

[206] James Briscoe, Alessandra Pierani, Thomas M. Jessell, and Johan Ericson. A homeodomain protein code specifies progenitor cell identity and neuronal fate in the ventral neural tube. *Cell*, 101(4):435–445, 5 2000.

[207] A. Pierani, L. Moran-Rivard, M. J. Sunshine, D. R. Littman, M. Goulding, and T. M. Jessell. Control of interneuron fate in the developing spinal cord by the progenitor homeodomain protein Dbx1. *Neuron*, 29(2):367–384, 2 2001.

[208] Akihiko Nakajima, Takako Isshiki, Kunihiko Kaneko, and Shuji Ishihara. Robustness under functional constraint: The genetic network for temporal expression in Drosophila neurogenesis. *PLoS Computational Biology*, 6(4):e1000760, 4 2010.

[209] James Briscoe and Johan Ericson. Specification of neuronal fates in the ventral neural tube. *Current opinion in neurobiology*, 11(1):43–49, 2 2001.

[210] Heather T. Broihier and James B. Skeath. Drosophila homeodomain protein dHb9 directs neuronal fate via crossrepressive and cell-nonautonomous mechanisms. *Neuron*, 35(1):39–50, 2002.

[211] Heather T. Broihier, Alexander Kuzin, Yi Zhu, Ward Odenwald, and James B. Skeath. Drosophila homeodomain protein Nkx6 coordinates motoneuron subtype identity and axonogenesis. *Development*, 131(21):5233–5242, 11 2004.

[212] Matthias Landgraf and Stefan Thor. Development and Structure of Motoneurons. 75:33–53, 1 2006.

[213] Juan Pablo Labrador, David O'Keefe, Shingo Yoshikawa, Randall D. McKinnon, John B. Thomas, and Greg J. Bashaw. The homeobox transcription factor even-skipped regulates netrin-receptor expression to control dorsal motor-axon projections in Drosophila. *Current Biology*, 15(15):1413–1419, 8 2005.

[214] Jay Uhler, James Garbern, Li Yang, John Kamholz, and Dervla M. Mellerick. Nk6, a novel Drosophila homeobox gene regulated by vnd. *Mechanisms of Development*, 116(1-2):105–116, 2002.

[215] Miki Fujioka, Bridget C. Lear, Matthias Landgraf, Galina L. Yusibova, Jian Zhou, Kristen M. Riley, Nipam H. Patel, and James B. Jaynes. Even-skipped, acting as a repressor, regulates axonal projections in Drosophila. *Development*, 130(22):5385–5400, 11 2003.

[216] Haluk Lacin, Jannette Rusch, Raymond T. Yeh, Miki Fujioka, Beth A. Wilson, Yi Zhu, Alice A. Robie, Hemlata Mistry, Ting Wang, James B. Jaynes, and James B. Skeath. Genome-wide identification of drosophila hb9 targets reveals a pivotal role in directing the transcriptome within eight neuronal lineages, including activation of nitric oxide synthase and fd59a/fox-d. *Developmental Biology*, 388:117–133, 4 2014.

[217] K. S. Broadie and M. Bate. Development of the embryonic neuromuscular synapse of drosophila melanogaster. *Journal of Neuroscience*, 13:144–166, 1 1993.

[218] Fernando Vonhoff and Haig Keshishian. Activity-dependent synaptic refinement: New insights from drosophila. *Frontiers in Systems Neuroscience*, 11:23, 4 2017.

[219] Alain Garces and Stefan Thor. Specification of Drosophila aCC motoneuron identity by a genetic cascade involving even-skipped, grain and zfh1. *Development (Cambridge, England)*, 133(8):1445–1455, 4 2006.

[220] A H D Watson and M Burrows. Cell and Tissue Research Input and Output Synapses on Identified Motor Neurones of a Locust Revealed by the Intracellular Injection of Horseradish Peroxidase. *Cell Tissue Res*, 215:325–332, 1981.

[221] Ryan J. Watts, Oren Schuldiner, John Perrino, Camilla Larsen, and Liqun Luo. Glia engulf degenerating axons during developmental axon pruning. *Current Biology*, 14(8):678–684, 4 2004.

[222] Jeffrey D. Martell, Thomas J. Deerinck, Yasemin Sancak, Thomas L. Poulos, Vamsi K. Mootha, Gina E. Sosinsky, Mark H. Ellisman, and Alice Y. Ting. Engineered ascorbate peroxidase as a genetically encoded reporter for electron microscopy. *Nature biotechnology*, 30(11):1143–1148, 11 2012.

[223] Chiao Lin Chen, Yanhui Hu, Namrata D. Udeshi, Thomas Y. Lau, Frederik Wirtz-Peitz, Li He, Alice Y. Ting, Steven A. Carr, and Norbert Perrimon. Proteomic mapping in live Drosophila tissues using an engineered ascorbate peroxidase. *Proceedings of the National Academy of Sciences of the United States of America*, 112(39):12093–12098, 9 2015.

[224] Kenneth J. Hayworth, C. Shan Xu, Zhiyuan Lu, Graham W. Knott, Richard D. Fetter, Juan Carlos Tapia, Jeff W. Lichtman, and Harald F. Hess. Ultrastructurally-smooth thick partitioning and volume stitching for larger-scale connectomics. *Nature methods*, 12:319, 3 2015.

[225] Juan Carlos Tapia, Narayanan Kasthuri, Kenneth J. Hayworth, Richard Schalek, Jeff W. Lichtman, Stephen J. Smith, and Joann Buchanan. High-contrast en bloc staining of neuronal tissue for field emission scanning electron microscopy. *Nature protocols*, 7(2):193–206, 2012.

[226] Benjamin Risse, Dimitri Berh, Nils Otto, Christian Klämbt, and Xiaoyi Jiang. Fimtrack: An open source tracking and locomotion analysis software for small animals. *PLOS Computational Biology*, 13:e1005530, 5 2017.

[227] Keiko Hirono, Minoree Kohwi, Matt Q. Clark, Ellie S. Heckscher, and Chris Q. Doe. The hunchback temporal transcription factor establishes, but is not required to maintain, early-born neuronal identity. *Neural Development*, 12, 1 2017.

[228] Joshua L. Lillvis, Hideo Otsuna, Xiaoyu Ding, Igor Pisarev, Takashi Kawase, Jennifer Colonell, Konrad Rokicki, Cristian Goina, Ruixuan Gao, Amy Hu, Kaiyu Wang, John Bogovic, Daniel E. Milkie, Linus Meienberg, Edward S. Boyden, Stephan Saalfeld, Paul W. Tillberg, and Barry J. Dickson. Rapid reconstruction of neural circuits using tissue expansion and lattice light sheet microscopy. *bioRxiv*, page 2021.11.14.468535, 11 2021.

[229] Matthias Siebert, Daniel Banovic, Bernd Goellner, and Hermann Aberle. Drosophila motor axons recognize and follow a sidestep-labeled substrate pathway to reach their target fields. *Genes Development*, 23:1052–1062, 5 2009.

[230] B. A. Stewart, H. L. Atwood, J. J. Renger, J. Wang, and C. F. Wu. Improved stability of drosophila larval neuromuscular preparations in haemolymph-like physiological solutions. *Journal of Comparative Physiology A 1994 175:2*, 175:179–191, 8 1994.